# Enhancement of Deregulated and Restructured Power Network Performance with Flexible Alternating Current Transmission Systems Devices


**Babatunde Olusegun Adewolu**

**218074756**

Thesis submitted in fulfillment of the requirements for the degree of

**Doctor of Philosophy (Ph.D.) in Electrical Engineering**

School of Electrical, Electronic and Computer Engineering, College of Agriculture, Engineering and Science, University of KwaZulu-Natal, Durban, South Africa.

August 2020

# Enhancement of Deregulated and Restructured Power Network Performance with Flexible Alternating Current Transmission Systems Devices

Submitted by

**Babatunde Olusegun Adewolu**

**218074756**

In fulfilment of the award of the degree of

**DOCTOR OF PHILOSOPHY IN ELECTRICAL ENGINEERING**

School of Electrical, Electronic and Computer Engineering, College of Agriculture, Engineering and Science, University of KwaZulu-Natal, Durban, South Africa.

Date of Submission

**August 2020**

Supervised by

**Prof. Akshay Kumar Saha**

As the candidate's supervisor, I agree to the submission of the thesis

Signed:…. …..

Date:……14/08/2020……

**UNIVERSITY OF KWAZULU-NATAL**
**COLLEGE OF AGRICULTURE, ENGINEERING AND SCIENCE**

## DECLARATION 1 - PLAGIARISM

I, **Babatunde Olusegun Adewolu**, declare that:

1. The research reported in this thesis, except where otherwise indicated, is my original research.
2. This thesis has not been submitted for any degree or examination at any other university.
3. This thesis does not contain other persons' data, pictures, graphs or other information, unless specifically acknowledged as being sourced from other persons.
4. This thesis does not contain other persons' writing, unless specifically acknowledged as being sourced from other researchers. Where other written sources have been quoted, then:
   (a) Their words have been re-written, but the general information attributed to them has been referenced.
   (b) Where their exact words have been used, then their writing has been placed in italics and inside quotation marks and referenced.
5. This thesis does not contain text, graphics or tables copied and pasted from the Internet, unless specifically acknowledged, and the source being detailed in the thesis and in the References sections.

Signed:……. …….

Date:……14/08/2020……

**UNIVERSITY OF KWAZULU-NATAL**
**COLLEGE OF AGRICULTURE, ENGINEERING AND SCIENCE**

# DECLARATION 2 - PUBLICATIONS

DETAILS OF CONTRIBUTION TO PUBLICATIONS that form part and/or include research presented in this thesis (include publications in preparation, submitted, *in press* and published and give details of the contributions of each author to the experimental work and writing of each publication)

**Articles in Peer Reviewed DHET Accredited Journals**

**Publication 1:**

**B. O. Adewolu** and A. K. Saha, "FACTS Devices Loss Consideration in Placement Approach for Available Transfer Capability Enhancement," *International Journal of Engineering Research in.Africa (IJERA)*, vol. 49, pp. 104–129, 2020. *doi.org/10.4028/www.scientific.net/JERA.49.104.*

**Publication 2:**

**B. O. Adewolu** and A. K. Saha, "Optimal Setting of Thyristor Controlled Series Compensator with Brain Storm Optimization Algorithms for Available Transfer Capability Enhancement." Accepted for publication on 24th December 2020 by *International Journal of Engineering Research in Africa (IJERA)*.

**Publication 3:**

**B. O. Adewolu** and A. K. Saha, "FACTS Controllers and Power System Networks Applications: A Review." *International Journal of Engineering Research in Africa (IJERA), vol. 51, pp. 147 – 175, 2020. doi.org/10.4028/www.scientific.net/JERA.51.147.*

**Publication 4:**

**B. O. Adewolu** and A. K. Saha, "Contingency Control Capability of an Optimized HVDC Based VSC Transmission System in Perspectives of Deregulated and Restructured Network" *IEEE Access, vol.* 9, pp. 4112 – 4128, 2021. doi.10.11109/ACCESS.2020.3048500.

**Peer Reviewed Conferences Papers**

**Publication 5:**

**B. O. Adewolu** and A. K. Saha, "Determination and Analyses of Available Transfer Capability: Deregulated and Restructured Power Systems Perspective," *Proc. - 2019 South. African Univ. Power Eng. Conf. Mechatronics/Pattern Recognit. Assoc. South Africa, SAUPEC/RobMech/PRASA 2019*, pp. 504–509, 2019, doi: 10.1109/RoboMech.2019.8704738.

**Publication 6:**

**B. O. Adewolu** and A. K. Saha, "Evaluation of Performance Index Methodology for Power Network

Contingency Ranking," in *2020 IEEE International SAUPEC/RobMech/PRASA Conference*, 2020, pp. 2–7, doi: https://doi.org/10.1109/SAUPEC/RobMech/PRASA48453.2020.9041137.

**Publication 7:**

**B. O. Adewolu** and A. K. Saha, "Performance Evaluation of FACTS Placement Methods for Available Transfer Capability Enhancement in a Deregulated Power Networks," in *2020 IEEE International SAUPEC /RobMech/PRASA Conference*, 2020, pp. 1–6, doi: 10.1109/SAUPEC/RobMech/PRASA48453.2020.9041146.

**Publication 8:**

**B. O. Adewolu** and A. K. Saha, "Available transfer capability enhancement with FACTS: Perspective of performance comparison," *2020 Int. SAUPEC/RobMech/PRASA Conf. SAUPEC/RobMech/PRASA 2020*, 2020, doi: 10.1109/SAUPEC/RobMech/PRASA48453.2020.9040995.

**Other Publications - Abstracts and Workshop Presentations**

**Publication 9:**

**B. O. Adewolu** and A. K. Saha "Enhancement of Available Transfer Capability with Facts Devices in a Deregulated and Restructured Power Systems,'' College of Agriculture, Engineering and Science, *Postgraduate Research and Innovation Symposium* 2019, University of KwaZulu-Natal, T Block, Westville Campus, 17 October 2019, pp. 60, 2019.

**Publication 10:**

**B. O. Adewolu** and A. K. Saha "Applications of FACTS Devices to Available Transfer Capability Enhancement in a Deregulated and Restructured Power System Network,'' College of Agriculture, Engineering and Science, *School of Engineering Research Exposition* 2019, University of KwaZulu-Natal, Unite Building, Howard Campus, 8 November 2019, https://caes.ukzn.ac.za/2019-research-expo-gallery/#.

Signed:……  …….

Date:……14/08/2020……

# DEDICATION

This work in its entirety is dedicated to the Almighty God, who is the source and giver of wisdom, knowledge and understanding. The realization of this dream was occasioned by HIS divine providence, may HE be praised forever.

## ACKNOWLEDGEMENTS

Firstly, my sincere appreciation goes to Almighty God, the beginning and the end, the alpha and omega, the ancient of days and the maker of all things on earth and in heaven, for HIS constant grace, wisdom, faithfulness, love, provisions, protections and enablement in all ramifications and especially towards the achievement and successful completion of this Ph.D. degree. God ensured the realization of this degree despite all odds; may HIS name be praised for ever (Philippians 4:13, Matthew 19:26).

I am deeply grateful to my supervisor, Professor Akshay Kumar Saha, for his leadership, mentorship, competence, inspiration, and clarity. I truly appreciate and value his esteemed counselling and encouragement from the beginning of my Ph.D. program to the end of thesis compilation. His trust, confidence and supports inspired me in the most important moments, and his style of guidance is worthy of emulation.

I express my gratitude to the Academic leader for the discipline of Electrical, Electronic and Computer Engineering, Professor Tom Wallingo, and other lecturers and staff of the department for their supports and provision of enabling environment throughout the period of my study.

My sincere appreciation goes to the following people in University of Ibadan, Ibadan, Nigeria. Firstly, The Vice Chancellor, Professor Abel Idowu Olayinka, for approval of my requests, which culminated into success of this program. Director of Works, Engr. O. A. Adetolu, for his endorsement of my leave requests and permission. Former Director of Works, Engr. J. K. Ajibola for his substantial role in the journey of this Ph.D. I appreciate the current Dean of Engineering, Professor O. A. Fakolujo and family for their supports and constant encouragement. Deputy Director of Works, Operations and Maintenance, Engr. S. A. Adeniji, for his supports. I appreciate Engr. O. A. Ajibade for his efforts at all times and for constant running around on my behalf especially on matters that pertain the success of this Ph.D program.

To those, whose suggestions and timely information yielded the choice and success of University of KwaZulu-Natal; to those, whose their companionships have greater impact on my sojourn at University of KwaZulu-Natal; to those, whom God used for the success of this thesis, through their countless contributions and valuable suggestions; and to those who graciously read, discussed and helped improve portions of the thesis, I say thank you all and God bless. Engr. (Dr.) D. O. Ayanda, Dr. (Mrs) A. E. Kayode, Akindele Mebawondu, Hammed Abbas, Oyewole Olawale, Kazeem Aremu, and James Akpan, you are all wonderful people. I equally remember my friend, Umayah Erhiega Nana, of blessed memory, may his soul rest in peace. My colleagues in the research group; Emmanuel Ogunwole, Peter Gbadega, and Oluwole Osaloni, I appreciate your corporation and thank you all. I also appreciate Pastor (Mrs.) Victoria Abbey for her concern, advice, and constant prayers. Many thanks also go to Pastor Ben Ilesanmi for his prayers and encouragement.

My gratitude goes to my parents Mr. Timothy Agboola Adewolu and Mrs. Lydia Ebunlomo Adewolu in whose care the Lord entrusted me. Your supports and prayers are of inestimable value in the realization of my set targets in life, one of which is the achievement of this higher degree. May you both live long to reap from the

fruits of your labour. I render my sincere appreciation to Elder and Deaconess A. O. Adewolu for through their inspiration and insight, the foundation of this program became a reality. May the Lord continue to strengthen and uphold you. Many thanks also, to all my brothers, sisters, the entire family and well-wishers who have contributed immensely to the success of this project. Your dispositions and moral supports are highly appreciated.

My deepest appreciation goes to my wife, the jewel of an inestimable value, Mrs. Opeyemi Ibiwumi Adewolu, for she stood in between the gap and for her limitless support, patience, perseverance, encouragement and understanding, throughout the period of the program. I thank and appreciate my children, Samuel, Abraham and Joshua Adewolu for their endurance and perseverance throughout the period of my absence at home.

# ABSTRACT

The increase in power transactions, consequent open access created by deregulation and restructuring has resulted into network operation challenges including determination as well as enhancement of available transfer capability (ATC), and congestion management among others. In this study, repeated alternating current power flow (RACPF) approach was implemented for determination of ATC. ATCs for inter-area line outage and generator outage contingency conditions were obtained and analyzed. Analyses of most severe line outage contingencies resulting from evaluation of different performance index (PI) ranking methods were carried out for severe line outage contingency identification. A comprehensive review of FACTS controllers with their various background, topological structures, deployment techniques and cutting-edge applications was carried out for network performance enhancement. In addition, different placement methods were investigated for optimal performance evaluation of FACTS devices. Following this, comparative performance of static var compensator (SVC) and thyristor-controlled series compensator (TCSC) models for enhancement of ATC, bus voltage profile improvement and real power loss minimization was investigated. In addition, particle swarm optimization (PSO) and brain-storm optimization algorithms (BSOA) were engaged for optimum setting of FACTS devices through multi-objective problem formulation and allocation purposes. Thereafter, sensitivity-based technique involving incorporation of proposed FACTS device loss with the general loss equation for the determination of optimum location with same objectives was developed and TCSC location was established based on this sensitivity factors analyses, obtained from partial derivatives of the resultant loss equations with respect to control parameters. Subsequently, investigation and analyses of capability of an optimized VSC-HVDC transmission system in enhancing power network performance were conducted. Furthermore, this optimized VSC-HVDC transmission system was applied for mitigation of bus voltage and line thermal limit violation as a result of n-1-line outage contingency. All these investigations and analyses were implemented for bilateral, simultaneous and multilateral transactions as characterized by network liberalization and IEEE 5 and 30 bus networks were used for implementation in MATLAB environment.

RACPF method found to be more accurate especially when compared with other methods with 11.574 MW above and 29.014 MW below recorded ATC values. Voltage and real power PI have also been proven to be distinctly dissimilar in severe contingency identification. In placement method comparison however, disparities in ATC enhancement ranges between 2% and 85% were achieved while real power loss minimization of up to 25% was obtained for different methods. Real power loss minimization of up to 0.06 MW and voltage improvement of bus 21 to 30 were achieved with SVC, while ATC enhancement of up to 14% were recorded for both devices. However, BSO behaved much like PSO throughout the achievements of other set objectives but performed better in ATC enhancement with 27.12 MW and 5.24 MW increase above enhanced ATC values achieved by the latter. The comparison of set objectives values relative to that obtained with PSO methods depict suitability and advantages of BSOA technique. Sensitivity based placement technique resulted into ATC enhancement of more than 60% well above the values obtained when TCSC was placed with thermal limit method. In addition, a substantial bus voltage improvement and active power loss reduction were recorded with

this placement method. With incorporation of a VSC-HVDC based transmission system into ac network however, there was an improvement in power flow up to 15.66% corresponding to 46 MW for various transactions, transmission line power loss minimization up to 0.38 MW and bus voltage profile deviation minimization. Besides, automatic alleviation of violated thermal and voltage limits during contingency present VSC-HVDC system as a solution for network performance optimization especially during various transactions occasioned by unbundling power processes. Therefore, ATCs were properly enhanced, bus voltage profile improved, and system real power loss minimized. Likewise, HVDC system enhanced network performance and automatically alleviated violated thermal and voltage limits during contingency.

# TABLE OF CONTENTS

# LIST OF FIGURES

**LIST OF TABLES**

## LIST OF ABBREVIATIONS

| | |
|---|---|
| ABC | Artificial Bee Colony |
| ABC | Artificial Bee Colony |
| ACPTDF | AC Power Transfer Distributed Factor |
| AGSA | Adaptive Gravitational Search Algorithm |
| AHP | Analytical Hierarchy Process |
| APF | Active Power Filter |
| APSOA | Adaptive Parallel Seeker Optimization Algorithm |
| ATC | Available Transfer Capability |
| BA | Bee Algorithm |
| BESS | Battery Energy Storage System |
| BF | Bacterial Foraging |
| CGSA | Cumulative Gravitational Search Algorithm |
| C-N | Casablanca Network |
| CO | Chaos Optimization |
| CPF | Continuation Power Flow |
| CRO | Chemical Reaction Optimization |
| CSA | Cuckoo Search Algorithm |
| CSC | Convertible Static Compensator |
| DCPTDF | DC Power Transfer Distributed Factor |
| DE | Differential Evolution |
| DG | Distributed Generator |
| D-GIPFC | Distributed Generalized Interline Power Flow Controller |
| D-GUPFC | Distributed Generalized Unified Power Flow Controller |
| D-HPFC | Distributed Hybrid Power Flow Controller |
| D-IPFC | Distributed Interline Power Flow Controller |
| D-SSC | Distributed Static Series Compensator |
| D-STATCOM | Distributed Static Synchronous Compensator |
| D-TCSC | Distributed Thyristor Controlled Series Capacitor |
| DVR | Dynamic Voltage Restorer |
| ELPSO | Enhanced Leader Particle Swarm Optimization |

| | |
|---|---|
| FA | Firefly Algorithm |
| FCN | Fuzzy-C-number |
| FL | Fuzzy Logic |
| FVSI | Fast voltage Stability Index |
| FWFR | Cluster Wise Fuzzy Regression Analysis |
| GA | Genetic Algorithm |
| GCPSO | Guarantee Convergence PSO |
| GIPFC | Generalized Interline Power Flow Controller |
| GSA | Gravitational Search Algorithm |
| GSF | Generation Shift Factor |
| GTO | Gate Turn Off |
| GUPFC | Generalized Unified Power Flow Controller |
| HPFC | Hybrid Power Flow Controller |
| HPFC | Hybrid Power Flow Controller |
| IC | Imperialistic Competitive |
| IGBT | Insulated Gate Bipolar Transistor |
| IGCT | Integrated Gate Commutated Thyristor |
| IPC | Interphase Power Controller |
| IPFC | Interline Power Flow Controller |
| ISB | Indian Southern Bus |
| ITLA | Improved Teaching Learning Algorithm |
| JADF | Java Agent Development Framework |
| MCA | Min Cut Algorithm |
| MILP | Mixed Integer Linear Programming |
| MINLP | Mixed Integer Non-Linear Programming |
| MPSO | Modified Particle Swarm Optimization |
| NLP | Non-Linear Programming |
| NSCPF | Network Structural Characteristics Participation Factor |
| OPF | Optimal Power Flow |
| PSOA | Particle Swarm optimization Algorithm |
| QOCRO | Quasi Oppositional CRO |
| RCGA | Real Code Genetic Algorithm |

| | |
|---|---|
| RGA | Real generic Algorithm |
| RPF | Repeated Power Flow |
| RTIZB | Real time Industrial Zone Bus |
| SA | Simulation Annealing |
| SADE | Self Adaptive Differential Evolution |
| SCR | Silicon Control Rectifier |
| SLIB | Single Load Infinite Bus |
| SMES | Superconducting Magnetic Energy Storage |
| SMIB | Single Machine Infinite Bus |
| SNB | Saddle Node Bifurcation |
| SP | Structure Preserving |
| SQP | Sequential Quadratic Programming |
| SSG | Static Synchronous Generator |
| SSSC | Static Synchronous Series Compensator |
| STATCOM | Static Synchronous Compensator |
| SVC | Static Var Compensator |
| SVG/A | Static Var Generator/Absorber |
| SVS | Static Var Systems |
| TAPSM | Two Area Power System Model |
| TCBR | Thyristor Controlled Breaking Resistor |
| TCPAR | Thyristor Controlled Phase Angle Reactor |
| TCPST | Thyristor Controlled Phase Shifting Transformer |
| TCR | Thyristor Controlled Reactor |
| TCSC | Thyristor Controlled Series Capacitor |
| TCSR | Thyristor Controlled Series Reactor |
| TCVL | Thyristor Controlled Voltage Limiter |
| TCVR | Thyristor Controlled Voltage Reactor |
| TDS | Time Domain Simulation |
| TLBO | Teaching Learning Based Optimization |
| TS | Tabu Search |
| TSC | Thyristor Switched Capacitor |
| TSR | Thyristor Switched Reactor |

| | |
|---|---|
| TSSC | Thyristor Switched Series Capacitor |
| TSSR | Thyristor Switched Series Reactor |
| TVAC | Time Varying Acceleration Coefficient |
| TVT | Tangent Vector Technique |
| UPFC | Unified Power Flow Controller |
| VCPI | Voltage Collapse Proximity Index |
| VSI | Voltage Stability Index |
| VSR | Variable Series Reactor |
| WOA | Whale Optimization Algorithm |
| WSCC | Western Science Coordinated Council |

# LISTS OF SYMBOLS

| | |
|---|---|
| $\boldsymbol{V_{ci}}$ | bus *i* converter voltage magnitude |
| $\boldsymbol{\theta_{ci}}$ | bus *i* converter voltage angle |
| $\boldsymbol{V_{cj}}$ | bus *j* converter voltage magnitude |
| $\boldsymbol{\theta_{cj}}$ | bus *j* converter voltage angle |
| $\boldsymbol{V_{i}}$ | bus *i* voltage magnitude |
| $\boldsymbol{\theta_{i}}$ | bus *i* voltage angle |
| $\boldsymbol{Y_{ci}}$ | shunt converter admittance |
| $\boldsymbol{G_{ci}}$ | shunt converter conductance |
| $\boldsymbol{B_{ci}}$ | shunt converter susceptance |
| $\boldsymbol{S_{ci}}$ | bus *i* injected converter complex power |
| $\boldsymbol{P_{ci}}$ | bus *i* injected converter real power |
| $\boldsymbol{Q_{ci}}$ | bus *i* injected converter reactive power |
| $\boldsymbol{I_{ci}}$ | bus *i* injected converter current |
| $\boldsymbol{P_{i}}$ | bus *i* injected real power |
| $\boldsymbol{Q_{i}}$ | bus *i* injected reactive power |
| $\boldsymbol{P_{dci}}$ | bus *i* converter dc power |
| $\boldsymbol{P_{dcj}}$ | bus *j* converter dc power |
| $\boldsymbol{P_{dcLoss}}$ | dc real power loss |
| $\boldsymbol{P_{ci}^{spec}}$ | bus *i* specified control real power |
| $\boldsymbol{Q_{ci}^{spec}}$ | bus *i* specified control reactive power |
| $\boldsymbol{V_{j}^{spec}}$ | bus *j* specified control voltage |
| $\boldsymbol{V_{j}}$ | bus *j* voltage magnitude |
| $\boldsymbol{V_{ci}^{min}}$ | bus *i* converter lower limit voltage magnitude |
| $\boldsymbol{V_{ci}^{max}}$ | bus *i* converter upper limit voltage magnitude |
| $\boldsymbol{V_{cj}^{min}}$ | bus *j* converter lower limit voltage magnitude |
| $\boldsymbol{V_{cj}^{max}}$ | bus *i* converter upper limit voltage magnitude |
| $G_{ij}$ | admittance between bus *i* and *j* |
| $G_{ii}$ | bus *i* total admittance |
| $P_{ji}$ | active power flow from bus *j*-*i* |

| | |
|---|---|
| $P_{ij}$ | active power flow from bus *i-j* |
| $\boldsymbol{I_{cj}}$ | bus *j* injected converter current |
| $\boldsymbol{I_{ci}^{max}}$ | bus *i* converter current limit |
| $\boldsymbol{I_{cj}^{max}}$ | bus *i* converter current limit |
| $\boldsymbol{Y_{ij}}$ | line *i-j* series admittance |
| $\boldsymbol{\theta_{ij}}$ | line *i-j* series admittance angle |
| $\boldsymbol{\theta_{n}}$ | bus *j* voltage angle |
| $\boldsymbol{P_{ci}^{spec}}$ | bus *i* specified active power |
| $\boldsymbol{P_{ci}^{cal}}$ | bus *i* calculated active power |
| $\Delta\boldsymbol{P_{ci}}$ | bus *i* change in injected real power |
| $\Delta\boldsymbol{P_{cj}}$ | bus *j* change in injected real power |
| $\Delta\boldsymbol{P^{VSC}}$ | active power mismatch |
| $\boldsymbol{I_{ij}}$ | current through admittance $\boldsymbol{Y_{ij}}$ |
| $I_i$ | bus *i* injected current |
| $I_j$ | bus *j* injected current |
| $P_{ij}^{l}$ | line *i-j* active power flow limit |
| $w_p$ | real power weighting factor |
| N | penalty function |
| $k$ | bus number |
| $X_{ij}$ | line *i-j* reactance |
| $R_{ij}$ | line *i-j* resistance |
| $\alpha_{ij}$ | real loss coefficient |
| $\beta_{ij}$ | imaginary loss coefficient |
| $R_{dc}$ | dc line resistance |

# CHAPTER ONE
# INTRODUCTION

## 1.1 Background of the study

The evolution of power sector all over the world was monopolistic in nature due to economy of scale. The electric power industry has over the years been handled by these large monopolistic utilities that had an overall authority over all activities in generation, transmission and distribution of power within its domain of operation. Based on definite policies and standards, they handle the overall planning and operations of the networks, with sole aim of maintaining reliable and uninterrupted supply to the loads [1]. These utilities are the sole provider of electricity in their domains and traditionally, operational structure appeared to be extremely stable. Hitherto, two major ownership structure subsisted: vertically integrated privately owned and publicly owned, otherwise referred to as state owned monopolies, such as in European and some developing countries of the world [2]. This structural tradition remains effectively in force without agitations for integration or separation of component parts comprising generation, transmission, and distribution, or change of ownership and/or policies governing critical decision variables affecting the operations [3].

In late 1970s however, with many different reasons that ranges from political to purely economical, which are also dissimilar from regions to countries, many electric power networks and utility companies globally have changed their mode of operation from vertically integrated structured to open market systems. This open market structure is also referred to as deregulated, restructured and liberalized power sector in the context of this study. Majorly, the quest for liberation of electricity industry emanated from poor performance and unwillingness for additional capital investment on the part of government of Chile and other Latin American nations. The change in attitudinal ideology against state ownership of utility infrastructures was responsible for liberalization in United Kingdom, while dissatisfaction of nature of power sector monopolies coupled with dependence on complex regulations and control policies prompted United States of America to adopt deregulation. In the case of Eastern Europe, the need to embark on massive industrialization through private sector driven initiative, coupled with change of government, resulted into embracement of deregulation of power network [4],[5].

Accordingly, Chile was the first to introduce restructuring into her electricity sector between 1978 to 1983 [6]. England adopted restructuring in 1989/90, United States, Argentina, Norway and Sweden in 1992, Bolivia and Colombia in 1993, Australia in 1994, New Zealand in 1996, Panama, El Salvador, Guatemala, Nicaragua, and Honduras and Costa Rica in 1997 [6],[7]. This wave of restructuring rapidly spread to other countries in Europe, North America, South America, New Zealand, Australia, part of Asian and African countries. This stride also induced other countries in Latin America and by extension the rest of the world to embrace restructuring [8]. Over this period, the pace of metamorphosis in electricity sector reform has increased tremendously with more sophisticated approach in its implementation. Many countries ranging from large to small, from developed to developing have embraced and adopted liberalization to their electricity sectors. This deregulation was

precipitated in the industrialized countries by the pressure to reduce costs and hence tariffs, while simultaneously increasing the competitiveness in the markets [9].

Generally, some of the factors that culminated into power sector reform have been categorized into: (a) inefficient performance of state owned and operated electricity sector regarding high cost of operation, poor expansion of electricity access to entire populace and unreliability of supply, (b) financial constraints on the part of the state for required obligations including facilities expansion and maintenance, (c) unavoidable pressure to focus on other pressing obligations and expenditures leading to removal of incentives in power sectors and, (d) the desire for revenue generation through auctions of state assets in power sector [2],[10]. Although, the implementations of these reforms have some associated controversies initially and have not ended into precise desired results, however, the trend in public policy has continued to gather accolade for power sector liberalization. Besides, the rapid technological advancement in power network components and parts has contributed immensely to the new structural adjustment of the industry. Nevertheless, the success of deregulation depends on creation of competitive electricity market which will provide avenue for better motivations for operational cost control and for encouragement of innovation in power supply chain technologies [11].

This recent changes in the power system structure have led to much more complexity in its operation. Deregulation resulted in reorganization of vertically integrated energy sector into a decentralized sector where generation, transmission and distribution were not to be owned by a single entity but differently owned and controlled by several entities [12]. The open access granted free access of existing transmission facilities to any individual with appropriate license to inject/draw power at any point into/from the system. Hence, deregulation of components structure of power system unavoidably introduces a change in planning and operational procedures of transmission systems. Due to evanescence of erstwhile ancillary services domiciled in vertically integrated structure, deliberate special arrangement is necessary for its replication in a restructured network. Ancillary services which include; black start capability, spinning reserve, reactive power provision and voltage support are indispensable for transmission network operations but are not readily accommodated in energy tariffs thereby resulting into additional cost for sector operators [13].

The operation of power system networks become difficult for power evacuation and injection, due to this open access. This is because, in a deregulated power system, both the power producers and the consumers make use of the same transmission network for transactions purposes [14]. In this open market strategy, all the participants are profits conscious and tend to purchase the energy from the cheapest source, hence this resulted into various challenges. The development of power network to fulfil consumption demand resulted in an unplanned power transaction which force transmission lines to operate in the region of their thermal limits. This usually results into overloading of these corresponding lines, known as congestion which in turn leads to contingency, which affects power system transmission network reliability [15]. This is because, in a pre-restructured network, most power transactions existed between neighboring utilities and such will not be embarked upon unless jointly agreed that system economy and security are guaranteed in the overall interests [16].

### 1.2 Problem Statement

Power transmission network differs in form to other transportation systems where between source and destination, there is freedom of choice amongst alternate paths, and such that storage of goods and services can be adopted in place of an inhibited flow. In contrast, electric energy cannot be substantially stored and there is limitation to the choice of transmission flow paths between energy source and sink among the clusters of power network branches [16]. Transmission capacity is already compressed due to various factors, and this must now meet the new demands created by deregulation. These demands consist of power flows for which transmission systems were not designed, arising from both open access and sitting of new generation with little concern for transmission requirements [17]. Largely, the incessant entry and exit of generators from the grid to satisfy contractual terms which resulted from their inability to sustain a specified market share usually lead to network limits violations. The presence of large number of market participants with conflicting interests is also responsible for increase in unscheduled transactions with no historic operational data, while the proliferations of small distributed generators usually of renewable origins are another source of problems for deregulated network [4].

The process of power network operation with due consideration for limits bounds is very vital to network security and reliability. One of the attributes of traditional network structure is the operation with sufficient reserve margins. In a deregulated network, this operational safety margin has been compromised, leading to high probability of power outage [16]. Blackouts that were experience in some countries in Northern America, (United States and Canada, between year 2003 and 2004) and Europe are partly attributed to the restructuring of the power industry [17],[18]. Notwithstanding, the current operating practices are based on reliability criteria that were established in response to certain events in the 1960s [19]. An improved flow control will be of immense benefits because of the restrictions in instantaneous network transmission transfer capability. These limitations are mostly imposed by transmission line thermal limits, bus voltage limits and system stability limits at any time. Unless something is done to reduce congestion or increase transmission capacity, there may be possibility of more blackouts or other unwanted scenarios. Network manipulation must be done to adjust system limitations to encompass normal and probable contingency cases such that uninterrupted power operation will be sustained at all time. Hence, this study seeks as follows;

(a) The issue of transmission capability determination become a herculean task because of upsurge in power transactions, consequent of open access. This study, therefore, investigate various methods of transmission capacity determination and presents repeated alternating current power flow (RACPF) based on implementation of full alternating current power flow equation on repeated power flow approach of available transfer capability computation.

(b) The orthodox ways of building new generation stations and transmission infrastructures in a bid to expand power transmission network capability are both technically and economically restricted. Therefore, this study investigates and presents flexible alternating current transmission systems (FACTS) as a solution for deregulated and restructured network transmission capacity enhancement.

(c) More power flow is necessary for available transfer capability (ATC) improvement, but more power flow is synonymous to power losses and it is inescapable to regulate network voltage within the limits and simultaneously satisfy power balance equations. Therefore, efforts were made in this research study to concurrently enhance ATC of a deregulated network and implement power loss control, with due consideration for bus voltage deviation minimization as part of the objective.

(d) Deregulated network is characterized by numerous and mostly unplanned power transfer trading. This forces transmission lines operation in the region of thermal capability, making overloading of some heavily loaded paths unavoidable, which will lead to congestion and eventual contingency of such lines. Therefore, because of inadvertent occurrence of network contingency, consequent of highlighted issues, the problem of n-1-line outage contingency mitigation for a deregulated and restructured power systems is also achieved and presented in this study.

### 1.3 Motivation for the Research

The wave of power network deregulation and restructuring is blowing intensely, leading to accruing in challenges for network operators whose determination hitherto, is to ensure economy of power operation with utmost consideration for maintenance of system security limits. The traditional way of physical network expansion is facing a lot of setback due to issues such as right-of-way, environmental and high cost of power facilities. Meanwhile, the recent advancement in power electronics devices have made tremendous contributions to the urgency for network capacity enhancement, constrained with sustainability and reliability improvement, with due consideration for minimization of cost, through injection of supplementary controllability and flexibility of operation. This improvement has created a renewed interest in FACTS applications. Therefore, FACTS devices are becoming intrinsic parts of network systems, especially for power network performance improvement among many other applications. This study investigates and implements enhancement of network performance, with FACTS devices, in a deregulated and restructured power system.

### 1.4 Key Research Questions

(a) How can the transmission capability be appropriately assessed in a deregulated and restructured power network?

(b) How can the transmission capability be appropriately enhanced in a deregulated and restructured power network?

(c) How can the bus voltage profile of a deregulated and restructured network be improved?

(d) How can the power loss of a deregulated and restructured network be controlled?

(e) How can the power flow of a deregulated and restructured power network be improved?

(f) How can the contingency be appropriately mitigated in a deregulated and restructured power network?

### 1.5 Aim and Objectives of the Research

The aim and objectives of this study are as follows;

#### 1.5.1 Aim of the Research

The primary aim of this study is to enhance electrical power performance of a deregulated and restructured power system through investigation and determination of network performance and provision of an effective flexible alternating current transmission systems (FACTS) devices for improvement of transfer capability, minimization of bus voltage profile deviation, control of system power losses and mitigation of network contingency.

### 1.5.2 Objectives of the Research

The objectives of this study are as stated below;

(a) determination of transmission capability of power network in a deregulated and restructured environment;

(b) evaluation of best approach for identification of the most severe n-1 outage contingency using performance index methodology;

(c) investigation of operational comparison of two different FACTS (TCSC and SVC) devices for network performance improvement.

(d) investigation of effectiveness of different FACTS devices placement approaches for network performance improvement of a deregulated and restructured power network;

(e) presentation of sensitivity-based analysis for optimal placement of FACTS devices for network performance enhancement of a deregulated and restructured power network.

Furthermore, the objectives of this study are also to provide an affirmative answers to the research questions raised in subsection 1.4 above.

## 1.6 Limitation of the Research

This research is limited to investigation of transfer capability determination and its enhancement with SVC and TCSC devices. It also investigated network bus voltage profile and power loss of a deregulated and restructure power network during transfer capability determination as well as its enhancement. Besides, it implemented contingency mitigation with VSC-HVDC transmission system, in addition to network performance enhancement with this device. All these were carried out for various power transactions at steady state and n-1 network element outage contingency conditions and did not implement symmetrical and asymmetrical faults on test networks. This study did not focus on cost related issues regarding FACTS device installation and operation.

## 1.7 Research Methodology and Design

This study involves deregulated and restructured power network performance enhancement with FACTS devices. In order to achieve these, the following are the major steps followed.

(a) Detailed study of existing literatures on transmission capability determination was carried out.

(b) Thorough study of severe line outage contingency evaluation was also conducted.

(c) Arising from (a) above, available transfer capability (ATC) was determined and implemented using IEEE RT system.

(d) Arising from (b) above, an effective means of the most severe line outage contingency identification, through contingency evaluation studies was aslo presented using IEEE RT system.

(e) Studies were conducted on applications of flexible alternating current transmission systems (FACTS).

(f) Brief presentations of simple models of three types of FACTS namely, TCSC, SVC and VSC-HVDC transmission systems were carried out.

(g) Implementation of TCSC and SVC for ATC enhancement of deregulated network was carried out.

(h) Investigations of FACTS device placement approaches for ATC enhancement, bus voltage deviation minimization and power loss control of a deregulated network were carried out.

(i) A sensitivity-based analysis approach, derived from (h) above, was presented for FACTS placement purposes.

(j) The approach in (i) above was implemented for network performance improvement including power flow enhancement and contingency mitigation of a deregulated and restructured power network.

(k) The results obtained in the above various steps were presented, analysed and validated.

### 1.8 Significance of the Research

One of the consequences of electrical power deregulation and restructuring is the resultant competitive electrical power transactions. This results into a herculean task for power system operators in order to maintain a secured and economic power trading amidst system constraints and other bounded operating conditions. Enhancement of ATC becomes imperative in a bid to handle the upsurge in power trading because sufficient and adequate ATC are necessary for both competitive and economic power transactions. Therefore, this study presents a unique and innovative approach for ATC enhancement, bus voltage deviation minimization and power loss reduction concurrently, through application of optimized FACTS devices based on sensitivity analysis method. Besides, network performance enhancement as well as contingency mitigation of a deregulated and restructured power system was achieved through optimized VSC-HVDC transmission system incorporated into an ac network.

### 1.9 Contribution of the current study to knowledge

Initially, repeated alternating current power flow (RACPF) method, based on implementation of full ac power flow equation on repeated power flow approach of ATC determination, was successfully implemented in determining the ATC of a deregulated and restructured system in this study. The accuracy of RACPF method was established when compared with the results of previous work in the literature. Various network operating conditions ranging from normal, contingency, bilateral and multilateral transactions were investigated with this method. ATC has been established to decrease with increase in power transactions. It has also been established that least ATC occurs with contingency occurrence of multilateral transaction. With these investigations, the importance of ATC to market participants in a deregulated power system has been substantiated.

Evaluation of performance index (PI) methodology as a tool for contingency evaluation was done with a view to presenting the most suitable method in deploying PI for contingency problems. The investigation conducted has demonstrated the behavioral attributes exhibited by different approaches of PI. It is therefore established in

this study that the disturbance which resulted into lines overload did not necessarily cause bus voltage limits violations. Subsequently, voltage and real power indices should be treated differently in order to obtain a separate but meaningful contingency rankings using PI, because the duo have been proven to be distinctly dissimilar.

Applications of FACTS devices for enhancement of ATC for engaged bilateral, simultaneous and multilateral transactions were implemented in this study. The performance comparison of TCSC and SVC were also carried out, during enhancements exercise. TCSC maintained bus voltage magnitude for bilateral and simultaneous transactions but with slight voltage droop during multilateral trading. In contrast, SVC slightly improved bus voltage profile for all the transactions. The introduction of SVC contributed to total system real power loss minimization for all the transactions while that of TCSC had no significant minimization for bilateral and simultaneous dealings but rather increased total real power loss for multilateral transaction. Therefore, for transfer capability enhancement with voltage improvement and real power loss minimization in focus, SVC is more relevant.

Review of FACTS devices which revealed that optimal location and parameter settings are sine-qua-non to device performance was implemented in this study. Therefore, comparison among various analytical placement techniques were carried out to present the best. Subsequently, a universal method for FACTS optimal placement was developed based on total real power loss minimization approach, through amalgamation of FACTS device loss with the total system loss with the objectives of ATC enhancement, voltage profile improvement and active power loss minimization. TCSC was also modeled analytically just like SSSC for purpose of implementation of this method.

An optimization technique known as brain storm optimization (BSO) algorithm was proposed for optimum setting of FACTS devices for multi-objective problem involving ATC enhancement, bus voltage profile deviation minimization and real power loss regulation. BSO performance in comparison with particle swarm optimization (PSO) during the achievement of set objectives was presented here which suggested an advantage of former over the latter. It has therefore been verified that BSO algorithm is effective in solving FACTS allocation multi-objective optimization problems.

Investigation of VSC-HVDC transmission system embedded into ac network was also presented in this study. With the incorporation of VSC-HVDC transmission system in an ac network, an improvement in system performance has been recorded, therefore, HVDC based VSC transmission systems have the capacity to support and enhance system behavior especially during power transactions to achieve system reliability and security of a restructured network.

In the same manner, contingency control capability of VSC-HVDC system integrated into an ac network was investigated in this study. Here also, sensitivity-based approach was applied for placement purposes. The objective of using sensitivity analysis based on controlled parameters of VSC was discerned through

consideration for the impacts of shunt devices on network loss characteristics. However, an n-1 transmission line outage contingency was created based on the most severe ranked outage line. The incorporation of VSC-HVDC system in-between ac buses in a network minimized bus voltage profile deviation for steady state and restored violated bus voltage limits during contingencies. Power flow were enhanced during steady state and thermal limit violation occasioned by contingencies were adequately controlled. During bilateral, simultaneous and multilateral transactions however, the presence of this HVDC in the ac network not only damped the impactful effects of power transfers on network dynamics but also control both voltage and thermal limit violations as a result of associated contingencies. Therefore, VSC-HVDC system incorporated into ac network has the capacity to influence system dynamics and it stands a solution to problems of contingency especially in a deregulated and restructured power network.

### 1.10 Organization of the Thesis

The subsequent parts of this study are as organized as follows.

**Chapter One: Introduction**

Chapter one gives the background to the research, highlights the problem statements presents research motivation, and pinpoints key research questions. It also discusses aim and objectives of the research, defines the research limitation, talks about the significance of the research, describes methodology of the research, and presents the thesis structure.

**Chapter Two: Literature Review**

This chapter discusses the concepts of power network deregulation and restructuring. It presents the review of various methods for available transfer capability determination and reviews various approaches for implementation of performance index methodology for identification of most severe line contingency. It presents comprehensive review of flexible alternating current transmission systems (FACTS), as relating to their generation, types, configurations and connection types. Various deployment techniques and cutting-edge applications of FACTS controllers as related to this research are also described in this chapter. The concepts of high voltage direct current based on voltage source converter (VSC-HVDC) are also discussed with brief review of its applications. This review work in this context has published in a peer-review journal.

**Chapter Three: Research Methodology**

This chapter presents the two methodologies used in available transfer capability determination. Repeated alternating current power flow (RACPF) and alternating current power transfer distribution factor (ACPTDF) are herein discussed. Performance index methodology for evaluation of the most severe line outage contingency is also presented here. Modelling of three types of FACTS devices namely, static var compensator (SVC), thyristor controlled series compensator (TCSC) and VSC-HVDC transmission system are presented in this chapter. Besides, the analytical modelling of TCSC for its adaptations for application of sensitivity-based method of optimization is also highlighted. Particle swarm optimization and Brain storm optimization algorithms used for optimization of TCSC device are also presented in this section. The implementation of

sensitivity-based approaches for placement of TCSC and VSC-HVDC devices as derived in this research are equally presented.

**Chapter Four: Network ATC Determination and Contingency Evaluation**

Available transfer capability of a deregulated and restructured network is presented here, using RACPF method. Evaluation of severity of line outage contingency is conducted in this chapter for clarification of misapplications of performance index (PI) methodology in identification of most severe outage contingency. Prior to this time, researchers have been applying the method indiscriminately using real power PI, voltage PI, reactive power PI, combination of any two of them and combination of all of them. Two published IEEE conference proceedings emanated from the results of this chapter.

**Chapter Five: Facts Devices Enhancement of Available Transfer Capability**

This chapter presents the enhancement of available transfer capability of a deregulated and restructured power network with two different types of FACTS. In the first section of this chapter, efforts were made to compare performance of SVC and TCSC for objectives of ATC enhancement, bus voltage profile deviation minimization and power loss control. In the second section of same chapter, different approaches for TCSC device placement were compared for the same objectives. The approaches considered are total real power loss, real power performance index, real power loss sensitivity with respect to line reactance, power transfer distribution factor (PTDF), line thermal limitation, available transfer capability (ATC) value, and least bus voltage magnitude. The contents of this chapter have been published. Two published IEEE conference proceedings emanated from the work presented in this chapter.

**Chapter Six: Optimization of thyristor control series compensator with Brain Storm Optimization Algorithm (BSOA)**

In chapter six, BSOA is engaged for the optimum setting of TCSC devices for enhancement of ATC of a deregulated electrical power system network. ATC enhancement, bus voltage deviation minimization and real power loss regulation are formulated into multi-objective problems for FACTS allocation purposes. ATC values are obtained for both normal and n-1-line outage contingency cases and these values are enhanced for different bilateral and multilateral power transactions. Obtained enhanced ATC values for different transactions during normal evaluation cases are then compared with enhanced ATC values obtained with Particle Swarm Optimization (PSO) set TCSC technique under same trading. The findings in this chapter has been accepted for publication in peer-review journal at the time of this thesis preparation.

**Chapter Seven: Sensitivity Based Approach for Thyristor Control Series Compensator Optimization**

In this chapter, a sensitivity based technique is developed for optimization of TCSC location in power network system. Here, FACTS device loss was incorporated with the general loss equation for the determination of optimum location for device placement in a deregulated power networks, with objectives of ATC enhancement, bus voltage profile improvement and loss reduction. A detailed mathematical model in terms of circuit system parameters is presented based on FACTS loss amalgamation approach. Like previous chapter, TCSC is

considered for simulation and analysis because of its capability to control active power among other parameters. The TCSC location is established based on analysis of sensitivity factors obtained from partial derivatives of the resultant loss equations (including FACTS) with respect to control parameters. ATC values are obtained using alternating current power transfer distribution factor (ACPTDF) method and with TCSC in place, these values are enhanced for different bilateral and simltaneous power transactions. The content of this chapter has been published in peer review journal.

**Chapter Eight: Network Performance Enhancement with High Voltage Direct Current Transmission Systems**

This chapter presents the results of an investigation and analyses of the capability of voltage source converter (VSC) based high voltage direct current (HVDC) transmission system in enhancing power network performance. A sensitivity-based technique of optimal location as presented in chapter seven was applied for incorporation of VSC-HVDC transmission system in this chapter. This placement is achieved with recourse to magnitude of injected voltage and control angle variables of the device through its active participation in total system loss derivatives. Performances of VSC-HVDC based transmission system during different power transfers resulting from bilateral and simultaneous transactions were observed. Bus voltage deviation minimization and power loss control involved in these various transactions are presented and analysed. The outcome of the research presented in this chapter is under consideration for publication at the time of compilation of this thesis.

**Chapter Nine: Contingency Mitigation with High Voltage Direct Current Transmission System**

This chapter presents the investigation of high voltage direct current (HVDC) based on voltage source converter (VSC) for power network contingency mitigation purposes. An optimized VSC-HVDC transmission system is applied for mitigation of bus voltage and line thermal limit violation as a result of n-1-line outage contingency occurrence during bilateral, simultaneous and multilateral transactions. Line contingency evaluation through real power performance index (RPPI) as earlier presented in chapter four was adopted for severe contingency identification purposes. Also as presented in chapter seven and as adopted in chapter eight, optimization of VSC-HVDC system was achieved through statically developed sensitivity-based analysis of VSC control parameters, while its performance for both steady state and contingency conditions are verified on IEEE standard network. The work presented in this chapter has been published in a Q1 peer review journal.

**Chapter Ten: Summary, Conclusion, Recommendations and Future Research**

The summaries of the findings of this research work are presented in this chapter of the thesis. The chapter also presents the conclusions that were drawn consequent these findings. Therefore, recommendations were made, and future research directions were also suggested in this chapter. Lastly, the succeeding Appendices contain IEEE bus systems and network data records as used in the study.

# CHAPTER TWO
# LITERATURE REVIEW

## 2.1 Introduction

This chapter undertakes the review of the literatures in relation to the concepts of this research study. It briefly discusses the ideas of electric power sector deregulation and restructuring. This power sector liberalization has changed the dynamics of network operation in relation to power system reliability, stability and security. Consequently, it has resulted into network operational challenges, which for the purpose of this study, are narrowed and restricted to available transfer capability (ATC) problems and contingency management. Therefore, the review of previous work on these issues are carried out in this section. Prior to the discussion on contingency mitigation, a review of performance index methodology of contingency evaluation is presented for identification of the most severe contingency line outage. Having recognized flexible alternating current transmission systems (FACTS) as an integral part of future power network operations especially for ATC enhancement and contingency mitigation application, a comprehensive review of FACTS devices is also conducted in this section. Reviews on applications of FACTS involving power flow control, contingency mitigation, voltage and power loss control are carried out. Besides, for power network to cope with upsurge in power demand consequent of deregulation however, the review of existing methods of ATC enhancement is also presented.

## 2.2. Power system network deregulation and restructuring

The evolution of power system all over the world was through monopolistic vertical integration with either highly regulated policies or ownership credited to the states. Here, all the functional components of power supply involving generation, transmission, distribution and other ancillary services are embedded within the jurisdiction of these electric utility companies [20]. However, with wide varying performance of these highly controlled monopolies across different countries, these companies have the de facto enfranchisements on all the activities regarding energy trading for residential, commercial as well as industrial consumers in the region of their geographical network coverage [1].

Thereafter, lately in 1980s, the experts in power sector including policy makers and members of academia unanimously agreed that energy production process should be undertaken through competitive and structured markets. It was foreseen that functionally separation into independent functional units of market structures erstwhile and traditionally undertaken by vertically integrated companies will create room for competitiveness, effectiveness and sustainability in energy markets [1],[10],[21],. However, due to these economic and efficiency reasons, the vertically integrated utilities are being deregulated globally [1]. As introduced and stated in chapter one, Chile was the first country to apply restructuring to her power sector between year 1978 and 1983 [22]. England adopted restructuring in 1989, United States in 1992 and this rapidly spread to other countries in Europe, North America, South America, New Zealand, Australia, part of Asian and African countries. This pace also encouraged other countries in Latin America and by extension the rest of the world to embrace

restructuring [8]. Fig. 2.1 [23] presents a simple pictorial view of both the vertically operated network and deregulated power networks. As shown in the figure, many components of the traditional power architecture have been structurally replaced and new functional unit incorporated in the transformation process. Generation, transmission and distribution units metamorphosized into generation companies (GENCOs), transmission companies (TRANSCOs) and distribution companies (DISCOs), with introduction of independent system operators (ISOs) and independent power producers (IPPs).

The occurrence of deregulation has transformed the practice of power transfer processes and has grossly increased power transfer between two areas. Therefore, there is a renewed interest and a regenerated attention in power industry, as a result of this new alteration in structural operations of power networks. Consequently, the operation of power network becomes difficult because of unhindered access brought about by deregulation [3].

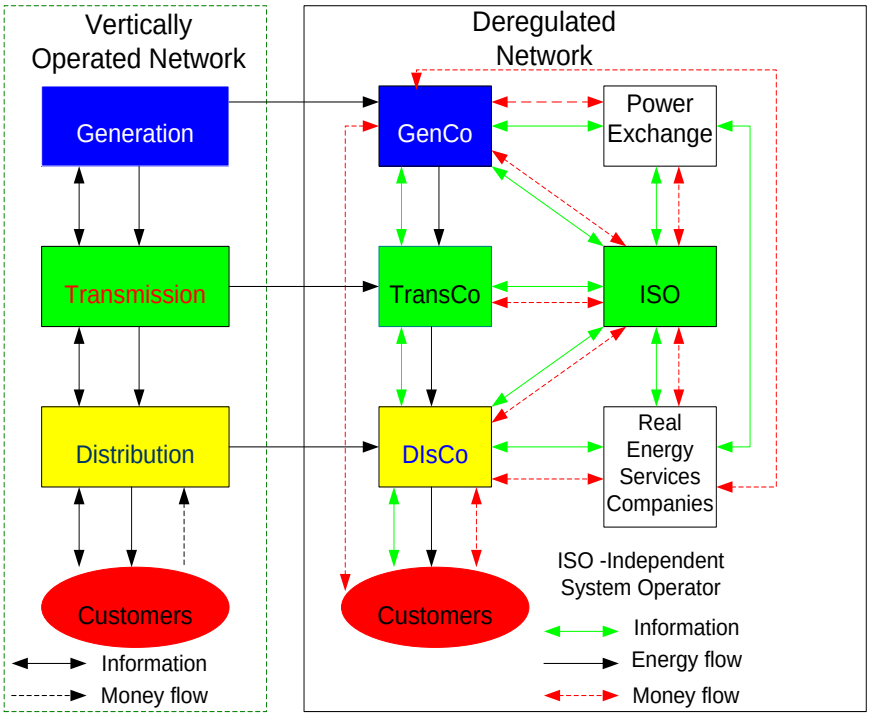


**Figure 2. 1: Structure of vertically operated network and restructured power system**

### 2.3 Review into ATC determination

Transmission of a very large quantum of power over a very long distance is a sine qua non for its reliability, security and economy of scale [24]. Nevertheless, there is limit to the maximum power that can be transferred over transmission lines due to thermal limit, voltage magnitude bounds, and security constraints [14]. In a deregulated and restructured environment, all power transactions take place over the same transmission network and due to economic reasons, market participants compete among themselves to purchase power from remote generators with the lowest generation costs [25]. When numerous power transactions are ongoing in market like this, and because of unplanned power transfer trading, there is tendency that transmission lines will be operated in the restrictions of their thermal capabilities. Therefore, overloading of some heavily loaded paths

will lead to congestion and eventual contingency of such lines [15]. Hence, for the market players in a deregulated market, values of ATC are cardinal pointer in making decisions. ATC perfectly depicts the transmission network's physical and system status as well as limits [25]. ATC of a deregulated network is an indication of transferrable quantity of power from one region to another in a network, with consideration for constraints [6]. Values of ATC are very crucial for transmission companies in indicating available transmission paths, by furnishing the generation and distribution companies the same information for power transaction purposes.

In determination of ATC, ac power flow method which was developed in MATLAB software environment was used for estimation of ATC in [6], where IEEE 30 bus network was adopted for investigation. In their study, the authors examined transfer capability of the test network under various loadings and different lines as well as generator outage conditions. A technique that employed optimization and Newton Raphson (NR) load flow called pattern search optimization based on NR power flow technique was used in [12]. Here, the power flow equations were formulated into maximization problem with both equality and inequality constraints. In the implementation of ATC of IEEE 24 bus network, an assumed value of capacity benefit margin (CBM) was adopted while transmission reliability margin (TRM) was not considered in estimation. This is also a challenge for accuracy of ATC values presented and besides, this method is complex as it involves a lot of objective functions to be minimized. Three methods comprising network response, network flow and linear sensitivity were used for ATC computation in [24]. The author implemented the determination of ATC for Bangladesh power system based on formulation of three mentioned network models in their work. Notwithstanding, these methods considered thermal constraints only, which is not sufficient for network stability. Linear programming based optimal power flow (OPF) for determination of ATC and ac power transfer distribution factor (ACPTDF) for determination of marginal costs for multi area system were implemented in [14]. These were implemented through multi-area sectionalization of the test system at both normal and contingency cases. Although, authors argued in their work that OPF made use of all possible regulating factors to reduce operational cost and reveal financial information significantly, however, this approach also involves problem formulation and linearization which make the method a complex one.

Direct current power transfer distribution factor (DCPTDF) method which is based on dc load flow for ATC estimation was used in [25]. In this work, ATC of IEEE 6 bus system was verified under normal and single element outage contingency cases. This method is quick to apply because of the assumptions involved in its formation preparation and calculations. Notwithstanding, the assumptions in equation formulation in this method have compromised the integrity of the results obtained. DCPTDF, ACPTDF and repeated power flow (RPF) methods were used for the calculation of ATC in [26]. Authors implemented their work on two types of network with different bilateral transactions. Based on the comparative results of both IEEE 6 and 14 bus systems, authors were able to further establish that DCPTDF is inaccurate and that though, ACPTDF gives better accurate result, it is more complex to implement. The results obtained for few transactions conducted indicate the accuracy of RPF over all other methods. DCPTDF, OPF, continuation power flow (CPF) and RPF

methods of deterministic load flow were used in [27] and [28]. In their works, authors in [27] implemented the investigation on IEEE standard test systems through sectionalization of the test systems into three, in order to obtain inter-area-ATC of the system while authors in the latter utilized Indian 246 system for their studies. The authors concluded with the fact that DCPTDF is fast but inaccurate, OPF incorporates a lot of complex constraints and that CPF cannot be used in real-time.

Linear sensitivity based DCPTDF was implemented in [29], where the estimated rate of change of line flow to that of generation in the network is computed from dc load flow. A comparative estimate using ACPTDF approach was implemented simultaneously in the same article. However, just as experienced in the previous work, ACPTDF method is complex, while DCPTDF is also inaccurate because of the dc load flow equations employed. Artificial neural networks (ANN) based method was used to evaluate ATC in [30]. This method can be used in real time but it involves many layers, requires data generation training, data normalization and testing, thereby making it complex to implement. Performance comparison between three heuristic algorithms namely GA, PSO, FA and generalized algebraic modelling system software (GAMS) were investigated for ATC determination in recent work implemented by the authors in [31]. Efforts were made to compare the performance of GAMS implemented through optimal power flow approach and ATC values obtained using other heuristic algorithms through same method. The former method resulted in better ATC values than the latter for normal case while no significant disparities observed for the two methods during contingency conditions. These heuristic algorithms and GAMS were used for solving optimal power flow problems of IEEE 24 bus reliability network with ATC determination in focus. However, this process involves a lot of parameterization, computations and coding which resulted in complexity of application of this approach.

Therefore, RPF which was found to be more accurate for ATC determination was later adopted and modified into repeated alternating current power flow (RACPF) through the implementation of full ac power flow using NR power approach for the first sets of ATC determination exercise in this study. Having established the accuracy through RACPF approach, ACPTDF method was later implemented for ATC determination and enhancement in the succeeding chapters.

### 2.4 Performance index (PI)

Evaluation of network reliability becomes major interest of power system transmission planners and operators because system reliability is the critical guarantor of steady power supply [32]. This is because, the occurrence of unscheduled and multiple trading due to liberalization will lead to overloading of some heavily loaded transmission paths which will aggravate the situation of congested network member and lead to eventual contingency of such component as earlier highlighted [15]. Contingency evaluation, which is synonymous to evaluation of network reliability intends to verify network's reliability standards especially in the event of inadvertent but urgent outages. Up till now, an n-1 criteria which necessitates that system endures an outage of singular network component member is in vogue and is being widely deployed in power operations [33]. However, as reported in the previous paragraphs, it was observed that some authors implemented an n-1 outage contingency but rather indiscriminately, without proper identification of the most severe contingent element.

Identifying severe critical line for implementation of n-1 line outage contingency becomes an issue because of network behaviors and responses especially when deploying performance index (PI) methodology among others.

One of the contingency ranking methods in use is performance index (PI). PI deals with the deviation of the system variables from their rated values. This makes it suitable for relative contingency evaluation because contingencies are ranked in line with response of PI to the change initiated by same contingencies. As a build up to similar work earlier carried out by Puttgen in University of Florida in 1976, Ejebe and Wollenberg in late 70's developed this approach for ranking and selection of contingency [34]. In their work, an algorithm was presented for classifying contingency in order of hierarchy, using active power and voltage with consideration for generators reactive power limits. However, power systems behaviours based on the specified contingency rank were not evaluated by the authors. Many authors have since adopted this approach in different ways for contingency ranking. The use of voltage PI was employed for contingency ranking of power network in the work implemented in [35]. Here, authors emphasized the need to optimize weighting factors to eliminate poor ranking effects.

Voltage fused with reactive power PI was applied for contingency screening and ranking in another work conducted in [36]. This was to ensure reactive power limit control as well as the voltage limit control of the network. The investigation which was implemented using fast decoupled load flow equations presented 249 possible outage contingency conditions for tested IEEE 14 bus system through and n-1 and n-2 network elements outage evaluations. However, these authors did not consider the effects of line power flow limits in their various rankings and besides, the post contingency evaluation of network system based on the rankings was not investigated. In the contingency ranking carried out in [37], real power PI was used for ranking and subsequent placement of interline power flow controller (IPFC) in a bid to investigate the performance of IPFC on network system. This method did not consider the effects of both voltage limits as well as reactive power control on the network system, having limited the evaluation to severity based on thermal effects alone. The network response to incorporation of IPFC was studied as compared uncompensated system vis-à-vis bus voltage profile and power flow in the same work. Similarly, real power PI was used for ranking in another work implemented in [38], where authors used the ranking for the placement of thyristor controlled phase angle regulator (TCPAR) in order to study its effects on power flow. This method, however, did not consider the effects of voltage magnitude bounds and reactive power enforcement on the network.

Sekhar and Mohanty [39] implemented contingency ranking of simple network system using real power and voltage PI methods. Authors evaluated the overall severe ranking, used in severity selection, through summation of the resultant indexes from the two approach, but without consideration for reactive power influence. This approach formed the basis for the contingency ranking in another work by authors in [40]. However, in their presentations, IEEE 5 and 6 bus networks were used for the analyses which was realized through full ac power flow equations. Ethiopian electric power system vulnerabilities were presented in [41], having identified the contingencies based on real power and voltage PI rankings but without reactive power control consideration.

Authors in [34] and [41] independently considered both the real power and voltage PI values in their ranking. However, PI computations method adopted differs in that authors in [41] did not consider the influence of generators reactive power limits on the bus voltages in their implemented work unlike the authors in [34]. It was therefore gathered from applications of PI methodology as reviewed that its diverse approach of implementation required further investigation for succinct clarifications to prevent mis application and for reliance as well as reliability of the concluding judgement on the subject matter. This issue was therefore dealt with in a clear manner as reported in chapter four of this thesis in order to unravel mystery behind PI methodology application especially for severe contingency raking purposes.

## 2.5 Flexible alternating current transmission systems (FACTS)

Flexible alternating current transmission systems (FACTS) deployments and applications are on the increase in modern day power network systems because of their advantages over conventional ways of power network physical expansion. FACTS devices have potency to enhance ATC, reduce power loses and stabilise network systems [42]. The need to enhance ATC was borne out of upsurge in power transactions consequent of open access created by deregulation and restructuring. According to [43], adequate ATC is required for an economic power transaction while its sufficiency is needed for a competitive electricity trading. Therefore, a comprehensive review of FACTS controllers with their various applications is carried out in this subsection. FACTS background alongside different techniques of deployments, leading to various applications and performance of these devices, hitherto organized structurally based on target objectives are also explored, presented and discussed. Summarily, this subsection provides an overview of the background, topological structures, deployment techniques and cutting-edge utilization of FACTS controllers.

### 2.5.1 The need for FACTS utilization

The quest for green and emission free energy has led to rapid development of renewable energy sources globally. This pursuit is partly due to concern for depletion of fossil energy fuels and largely to debilitating and detrimental impacts of these conventional energy sources on the environment. Incorporation of renewable energy into the grid in form of distributed energy resources are being facilitated by the ongoing power sector deregulation and restructuring [1],[20],[44]. As parts of its attendant benefits however, issues of system stability, security and reliability among others are the major challenges of power system network operation in a restructured power system [45]. This is because, there is a reduction in reactive power backing, hitherto being provided by the generation subsystem consequent of eradication of incentives for provision of this functional potentialities [43]. Therefore, sustainability of system security in the wake of growth power transfers, consequent of open access becomes increasingly herculean task [46].

Implementation of FACTS controllers for the management of both power transmission and distribution systems is evolving because of the limitations imposed by conventional methods of network expansions [47]. Economic and technical factors involving high cost of procurement of power network materials, environmental consideration, right-of-way, stringent regulations and other issues are some of these major restrictions regarding

physical network structure expansion [48],[49],[50]. In order to surmount these restrictions, FACTS is therefore intrinsically becoming parts of modern-day power system networks.

### 2.5.2 FACTS description

FACTS devices are applied for improvement of network performance of a deregulated and restructured network in this study; therefore, this section briefly discuss its concepts. FACTS can be defined as alternating current transmission systems that combines power electronic enabled regulators to heighten power transfer capability and its control [50]. The concept of FACTS was introduced to technical environment in 1984 when Hingorani invented the first series connected controller which was demonstrated by Siemens in California [51]. Although, static var compensator (SVC) for control of voltage which was commercialized by General Electric in 1974 and by Westinghouse in Minnesota in 1975 had been first established in Nebraska [51],[52], FACTS ingenuity was to enhance transmission line power transfer capability and for appropriate power flow control [43]. The capability of FACTS to control current, voltage, impedance (series and shunt), phase angle (current and voltage) and various damping frequency oscillations unfolded ways for these diverse opportunities [51].

#### 2.5.2.1 Classifications of FACTS

FACTS are classified into four groups in this study depending on their evolution, the technological characteristics and control modalities into first, second, third and fourth generations [53].

**(a) First generation**

FACTS in this group are described as thyristor based devices that used thyristor coupled with gate controlled firing system, typically silicon control rectifier (SCR). These devices have limited applicability in the range of power electronics, and they act like element whose impedance is controllable [54]. Devices in this group include SVC, thyristor controlled static compensator (TCSC), convertible static compensator (CSC) and thyristor control phase angle reactor (TCPAR) [55],[56].

**(b) Second generation**

Devices in this group make use of power electronics with turn off ability e.g gate turn off (GTO), insulate gate bipolar transistor (IGBT), integrated gate commutated thyristor (IGCT) etc. These devices based on converters are typically current/voltage sources [56]. In other words, the incorporation of later developed semiconductors with both ignition as well as extinction controllability in these devices differentiates them from the first generation types. Their advantage over first generation include size, speed, quantum of harmonic generation, flexibility, reactance ratings, capacitor size among others [43]. Another major difference between these two FACTS generations are reactive power generation and active power exchange with connected system. The device in this category include static synchronous compensator (STATCOM), static synchronous series compensator (SSSC) and unified power flow controller (UPFC) among others, derived from SVC, CSC and TCPST respectively [55], [57],[58].

**(c) Third generation**

The development of independent capability control of multiple network parameters consequent of advanced technological concepts led to the FACTS in this generation. FACTS devices in this group include but not limited to interline power flow controller (IPFC), generalized unified power flow controller (GUPFC), and hybrid power flow controller (HPFC) [56], [59].

**(d) Fourth generation**

This is the generation of distributed FACTS (D-FACTS) where the problems arising from GTO thyristors such as forced commutation, uncontrollable switching losses and modulation, resulted into development and practical applications of FACTS into distribution section of the network, hence the name D-FACTS [60]. Some common types of FACTS in this group are distributed STATCOM (D-STATCOM), distributed static series compensator (DSSCs), distributed thyristor controlled series compensator (D-TCSC), etc. [61],[62],[63].

#### 2.5.2.2 Categories of FACTS

Based on connection, FACTS controllers are categorized into four groups, namely Series, Shunt, Series-Series and Series-Shunt controllers [51],[55],[64],[65],[66]. These categories are explained below.

**(a) Series controllers**

These controllers are connected in series with the power line and thereby injecting voltage in series with the line as a result of reactive power they supplied or consumed. They include TCSC, SSSC, etc.

**(b) Shunt controllers**

They also consume or supply reactive power as they are shunt connected, thereby injecting current, at the point of connection into the system. STATCOM and SVC are examples of these controllers.

**(c) Combined series-series controllers**

These controllers balance real and reactive power through the connection of the inherent dc terminals. They could either be coordinated controlled separate series controllers or unified controllers. Examples are IPFC, thyristor controlled voltage reactor (TCVR), thyristor controlled voltage limiter (TCVL) etc.

**(d) Combined shunt-series controllers**

Controllers in this group could be coordinated controlled separate shunt and series controllers or unified controllers. Current and voltage injection through shunt and series part of the controllers make active power exchange possible through power linkage. These controllers include thyristor controlled phase shifting transformer (TCPST), UPFC.

Table 2.1 summaries the classifications and categories of FACTS for a clearer presentation, while basic structures of some of these controllers are depicted in Fig. 2.2 [48],[51],[55] – [63].

Table 2. 1: Summary of classifications and categories of FACTS controllers

| FACTS | Series | Shunt | Series-Series | Shunt-Series |
|---|---|---|---|---|
| **First Generation** | TCSC, CSC, TSSC, TCSR, TSSR, | SVC, SVS, SVG/A, TCR, TSC, TCBR, TCVL, TSR | | TCPST (TCPAR), IPC, TCVR |
| **Second Generation** | SSSC | STATCOM, SSG, SMES, BESS | | UPFC |
| **Third Generation** | | | IPFC, GIPFC | GUPFC, HPFC |
| **Fourth Generation** | D-TCSC, D-SSC | D-STATCOM | D-IPFC | D-GUPFC, D-HPFC |

### 2.5.3 FACTS devices incorporation and placement techniques

In order to enhance the target network system performance and for optimum economic advantages, optimal location and parameter settings of FACTS devices are of utmost importance. A survey of various existing placement techniques summaries the methodologies into four groups namely; Analytical, Optimization, Artificial Intelligence and Hybrid Artificial Intelligence [67].

#### 2.5.3.1 Analytical technique

This technique is also referred to as conventional, sensitivity and numerical method. This technique is computational efficient but in the event of non-inclusion of nonlinearity of power flow equation in the model, it may impacts on the accuracy of the outcome result [68]. This method lacks the capability to simultaneously handle both the optimal position and parameter settings of FACTS devices, but efficient in resolving either of the two independently [69]. Various analytical methods include modal analysis, index analysis, eigen-value based, eigen-vector analysis, residue based, sensitivity-based method, loss index etc [55],[70],[71],[72],[73], [74].

#### 2.5.3.2 Optimization technique

This method is known for efficient convergence attributes although, there is an issue with the management of optimization constrained problems [75]. In this category are NR optimal power flow algorithm, linear, penalty successive linear, nonlinear, mixed integer nonlinear, dual, stochastic dual, dynamic, and sequential quadratic programming, ordinal optimization, exhaustive search algorithm, interior-point method, OPF based method, biogeography based method, gradient search and continuation power flow among others [55],[76],[77],[78], [79],[80].

#### 2.5.3.3 Artificial intelligence technique

This method is also referred to as heuristic or meta-heuristic approach and is about the commonest in usage of all the methodology in recent times [69]. Techniques in this category are stochastic and optimization algorithms that are based on population with efficient capability in handling multi-objective, multimodal and constrained discrete problems [63],[81]. Meta-heuristic algorithms are described as generic and search method capable of solving, combinational, complex and challenging problems [82]. In this group are; Fuzzy logic (including FCN,

CWFR), genetic algorithm (GA), non dominating sorting genetic algorithm two (NDSGA-II), artificial neural network (ANN), general regression ANN (GRANN), plant growth simulation algorithm (PGSA), body immune algorithm (BIA), particle swarm optimization (PSO), modified PSO, discrete PSO, phasor discrete PSO, whale optimization (WOA) ant colony search (ACS), artificial bee colony (ABC), and modified ABC among others [63],[70],[79],[83],[84],[85],[86],[87],[88]

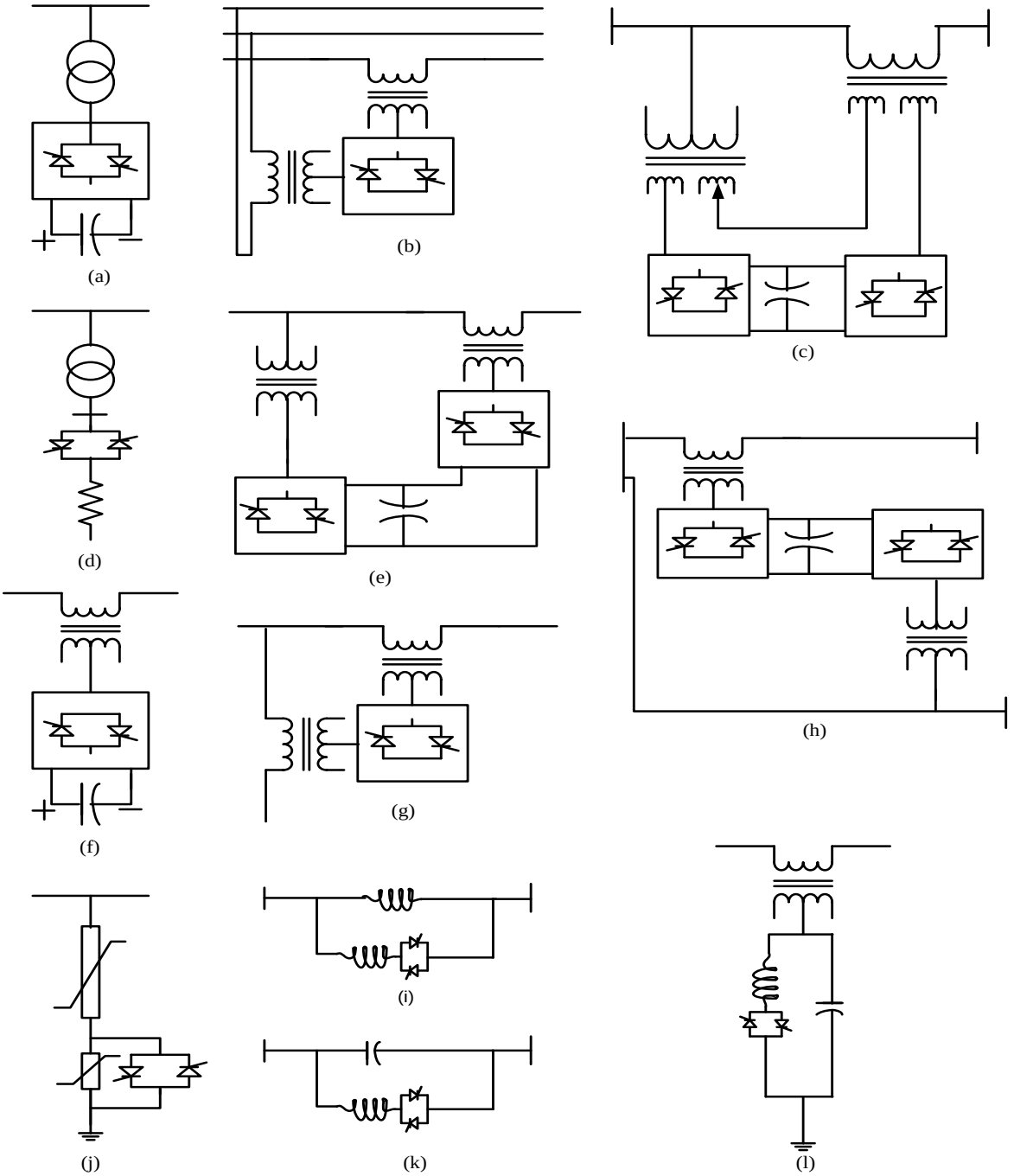


**Figure 2. 2: Basic Structures of (a) STATCOM, (b) TCPST/TCPAR, (c) OUPFC, (d) TCBR, (e) UPFC, (f) SSSC, (g) TCVR, (h) IPFC, (i) TCSR/TSSR, (j) TCVL, (k) TCSC, (l) SVC**

#### 2.5.3.4 Hybrid artificial intelligence technique

This basically involve mixing any two or more of the above methods in the device location and parameter settings. Analytical and optimization or analytical and artificial intelligence techniques could be used together in FACTS placement. This usually results into fast and efficient computational period [89],[90],[91],[92]. However, the definitions and characteristics including detailed descriptions, importance, advantage, disadvantages as well as various applications of these various techniques are contained in the literatures [82],[93],[94],[95],[96],[97],[86],[98],[99],[100],[101],[102],[103].

### 2.5.4 Benefits of applications of FACTS controllers to power networks

FACTS devices play important roles in various power applications ranging from active and reactive power flow control, voltage regulation, improvement of power quality, harmonic mitigation, real and reactive power loss control, transient and steady stability improvement, oscillation damping, dynamic stability among others [104],[105]. This segment presents the review of diverse benefits and applications of FACTS controllers as related to this work. These benefits are as highlighted while FACTS applications to power flow control, contingency mitigation, voltage control and power loss regulations, multi objective application of FACTS involving more than one of these highlighted sub-headings as well as ATC enhancement, formed bulk of the discussions because these are the main focuses of this research thesis.

#### 2.5.4.1 Power flow control

This study undertakes power flow enhancement capability of FACTS in the latter chapters of this study, hence the need to present various previous works in this area. Power flow control capability of FACTS devices was implemented in [106] where GIPFC was engaged. In their work, authors implemented voltage source converter based on 48-pulse neutralized harmonic gate turn off converter (GTO) for the device synthesis. Authors demonstrated the capability of GIPFC to control real power flow simultaneously on more than one transmission lines without adverse effects on the adjacent line as compared UPFC whose line power control is limited in this capacity. Three devices including SVC, STATCOM, and UPFC were used for power flow control in another work implemented by [107]. In this work, three different location namely sending, receiving and middle of the designed transmission line were the choice for the device location in the investigation. It was observed from the analysis that the devices performed better at the middle of the line for the compensated line and besides, the results indicated that power flow control of the compensated networks was better than that of the uncompensated ones where SVC took the lead in term of performance.

Authors in [108] presented the performance of the coordinated utilization of SVC and TCSC for management of power flow of IEEE 14 bus network. The device was incorporated based on network loss and least bus terminal voltage at base case, while PSO was used for devices parameter settings. Network performance based on the presence of each device was investigated independently for power flow control. However, the climax of the investigation was achieved through coordination of the two devices for network response during faults occurrence. The analysis revealed good response to three-phase to ground fault through proper coordination of

SVC and TCSC devices. The network loadability improvement through FACTS, formed the basis of the investigation conducted in [109]. With this objective in focus, formulation of three devices namely TCSC, TCPST and STATCOM was based on the best device, best location, and the best device setting. All these were implemented to study the appropriate budget which will result in optimal device application. It was observed in their study that increase in budget will increase the device size, which will in turn lead to increase in the system loadability. It was concluded that nonlinear relationship exists between the budget and system loadability because at a point beyond the equilibrium, an increase in budget will no longer lead to increase in network loadability. In another work by Dash *et al.*, Ant Lion-Moth and Flame-Salp Swarm hybrid metaheuristic optimization algorithm was used for optimization of TCSC, UPFC and SVC devices to improve network system loadability [110]. The use of optimization algorithm was to save cost through optimal location of the devices which were implemented singularly and combinatorial on IEEE 6 and 30 bus systems. It was observed that Salp swarm algorithm performance was more beneficial compared others through network loadability recorded when engaged. A sensitivity optimal placement approach based on the relationship between changes in load reduction and changes in series control variables of UPFC was implemented through optimal load flow formulation [111]. An investigation conducted on 14 and 30 bus IEEE networks through this formulation and optimization procedure resulted into achievement of the desired objective of load curtailment minimization.

#### 2.5.4.2 Contingency management

The review of works in the area of contingency management is of utmost value to this research work because, efforts were made in the latter chapters of this research work to mitigate network contingency using FACTS devices. Placement of TCSC and STATCOM were demonstrated in [112] for power flow control and voltage regulation, especially to relieve congestion. This was demonstrated on IEEE 14 bus system in MATLAB software environment. The location of TCSC was achieved through loss sensitivity obtained by derivatives of reactive power loss with respect to line reactance while that of STATCOM was achieved by minimum loss consideration at base case, and concurrent observation of voltage limit violation, with moderate cost evaluation. The result presents power flow redistribution for the compensated network and this implies the possibility for congestion relieve in case it occurs. In their work, authors in [48] formulated placement approach based on sensitivity for achievement of transmission line overloading reduction using UPFC, OUPFC and IPFC devices. Although, an example with network demonstration of an overloading removal was not presented, however, authors established that optimal placement of FACTS devices will surely relieve network congestion.

Network contingency was alleviated with SVC in another work implemented in [113]. Authors formulated optimal power flow for network system, while artificial bee colony (ABC) optimization algorithm was used for SVC parameter setting. The occurrence of bus voltage violations resulting from contingency was mitigated with presence of SVC. TCSC, SVC and UPFC were incorporated into the network with meta-heuristic algorithm for the purpose of congestion minimization while considering power loss and operational cost reduction at same time [52]. The investigation conducted through optimal power flow was implemented with gravitational search

optimization algorithm for device placement. This algorithm whose performance was compared with genetic algorithm, differential evolution, and particle swarm optimization algorithms when implemented on IEEE 30 and 57 bus resulted into better results for the target objectives of congestion management, loss reduction and eventual operational cost reduction.

#### 2.5.4.3 Voltage control and power loss reduction

In this section, the review into capability of FACTS for voltage profile control as well as network power loss reduction is undertaking. The performance of dynamic voltage restorer (DVR) and D-STATCOM were investigated on network system, for voltage sag mitigation purposes [114]. These devices which were modelled through Thevenin's approach were equally incorporated into IEEE 33 bus test system using system average root mean square frequency index (SARFI) method for performance comparison between the two of them. It was substantiated that D-STATCOM performed better than DVR in the area of global voltage sag mitigation. TCSC and UPFC were also used for voltage control in [47] with incorporation of wind turbine generator (WTG), place on bus 9 of tested IEEE 14 bus system. This was to simulate deregulated power network, which allows for accommodation of distributed generators. The optimization method was achieved through step by step variation of the control parameters of UPFC and TCSC in which the location that resulted into maximization of social welfare and that of the target objective becomes optimal location. The investigation for various conditions ranging from network without WTG, with WTG, with WTG and FACTS in each case conducted revealed that network voltage deviation minimized with WTG, and further minimized with WTG and FACTS presence in the network. IEEE 118 bus system also resulted into similar scenario as occurred for IEEE 14 bus test system, such that in each test case, the objective which was bus voltage profile improvement was achieved.

Artificial bee colony (ABC) was applied for setting of SVC device which was implemented through OPF method in [113] for system bus voltage profile improvement. The investigation conducted on IEEE 30 bus system for normal and contingency conditions presents an improved in bus voltage profiles during this exercise. D-FACTS was used for power loss minimization of IEEE 118 bus test system with the incorporation of D-SSC using loss sensitivity approach with respect to changes in line impedance in [61]. Authors were able to implement ± 20% of line reactance for different 15 transmission lines of the tested network. The incorporation of D-SSC resulted into loss reduction in the study. Enhancement of bus voltage profile, as well as real and reactive power loss control were achieved with the incorporation of SVC, with its firing angle modeled mathematically in [66]. The location of this device was based on base case least bus voltage for optimal performance. Authors conducted the investigation through injection of different values of reactance to the connected network. Although, authors failed to indicate the optimal values of SVC for better performance, the implementation of the investigation conducted on IEEE 9 and 30 buses resulted into improvement in bus voltage profile and power loss control of the test networks as demonstrated in the study. Bus voltage profile were verified with different injected reactive power ranging from ± 5 to ± 45 MVAR consequent of incorporated SVC.

These same subjects of bus voltage deviation minimization and power loss control were also investigated in [115]. Adaptive multi-objective parallel seeker optimization algorithm was used for optimal setting of TCSC device implemented through optimal power flow process. The capability of this device for achievement of set objectives was demonstrated on various IEEE networks systems comprises 9, 30, 57 and 118 buses. A remarkable loss reduction and voltage minimization were achieved in this study compare to similar studies of same criteria. In another work contained in [116], the presence of renewable energy resources was analysed while considering TCSC and SVC for voltage regulation and power loss control on IEEE 5 bus system. Both wind and solar energy resources which were modelled through Weibull and Beta distribution functions respectively and were applied to the test system at buses 4 and 5 respectively. The investigation was also conducted for line 2 – 4 outage contingency case, with SVC at bus three, and TCSC on line 3 – 4 in each case. It was observed in these studies that for both normal and contingency conditions, the voltage deviation was improved with renewables and further improved with SVC and similarly, power loss was minimized with renewable and further reduced with incorporation of TCSC device. Active power loss minimization, and voltage improvement were achieved with the incorporation of TCSC, SVC and UPFC into IEEE 30 bus network in the work presented by [117] with the observation that loss control led to reduction and operational cost. Differential evolution and genetic algorithms were applied for optimal placement of these FACTS while the network reactive power loading was varied from base case to 200% rating. This study investigated simultaneous application of TCSC and SVC with UPFC and this resulted into better performance as against only UPFC deployment. Summarily, the investigation resulted into system loss reduction and voltage profile improvement of the test system.

#### 2.5.4.4 Multiple objective applications of FACTS

In some cases, FACTS were applied for multi-objective purposes involving combination of any or all of voltage improvement, power loss reduction, power flow improvement, cost minimization and so on. In this section, the review of closely related work, containing multiple of the target objectives in relation to this research thesis is carried out. Modelling and simulations of 11 kV network system which was incorporated with SVC, STATCOM, TCSC, SSSC and UPFC with a view to enhancing network performance resulted into power improvement, bus voltage profile enhancement and system stability improvement in [118]. The investigation was conducted with capacitance of each FACTS varied between 50 $\mu F$ and 100 $\mu F$ having stated that their performance depends on their capacitance levels. In their analysis, it was observed that STATCOM injected more real power than SVC while the reverse was the case for reactive power injection. Injection of real power of TCSC outweighed that of SVC while its reactive power injection surpasses that of SSSC and STATCOM. In this investigation under same reactance (same capacitance) therefore, UPFC performed better than all other devices in achieving set objectives. STATCOM and TCSC were the devices used to improve bus voltage profile, reduce power loss of the tested IEEE 14 bus system and enhance steady state stability limit of the network [119]. In their work, optimal locations of FACTS devices were achieved with voltage collapse proximity index, and through line stability index for each of them. The realization of improved bus voltage and reduced power loss resulted into steady state stability of the test network in the exercise. In short review conducted in [120],

applications of UPFC for oscillation damping, voltage stability enhancement and power flow control were reported, where the efficacy of this device was emphasized. This device was also compared with others like TCSC, SVC and STATCOM in the same study.

In another work by [86], the incorporation of UPFC and IPFC into IEEE 30 bus system was achieved using hybrid particle swarm optimization and gravitational search algorithms. The analysis was conducted using NR power flow approach and the resultant network power flow, power loss and bus voltage analysis revealed loss reduction and voltage stability improvement of the test system. Bus voltage deviation minimization, power loss reduction and power flow control were the objectives for incorporation of D-TCSC device into both IEEE 14 and 118 bus networks in [63]. In their work, authors formulated the D-TCSC into multi-objective problems involving those earlier stated, where the reactance of the device was used as the decision vector, having placed the device in all possible branches with the exceptions of lines containing transformer regulating elements. Thereafter, with the help of enhanced leader particle swarm optimization (ELPSO) algorithm, which was compared with conventional PSO, genetic, gravitational search, galaxy-based search, invasive weed optimization, asexual reproduction optimization, threshold acceptance, pattern search and non-linear programming algorithms, the device parameters were achieved. In all these optimization algorithms, ELPSO performed better in achieving the set objectives of bus voltage deviation minimization, power loss reduction and system overload control.

Transmission loss minimization, voltage profile improvement and voltage stability enhancement were achieved with STATCOM device, which was placed with artificial intelligence method of chemical reaction optimization (CRO) as presented in the work of Dutta *et al.* [121]. Although, the emphasis on the part of authors was on the suitability of CRO for optimal placement of the device, notwithstanding, the obtained results through implementation of this research approach on IEEE 30 and 57 networks substantiated the achievement of the set objectives. In [122], TCSC which was optimally set with PSO was used to reduce network transmission loss, reduce installation cost and minimized bus voltage profile deviations. Here, these target network parameters were formulated into multi-objective functions for NR power flow execution and this was implemented on IEEE 14 and 30 bus networks and Indian 75 bus system. The comparative analysis of both uncompensated and compensated network presented the achievement of voltage profile deviation minimization, power loss reduction and installation cost reduction of the test networks. In order to achieve radial system load balancing and power loss reduction, a novel grey wolf optimizer algorithm was implemented for solving installation and reconfiguration problems of D-STATCOM device, whose candidate location had earlier been suggested by index vector approach [123]. The device effectiveness based on the employed approaches was tested on three radial networks involving 33, 66 and real time 31 bus systems and the outcome recorded significant power loss control.

Bus voltage profile improvement, reduction in installation cost as well as real and reactive power loss reduction were the target of authors in [97] before placement of TCSC in the network system using TLBO artificial

intelligence technique. Just like in their previous work, the performance of TCSC was implemented on IEEE 14 and 30 bus networks and Indian 75 bus system. Here also, with well-defined equality and inequality constraints, these objectives were formulated into multi-objective functions for the device to handle. TLBO was compared with PSO, and ABC algorithms for performance verification and it was apparent that TLBO outperformed PSO and ABC. In another work involving separate placement of TCSC, SVC, UPFC and concurrent placement of TCSC and SVC, conducted by [94], three objectives involving cost, system line loading and load voltage deviation were proposed for achievement. In this study, PSO, improved weighted parameters PSO (WIPSO) and biogeography optimization (BBO) were utilized for device parameter settings. Analyses were conducted on IEEE buses 14 and 30 and the performances of devices set BBO were found to be better than other used algorithms. With cost of installation in focus, authors also established that combination of TCSC and SVC achieved better results as compared with autonomous UPFC.

#### 2.5.4.5 Available transfer capability enhancement

This study focuses largely on ATC enhancement of a restructured network, hence efforts into analyses of previous work under this subheading is very beneficial to this study. The first sets of enhancement review conducted here are predominantly single objective in nature, meaning that only ATC enhancement formed the focus of the works presented here. Impacts of TCSC on ATC enhancement was implemented in [124] with the device optimal placement achieved based on utmost performance of the device reference to the location. In their study, authors investigated the impacts of renewable energy sources on the network ATC, having considered wind and hydro power plant as the two renewable sources. Different scenarios were considered for ATC determination with network comprises wind and hydro power independently and with introduction of TCSC in each case. It was concluded that network ATC improved with renewable presence while the introduction of TCSC further enhanced ATC values.

Artificial intelligent algorithms comprises real genetic and hybrid real genetic algorithms were applied to TCSC placement in another work presented by Rashidinejad *et al.* [125], where the result of ATC enhancement of IEEE 9 and 30 bus systems revealed some improvement with presence of the device. Interline power flow controller (IPFC) was the device used for ATC improvement presented in [126], where the device location was achieved with recourse to transmission line limiting element. PSO was employed for device setting and ACPTDF approach was applied for determination of transfer capability of IEEE standard 30 bus network. Although, authors presented the individual transfer capability vis-à-vis network value of an uncompensated network, a critical look at these values indicate an improvement in overall system ATC. In ATC enhancement work through static synchronous series compensator SSSC device as presented in [127], line with highest loss values, obtained with respect to system loss equation was the location of the device. However, optimal setting of the device was done via firefly optimization algorithm, while the improvement in ATC was obtained through optimal power flow of the test system. The result of their study presents some improvement in ATC values.

In a similar work presented in [128] by the same authors, but with STATCOM device in this other work, the effects of variation of both shunt voltage and voltage angle of the device were verified on the ATC of the test

system. Authors were able to conclude that linear variation exists between control voltage magnitude of STATCOM device and ATC, while the relationship between the device control angle and ATC are non-linear. In their reported research, one can infer that, though, ATC values were improved with STATCOM incorporation, however, the impacts of device control angle variation on ATC enhancement was more significant when compared with that of device voltage magnitude. Efforts were also made in [129] to improve ATC of a designed system using SSSC through redistribution of system loading. The system load redistribution was achieved through soft signal technology of distribution system referred to as multi-agent in the study. It was concluded that proper coordination of SSSC through the multi-agent as described led to improvement in network ATC. With all the efforts in these previous works, only ATC was the focus of these researches. The network responses to other parameters during the incorporation of FACTS device were not investigated. The next paragraph presents the achievement of ATC improvement with other network parameter enhancement.

OPF based analytical method was used for evaluation of ATC with multiple transactions using STATCOM, SSSC and UPFC devices [130]. Efforts were also made by these authors in their study to implement contingency conditions, with verification of ATC values under these conditions. This study indicates that ATCs were improved with different FACTS controllers and that occurrence of contingency impacted the ATCs values. Authors concluded that UPFC performance during ATC enhancement outweighs other deployed devices. Total transfer capability enhancement was achieved with TCSC, TCPS, UPFC and SVC in another work carried out in [131], where placement of these devices were achieved through hybrid PSO algorithm. It was observed in their work also that transfer capability of the network was improved with FACTS devices. TCSC and SVC are the devices used for ATC enhancement in [132], with optimal setting of devices implemented through real code genetic algorithm in conjunction with voltage dominant for SVC and thermal dominant for TCSC device. Authors were able to conclude through the investigation of ATC enhancement only that TCSC performed better than SVC. IPFC and GUPFC were used to enhanced ATC in another work conducted by A. Kumar and J. Kumar in [133]. Here, ATC of IEEE 24 bus system was obtained using OPF approach, while different line outages were also implemented during network performance enhancement. Different power transactions were implemented and the comparison between the two devices revealed that the location of the device is symbolical to its performance as no conclusion could be drawn from the presented results.

The placement of TCSC was achieved with due consideration for line thermal limits while SVC was incorporated with consideration for least bus voltage at base case [99]. The settings of these devices were achieved with cat swarm optimization algorithm. Continuation power flow was the approach used for implementation of ATC alongside its enhancement, through TCSC and SVC devices. In their work, ATCs of IEEE 14 bus test network which was divided into different areas based on different voltage level were obtained with incorporation of theses device independently. Line outage contingency which was identified through real power performance index was implemented in the study at the same time. Here, ATCs were improved with minimum values occurred during contingency and with this achievement, TCSC was observed to have performed better than SVC. In these researches, multi-FACTS devices were used but with single objective of ATC enhancement, just like in the case of single FACT device earlier discussed.

Various works involving multi objectives are reviewed in this paragraph. The work carried out by authors in [134] involved ATC enhancement and system loss minimization, using STATCOM, SSSC and UPFC, which were modelled based on current injection approach. An OPF method was used for implementation, placements were realized based on incorporation that resulted into minimal system loss, while the device setting were achieved with firefly algorithm. This study showcased UPFC as the best device in this context among others. This performance can be premised on the fact that UPFC is a combination of STATCOM and SSSC. In [135], authors engaged TCSC for ATC enhancement, bus voltage deviation minimization and installation cost reduction. The device setting was achieved using differential and modified differential evolution algorithms, while RPF approach was used for ATC computation. It was inferred from the work that while ATC improved and bus voltage deviation reduced, at optimal device cost, modified differential algorithm presents a better optimization algorithm for complex problem of this kind.

In [136], real parameter generic algorithm (RGA) was also engaged for optimal setting of both SVC and TCSC devices for ATC improvement. The ATC which was determined using continuation power flow was conducted on 24 bus system for both normal and contingency conditions. TCSC was observed to perform better than SVC for this ATC improvement objective. Hybridization of evolutionary algorithm (EA), tabu search algorithm (TS) and PSO was implemented by authors in [137] for settings of TCSC, SVC, UPFC and thyristor controlled phase shifter (TCPS). The integration of EA and TS using PSO as the main algorithm was applied for enhancement of total transfer capability of power network. The methodology applied was through optimal power flow to achieve the set objective. When applied to 24, 30 and 118 IEEE networks, the hybrid algorithm resulted into better result compare individual evolutionary, tabu search and particle swarm optimization algorithms in this study.

Most of the survey on the previous ATC enhancement works hardly undertake ATC improvement alongside power loss control. The survey majorly revealed either ATC enhancement only or alongside voltage profile improvement especially where shunt type FACTS devices were deployed. As earlier stated, the need to enhance network ATC was born out of necessity to cater for upsurge in network demand because adequate ATC is required for economic power transaction while its sufficiency is needed for a competitive electricity trading. Notwithstanding ATC improvement is synonymous to network power flow enhancement and it is inescapable to regulate the network voltage within the limits and concurrently satisfy power balance equations. Besides, more losses usually accompany more power flow which is necessary for ATC improvement. Therefore, efforts were made in this research study to enhance ATC of a deregulated network and at the same time implement power loss control, with due consideration for bus voltage deviation minimization as part of the objective.

### 2.6 Previous works on analytical techniques of FACTS placement for ATC enhancement

The comparison of effectiveness of some analytical methods of FACTS placement was conducted in this research also. This formed the basis for development of sensitivity-based placement approach for optimal performance of FACTS devices as implemented in latter chapters of this report, hence the need for selected review of this kind. In the first section of chapter five of this thesis, the implementation of TCSC and SVC for

ATC enhancement was reported, while the performance comparison of selected few of placement techniques was presented in the second section of same chapter. In this section however, these selected placement approaches are briefly reviewed to give an insight into previous work on these methods.

In the placement of TCSC for ATC enhancement carried out by Prajapti and Gandhi in [138], real power performance index was used for the location of the device, with 70 and 30 percent of capacitive and inductive reactance settings respectively. The process involved ranking of the most severe line based on thermal limit as resulted from real power PI method and the placement of TCSC device on this line. The device optimization with this process resulted into enhancement of ATC of 6 bus IEEE tested network. Transmission line thermal limiting element was considered in locating TCSC for transmission capability enhancement presented in [139]. In their work, network thermal limiting element at base case was considered for placement of TCSC, having treated the limiting lines and buses as congested element, and the resultant network transmission capability indicated an improvement of compensated network. ATC enhancement with TCSC was also conducted in [140], where the device placement was achieved through transmission line thermal limit consideration and its setting done using particle swarm optimization algorithm. Efforts were also made to investigate different bilateral transactions in this study, using two test systems involving IEEE 6 and 30 buses. The ATC obtained through DCPTDF approach, which was conducted on these standard networks resulted into an improved value with placement of TCSC device.

In [141] and [142], Static Synchronous Series Compensator (SSSC) and STATCOM respectively were placed for ATC enhancements based on least bus voltage magnitude at base case power flow. SSSC was applied for improvement of transfer capability of IEEE 24 bus system with transmission line connecting bus with least voltage terminal at base case serving as the location for the device [141]. The control of SSSC was achieved through variation of its angle between 0 degree and 6.28 degree in this study while ACPTDF was adopted as the method for ATC computation. The focus of that research work was to present the variation of SSSC angle with ATC values in each of the undertaking transactions. The impacts of variations of both the magnitude and voltage angle parameters of STATCOM device were studied on the ATC enhancement in [142], with conclusion that shunt angle has predominant effect on ATC values. In their work conducted on IEEE 24 bus system, it was observed that ATC value initially decreased with increase in STATCOM shunt angle and subsequently increase with increase in this angle. This shunt angle variation marginally impacted ATC values because beyond certain shunt angle, no further increase was recorded but in contrary, further increase in STATCOM shunt angle led to reduction in ATC values.

Total real power loss sensitivity was used for SSSC device placement in the ATC improvement research work presented in [143]. Here, the model of SSSC was achieved through current based approach while its parameter setting realization was made possible with firefly algorithm. Optimal power flow method formulated with due consideration for equality and inequality constraints resulted into ATC enhancement. Power transfer distribution factor (PTDF) was the basis for placement of STATCOM, SSSC and UPFC while PSO was used for their parameter setting in [144]. Author emphasized that lines with higher PTDFs will not result into

appreciable ATC enhancement but rather considered lines with high slope and lower PTDF magnitude in implementation. It was observed from their study that UPFC outperformed STATCOM and SSSC devices.

TCSC, TCPAR and SVC were the devices used in another work by [145], where the placement of the devices were achieved through sensitivity approach obtained from the derivatives of the system reactive power loss with respect to involved transmission line reactance. The values obtained when the devices were inserted into the IEEE 14 bus network indicate some improvement in ATCs. In a similar work presented by authors in [146], the devices were limited to TCSC and TCPAR for the same ATC enhancement purpose. The same sensitivity base method was used for incorporation but in the case of TCPAR, the sensitivity was obtained with respect to its control angle. Efforts were made in their study to compare these devices with the conclusion that optimally placed TCSC performed better. In the comparative performance analyses between TCSC and TCPAR for ATC enhancement, loss sensitivity approach was adopted for their placement in [147]. The location for placement of TCSC was based on var loss sensitivity in which the line having the most positive loss sensitivity index was prioritized. Angle control parameter with the line having highest absolute value of loss index was used in setting the TCPAR.

In another work presented in [148], TCSC was also deployed for ATC enhancement purposes. Here, the choice for the device placement was achieved through due consideration for base case ATC values while the device settings were obtained using PSO. The ATC which was determined using DCPTDF was improved with incorporation of TCSC device on IEEE 6 bus test network. The locations for SSSC, STATCOM and UPFC, which were current based modelled for the purpose of evaluation and enhancement of ATC as implemented in [100], was through power loss sensitivity. The determination of ATC was through optimal power flow approach, while setting of the devices achieved with firefly algorithm. The investigations which were conducted on IEEE 30 and 57 buses, independently placed devices in all possible locations in the networks and the placement that resulted into least power loss was considered as the optimal location. The test networks recorded ATC enhancement afterward and it was observed that UPFC was more effective than other devices during the investigation.

### 2.7 Brief review on applications of HVDC transmission systems

In this study, efforts were made to investigate and present high voltage direct current (HVDC) based voltage source converter (VSC) for various network performance improvements and contingency mitigations. Applications of voltage source converter (VSC) based HVDC in transmission system is gaining attraction because of the recent recorded successes and improvements in VSC based power electronic systems. Recently, power electronics devices have made tremendous contributions to the urgency for network capacity enhancement, constrained with sustainability and reliability improvement, with due consideration for minimization of cost, through injection of supplementary controllability and flexibility of operation [149]. The advancement in voltage source converter based technology enables FACTS devices and HVDC systems to play these substantive roles in grid infrastructure sustainability and supports [150]. Among other benefits however, HVDC has been established to be economical for power system transmission over long distance and its

application apart from being significant, will determine network grid operation in the future [151]. HVDC surpasses HVAC in asynchronous interconnection of grids, broadened connection of underground cables, minimization of fault currents, mitigation of impacts on environment and network congestion control [152].

The major technology behind the realization of HVDC is via power electronic based semiconductor converters grouped into line commutated converter (LCC) and VSC [153]. Some of the prominent characteristics in favor of VSC-HVDC over LCC-HVDC based systems include but not limited to independent active and reactive power control, black start capability, passive network supply fitness, fast and reliable dynamic performance, stability of ac operation, compact station structure, flexibility of operation among others [154],[155]. Increase in application of VSC-HVDC will increase the integration of more renewable generations, expand bidirectional flow of ac grid current, expand efficiency of grid transmission, enhance distributed generation connections and improve system security as well as reliability which will eventually redirect forthcoming grid operations and redefine future grid architectures [156],[157].

The guidelines for both technical and standardization requirement for the first VSC-HVDC grids were reported in the work of Akhmatov *et al.*, to give insight into basic design requirements, operation principles and for ground preparation for detailed work that will conform to the set standard [158]. Hitherto, the design and application of VSC-HVDC had been investigated with the conclusion that this devise transmits active power and control reactive power between ac grids in addition to possession of STATCOM capability [159]. The transient and dynamic stability studies of an ac infinite bus single machine system with an embedded VSC-HVDC were conducted based on equivalent mathematical modelling by Wang *et al.*, while concluding that voltage supports provided by VSC-HVDC during ac grid disturbance led to quick voltage recovery and transient stability of the grid network [160]. Frequency control capability of VSC-HVDC was investigated in [161], where it was concluded that power system frequency stability can be improved through proper coordination of the interconnected systems. An investigation was conducted through optimal power flow into a VSC-HVDC transmission system by the development of a generalized approach for radial and meshed networks in order to minimize power loss [162]

A multi terminal VSC-HVDC, which was investigated through small signal stability on inter area oscillation damping with intention to examine its impacts on power transfer capability enhancement of network grid was presented [163]. The article presented VSC-HVDC as having exploitative tendency to improve power transfer as inferred from the investigative study. This was corroborated by Kim *et al.,* [164], where it was established through small signal stability study that ac networks incorporated VSC-HVDC enjoys stable system operations. The effectiveness of VSC-HVDC in conjunction with model predictive control in power system network stabilization was conducted in [165], where the latter was used to manipulate the reactive power injection of the former for damping the oscillation of the ac network system. Recently, the awareness created by westward continuous expansion of Southwest China power grid necessitated inquisitive study into optimization of interconnection of cross-region network grid via the use of VSC-HVDC [166]. The study revealed the possibility of an improved bidirectional power flow support capability, grid support optimization and an

improvement in capability of power transmission. Steady state modelling of a grid VSC-HVDC interconnecting offshore wind farm was implemented in [167], to investigate optimal network transmission capability, the outcome of which demonstrated the possibility of optimal operation of power network through the use of VSC-HVDC.

VSC-HVDC, UPFC, SSSC and other related FACTS devices that are embedded with VSC, have the capacity to noticeably improve diverse power system characteristics. Hence, their optimization become very important for effective and economic reasons [83]. Steady state model of VSC-HVDC system feeding ac grid was presented in [168] for the purpose of derivation of active and reactive power flow constraints satisfaction. Fault current protection capability of VSC-HVDC interconnecting wind farm and ac grid was demonstrated in [169]. It was concluded in the study that, traditional protection systems were impacted as a result of manipulation of both magnitude and phase angle of fault current by the presence of VSC-HVDC transmission system. Deployment of VSC-HVDC network interconnection for frequency support service provision was studied using temperature dependent overload capability in [170], while small signal stability investigation conducted through controlled OPF in [164] revealed that, an ac network embedded with VSC-HVDC system is more stable. With focus on maintaining transmission equilibrium and stability of the grid, an OPF approach based on minimum power loss was developed for a multiterminal VSC-HVDC grid [171].

Assessment of stability performance of an embedded VSC-HVDC transmission system through interactive dynamic behavior was investigated with inference of an improved system dynamic performance [172]. In order to improve dynamic performance and enhance system stability however, artificial bee colony (ABC) was engaged for optimal scheduling of VSC-HVDC gain in the work presented by Ramadan *et. al.*, [173]. In a similar work, the control parameters of VSC were tuned using particle swarm optimization algorithm (PSO) for steady state and dynamic performance enhancement of VSC-HVDC system [174]. Wang *et. al.*, studied the effects of dissimilar reactive power control strategies on transient and dynamic stability of an ac system, with conclusion that oscillation control and voltage sustenance were influenced especially at the instance of grid disturbance [160]. It was concluded in [175] however, that VSC-HVDCs have an impact on interdependency of power system dynamics and that further studies are required to fully understand their impact on system stability improvement and ancillary support services. Hence, in chapters eight and nine of this thesis, VSC-HVDC transmission systems were presented for network performance improvement and congestion mitigation respectively, as parts of investigation of VSC-HVDC ancillary support capabilities.

### 2.8 Summary of chapter two

The concept of power sector deregulation and restructuring alongside the associated problems have been discussed in this chapter. These problems which include determination and enhancement of ATC as well as contingency evaluation were also discussed and previous work on these issues reviewed. An up-to-date and comprehensive literature review of FACTS controllers starting from description, generations, classifications, categories and connection types, have also been presented. The basic schematics of some of these controllers were also described. FACTS devices optimal location and parameter settings which were categorized into four

major groups in this work have also been exhaustively and properly discussed. Essentially, the importance of FACTS controllers to network performance improvement which include power flow control, contingency mitigation, voltage control and power loss control, as well as ATC enhancement, were categorized and discussed. Few analytical methods for FACTS placement especially for ATC improvements were also presented.

Consequent the review conducted and reported in this chapter, TCSC and SVC were further explored for ATC enhancement, bus voltage profile improvement and real power loss minimization of a deregulated and restructured power network in subsequent chapters. In addition, VSC-HVDC transmission system which was reviewed alongside other FACTS in the earlier paragraphs was also investigated in a liberalized power sector, for power flow enhancement, voltage profile deviation minimization, power loss control and contingency mitigation in the latter part of this thesis.

# CHAPTER THREE
# RESEARCH METHODOLOGY

## 3.1 Introduction

This chapter presents the two major methods of available transfer capability (ATC) computation implemented in this thesis. The repeated alternating current power flow (RACPF) and alternating current power transfer distribution factor (ACPTDF) are properly described in this section. In addition, contingency evaluation methodology through performance index (PI) are presented. Modelling of static var compensator (SVC) based on its equivalent diagram is presented, while thyristor control series compensator (TCSC) equivalent network model and its analytical model are also presented for deployment into ATC enhancement and network performance improvement. Procedures for proposed brain storm optimization algorithms (BSOA) used for optimal setting of TCSC device in this research work is also presented alongside particle swarm optimization (PSO) algorithm used in performance comparison with former. Thereafter, sensitivity-based approaches for placement of TCSC and high voltage direct current (HVDC) based voltage source converter (VSC) transmission system for network performance enhancement are presented.

## 3.2 Available transfer capability (ATC)

According to North American Electric Reliability Council (NERC) [176], and as reported in [26], ATC is explained to mean the remaining corridor above the existing transmission network usage for trading activities. Values of ATC computed have to be published quickly in open access same time information system (OASIS) for power planning, booking, or trading [6],[26],[27],[176].

$$ATC = TTC - (TRM + ETC + CBM) \tag{3.1}$$

In mathematical interpretation as presented in equation (3.1), ATC can best be explained as the total transfer capability (TTC) less the summation of transmission reliability margin (TRM), existing transmission commitments (ETC), and capacity benefit margin (CBM) [24],[25],[26],[27] and [176]. The physical relationship among the components of equation (3.1) is illustrated in Fig. 3.1.

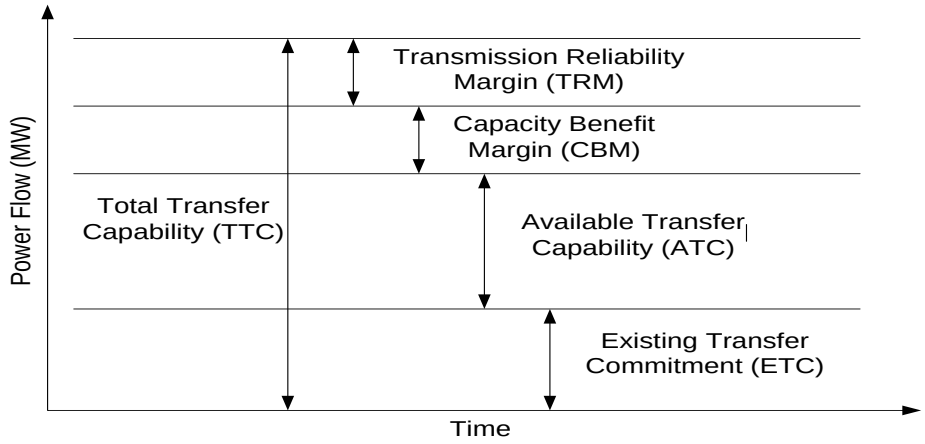


**Figure 3. 1: ATC and related definitions** [25]

From Fig. 3.1, the maximum reliable power that the entire transmission network is capable to handle is TTC. The power flowing at the instant when ATC is to be determined is ETC and it is the base case power flow at that instant of time. TRM and CBM are used for network system security and their values vary alongside system operators and market players policies [14].

Categorically, some methods in use for computation of ATC include direct current power transfer distribution factor (DCPTDF), ACPTDF, continuation power flow (CPF), artificial neural network (ANN), optimal power flow (OPF) and repeated power flow (RPF) [26]. DCPTDF technique is fast and simple to implement however, voltage and reactive power are not being considered in its computation. The resistance is taken as zero because a particular line reactance is considered to be far greater than its resistance. This has implications on the accuracy of the results. ACPTDF approach gives better accurate results compared to DCPTDF because transmission line real and reactive power flows are well thought-out in its computation [14]. Implementation of CPF method is mathematically complicated and besides, it involves predator, a particular set of parameters, adjustment and constant control. This complexity puts CPF at a disadvantage despite being popular [30].

RPF method yields a better result over ACPTDF and DCPTDF approaches because of its consideration for thermal and voltage magnitude constraints [28]. In RPF method, the main information obtained are voltage magnitudes and phase angles of the load buses, real and reactive power flows of transmission lines and generator buses reactive powers. It was argued in [29] that the results obtained using RPF method are always accurate but time consuming. However, the word time in this context is relative and cannot be substituted for accuracy especially for the sensitive nature of the analysis of power network. Many factors in consideration for power system planning and operation depend on value of ATC obtained especially in deregulation environment, hence its precision cannot be substituted. This fact is also corroborated by the information presented in [26] that RPF method is easy and suitable for bigger electrical power systems. Among the advantages of this method are effortlessness of execution and quick convergence [29],[30]. In order to consider reactive power, voltage magnitude and line thermal limit consequences, RPF was adopted and modified into repeated alternating current power flow (RACPF) method and this was applied to first sets of ATC determination in this thesis.

### 3.2.1 RACPF methodology for ATC determination

In RACPF, the conventional power flow equations are solved in a chronological sequence along a definite direction. Power transfer is achieved by an increment in complex load of the target bus within the energy sink region, following which the generator bus real power at the source region will be correspondingly increased. This is continued pending when a limit is observed. For instance, the transfer of 10 MW from bus 5 to bus 7 means addition of 10 MW to generator real power at bus 5 and removal of 10 MW generator real power at bus 7, while inverse of this is re-dispatch. Power transfer between generator and load bus was established by this approach.

In implementing this RACPF method, NR equations were used for load flow. This method is easily implemented while taking security constraints into consideration. The power equations which were presented in [177] [178] are given as follows;

$$P_i = \sum_{j=1}^{N} |V_i||V_j||Y_{ij}| \cos(\theta_{ij} - \delta_i + \delta_j) \quad (3.2)$$

$$Q_i = -\sum_{j=1}^{N} |V_i||V_j||Y_{ij}| \sin(\theta_{ij} - \delta_i + \delta_j) \quad (3.3)$$

Where, $N$ stands for total number of bus, injected real and reactive power are $P_i$ and $Q_i$ at any bus $i$, voltage magnitude are $|V_i|$ $and$ $|V_j|$ at the buses $i$ and $j$, $|Y_{ij}|$ and $\theta_{ij}$ represent magnitude and angle of bus admittance for bus $i$ and $j$, while $\delta_i and\ \delta_j$ equal the voltage angle at bus $i$ and $j$. Using Taylor series expansion for equations (3.2) and (3.3), the Jacobian representation for the change in power flows at any bus $i$ is given as follows;

$$\begin{bmatrix}\Delta P \\ \Delta Q\end{bmatrix} = \begin{bmatrix}J_1 & J_2 \\ J_3 & J_4\end{bmatrix} \begin{bmatrix}\Delta\delta \\ \Delta|V|\end{bmatrix} \quad (3.4)$$

where $\Delta P$ and $\Delta Q$ are equal to change in real and reactive power flow respectively.

$$[J_1] = \frac{\partial P}{\partial \delta}\ ; [J_2] = \frac{\partial P}{\partial |V|}\ ; [J_3] = \frac{\partial Q}{\partial \delta} \text{ and } [J_4] = \frac{\partial Q}{\partial |V|} \quad (3.5)$$

The elements of $J_1$ are;

$$\frac{\partial P_i}{\partial \delta_i} = \sum_{j\neq 1}^{N} |V_i||V_j||Y_{ij}| \sin(\theta_{ij} - \delta_i + \delta_j) \quad (3.6)$$

$$\frac{\partial P_i}{\partial \delta_j} = -|V_i||V_j||Y_{ij}| \sin(\theta_{ij} - \delta_i + \delta_j) \quad j \neq 1 \quad (3.7)$$

The elements of $J_2$ are;

$$\frac{\partial P_i}{\partial |V_i|} = 2|V_i||Y_{ii}| \cos\theta_{ii} + \sum_{j\neq 1}^{n} |V_j||Y_{ij}| \cos(\theta_{ij} - \delta_i + \delta_j) \quad (3.8)$$

$$\frac{\partial P_i}{\partial |V_j|} = |V_i||Y_{ij}| \cos(\theta_{ij} - \delta_i + \delta_j) \quad j \neq 1 \quad (3.9)$$

The elements of $J_3$ are;

$$\frac{\partial Q_i}{\partial \delta_i} = \sum_{j\neq 1}^{N} |V_i||V_j||Y_{ij}| \cos(\theta_{ij} - \delta_i + \delta_j) \quad (3.10)$$

$$\frac{\partial Q_i}{\partial \delta_j} = -|V_i||V_j||Y_{ij}| \cos(\theta_{ij} - \delta_i + \delta_j)\ j \neq 1 \quad (3.11)$$

The elements of $J_4$ are;

$$\frac{\partial Q_i}{\partial |V_i|} = -2|V_i||Y_{ii}| \sin\theta_{ii} - \sum_{j\neq 1}^{n} |V_j||Y_{ij}| \sin(\theta_{ij} - \delta_i + \delta_j) \quad (3.12)$$

$$\frac{\partial Q_i}{\partial |V_j|} = -|V_i||Y_{ij}| \sin(\theta_{ij} - \delta_i + \delta_j) \quad j \neq 1 \quad (3.13)$$

The change in the angle and voltage magnitude can be determined as equation (3.14), where the inverse of Jacobian matrix element is assumed to exist for this particular calculation.

$$\begin{bmatrix} \Delta\delta \\ \Delta|V| \end{bmatrix} = \begin{bmatrix} J_1 & J_2 \\ J_3 & J_4 \end{bmatrix}^{-1} \begin{bmatrix} \Delta P \\ \Delta Q \end{bmatrix}. \quad (3.14)$$

In ATC calculation, especially for bilateral transaction, real power changes at each bus are functions of $\lambda$ [29], therefore,

$$P_{gi} = P_{gi}^{0}(1 + \lambda K_{gi}) \quad (3.15)$$

$$P_{dj} = P_{dj}^{0}(1 + \lambda K_{dj}) \quad (3.16)$$

The injected and extracted actual power at bus *i* and *j* are represented by $P_{gi}\ and\ P_{dj}$, while the base case real power generation at bus *i* and real power demand at bus *j* are $P_{gi}^{0}\ and\ P_{dj}^{0}$ respectively. $\lambda$ is a variable quantity, that is, a scalar parameter, whose value determines the alteration in real power for the implemented transactions, while $K_{gi}$ and $K_{dj}$ are power factor regulators. However, for this work, power factor is maintained at unity, TRM and CBM are regarded as zero quantity because, their values vary and are market dependent [28], hence ATC is calculated from the TTC value obtained as follows;

$$TTC = \min\left[\sum_{j\epsilon k} P_{dj}\ (\lambda_{max}) - \sum_{j\epsilon k} P_{dj}\ (\lambda_0)\right]. \quad (3.17)$$

In equation (3.17), the subscript *k* implies the buses in the energy sink area, $\sum_{j\epsilon k} P_{dj}\ (\lambda_{max})$ is sum total load in energy sink area when $\lambda = \lambda_{max}$ and $\sum_{j\epsilon k} P_{dj}\ (\lambda_0)$ is sum total load in energy sink area when $\lambda = 0$.

### 3.2.2 RACPF Algorithm

The implementation process presented in [26] is modified for this approach as follows:

(a) Define and identify power transaction whose ATC is to be determined and computed.
(b) Run a base case power flow such that constraint violations are not violated, using Newton Raphson (NR) method.
(c) Stepwise perform the power transfer, by increasing the load at sink load bus and increasing the generation at source bus with the injection of same amount of power.
(d) Set up and run a RACPF in MATLAB program.
(e) Check for constraint violation in (d) above.
(f) If there is/are violation/s then reduce step size by half and return to (d); otherwise return to (c).
(g) Otherwise end.
(h) Determine and hold the numerical values of real power flow for the target transaction as TTC.
(i) Calculate ATC by subtracting TRM, CBM, and ETC from TTC, using equation (3.1).

### 3.2.3 Flow Chart of RACPF

In order to implement the steps above, the algorithm has been developed into the flow chart shown in Fig. 3.2. The manual input in the third block is for human intervention to define the subsequent desired transactions.

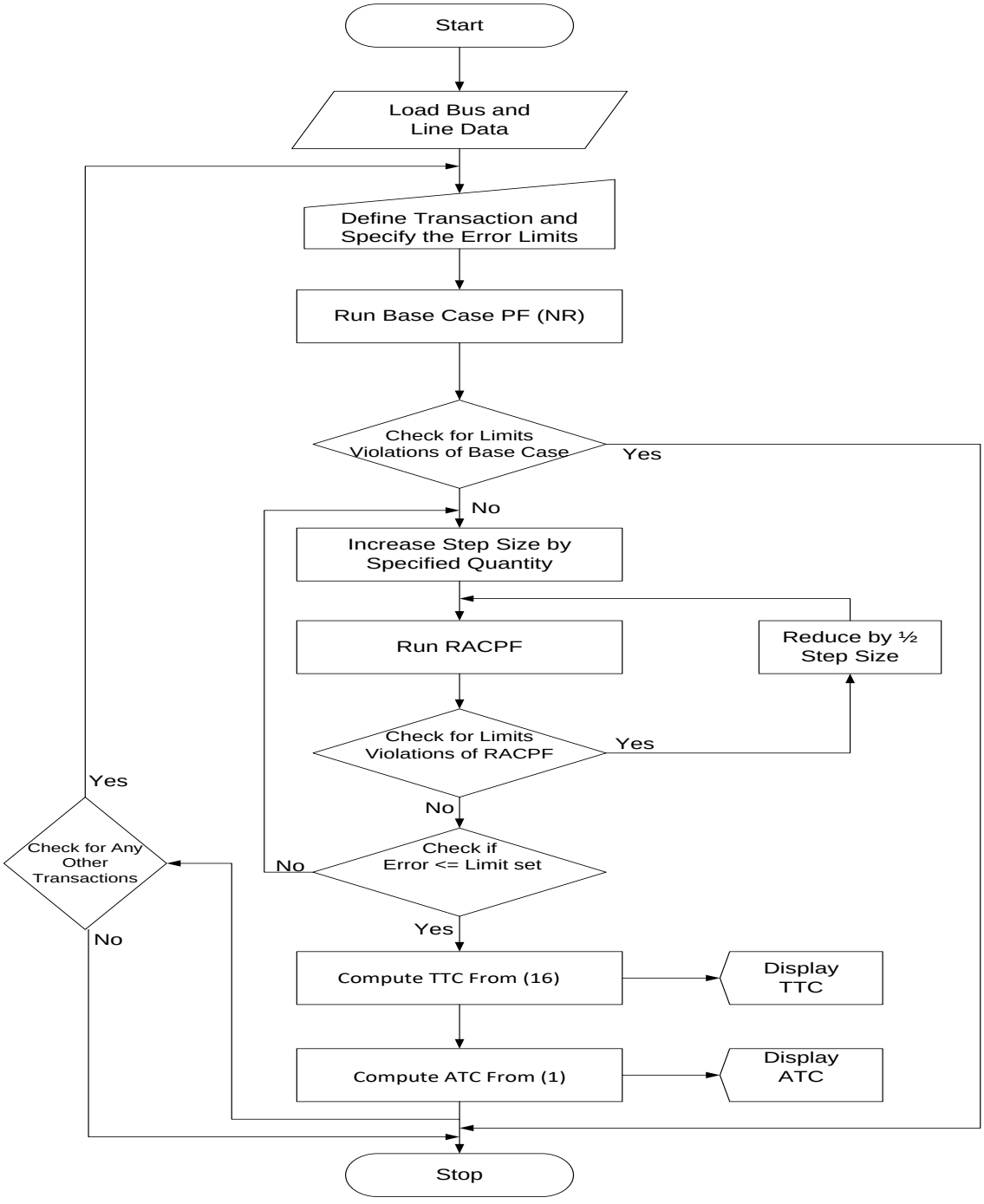


**Figure 3. 2: Flowchart of the RACPF**

### 3.3 ACPTDF method of ATC calculation

ACPTDF method of ATC computation which requires less time of computation has been adjudged simple, easy and non-iterative by [100],[140],[143],[144] hence, it is used for subsequent ATC determination after establishment of accuracy of the earlier method. ACPTDF gives the sensitivity factors of transmission line real power flow to line active power transfer [140].

Assuming $\Delta G_{xy}\ MW$ is the change in active power generation for a specific transaction between buyer bus y and seller bus x and that based on this transaction, there is a change in active power flow on the interconnected transmission line *i* and *j*, denoted by ($\Delta P_{ij}\ MW$) then, ACPTDF is represented by equation (3.18).

$$ACPTDF_{ij,xy} = \frac{\Delta P_{\ ij}\, MW}{\Delta G_{\ xy}\, MW}. \tag{3.18}$$

Where $\Delta P_{ij}\ MW$ is either the active power flow from bus *i* to *j* ($P_{ij}$) or from bus *j* to *i* ($P_{ji}$). These changes in real power flow can be obtained from Newton Raphson Jacobian elements at base case load flow as presented in equations (3.2) and (3.3).

The Jacobian polar coordinate is mathematically presented as follows;

$$\begin{bmatrix}\Delta\theta\\ \Delta V\end{bmatrix} = \begin{bmatrix}\frac{\partial P}{\partial\theta} & \frac{\partial P}{\partial V}\\ \frac{\partial Q}{\partial\theta} & \frac{\partial Q}{\partial V}\end{bmatrix}^{-1}\begin{bmatrix}\Delta P\\ \Delta Q\end{bmatrix} = [J_T]^{-1}\begin{bmatrix}\Delta P\\ \Delta Q\end{bmatrix} \tag{3.19}$$

Changes in real power flows along line $i-j$ as a result of the change in power transaction are presented in equation (3.20) and (3.21);

$$\frac{\partial P_{ij}}{\partial\theta_k} = \begin{Bmatrix}0 & for\ k\neq i,j\\ -V_iV_jY_{ij}\sin(\theta_i-\theta_j-\theta_{ij}) & for\ k=i\\ V_iV_jY_{ij}\sin(\theta_i-\theta_j-\theta_{ij}) & for\ k=j\end{Bmatrix}. \tag{3.20}$$

$$\frac{\partial P_{ij}}{\partial V_k} = \begin{Bmatrix}0 & for\ k\neq i,j\\ 2V_iV_jY_{ij}cos\theta_{ij}+V_iY_{ij}\cos(\theta_i-\theta_j-\theta_{ij}) & for\ k=i\\ V_iY_{ij}\sin(\theta_i-\theta_j-\theta_{ij}) & for\ k=j\end{Bmatrix}. \tag{3.21}$$

It should be noted that there will be a change in succeeding power mismatch in equation (3.19), if there is a change in power transaction as a result of $\Delta G_{xy}\ MW$. The values of these changes are non-zero and are represented by equation (3.22). This is also presented in equation (3.23) as real power mismatch vector $[\Delta P_i]$ representations.

$$\Delta P_i = \Delta G_{xy}\ MW;\ and\ \Delta P_j = -\Delta G_{xy}\ MW \tag{3.22}$$

$$[\Delta P_i] = \begin{bmatrix}0\\ (x)/\Delta G\\ \vdots\\ 0\\ \vdots\\ 0\end{bmatrix};\ [\Delta P_j] = \begin{bmatrix}0\\ 0\\ \vdots\\ (y)/-\Delta G\\ \vdots\\ 0\end{bmatrix},\ [\Delta Q_i] = [\Delta Q_j] = \begin{bmatrix}0\\ 0\\ \vdots\\ 0\\ \vdots\\ 0\end{bmatrix}. \tag{3.23}$$

For a deregulated market which is characterised by multiple transactions, the same procedure for bilateral holds for multiple transactions except for change in injected power matrix. Therefore, if there are group sellers *x* and *p*, involving in bilateral trading with another group of buyers *y* and *q*, whatever change experienced in trading is shared equally by both traders then, equation (3.23) becomes (3.24).

$$[\Delta P_i] = \begin{bmatrix} 0 \\ 0 \\ (x)/\Delta G \\ \vdots \\ 0 \\ (p)/\Delta G \\ \vdots \\ 0 \end{bmatrix}; [\Delta P_j] = \begin{bmatrix} 0 \\ 0 \\ \vdots \\ (y)/-\Delta G \\ 0 \\ (q)/-\Delta G \\ \vdots \\ 0 \end{bmatrix}, [\Delta Q_i] = [\Delta Q_j] = \begin{bmatrix} 0 \\ 0 \\ \vdots \\ 0 \\ 0 \\ 0 \\ \vdots \\ 0 \end{bmatrix}. \quad (3.24)$$

The mismatch elements from equations (3.19) to (3.21) are used to determine bus voltage magnitudes and voltage angles at all the buses. These new voltage magnitudes and angles are then used to obtain power flow in all the connected transmission lines and hence, change in power flow can be determined. ACPTDF can therefore be determined in each transmission line using equation (3.18), for any given power transaction. Equation (3.25) is used to obtain ATC between buses *x* and *y* for any given transaction.

$$ATC_{xy} = min\{T_{ij,xy}\} \; ; ij \in n_l \quad (3.25)$$

Transaction $T_{ij,xy}$ can be calculated as follows;

$$T_{ij,xy} = \begin{cases} \frac{P_{ij}^{max} - P_{ij}^{0}}{ACPTDF_{ij,xy}} & ; ACPTDF_{ij,xy} > 0 \\ \infty & ; ACPTDF_{ij,xy} = 0 \\ \frac{-P_{ij}^{max} - P_{ij}^{0}}{ACPTDF_{ij,xy}} & ; ACPTDF_{ij,xy} < 0 \end{cases}. \quad (3.26)$$

Where $P_{ij}^{max}$ *and* $P_{ij}^{0}$ are the maximum real power limit in MW and base case power flow between bus *i* and *j*. $T_{ij,xy}$ is power transfer's limits of transmission line.

### 3.4 Performance indices technique

Performance index (PI) deals with the deviation of the system variables from their rated values. This makes it suitable for relative contingency evaluation because contingencies are ranked in line with response of PI to the change initiated by same contingencies. Line flow real power loading, bus voltage magnitude limits and generators reactive power limits are considered in this PI estimate. In contingency study however the followings are involved;

#### 3.4.1 Contingency study and analysis

Contingency study and analysis involve three basic steps, namely; contingency creation, selection and evaluation. The definitions and explanations of these three steps are well reported in [40]. Here, line outage contingency was created while PI approach which involves real power line overload, voltage limit and generator reactive power limit are used for contingency selection.

##### 3.4.1.1 Line outage contingency creation

The load flow study of the transient steady state condition consequent each line outage has been adjudged the standard approach for contingency scrutiny of the steady state power system [178]. This is because outage of some lines may result into thermal and voltage limits violations, consequent of alterations in line parameters

following the outage. Line outage only was considered for this work after full ac load flow has been performed on the test system. Newton Raphson (NR) based ac load flow approach whose details are contained in [178] was adopted because of its accuracy. The real power and reactive power equations are as presented in equations (3.2) and (3.3).

#### 3.4.1.2 Ranking of contingency

The load flow is performed after each line outage and the ranking is done according to their sensitivities to the disturbance. The ranking of real power overload, voltage problems and generator reactive power limits are done separately. Sensitivity of each PI to outages determines order of ranking, usually from the most severe to the least ones. This is done with a view to evaluating and properly analyzing the performance of different ranking methods.

#### 3.4.1.3 Selection of contingency

The most severe contingency cases are evaluated and further analyzed. This is to be able to identify the most severe outage from the purposeful investigation. The pre and post contingency conditions are then comparatively analyzed.

### 3.4.2 Performance index methodologies

The diffferent performance index methodology involving real power, reactive power and voltage based PI as impelemented in this study are discussed as follows [34],[35],[36],[37],[38],[41];

#### 3.4.2.1 Performance index of real power flow ($PI_{\_P}$)

Equation (3.27) is the real power PI ($PI_{\_P}$), which reveals measures of line real power overload.

$$PI_{\_P} = \sum_{i}^{N} \frac{w_p}{2r} \left\{\frac{P_{ij}}{P_{ij}^{m}}\right\}^{2r} \tag{3.27}$$

$$P_{ij}^{m} = \frac{V_i V_j}{X_{ij}}. \tag{3.28}$$

Where $N$ is the bus number, $w_p$ is the real power non-negative weighting factor, $r$ is penalty function, $P_{ij}$ is real power flow on line *i-j*, $P_{ij}^{m}$ is the real power capacity limit, $V_i$ and $V_j$, are the voltages at bus *i and j* respectively while $X_{ij}$ is the line reactance between bus *i* and *j*.

#### 3.4.2.2 Voltage performance index ($PI_{\_V}$)

The deficiency of the system based on bus limit violation is measured by voltage PI ($PI_{\_V}$), therefore,

$$PI_{\_V} = \sum_{i}^{n} \frac{w_V}{2r} \left\{\frac{|V_i| - |V_i^{spec}|}{\Delta V_i^{limit}}\right\}^{2r}. \tag{3.29}$$

Here, $|V_i|$ is the bus *i* voltage magnitude, $|V_i^{spec}|$ is the bus *i* specified voltage magnitude, $w_V$ is the real non-negative weighting factor, while voltage deviation limits $\Delta V_i^{limit}$, is the value beyond which voltage becomes unacceptable, it is obtained from the mean value of minimum and maximum allowable voltage at bus *i*.

$\Delta V_i^{limit}$ reveals the severity of bus limit voltage violations because $PI_{\_V}$ becomes small when all voltage deviations fall within its value.

#### 3.4.2.3 Performance index of reactive power ($PI_{\_Q}$)

This index gives the constraints of reactive power capability of generators for contingency ranking. Reactive power flows determine bus voltages levels therefore once generating units are within their reactive power limits, values obtained for $PI_{\_V}$ gives reliable measurement of abnormal voltage severity otherwise, these values become unreliable. The inclusion of $PI_{\_Q}$ is to reveal the potency of reactive power flow constraints of generators in contingency analysis, therefore;

$$PI_{\_Q} = \sum_i^{ng} \frac{w_Q}{2r} \{\frac{Q_i}{Q_i^m}\}^{2r}. \quad (3.30)$$

Where $Q_i$ and $Q_i^m$ are bus *i* reactive power and reactive power limits, $ng$ is the number of generators and $w_Q$ is the real non-negative weighting factor.

#### 3.4.2.4 Contingency algorithm using PI

The algorithm developed for implementation of this study is itemized below:

(a) Obtain system data for network under study.
(b) Run a base case power flow such that network constraints are not violated, using NR approach.
(c) Implement a line outage contingency on a specified transmission line *i to j* by eliminating it from the network performance.
(d) Run network power flow after line outage.
(e) Compute values for $P_{ij}^m$ from equation (3.28) on the intact lines and hence determine corresponding $PI_{\_P}$ for numbers of lines using equation (3.27).
(f) Obtain the values for bus voltage magnitude, $|V_i|$.
(g) Compute corresponding values of $PI_{\_V}$ based on step (f) for numbers of buses using equation (3.29).
(h) Obtain values for $Q_i$ for numbers of generators.
(i) Obtain corresponding $PI_{\_Q}$ values with equation (3.30), based on step (h) for numbers of generators.
(j) Combine outage values of $PI_{\_P}$, $PI_{\_V}$ and $PI_{\_Q}$.
(k) Repeat steps (c) to (j) for remaining lines.
(l) Rank $PI_{\_P}$, $PI_{\_V}$ and $PI_{\_Q}$ values in descending order indicating the most severe to the least.
(m) Display various values of $PI_{\_P}$, $PI_{\_V}$ and $PI_{\_Q}$ obtained for all transmission lines in step (j.).
(n) Perform power flow on the most severe contingency for each of $PI_{\_P}$, $PI_{\_V}$ and $PI_{\_Q}$.

The above steps as itemized are presented in the flowchart shown in Fig. 3.3.

### 3.5 Static var compensator (SVC) Model

SVC is a general term used to describe single operation or combinations of thyristor controlled reactor, thyristor switched reactor and/ or thyristor switched capacitor shunt devices. A shunt connected SVC operates through constant variation or adjustment of its output shunt reactance to exchange inductive or capacitive current with connected system in order to regulate or control target and specific power network parameter(s). Typically, thyristor without competence for turn off capability through lack of gate signal formed basis of operation of

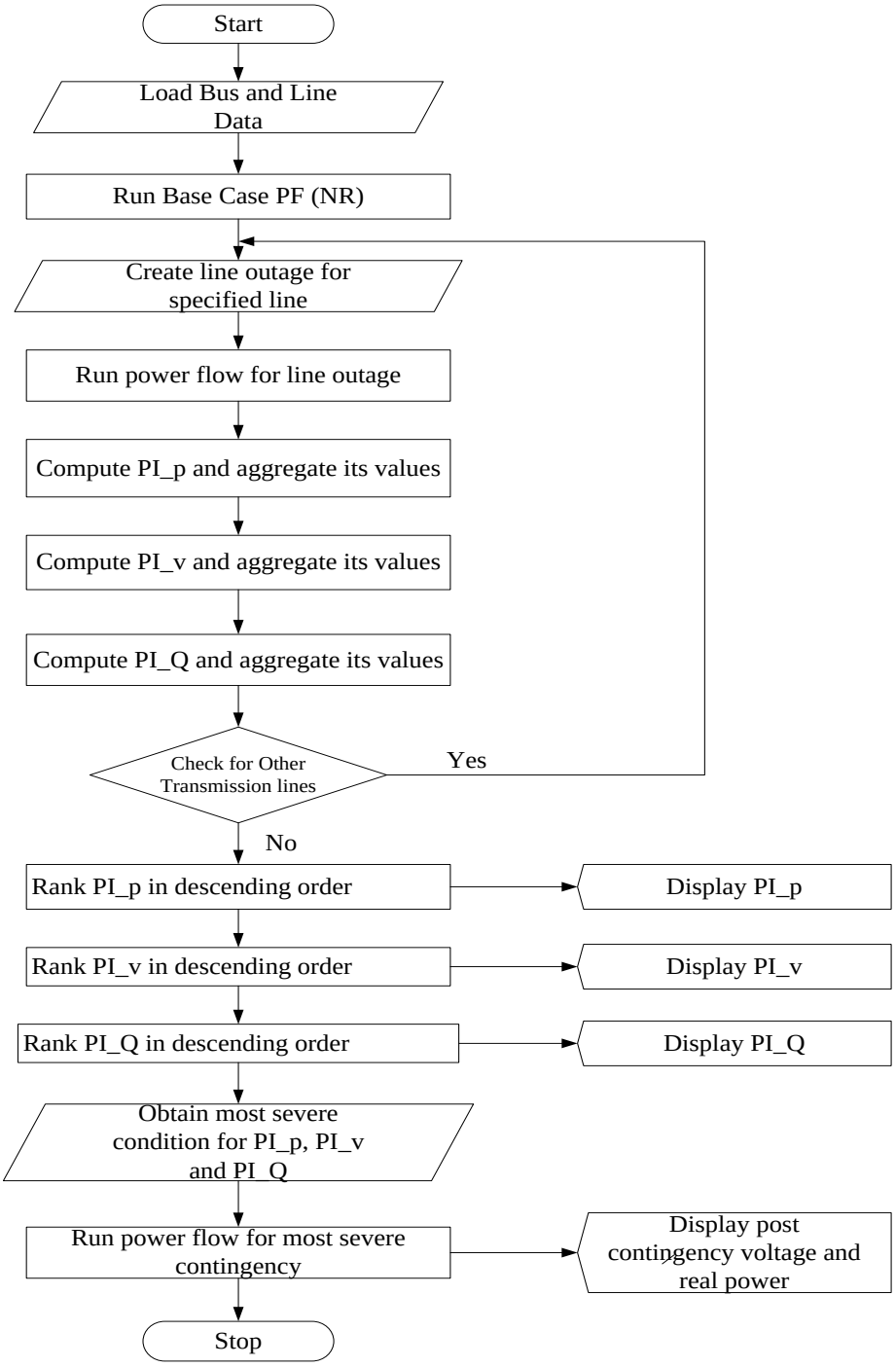


**Figure 3. 3: Flowchart for implementation of performance index methodology**

SVC. In SVC operation, the provision for leading var, that is reactive power absorption, is achieved through thyristor controlled reactor or thyristor switched reactor while that of reactive power generation, that is lagging var is accomplished through thyristor switched capacitor [51],[179].

The extensive and major applications of SVC are in the provision of quick reactive power control and voltage regulation services. These are made possible through instantaneous response speed of SVC occasioned by thyristor controlled firing angle [108]. The general representation of SVC is as presented in Fig. 3.4 [51], where from the figure, TCR implies thyristor controlled reactor, TSR connotes thyristor switched reactor, TSC entails thyristor switched capacitor, SVC means static var system and SVG implies static var generator

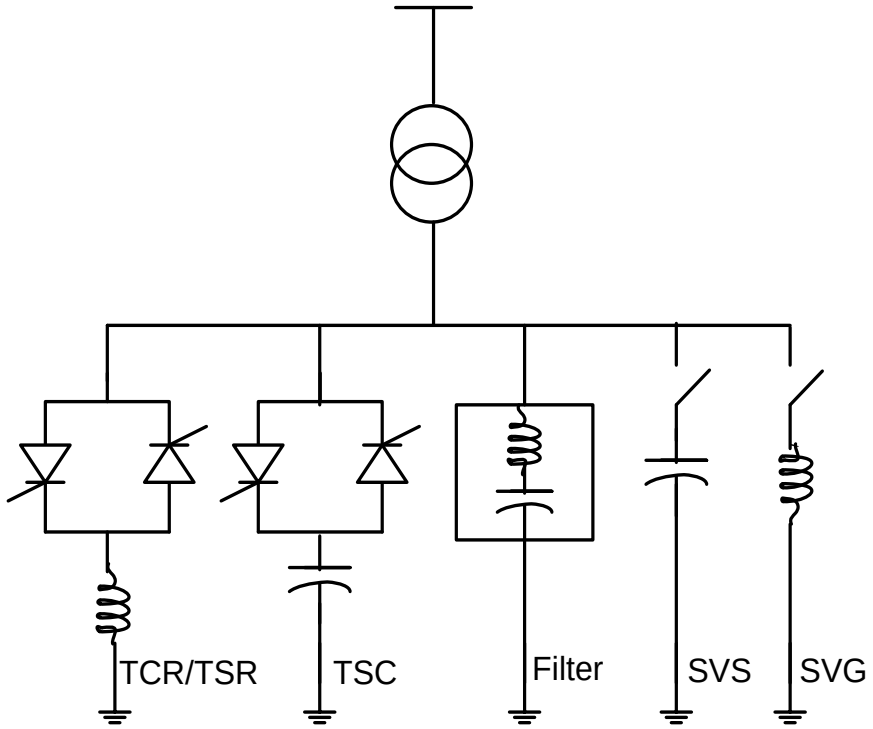


**Figure 3. 4: Structure of SVC**

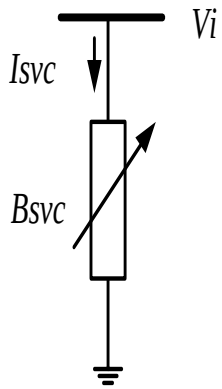


**Figure 3. 5: Equivalent circuit of SVC**

SVC equivalent model according to [51] is presented in Fig. 3.5. It is represented as an adjustable reactance with either reactance or firing angle limits. According to Fig. 3.4, the linearized and non linear power equations suitable for incorporation into Newton Raphson power are presented as follows:

Current and reactive power drawn by SVC from Fig. 3.5, are:

$$I_{SVC} = jB_{SVC}V_i \tag{3.31}$$

$$Q_{SVC} = Q_i = -V_i^2 B_{SVC}. \tag{3.32}$$

The linearized equation is presented as equation (3.33), while equivalent susceptance was considered as state variable.

$$\begin{bmatrix}\Delta P_i \\ \Delta Q_i\end{bmatrix}^k = \begin{bmatrix}0 & 0 \\ 0 & Q_i\end{bmatrix}^k \begin{bmatrix}\Delta\theta_i \\ \Delta B_{SVC}/B_{SVC}\end{bmatrix}^k. \tag{3.33}$$

Then at the end of iteration (k), shunt susceptance variable $B_{SVC}$ is updated according to equation (3.34).

$$B_{SVC}^k = B_{SVC}^{k-1} + \left(\frac{\Delta B_{SVC}}{B_{SVC}}\right)^k B_{SVC}^{k-1}. \tag{3.34}$$

This changing susceptance is the total susceptance of SVC required to maintain bus voltage magnitude at a fixed value.

### 3.6 Thyristor control series compensator/capacitor (TCSC) model

TCSC is made up of fixed capacitor in parallel with thyristor controlled reactor (TCR). This arrangement can be one or more segments for variation of resultant compensating series impedance and corresponding voltage. Within its range of operation, and having sufficient segment of schemes, TCSC can maintain and regulate voltage with reduced line current [180]. TCSC is similar to SVC in principle but while TCSC is series connected with transmission line, SVC is shunt connected with the bus. With an appropriate designed of TCR, TCSC can also offer inductive compensation, which because of practical realities, is an abridge form of its capacitive counterpart due to losses, reactor rating and thyristor valve voltage/current ratings [51],[181],[182].

Vithayathil and others in 1986 proposed basic scheme of TCSC as shown in Fig. 3.6. It was projected to be a fast adjustment method of network impedance which consists of a compensating capacitor shunted by a TCR [51]. The principle behind TCSC arrangement is the continuous provision of an adjustable capacitor through partial cancellation of operative compensating capacitance. Steady state impedance of TCSC ($X_{TCSC}(\alpha)$), comprises of fixed capacitive impedance $X_C$ and variable inductive impedance $X_L(\alpha)$ is specified by equation (3.35).

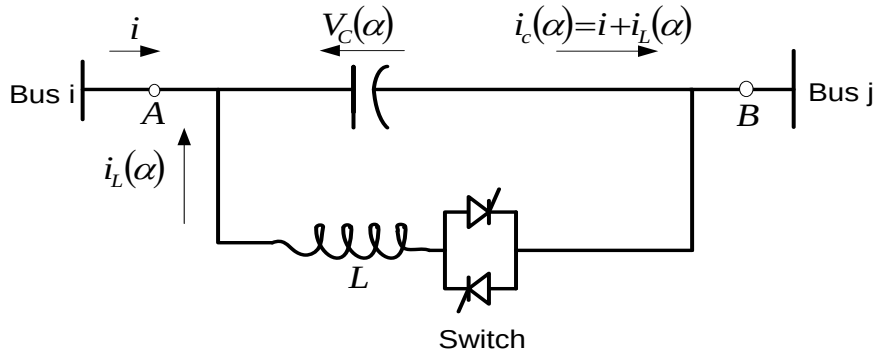


**Figure 3. 6: Basic scheme of TCSC**

$$X_{TCSC}(\alpha) = \frac{X_C X_L(\alpha)}{X_L(\alpha) - X_C}. \tag{3.35}$$

TCSC equivalent circuit can be represented as follows in Fig. 3.7, [140]. Where following limits holds; $\alpha_{C\_limit} \leq \alpha \leq \frac{\Pi}{2}$ for capacitive reactance, and $0 \leq \alpha \leq \alpha_{L\_limit}$ for inductive reactance.

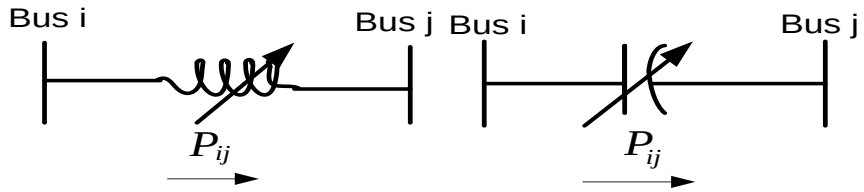


**Figure 3. 7: Equivalent circuit of TCSC**

Active and reactive power flow equations for bus $i$ when TCSC is connected between bus $i$ *and* $j$ are given by equations (3.36) and (3.37). Subscript $i$ is interchanged for $j$ for same power at bus $j$ and $X_{TCSC}$ is the TCSC reactance value.

$$P_i = V_i V_j B_{ij} \sin(\theta_i - \theta_j) \tag{3.36}$$

$$Q_i = -V_i^2 B_{ii} - V_i V_j B_{ij} \cos(\theta_i - \theta_j) \tag{3.37}$$

$$B_{ij} = 1/X_{TCSC}. \tag{3.38}$$

Equation (3.39) is the linearized Newton Raphson power flow Jacobian matrix equations when TCSC is controlling real power flowing from bus $i$ *to* $j$ at a specified value [140].

$$\begin{bmatrix} \Delta P_i \\ \Delta P_j \\ \Delta Q_i \\ \Delta Q_j \\ \Delta P_{ij}^{TCSC} \end{bmatrix} = \begin{bmatrix} \frac{\partial P_i}{\partial \theta_i} & \frac{\partial P_i}{\partial \theta_j} & \frac{\partial P_i}{\partial V_i} V_i & \frac{\partial P_i}{\partial V_j} V_j & \frac{\partial P_i}{\partial X_{TCSC}} X_{TCSC} \\ \frac{\partial P_j}{\partial \theta_i} & \frac{\partial P_j}{\partial \theta_j} & \frac{\partial P_j}{\partial V_i} V_i & \frac{\partial P_j}{\partial V_j} V_j & \frac{\partial P_j}{\partial X_{TCSC}} X_{TCSC} \\ \frac{\partial Q_i}{\partial \theta_i} & \frac{\partial Q_i}{\partial \theta_j} & \frac{\partial Q_i}{\partial V_i} V_i & \frac{\partial Q_i}{\partial V_j} V_j & \frac{\partial Q_i}{\partial X_{TCSC}} X_{TCSC} \\ \frac{\partial Q_j}{\partial \theta_i} & \frac{\partial Q_j}{\partial \theta_j} & \frac{\partial Q_j}{\partial V_i} V_i & \frac{\partial Q_j}{\partial V_j} V_j & \frac{\partial Q_j}{\partial X_{TCSC}} X_{TCSC} \\ \frac{\partial P_{ij}^{TCSC}}{\partial \theta_i} & \frac{\partial P_{ij}^{TCSC}}{\partial \theta_j} & \frac{\partial P_{ij}^{TCSC}}{\partial V_i} V_i & \frac{\partial P_{ij}^{TCSC}}{\partial V_j} V_j & \frac{\partial P_{ij}^{TCSC}}{\partial X_{TCSC}} X_{TCSC} \end{bmatrix} \begin{bmatrix} \Delta\theta_i \\ \Delta\theta_j \\ \frac{\Delta V_i}{V_i} \\ \frac{\Delta V_j}{V_j} \\ \frac{\Delta X_{TCSC}}{X_{TCSC}} \end{bmatrix} \tag{3.39}$$

$$\Delta P_{ij}^{X_{TCSC}} = P_{ij}^{reg} - P_{ij}^{X_{TCSC,cal}} \quad (3.40)$$

$$\Delta X_{TCSC} = X_{TCSC}^{(k)} - X_{TCSC}^{(k-1)}. \quad (3.41)$$

TCSC mismatch active power flow is $\Delta P_{ij}^{X_{TCSC}}$, incremental change in series reactance is $\Delta X_{TCSC}$, while $P_{ij}^{X_{TCSC,cal}}$ is the calculated power given by equation (3.36).

## 3.7 FACTS placement methods

Placement of FACTS devices is very crucial to its performance. Briefly, the following are some of the analytical placement methods, especially for enhancement of ATC.

### 3.7.1 Base case real power loss placement method (PTLB)

Transmission line real power losses are obtained at base case power flow and ranked in order of severity. The line with highest loss magnitude is considered for device location [108],[143].

### 3.7.2 Performance index placement method (PI)

Real power performance index of a given network is obtained and the highest ranked value of real power performance index obtained is used for device placement in this method [138]. Equations (3.27) and (3.28) form the basis of ranking in this context.

### 3.7.3 Total real power loss sensitivity (PTLS)

Transmission line with highest ranked sensitivity index based on total real power loss equation is used for device placement in this method [146].

### 3.7.4 Loss sensitivity with respect to line reactance (XTL)

Line having the most positive loss sensitivity index when total reactive power loss equation is differentiated with respect to line reactance is considered for device placement. The resultant derivatives of reactive power of the total loss equation with respect to line reactance gives the sensitivity index [145].

### 3.7.5 Power transfer distribution factor (PTDF)

Line with lower magnitude of sensitivity variation based on PTDF values for the considered transaction is used for device placement as in [144]. However, PTDF can be alternating current or direct current based as earlier discussed in this thesis.

### 3.7.6 Line thermal limiting element (TL)

The limiting transmission line of network system was identified and used for device location as in [139],[140]. Line with the least thermal limit will impact on the transmission capability of the network.

### 3.7.7 Least bus voltage magnitude (LBV)

Bus voltage magnitudes are critically examined for a particular transaction and the bus with least voltage magnitude is considered for device placement as in [128],[141].

### 3.7.8 Value of line transfer capability (LTC)

Just as implemented in [148], line with lowest value of transfer capability is incorporated with device in order to enhance the transfer capacity of that line.

## 3.8 Optimization algorithms methodology

Two optimization algorithms involving brain storm optimization and particle swarm optimization algorithms are implemented for FACTS device placement in this study and are discussed as follows;

### 3.8.1 Brain storm optimization algorithm (BSOA)

This section presents the methodology involved in implementation of BSOA. An overview of BSOA, the basic operation and its flow charts are described in subsequent paragraphs.

#### 3.8.1.1 BSOA

BSOA is a new and promising heuristic algorithm premeditated upon brainstorming process. It is problem solving capability mimics collective behavior of human beings, having the notion that humans are the most intelligent of all creatures [95],[183]. The idea of brainstorming process which was first promulgated in 1953 by Osborn was developed into a novel optimization algorithm by Shi in 2011 [95],[183],[184]. Osborn's four rules which form the basis of BSO algorithm are: (i) all ideas are acceptable at the inception of ideation, (ii) during ideation, criticism is not allowed, (iii) welcome diverse and unconventional ideas as the focus is on quantities of ideations and, (iv) cross-fertilize, exchange, combine and amalgamate ideas to produce more and better ideas [21]. The algorithm processes involved in human brainstorming are as follows [96],[184]:

(a) Initialization – People with different profiles and dissimilar backgrounds are gathered.
(b) New quantity ideas based on Osborn's rules are generated.
(c) Related ideas having same subject matter are clustered into groups.
(d) The ideas in (c) are assessed and authenticated by experts.
(e) More ideas picked at random are used to obtain new and more ideas.
(f) New ideas stirred from old ones are generated.
(g) Repeat steps (b) – (f) to obtain a better solution for the problem in question.

The basic operation of BSOA is categorized into four fundamental procedures from above process involve initialization, clustering, cluster center disruption and individual perturbation [185],[186]. These are briefly explained as follows:

i. Initialization - This involves randomly generation of N-individuals and evaluate N-individuals.
ii. Clustering - Convergent operation of partitioning of individual population into clusters. K-implies clustering algorithm used.
iii. Cluster center disruption – Cluster center which corresponds to best idea is the best individual in a cluster. With a small probability $P_s$, cluster center is replaced with a randomly generated individual. Value of $P_s$ is important for the control capability of BSOA, the higher it is the better is performance capability.

iv. Individual perturbation – New individuals in the clusters are obtained according to original BSOA as presented in equations (3.41) – (3.42) [95],[183],[184],[185],[186];

$$x_{new}^{i}(t) = x_{old}^{i}(t) + \xi(t) \times N(\mu, \sigma^2) \tag{3.42}$$

$$\xi(t) = logsig\left(\frac{0.5 \times T - t}{k}\right) \times rand(0,1) \tag{3.43}$$

The notation $N(\mu, \sigma^2)$ is a random variable obtained with Gaussian distribution with mean zero and standard deviation one. Current iteration is $t$, while $T$ is the total number of iterations. $\xi(t)$ is the step-size-function utilized to equalize the speed of convergence of algorithm, while k is the coefficient that changes slope of $logsig()$ function. $x_{new}^{i}$ and $x_{old}^{i}$ denote dimension $i$th iteration of $x_{new}$ and $x_{old}$ respectively. Random function $rand(0,1)$ is used to generate uniformly but random numbers between zero and one. The process of cluster center disruption and individual perturbation continues until stopping criteria is fulfilled.

The flow chat of BSO process as itemized above is depicted as follows in Fig. 3.8 [96],[184];

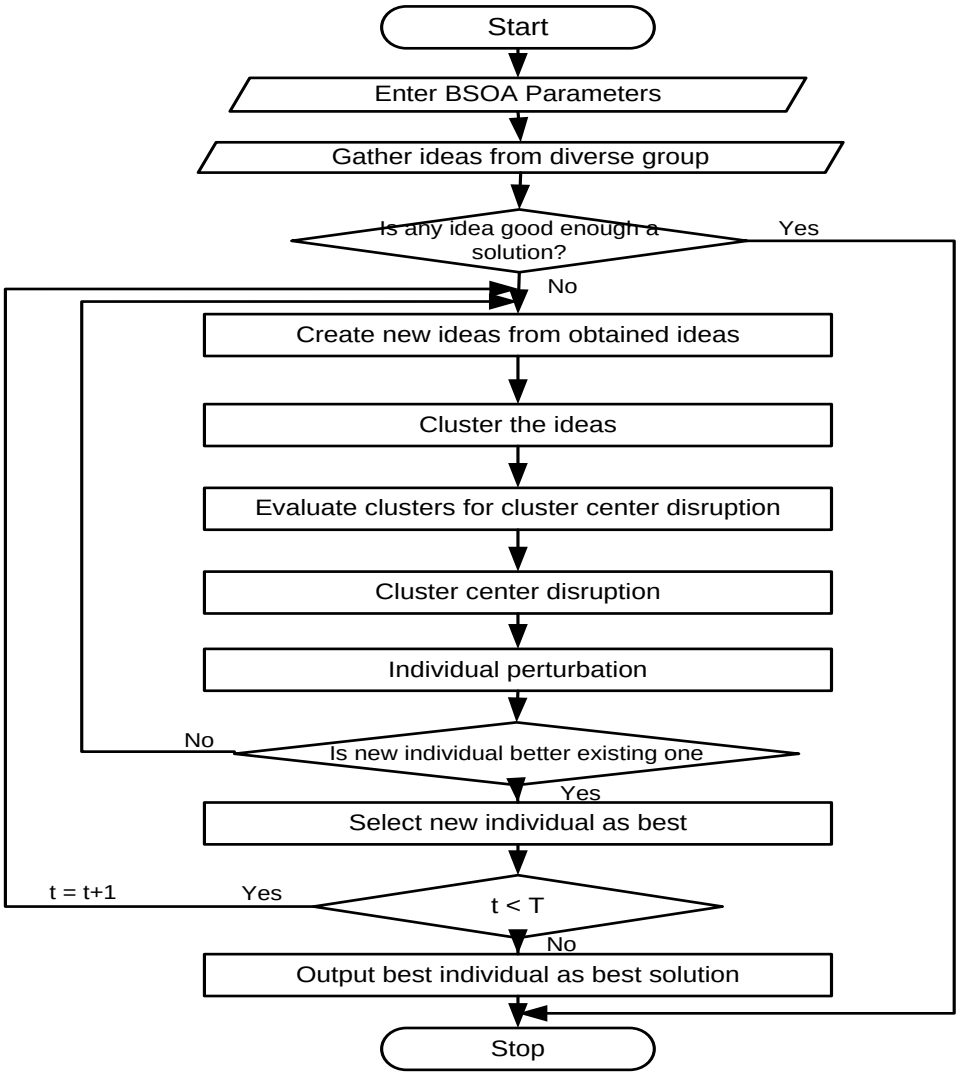


**Figure 3. 8: Flow chat of the processes involved in BSOA solution**

Transmission line total reactance ($X_{Total}$) incorporating TCSC comprises both TCSC and line reactance. Therefore equation (3.35) becomes

$$X_{Total} = X_{line} + X_{TCSC}(\alpha) \tag{3.44}$$

Introducing α as an expression for degree of compensation of line reactance, and substitute this in equation (3.44), results into equations (3.45) – (3.47) [97].

$$X_{TCSC}(\alpha) = \alpha \times X_{line} \tag{3.45}$$

$$X_{Total} = X_{line} + \alpha \times X_{line} \tag{3.46}$$

$$X_{Total} = (\alpha + 1)X_{line} \tag{3.47}$$

### 3.8.2 Multi-objective optimization problem formulation

In order to benefit maximumly from FACTS installation for the desired objectives, optimal setting of the device must be ensured. The objectives functions in this study are; ATC maximization (enhancement), bus voltage profile deviation minimization and real power loss control.

#### 3.8.2.1 Available transfer capability maximization

Enhancement of ATC is very crucial for secure and economic power system transactions. ATC enhancement between two buses *i* and *j* is represented as max ($ATC_{xy}$), where $ATC_{xy}$ is given as equation (3.25), therefore,

$$\mu_1 = \frac{ATC_{xyTCSC}}{ATC_{xy}} \tag{3.48}$$

Where $ATC_{xy}$ is transfer capability without TCSC and $ATC_{xyTCSC}$ is the transfer capacity with TCSC.

#### 3.8.2.2 Transmission line real power loss regulation

The active power loss presented by equation (3.49) has to be minimized if transfer capability will be maximized [100]. This is required in addition to power flow control of the FACTS device.

$$P_{TL} = \sum_{k=1, i \neq j}^{nl} G_{ij}\left(V_i^2 + V_j^2 - V_i V_j \, Cos(\theta_i - \theta_j)\right) \tag{3.49}$$

$$\mu_2 = \frac{P_{TL(TCSC)}}{P_{TL}} \tag{3.50}$$

$P_{TL}$ and $P_{TL(TCSC)}$ are the total power loss without and with TCSC respectively. $G_{ij}$ is the conductance between lines *i and j*, $nl$ is the number of transmission lines, $V_i$ & $V_i$ *and* $\theta_i$ & $\theta_j$ are the voltages and voltage angles at bus *i* and *j* respectively.

#### 3.8.2.3 Bus voltage profile deviation minimization

Voltage instability consequence of swell or sag usually resulted into system security violation. Bus voltage is expected to be within the upper limit of 1.05 and lower limit of 0.95 p.u. Voltage deviation minimization function is given as [97],[122];

$$VD = \sum_{i=1}^{N} \left| V_{iref} - V_i \right| \tag{3.51}$$

$$\mu_3 = \frac{VD_{TCSC}}{VD} \tag{3.52}$$

$VD_{TCSC}\ and\ VD$ are the voltage deviation with and without TCSC.

These objectives are then normalized and translated into a single objective having fitness function denoted by $\mu$, as in equation (3.53).

$$\mu = \beta_1\mu_1 + \beta_2\mu_2 + \beta_3\mu_3 \tag{3.53}$$

$\beta_1, \beta_2, and\ \beta_3$ are scaling factors which are described by the following conditions in equation (3.54).

$$\beta_1 + \beta_2 + \beta_3 = 1 \qquad \& \quad 0 < \beta_1, \beta_2, \beta_3 < 1. \tag{3.54}$$

Most importantly the following power equality constraints equations must be satisfied. Where $P_{Gi}$ , $P_{Di}$, and $P_{Ci}$ are the generated, demand/load and calculated real powers in that order; $Q_{Gi}$ , $Q_{Di}$ and $Q_{Ci}$ are the generated, demand/load and calculated reactive powers respectively [100].

$$P_{Gi} - P_{Di} = \sum_{j=1}^{N} |V_i||V_j||Y_{ij}| \cos(\theta_{ij} - \theta_i + \theta_j) \tag{3.55}$$

$$Q_{Gi} - Q_{Di} = \sum_{j=1}^{N} |V_i||V_j||Y_{ij}| \sin(\theta_{ij} - \theta_i + \theta_j) \tag{3.56}$$

In addition, and among others, the following inequality equations (3.57) – (3.58) must also be met. Bus voltage lower and upper limits described by equation (3.57) and the decisive TCSC reactance limits described by equation (3.58).

$$V_{imin} \leq V_i \leq V_{imax} \tag{3.57}$$

$$X_{TCSCmin} \leq X_{TCSC} \leq X_{TCSCmax} \tag{3.58}$$

### 3.9 Particle swarm optimization algorithm (PSO)

PSO is a stochastic, swarm based intelligent optimization technique, inspired through biological processes. It was first introduced by Kennedy and Eberhart in 1995 [187]. The concepts of PSO emanated from mimicking behavioral tendencies of animal cultures, devoid of leader in the swarm or group, such as fish schooling and bird flocking, by simulating these attributes in multidimensional space. Naturally, the search of food by group of animals without a leader becomes random and there is tendency to explore in the region of a member with proximity to food source, referred to as potential solution. This continues and the animals accomplish their best concurrently through constant exchange of information among their peers who already achieved better condition. Simultaneous movement of the flocks toward source of food will follow the information disseminated from animal with better food source and this occurs repeatedly until the best source of food is discovered [187],[188],[189]. Similarly, PSO algorithm adopts this animal interactive processes in finding optimal solution to a particular problem. Summarily, PSO consists clouds, in which a potential solution is represented by a particle.

PSO like most search algorithms is characterized with explorative and exploitative abilities. Exploration implies its ability to explore diverse area of search infinite with a view to locating good optimal, while exploitation indicates its aptitude to focus the search around the locality of the predicting region for perfecting candidate solution. With these characteristics, swarm particles hover in space with two major indispensable cognitive capabilities involving memory of particle's individual best location referred to as 'local best' and memory of neighborhood or global particles best position also referred to as 'global best'. Meanwhile, the position of particle *i* in space and at time *t* denoted by $x_i(t)$ is determined by velocity $v_i(t)$. The velocity $v_i(t)$ is defined by equation (3.59) [140], [144], [145].

$$v_i(t) = v_i(t-1) + c_1 r_1\big(localbest(t) - x_i(t-1)\big) + c_2 r_2(globalbest(t) - x_i(t-1)) \quad (3.59)$$

The change in position of a particle is achieved with addition of velocity $v_i(t)$ to its current position, as presented in equation (3.60)

$$x_i(t+1) = x_i(t) + v_i(t+1) \quad (3.60)$$

Where $c_1$ & $c_2$ are acceleration coefficients and $r_1$ & $r_2$ are random vectors. The flowchart for implementation of PSO is as presented in Fig. 3.9 [140],[148].

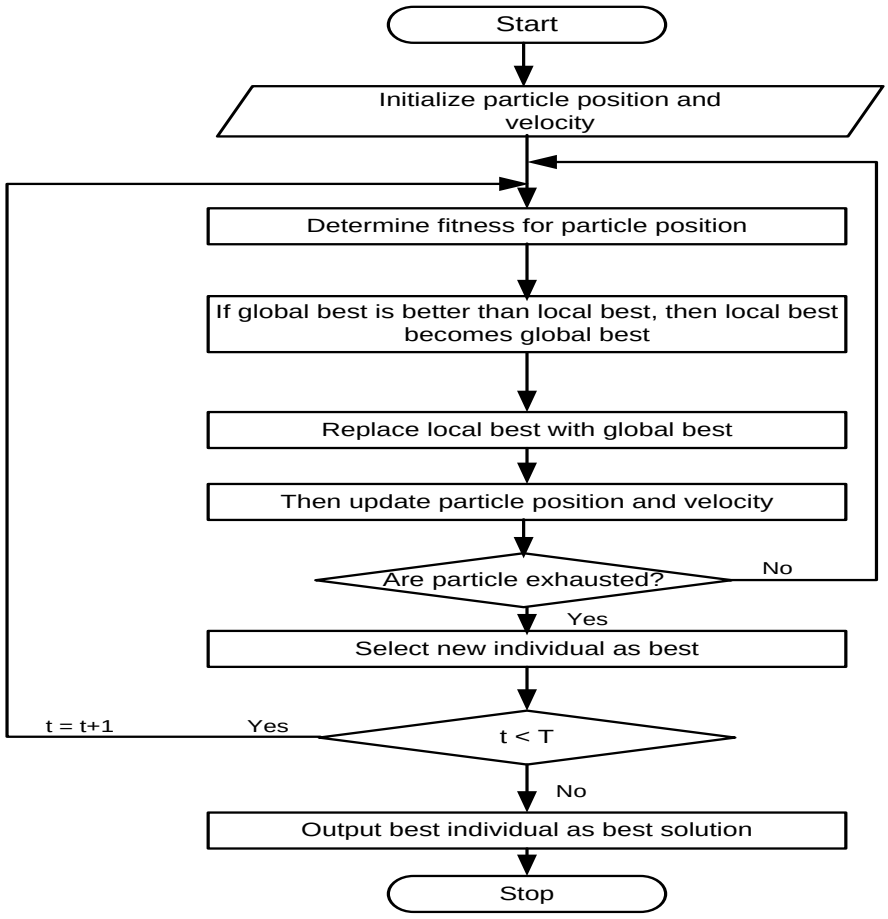


**Figure 3. 9: Flow chat for implementation of PSO algorithm**

### 3.10 Sensitivity based placement method for TCSC device

Sensitivity based method of FACTS device placement is proposed in this subheading for its optimal performance. This approach cannot be Implemented for TCSC if it is not modelled analytically as against the conventional model. The model is to obtain both voltage magnitude and angle of voltage injection which are the factor to be considered for placement of this device. Likewise, this sensitivity-based method for VSC-HVDC transmission system optimal placement is presented in subsequently.

#### 3.10.1 Analytical model of TCSC

A typical TCSC as shown in Fig. 3.6, can provide continuous control of power on ac line with a variable series capacitive reactance. In principle, and as stated earlier, TCSC is very similar to a Static var compensator (SVC), except that the former is regularly series connected with a transmission line while the latter is usually shunt connected with targeted bus [51]. Likewise, a TCSC can be represented analytically by an equivalent static synchronous series compensator (SSSC) for power flow analysis [180]. For the purpose of this analysis, TCSC is analytically represented by equivalent circuit of SSSC as shown in Fig. 3.10, as different from the usual representation presented in Fig. 3.7 [97],[108],[139],[140],[145],[146],[148]. The equivalent $X_{TCSC}\ (\alpha)$ can be represented by series impedance $Z_s$ with a regulated voltage source $V_s$ as shown in Fig. 3.10. In the practical operations, $V_s$ can be regulated in order to control line power flow $P_{ij}\ or\ P_{ji}$.

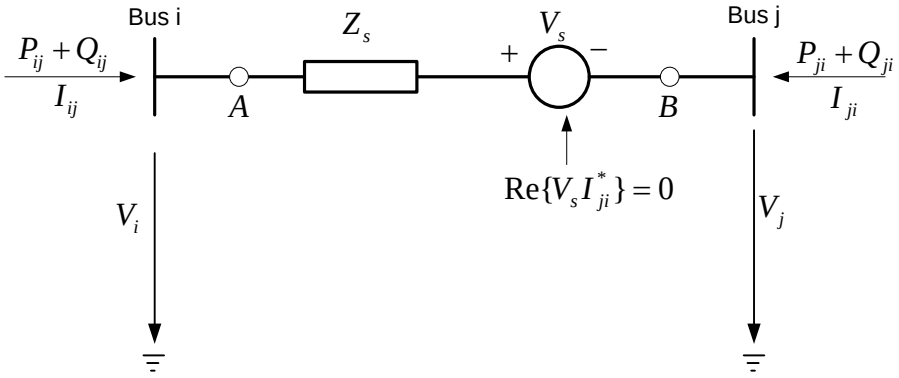


**Figure 3. 10: Analytical equivalent circuit of thyristor controlled series compensator**

In line with equivalent circuit above, $V_s = V_s\angle\,\theta_{s,}\ V_i = V_i\angle\,\theta_{i,}\ V_j = V_j\angle\,\theta_{j,}$ therefore, the power flow constraints at bus $i\ and\ j$ are [83],[180];

$$P_{ij} = V_i^2 G_{ii} - V_i V_j\left(G_{ij}cos\,\theta_{ij} + B_{ij}sin\,\theta_{ij}\right) - V_i V_s\left(G_{ij}\cos\left(\theta_i-\theta_s\right) + B_{ij}\sin\left(\theta_i-\theta_s\right)\right) \quad (3.61)$$

$$Q_{ij} = -V_i^2 B_{ii} - V_i V_j\left(G_{ij}sin\,\theta_{ij} - B_{ij}cos\,\theta_{ij}\right) - V_i V_s\left(G_{ij}\sin(\theta_i-\theta_s\right) - B_{ij}\cos\left(\theta_i-\theta_s\right)) \quad (3.62)$$

$$P_{ji} = V_j^2 G_{ii} - V_i V_j\left(G_{ij}cos\,\theta_{ji} + B_{ij}sin\,\theta_{ji}\right) + V_j V_s\left(G_{ij}\cos(\theta_j-\theta_s\right) + B_{ij}\sin\left(\theta_j-\theta_s\right)) \quad (3.63)$$

$$Q_{ji} = -V_j^2 B_{jj} - V_i V_j\left(G_{ij}sin\,\theta_{ji} - B_{ij}cos\,\theta_{ji}\right) + V_j V_s\left(G_{ij}\sin(\theta_j-\theta_s\right) - B_{ij}\cos\left(\theta_j-\theta_s\right)) \quad (3.64)$$

where $G_{ij} + B_{ij} = 1/Z_s$, $G_{ii} = G_{ij}$, $B_{ii} = B_{ij}$, $G_{jj} = G_{ij}$, $B_{jj} = B_{ij}$.

It should be noted that the first and second terms of equations (3.61) and (3.62) are the real and reactive power flows from bus *i to j* and that of equations (3.63) and (3.64) are the real and reactive power flows from bus *j to i* as can be derived from equivalent $\pi$-network representation of a transmission lines with lump parameters connected bus *i to j*.

The operating constraint of TCSC for real power exchange through dc link is given by [141]:

Power exchange = $Re\ (V_s\, I_{ji}^*) = 0.$ (3.65)

$$Re\ (V_s\, I_{ji}^*) = -\,V_i V_s \left(G_{ij}\ \cos(\theta_i - \theta_s\right) +\ B_{ij} \sin\ (\theta_i - \theta_s))\ +\ V_j V_s \left(G_{ij}\ \cos(\theta_j - \theta_s\right) +\ B_{ij} \sin\ (\theta_j - \theta_s)) \quad (3.66)$$

In practical applications with this model, and considering equation (3.65), the device can be used for control of any of active or reactive power flow of the transmission line, bus voltage as well as impedance of the transmission line [180]. Since the main objective is to enhance ATC, the impedance (reactance) control which is a function of $V_s$ is implemented. $V_s$ is regulated to control equivalent reactance of the device to a specified value, bounded by stated $X_{TCSC}$ lower and upper limits which ranges from -0.05 to 0.05 for this work. Therefore, the control parameters are $V_s$ and $\theta_s$.

### 3.10.2 FACTS device loss consideration for optimal location and placement

The inclusion of FACTS device loss in this formulation is to enhance ATC, improve bus voltage and reduce the total system loss as the part of the objectives in this study. This is because the set objective may not be properly achieved with improper deployment of FACTS. Therefore, to reduce system loss, FACTS loss must be included in the system loss. Hence,

Total system loss with FACTS ($P_{TL}$ ) = System Loss + FACTS Loss. (3.67)

Equation (3.67) can be written as equation (3.68) for TCSC device that is connected between bus *i* and *j* as in Fig. 3.6*;*

$$P_{TL}\ = P_L + \left(P_{i\_TCSC} +\ P_{j\_TCSC}\right). \quad (3.68)$$

System loss formula as given by [145],[146], and [190], is;

$$P_L\ =\ \sum_{i=1}^{N}\sum_{j=1}^{N}\left[\alpha_{ij}\ \left(P_i P_j +\ Q_i Q_j\right) +\ \beta_{ij}\left(Q_i P_j -\ P_i Q_j\right)\right]. \quad (3.69)$$

Where, $P_i\ and\ P_j$ are real powers injected at bus *i* and *j*, $Q_i\ and\ Q_j$ are reactive powers injected at bus *i* and *j*, while $\alpha_{ij}\ and\ \beta_{ij}$ are the loss coefficients and are given by;

$$\alpha_{ij} = \frac{R_{ij}}{V_i V_j}\cos\left(\theta_i -\ \theta_j\right)\ and\ \beta_{ij} = \frac{R_{ij}}{V_i V_j}\sin\left(\theta_i -\ \theta_j\right). \quad (3.70)$$

Here, $R_{ij}$ is the real part of row *i* and column *j* element of the impedance (Z) bus matrix. This can be obtained from the inverse of admittance matrix elements.

The sensitivity factors are obtained with partial derivatives of total system real power loss with respect to the control parameters $V_s$ and $\theta_s$ of TCSC placed on transmission line T, connecting bus *i* and *j*. These factors are defined below, where T = 1, 2, 3 …..*nl*, and *nl* is the total number of transmission lines.

In this study and as presented in chapter seven, total loss sensitivity with respect to $V_s$ at $V_s = 0$ is denoted by $a_1^{TCSC}$, and this is mathematically obtained from equation (3.69) by partial derivatives as presented in equation (3.71).

$$a_1^{TCSC} = \frac{\partial P_L}{\partial V_s}\Big|_{V_{s=0}} \tag{3.71}$$

Also, total loss sensitivity with respect to $\theta_s$ at $\theta_s = 0$ is denoted by $a_2^{TCSC}$, obtained mathematically from equation (3.69) by partial derivatives as presented in equation (3.72).

$$a_2^{TCSC} = \frac{\partial P_L}{V_s \partial \theta_s}\Big|_{\theta_{s=0}} \tag{3.72}$$

These factors $a_1^{TCSC}\ and\ a_2^{TCSC}$ which are then computed from equations (3.68) and (3.69) are presented as equations (3.72) and (3.73), for a transmission line connecting bus *i* and *j*,

$$a_1^{TCSC} = \frac{\partial P_L \partial P_i}{\partial P_i \partial V_s}\Big|_{V_{s=0}} + \frac{\partial P_L \partial P_j}{\partial P_j \partial V_s}\Big|_{V_s=0} + \frac{\partial P_L \partial Q_i}{\partial Q_i \partial V_s}\Big|_{V_s=0} + \frac{\partial P_L \partial Q_j}{\partial Q_j \partial V_s}\Big|_{V_s=0} - \left(\frac{\partial P_i}{\partial V_s} + \frac{\partial P_j}{\partial V_s}\right)\Big|_{V_{s=0}} \tag{3.73}$$

$$a_2^{TCSC} = \frac{\partial P_L \partial P_i}{\partial P_i V_s \partial \theta_s}\Big|_{\theta_{s=0}} + \frac{\partial P_L \partial P_j}{\partial P_j V_s \partial \theta_s}\Big|_{\theta_s=0} + \frac{\partial P_L \partial Q_i}{\partial Q_i V_s \partial \theta_s}\Big|_{\theta_s=0} + \frac{\partial P_L \partial Q_j}{\partial Q_j V_s \partial \theta_s}\Big|_{\theta_s=0} - \left(\frac{\partial P_i}{V_s \partial \theta_s} + \frac{\partial P_j}{V_s \partial \theta_s}\right)\Big|_{\theta_{s=0}}. \tag{3.74}$$

Arising from equation (3.69),

$$\frac{\partial P_L}{\partial P_i} = 2\sum_{i=1}^{N} \alpha_{ij} P_j - \beta_{ij} Q_j \tag{3.75}$$

$$\frac{\partial P_L}{\partial P_j} = 2\sum_{j=1}^{N} \alpha_{ij} P_i + \beta_{ij} Q_i \tag{3.76}$$

$$\frac{\partial P_L}{\partial Q_i} = 2\sum_{i=1}^{N} \alpha_{ij} Q_j + \beta_{ij} P_j \tag{3.77}$$

$$\frac{\partial P_L}{\partial Q_j} = 2\sum_{j=1}^{N} \alpha_{ij} Q_i - \beta_{ij} P_i. \tag{3.78}$$

The derivatives of terms $\frac{\partial P_i}{\partial V_s}\Big|_{V_{s=0}}, \frac{\partial P_j}{\partial V_s}\Big|_{V_{s=0}}, \frac{\partial P_i}{V_s \partial \theta_s}\Big|_{\theta_{s=0}}, and\ \frac{\partial P_j}{V_s \partial \theta_s}\Big|_{\theta_{s=0}}$ with respect to FACTS parameters are determined from equations (3.61) and (3.63) and are presented below:

$$\frac{\partial P_i}{\partial V_s}\Big|_{V_s=0} = \frac{\partial P_{ij}}{\partial V_s}\Big|_{V_s=0} = -V_i\,(G_{ij} cos\,\theta_i + B_{ij}\, sin\theta_i) \tag{3.79}$$

$$\frac{\partial P_j}{\partial V_s}\Big|_{V_s=0} = \frac{\partial P_{ji}}{\partial V_s}\Big|_{V_s=0} = +V_j\,(G_{ij} cos\,\theta_j + B_{ij}\, sin\theta_j) \tag{3.80}$$

$$\left.\frac{\partial P_i}{V_s \partial \theta_s}\right|_{\theta_s = 0} = \left.\frac{\partial P_{ij}}{V_s \partial \theta_s}\right|_{\theta_s = 0} = -V_i\,(G_{ij} sin\,\theta_i - B_{ij}\,cos\theta_i) \tag{3.81}$$

$$\left.\frac{\partial P_j}{V_s \partial \theta_s}\right|_{\theta_s = 0} = \left.\frac{\partial P_{ji}}{V_s \partial \theta_s}\right|_{\theta_s = 0} = +V_j\,(G_{ij} sin\,\theta_j - B_{ij}\,cos\theta_j). \tag{3.82}$$

Likewise, the derivatives of terms $\left.\frac{\partial Q_i}{\partial V_s}\right|_{V_s=0}, \left.\frac{\partial Q_j}{\partial V_s}\right|_{V_s=0}, \left.\frac{\partial Q_i}{V_s \partial \theta_s}\right|_{\theta_s=0}, and\ \left.\frac{\partial Q_j}{V_s \partial \theta_s}\right|_{\theta_s=0}$, with respect to FACTS parameters are determined from equations (3.62) and (3.64) and are presented below:

$$\left.\frac{\partial Q_i}{\partial V_s}\right|_{V_s = 0} = \left.\frac{\partial Q_{ij}}{\partial V_s}\right|_{V_s = 0} = -V_i\,(G_{ij} sin\,\theta_i - B_{ij}\,cos\theta_i) \tag{3.83}$$

$$\left.\frac{\partial Q_j}{\partial V_s}\right|_{V_s = 0} = \left.\frac{\partial Q_{ji}}{\partial V_s}\right|_{V_s = 0} = +V_j\,(G_{ij} sin\,\theta_j - B_{ij}\,cos\theta_j) \tag{3.84}$$

$$\left.\frac{\partial Q_i}{V_s \partial \theta_s}\right|_{\theta_s = 0} = \left.\frac{\partial Q_{ij}}{V_s \partial \theta_s}\right|_{\theta_s = 0} = +V_i\,(G_{ij} cos\,\theta_i + B_{ij}\,sin\theta_i) \tag{3.85}$$

$$\left.\frac{\partial Q_j}{V_s \partial \theta_s}\right|_{\theta_s = 0} = \left.\frac{\partial Q_{ji}}{V_s \partial \theta_s}\right|_{\theta_s = 0} = -V_j\,(G_{ij} cos\,\theta_j + B_{ij}\,sin\theta_j) \tag{3.86}$$

The factors $a_1^{TCSC}\ and\ a_2^{TCSC}$ are obtained by substituting equations (3.75) – (3.86) into equations (3.73) – (3.74) appropriately.

### 3.10.3 Conditions for TCSC placement

(a) TCSC is installed on the transmission line with the least loss sensitivity with respect to control voltage magnitude.

(b) TCSC is installed on the transmission line with the most positive absolute value of loss sensitivity with respect to control voltage angle.

(c) TCSC are not installed on the transmission line containing tap changing transformer [100],[143], even if the sensitivity obtained is in favors of that location, the next on the ranking will be considered.

(d) TCSC are not installed on the transmission lines in between the buses that contained generators and shunt compensators [100],[143],[190], even if the sensitivity favors the installation.

## 3.11 VSC-HVDC transmission system

Power electronic devices such as insulated gate bipolar transistor (IGBT) and gate tur-off (GTO), with turn off capability through a control signal by pulse width modulation (PWM) constitute the major operation of voltage source converter (VSC). Basically, high voltage direct current based VSC (VSC-HVDC) consists of two VSCs, which for the purpose of this study are interconnected with dc conductor. One of the VSCs operates as a rectifier for the purpose of transmitting constant and highly controllable power to its counterpart that functions as an inverter [191]. In Fig. 3.11, the basic schematic of VSC-HVDC interconnecting two ac network buses is presented [192]. One of the converters controls the dc link voltage while the other controls the active power transmission through the link represented as HVDC cable in Fig. 3.12 [172]. Typically, there is capability of

injected ac active power regulation at both converter stations, with each converter having the possibility of controlling either voltage magnitude or injected reactive power at their respective ac buses, but for power flow analysis purposes, one converter is considered to be master station and the other being designated slave station [180]. Further details of operational principles are contained in the literature[180],[191],[193].

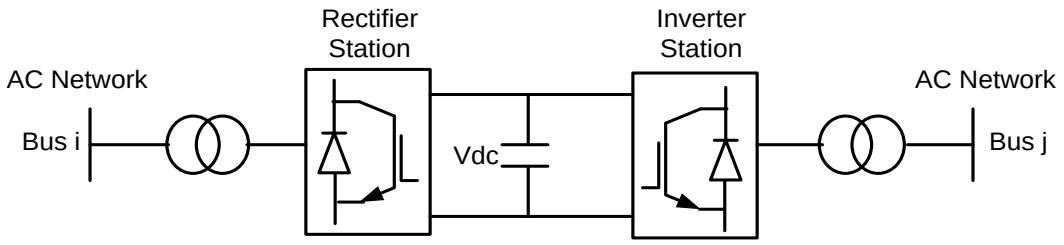


**Figure 3. 11: Basic schematic of VSC-HVDC system interconnecting AC network**

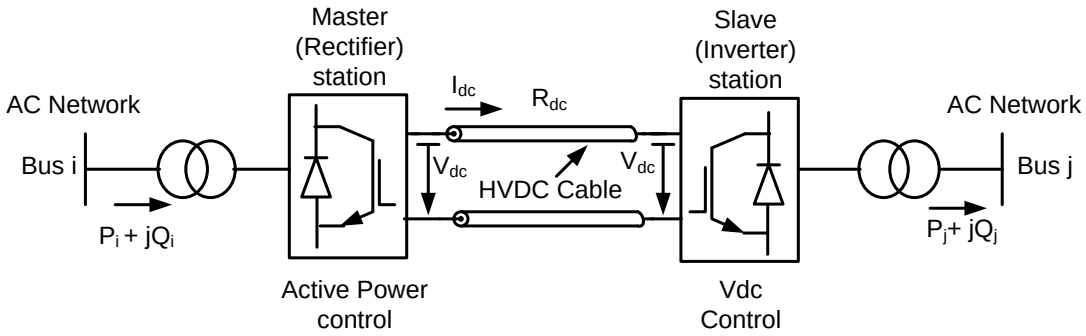


**Figure 3. 12: Representation of HVDC cable and typical VSC control of VSC-HVDC system**

### 3.11.1 Steady state modelling of VSC-HVDC

The steady state modelling of VSC-HVDC at fundamental frequency can be realized with the following assumptions[167].

(a) Both network and VSC have balanced three phase voltage with constant frequency and amplitude.
(b) All harmonics relating to current and voltage generated by converters are negligible.
(c) Converter valves are treated as an ideal type without voltage drop and hence, internal losses are also negligible.
(d) The dc voltage as well as current is assumed perfect without ripples.

Therefore, VSC-HVDC presented in Fig. 3.11 can be represented equivalently [180],[194] as diagram shown in Fig. 3.13. The phasor voltage through the converters at buses *i* and *j* are $V_{ci} = V_{ci}\angle\theta_{ci}$ and $V_{cj} = V_{cj}\angle\theta_{cj}$, where $V_c$ and $\theta_c$ are the voltage converter voltage magnitude and angle respectively. The shunt converter admittance is also given by $Y_c = G_c + B_c$ as denoted by their respective bus notations, with $G_c$ and $B_c$ being the conductance and susceptance respectively.

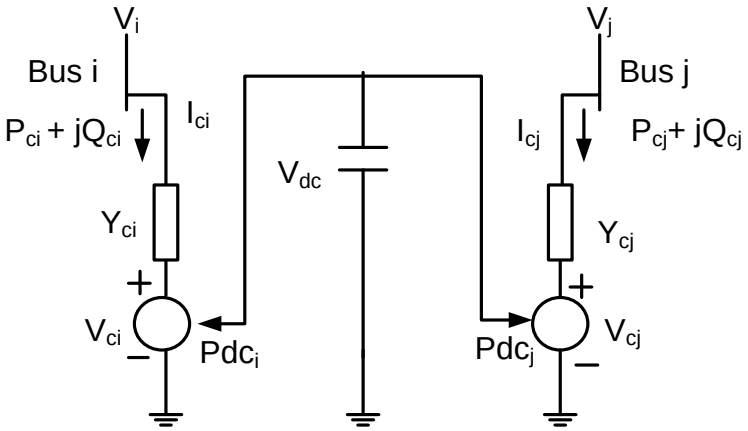


**Figure 3. 13: Equivalent circuit diagram of VSC-HVDC system interconnecting ac buses *i* and *j***

The complex voltage through the converter connected at bus *i*, and the complex voltage at bus *i* can be written as equations (3.87) and (3.88) respectively.

$$V_{ci} = V_{ci}\,(cos\theta_{ci} + j\,sin\theta_{ci}). \tag{3.87}$$

$$V_i = V_i\,(cos\theta_i + j\,sin\theta_i). \tag{3.88}$$

Therefore, the ac complex power denoted by $S_{ci}$ that flows into the converter connected at bus *i* can be represented by equation (3.89) where $S_{ci}$ is a function of shunt current and converter voltage.

$$S_{ci} = P_{ci} + j\,Q_{ci} = V_{ci}I_{ci}^{*}. \tag{3.89}$$

Therefore, with similar situation for bus *j*, active and reactive power flow into VSC-HVDC connected at bus *i* can be obtained as equations (3.90) and (3.91), where the active and reactive power injected at bus *i* can be obtained as equations (3.92) and (3.93) respectively [180];

$$P_{ci} = V_{ci}^2G_{ci} + V_{ci}V_i(G_{ci}\,cos(\theta_{ci} - \theta_i) + B_{ci}\sin(\theta_{ci} - \theta_i)) \tag{3.90}$$

$$Q_{ci} = -V_{ci}^2B_{ci} + V_{ci}V_i(G_{ci}\,sin(\theta_{ci} - \theta_i) - B_{ci}\cos(\theta_{ci} - \theta_i)) \tag{3.91}$$

$$P_i = V_i^2G_{ci} + V_iV_{ci}(G_{ci}\,cos(\theta_i - \theta_{ci}) + B_{ci}\sin(\theta_i - \theta_{ci})) \tag{3.92}$$

$$Q_i = -V_i^2B_{ci} + V_iV_{ci}(G_{ci}sin(\theta_i - \theta_{ci}) - B_{ci}\cos(\theta_i - \theta_{ci})). \tag{3.93}$$

In this application the converters are interconnected by a dc cable, the rectifier converter performs power control operation while inverter station controls the voltage, therefore, the equality constraint equations are presented as follows;

$$P_{dci} + P_{dcj} + P_{dcLoss} = 0 \tag{3.94}$$

$$P_{ci} - P_{ci}^{spec} = 0 \tag{3.95}$$

$$Q_{ci} - Q_{ci}^{spec} = 0 \tag{3.96}$$

$$V_j - V_j^{spec} = 0 \tag{3.97}$$

The inequality constraint equations are also as follows;

$$V_{ci}^{min} \leq V_{ci} \leq V_{ci}^{max}, \quad V_{cj}^{min} \leq V_{cj} \leq V_{cj}^{max} \tag{3.98}$$

$$0 \leq \theta_{ci} \leq 2\pi \, , 0 \leq \theta_{cj} \leq 2\pi \tag{3.99}$$

$$I_{ci} \leq I_{ci}^{max} \, , I_{cj} \leq I_{cj}^{max} \tag{3.100}$$

The representation of power flow equations in polar form are as earlier given by equations (3.2) and (3.3) [195]. The resulting modified NR power flow equations to accommodate VSC-HVDC can be written as equation (3.101) [180],[194], for the purpose of this study where active power is regulated at converters rectifier side.

$$\begin{bmatrix} \Delta P_i \\ \Delta P_{ci} \\ \Delta Q_i \\ \Delta Q_{ci} \\ \Delta P^{VSC} \end{bmatrix} = \begin{bmatrix} \frac{\partial P_i}{\partial \theta_i} & \frac{\partial P_i}{\partial \theta_{ci}} & \frac{\partial P_i}{\partial V_i} V_i & \frac{\partial P_i}{\partial V_{ci}} V_{ci} & 0 \\ \frac{\partial P_{ci}}{\partial \theta_i} & \frac{\partial P_{ci}}{\partial \theta_{ci}} & \frac{\partial P_{ci}}{\partial V_i} V_i & \frac{\partial P_{ci}}{\partial V_{ci}} V_{ci} & 0 \\ \frac{\partial Q_i}{\partial \theta_i} & \frac{\partial Q_i}{\partial \theta_{ci}} & \frac{\partial Q_i}{\partial V_i} V_i & \frac{\partial Q_i}{\partial V_{ci}} V_{ci} & 0 \\ \frac{\partial Q_{ci}}{\partial \theta_i} & \frac{\partial Q_{cj}}{\partial \theta_{ci}} & \frac{\partial Q_{ci}}{\partial V_i} V_i & \frac{\partial Q_{ci}}{\partial V_{ci}} V_{ci} & 0 \\ \frac{\partial P^{VSC}}{\partial \theta_i} & \frac{\partial P^{VSC}}{\partial \theta_{ci}} & \frac{\partial P^{VSC}}{\partial V_i} V_i & \frac{\partial P^{VSC}}{\partial V_{ci}} V_{ci} & \frac{\partial P^{VSC}}{\partial V_{cj}} \end{bmatrix} \begin{bmatrix} \Delta \theta_i \\ \Delta \theta_{ci} \\ \frac{\Delta V_i}{V_i} \\ \frac{\Delta V_{ci}}{V_{ci}} \\ \Delta \theta_{cj} \end{bmatrix}. \tag{3.101}$$

As stated earlier, the active power is regulated at bus *i*, and voltage at bus *j*, $\Delta P_{ci} = P_{ci}^{spec} - P_{ci}^{cal}$, $\Delta P_j$ and $\Delta P_{cj}$ are not used in equation (3.101). Likewise, $\Delta Q_j$ and $\Delta Q_{cj}$ become redundant because voltage magnitude is held constant at bus *j*. From the above equation, $\Delta P^{VSC}$ is the mismatch in active power flow and it can be obtained from equation (3.102 as follows.

$$\Delta P^{VSC} = \Delta P_{ci} - \Delta P_{cj} = P_{ci}^{spec} - P_{ci}^{cal}. \tag{3.102}$$

### 3.11.2 Static modelling of transmission line incorporated with VSC-HVDC

The static modelling of a transmission line containing VSC-HVDC is fundamental to obtaining power loss on such transmission line. This is with a view to including VSC-HVDC loss in the total network loss for active participation of controller in the proposed optimal device location. The π-equivalent representation of schematic diagram of VSC-HVDC transmission line depicted in Fig. 3.12 is presented in Fig. 3.14. The power flow from bus *i* to *j*, is $P_{ij}$ and from bus *j* to *i*, is $P_{ji}$ and they can be obtained through the relationship between the corresponding current flow and transmission line admittance. The current flow from bus *i* to *j*, denoted as $I_{ij}$ can therefore be gotten from the figure as equation (3.103), and the corresponding power as equation (3.104).

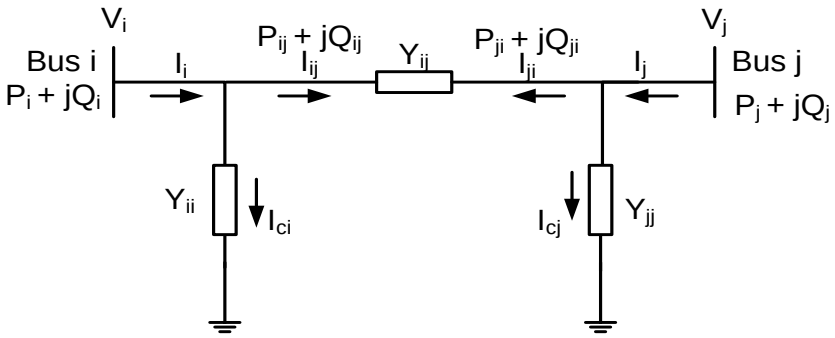


**Figure 3. 14: Equivalent $\pi$ representation of VSC-HVDC transmission system interconnecting ac buses *i* and *j*.**

$$I_{ij} = -I_{ji} = Y_{ij}(V_i - V_j) \; and \; I_{ij} = I_i - I_{ci} \tag{3.103}$$

$$P_{ij} = V_i I_i = (Y_{ii} + Y_{ij})V_i^2 - Y_{ij}V_iV_j \tag{3.104}$$

Where $Y_{ii}$ and $Y_{ij}$ are the sum of the admittances between buses *i* and *j* including ground and the net admittance between buses *i* and *j* as appeared at bus *i.* During steady state however, both the capacitive and inductive components disappears for HVDC transmission line interconnecting bus *i* to *j.* Therefore,

$$P_{ij} = (G_{ii} + G_{ij})V_i^2 - G_{ij}V_iV_j \tag{3.105}$$

$$P_{ji} = (G_{ii} + G_{ij})V_j^2 - G_{ij}V_jV_i \tag{3.106}$$

Power loss on VSC-HVDC line interconnecting bus *i* to *j* can be written as;

$$P_{dcLoss} = P_{ij} + P_{ji} = (G_{ii} + G_{ij})V_i^2 + (G_{ii} + G_{ij})V_j^2 - 2G_{ij}V_iV_j \tag{3.107}$$

### 3.11.3 Proposed sensitivity based optimal location of VSC-HVDC

Network power losses are mostly influenced by networks containing shunt devices like VSC [196] and hence power loss as a parameter was considered as a sensitive factor in determining the optimal location for VSC-HVDC system in this work. The main focus here was to propose a sensitive based approach to derive maximum benefits for VSC-HVDC placement for achievement of power flow enhancement in the network. The exact system loss formula has been presented as equations (3.69) and (3.70) [146];

The algebraic loss on the network containing VSC-HVDC ($P_{TL}$ ), can be written as loss without VSC-HVDC ($P_L$) and loss on the line containing VSC-HVDC ($P_{dcLoss}$) . This can also be written mathematically as;

$$P_{TL} = P_L + P_{dcLoss} = P_L + (P_{ij} + P_{ji}). \tag{3.108}$$

The loss sensitivity, due to VSC-HVDC transmission line connecting bus *i* to *j*, can be obtained by taking partial derivatives of the resulting total system real power loss in equation (3.108) with respect to the control

parameters $V_{ci}$ and $\theta_{ci}$. Total loss sensitivity considering $V_{ci}$, at $V_{ci} = 0$ and $\theta_{ci}$, at $\theta_{ci} = 0$ are represented by $\psi_1$and $\psi_2$. These are defined below;

$$\psi_1 = \frac{\partial P_{TL}}{\partial V_{ci}}\Big|_{V_{ci}=0} \tag{3.109}$$

$$\psi_2 = \frac{\partial P_{TL}}{\partial \theta_{ci}}\Big|_{\theta_{ci}=0} \tag{3.110}$$

These factors are obtained from the following as derived from resulting equations;

$$\psi_1 = \frac{\partial P_{TL}}{\partial V_{ci}}\Big|_{V_{ci}=0} = \frac{\partial P_L \partial P_{ci}}{\partial P_{ci}\partial V_{ci}}\Big|_{V_{ci}=0} + \frac{\partial P_L \partial P_{cj}}{\partial P_{cj}\partial V_{cj}}\Big|_{V_{cj}=0} + \frac{\partial P_L \partial Q_{ci}}{\partial Q_{ci}\partial V_{ci}}\Big|_{V_{ci}=0} + \frac{\partial P_L \partial Q_{cj}}{\partial Q_{cj}\partial V_{cj}}\Big|_{V_{cj}=0} + \left(\frac{\partial P_{ij}}{\partial V_i} + \frac{\partial P_{ji}}{\partial V_j}\right)\Big|_{V_{ci},\, V_{cj}=0} \tag{3.111}$$

$$\psi_2 = \frac{\partial P_{TL}}{\partial \theta_{ci}}\Big|_{\theta_{ci}=0} = \frac{\partial P_L \partial P_{ci}}{\partial P_{ci} V_{ci}\partial \theta_{ci}}\Big|_{\theta_{ci}=0} + \frac{\partial P_L \partial P_{cj}}{\partial P_{cj} V_{cj}\partial V_{cj}}\Big|_{\theta_{cj}=0} + \frac{\partial P_L \partial Q_{ci}}{\partial Q_{ci} V_{ci}\partial \theta_{ci}}\Big|_{\theta_{ci}=0} + \frac{\partial P_L \partial Q_{cj}}{\partial Q_{cj} 0 V_{cj}\partial \theta_{cj}}\Big|_{\theta_{cj}=0} + \left(\frac{\partial P_{ij}}{V_i \partial \theta_i} + \frac{\partial P_{ji}}{V_j \partial \theta_j}\right)\Big|_{\theta_{i},\theta_{j}=0} \tag{3.112}$$

The derivatives $\frac{\partial P_{ci}}{\partial V_{ci}}\Big|_{V_{ci}=0}$, $\frac{\partial P_{cj}}{\partial V_{cj}}\Big|_{V_{cj}=0}$, $\frac{\partial P_{ci}}{V_{ci}\partial \theta_{ci}}\Big|_{\theta_{ci}=0}$, and $\frac{\partial P_{cj}}{V_{cj}\partial \theta_{cj}}\Big|_{\theta_{cj}=0}$ can be obtain from equations (3.90) for bus *i* and in similar manner for bus *j*, with respect to the control factors of VSC-HVDC as follows;

$$\frac{\partial P_{ci}}{\partial V_{ci}}\Big|_{V_{ci}=0} = V_i\,(G_{ci} cos\,\theta_i - B_{ci}\, sin\theta_i) \tag{3.113}$$

$$\frac{\partial P_{cj}}{\partial V_{cj}}\Big|_{V_{cj}=0} = V_j\,(G_{cj} cos\,\theta_j - B_{cj}\, sin\theta_j) \tag{3.114}$$

$$\frac{\partial P_{ci}}{V_{ci}\partial \theta_{ci}}\Big|_{\theta_{ci}=0} = V_i\,(G_{ci} sin\,\theta_i + B_{ci}\, cos\theta_i) \tag{3.115}$$

$$\frac{\partial P_{cj}}{V_{cj}\partial \theta_{cj}}\Big|_{\theta_{cj}=0} = V_j\,(G_{cj} sin\,\theta_j + B_{cj}\, cos\theta_j) \tag{3.116}$$

The corresponding reactive power derivatives $\frac{\partial Q_{ci}}{\partial V_{ci}}\Big|_{V_{ci}=0}$, $\frac{\partial Q_{cj}}{\partial V_{cj}}\Big|_{V_{cj}=0}$, $\frac{\partial Q_{ci}}{V_{ci}\partial \theta_{ci}}\Big|_{\theta_{ci}=0}$, and $\frac{\partial Q_{cj}}{V_{cj}\partial \theta_{cj}}\Big|_{\theta_{cj}=0}$ can be obtain from equations (3.91) for bus *i* and in similar manner for bus *j*, with respect to the control factors of VSC-HVDC as follows;

$$\frac{\partial Q_{ci}}{\partial V_{ci}}\Big|_{V_{ci}=0} = V_i\,(G_{ci} sin\,\theta_i + B_{ci}\, cos\theta_i) \tag{3.117}$$

$$\frac{\partial Q_{cj}}{\partial V_{cj}}\Big|_{V_{cj}=0} = V_j\,(G_{cj} sin\,\theta_j + B_{cj}\, cos\theta_j) \tag{3.118}$$

$$\left.\frac{\partial Q_{ci}}{V_{ci}\partial\theta_{ci}}\right|_{\theta_{ci}=0} = V_i\,(G_{ci}cos\,\theta_i - B_{ci}\,sin\,\theta_i) \tag{3.119}$$

$$\left.\frac{\partial Q_{cj}}{V_{cj}\partial\theta_{cj}}\right|_{\theta_{cj}=0} = V_j\,(G_{cj}cos\,\theta_j - B_{cj}\,sin\theta_j). \tag{3.120}$$

The derivatives of the loss components of voltage magnitude from equations (3.105) and (3.106), are $\left.\frac{\partial P_{ij}}{\partial V_i}\right|_{V_i=0}, \left.\frac{\partial P_{ji}}{\partial V_j}\right|_{V_j=0}$ and are derived as follows while the derivatives of angle loss components are zero because of pure dc component.

$$\left.\frac{\partial P_{ij}}{\partial V_i}\right|_{V_i=0} = -V_jG_{ij} \tag{3.121}$$

$$\left.\frac{\partial P_{ji}}{\partial V_j}\right|_{V_j=0} = -V_iG_{ij} \tag{3.122}$$

The sensitivity factors $\psi_1$ and $\psi_2$ can therefore be obtain from equations (3.111) and (3.112) using equations (3.75 to (3.78) and equations (3.113) to (3.122).

### 3.12 Summary of chapter three

This chapter described two distinct methodologies of ATC determination known as RACPF and ACPRDF. It presented the principle of implementation of performance index methodology for identification of severe line outage contingency evaluation purposes. Three types of FACTS devices namely; SVC, TCSC and VSC-HVDC system were described and also presented for network performance improvement. Basic principles of different FACTS placement methods were discussed in this chapter and based on this, a sensitivity-based approach which involves incorporation of FACTS loss into network system loss was proposed. The devise location was based on the sensitivity factor obtained from the derivatives of the algebraic sum of the resultant system loss with respect to magnitude and angle of injection voltage of the device. This sensitivity-based method is therefore applied for FACTS placement in later chapters as described in this chapter. The methodologies described in this chapter, were applied for ATC determination, contingency evaluation, ATC enhancement, voltage profile improvement, loss reduction and contingency mitigation using described FACTS devices as presented in the subsequent chapters in this thesis. SVC and TCSC are presented in the subsequent chapter for ATC enhancement, bus voltage deviation minimization and power loss reduction, while VSC-HVDC transmission system is presented for network power flow enhancement and contingency mitigation.

# CHAPTER FOUR

# NETWORK ATC DETERMINATION AND CONTINGENCY EVALUATION

## 4.1 Introduction

This chapter consists of two major parts. The first part presents repeated alternating current power flow approach, for the determination of Available Transfer Capability (ATC) of a network system. In a deregulated environment, ATC values accurately depict the transferable quantum of power over the transmission network with due consideration for limits violations. In this work, RACPF based on Newton Raphson (NR) power flow equation was developed in a MATLAB software environment to obtain various values of ATC using IEEE 30 bus reliability test system presented in Appendix A-1. ATC values for each transmission line as determined through RACPF approach are presented, while the resultant value of network ATC then indicated. Also, ATC values for inter-area line outage and generator outage contingency conditions are obtained and analyzed. Likewise, in the same section, ATC values for bilateral and multilateral transactions are presented. Various ATC values obtained during inter-area tie lines outages for these conditions are also presented. In order to establish the accuracy of RACPF method, ATC values obtained in this study are then compared with values obtained through other method as presented in the literature.

The second aspect of this chapter deals with identification of the most severe line outage contingency. This becomes necessary in order to prioritize and properly identify the most severe contingent line arising from line outage of tie lines implemented in first section of this chapter. Here, investigation of line outage contingency ranking and analyses using various Performance Index (PI) approaches are conducted and reported. Independent contingency rankings based on voltage, real power, reactive power, voltage fused with reactive power and real power amalgamated with voltage fused reactive power PI are the ranking methods used. Analyses of most severe contingencies resulting from different ranking methods are carried out and the behavioural patterns of the affected transmission lines investigated and validated. Newton Raphson power flow equations developed in MATLAB environment are used for these analyses while the same IEEE 30 bus network is the test system. The results obtained in this section clearly presents the methodology of deploying PI in contingency identification and ranking using various power network parameters.

## 4.2 Present status of power structure

The operational structure of electric power industry has been under the control of a big but vertically integrated companies (usually public services) for many years. Within their confines of operation, all the rights of electric power activities on generation, transmission and distribution reside with these companies. However, due to economic and efficiency reasons, the vertically integrated utilities are being deregulated globally [9]. As earlier reported, starting from Chile to other countries in Latin America and by extension the rest of the world, restructuring becomes the order of the day and this brought about a regenerated attention in power industry, in response to this new alteration in structural power operations. Consequently, the operation of power network becomes difficult because of unhindered access brought about by deregulation [12].

One of the essential requirements of economic and secured electric supply is the bulk transfer of power over long distance [24]. Nevertheless, this maximum bulk power transfer is constrained by network limitations as bounded by thermal, voltage magnitude and other security constraints [14]. Due to power liberalization, the competition among market participants as a result of desired economic benefits is a major challenge for network operation because all power transactions exist on the same transmission network system. The consideration for nearby power wheeling between the source and the energy sink with mutual agreement for network security is no longer valid [25]. Numerous, concurrent and sometimes unscheduled power transaction becomes the order of energy trading and with this characterization, overloading of heavily loaded network path will result into affinity for network congestion and eventual contingency. This situation requires constant determination of ATC value especially for decision making to guide market participants [15]. ATC becomes fundamental as it presents network's physical conditions and transmission limits [25]. Generally, and with due consideration for network constraints, ATC gives transferrable quantum of power among inter areas connections of a deregulated power network [6]. Transmission companies rely on this crucial value for declaring available transmission corridors among the duo of generation and distribution sectors of power system for transaction purposes.

Likewise, contingency analysis is also very crucial to modern power system planning and operation. This is because, modern power system network is undergoing structural changes in a bid to acquire economy of scale and surmount technical challenges. Restructuring aims at achieving flexibility of operation, economy of scale and stability of supply among others [20]. Consequently, power network operation is becoming more difficult because of open access created by deregulation as highlighted. The resultant competitive trading keeps stressing saturated transmission network further and increases its propensity to failure. There is tendency for power networks in a deregulated environment to suffer system overload due to frequent multiple but unplanned power transactions. This susceptibility of transmission lines to overloading otherwise known as congestion always resulted into contingency [15]. Contingency though undesirable, is the temporary loss of one or more power network components [40]. One of the challenges of system operators is the operation of network systems in a way that transmission limits are properly controlled [1]. However, the identification and ranking of transmission lines in order of their severity precede congestion management. This is quite indispensable for security assessment and congestion management as a prerequisite for further power system steady state critical analysis. System security assessment is the process of keeping the system secured against operational limits violations [38].

In the subsequent paragraphs, ATC values of the test network during various conditions are obtained and presented using various governing equations presented in chapter three. Likewise, the diverse utilization of PI as a contingency screening and selection method is further scrutinized and investigated to avoid misapplication in the succeeding sections. Hitherto, PI is being applied indiscriminately, hence, the methodology of deploying PI in contingency ranking is ultimately justified with assertion, through assessment of the effects of the most severe ranked contingency on the network system parameters.

### 4.3 Results and discussions

In this section, the ATC values of the test network are obtained without power trading and for bilateral and multilateral power transactions. ATCs during various tie line and generator outage contingency conditions are also obtained. Results obtained for various simulations are as discussed subsequently.

#### 4.3.1 ATC for normal power transfer condition

ATC values have been obtained for different single power transfers. Normal condition in this context implies that the test system parameters are intact except the single source-sink bus where power transfer that resulted into ATC determination took place. This is done with a view to establishing test system's ATC prior to power transactions. Deregulation is characterized by various power transactions including bilateral and multilateral power transactions, hence, ATC values obtained during normal power flow are very useful for system planning and operations. Fig. 4.1 shows values of ATC obtained using the RACPF method as discussed.

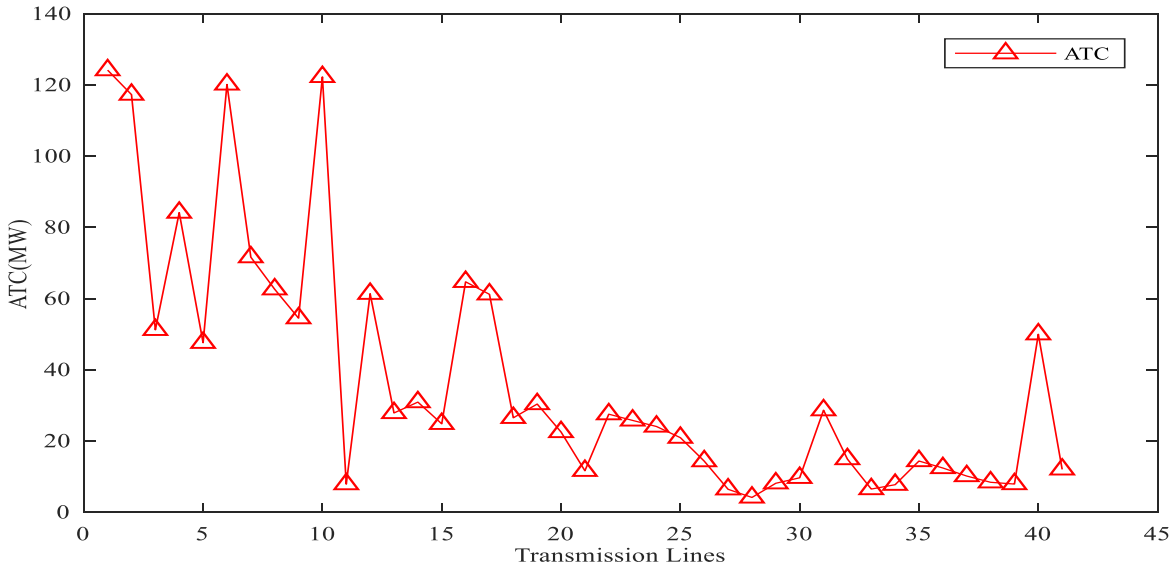


**Figure 4. 1: ATC values during normal transfer condition**

The ATC values for all transmission lines are as presented, where each line presents different values based on their transfer capability limits. In this case, the minimum value of 4.175 MW is obtained on the transmission line 15 – 23, corresponding to line number 28. This value is the ATC value for the entire network as earlier presented in equation ((3.17) of chapter three). This implies that although, other transmission lines can accommodate well above 4.175 MW for any schedule power transfer however, the network cannot allow beyond this value for a secured and reliable power system operation.

In the analysis, the highest transferable quantity of power with due consideration for network security and stability is overtly presented for operators' consideration. The amount of power that can violate network thermal loading and megavolt-amperes (MVA) limit is known. Going by system data, transmission lines 1-2, 1-3, 2-5, and 3-4 have the highest thermal limit of 130 MVA each, hence the highest ATCs as shown in the graph, while

lines 14-15, 15-18, 15-23, 16-17, 18-19, 22-24, 23-24, 24-25, 25-25, 25-27, 27-29, 27-30, and 29-30 have the lowest ATCs which are synonymous to thermal limit of 16 MVA. Obviously thermal limit restricts ATC.

Fig. 4.2 shows the relationship among Base case, ATC and TTC. Base case is the default power flow of the test system based on its parameters, while TTC is the total reliable power flow that the test system has the capability to sustain. There is a substantial clearance between the base case and ATC of the network for the first twenty transmission lines except for transmission line number eleven. These lines with higher thermal limit capability have higher transfer capability for additional power flow, beyond their counterpart in the remaining part of the network because of these thermal ratings. ATC at every instance is shown with reference to TTC of the network, this method obtained ATC with due consideration for the thermal limit violation.

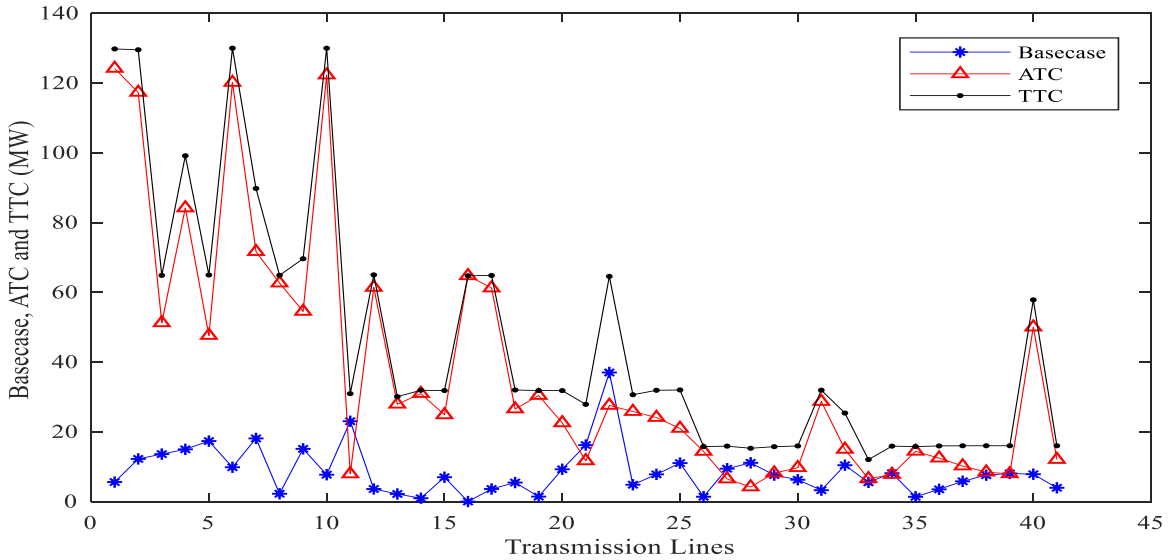


**Figure 4. 2: Base case, ATC and TTC values of the test case**

In order to validate this work, values of ATC obtained are compared with results in [6], where authors used ac power flow approach. This is done for similarity purposes because in that work, the same IEEE 30 bus test system was also used for analysis as in in this work. As shown in Fig. 4.3, 11.574 MW and 8.892 MW ATC values are obtained in this work above the values obtained in [6], especially for same transmission lines 1-2 and 1-3 respectively, while on the lines 2-5 and 6-8, ATC values of 25.535 MW and 29.014 MW below that of [6] are obtained. Differences are also noticed for transmission lines 1-2, 1-3, 2-4, 2-5, 2-6, 3-4, 4-6, 6-7, 6-8, 6-9, 9-10, 10-21, 10-22, 22-24 and 28-27. A wider ATC bound values here means a better accuracy. It is observed from the results that RACPF approach is more accurate when compared with the results obtained using ac power flow in previous work. It is also established from the results that ATC values present an understanding of transmission network conditions and limits needed for operational purposes especially in a deregulated power sector. This implies that the results obtained in this exercise is very accurate. This method is therefore suitable for independent system operator (ISO) in determining ATC values needed in taking unambiguous decisions.

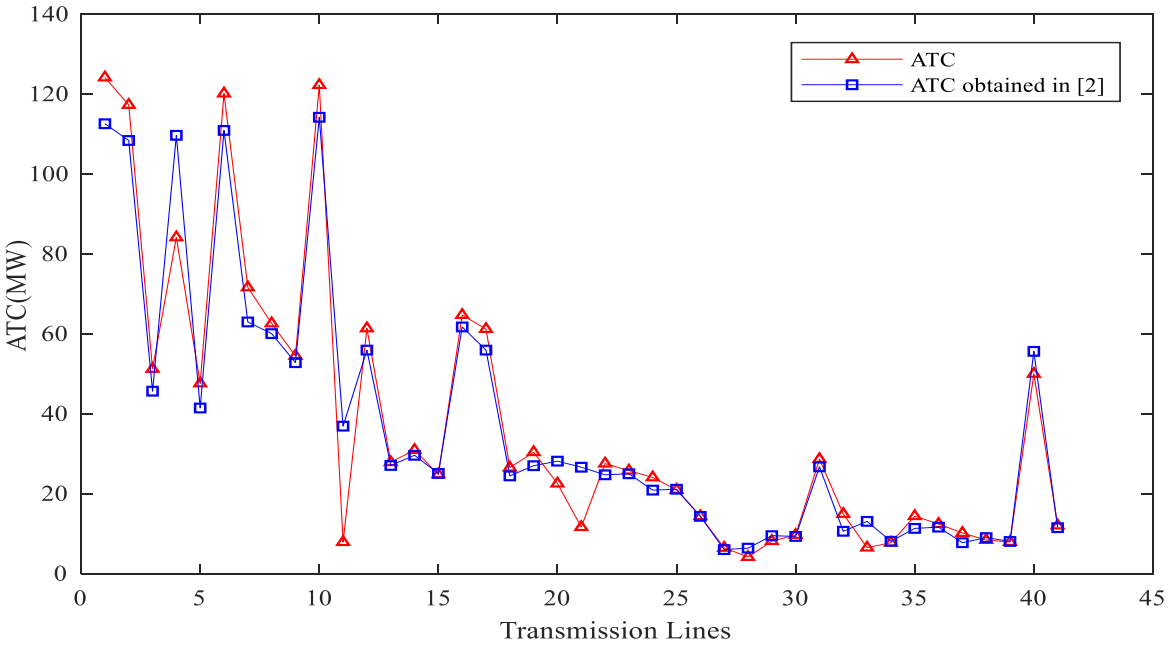


**Figure 4. 3: Comparison of the values of ATC obtained with that in [6]**

### 4.3.2 ATC for contingency conditions

In modern day power operation, which is characterised by various power transactions consequents of power network liberalization, power networks are made to operate around their thermal limits, hence contingency may inadvertently occur. The subsequent paragraphs present outcome of an investigation of some common contingency occurrences.

#### 4.3.2.1 Line outage contingency condition

Line(s) contingency usually occur(s) when such lines are operated in violation to their thermal limits, consequent of overloading [15]. To demonstrate this, the test bus system was modified by dividing it into three areas; Areas A, B, and C, as shown in Fig.4.4. The test system is divided as such, for simplicity of analysis. Line outage contingency was then considered for tie line between the areas. Tie lines are the transmission lines that connect an area to its neighboring areas in a power network and power sharing between two areas occur through these tie lines [178]. The mapped areas, bus numbers and the transmission lines linking one area to another are as shown in Table 4.1.

Table 4. 1: Areas of the network in relation to affected buses and tie lines

| Areas | Bus | Area to Area | Tie Lines |
|---|---|---|---|
| A | 1, 2, 3, 4, 5, 6, 7, 9, 11 | A-B | 4-12, 9-10, 6-10 |
| B | 10, 12, 13, 14, 15, 16, 17, 18, 19, 20, 21,22, 23, 24 | A-C | 6-8, 6-28 |
| C | 8, 25, 26, 27, 28, 29, 30 | B-C | 24-25 |

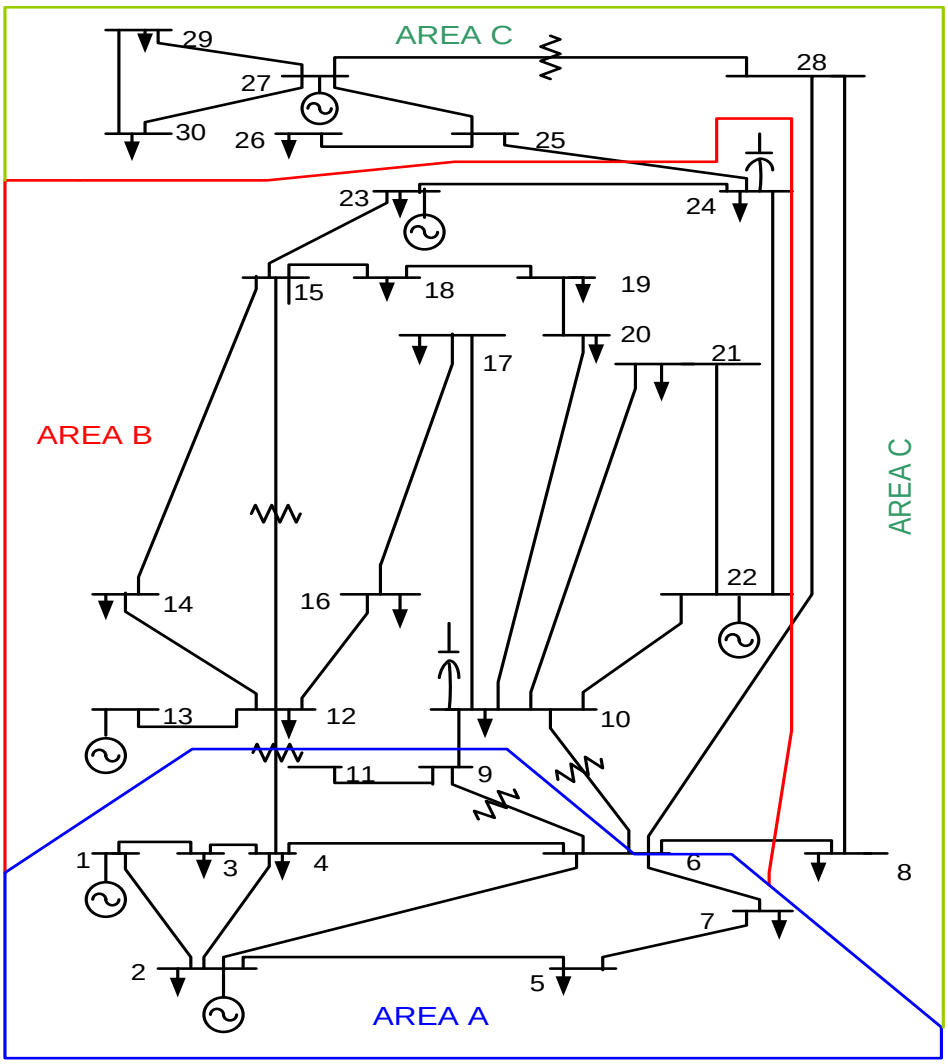


**Figure 4. 4: Modified diagram of IEEE 30 bus test system**

It can be seen from the table that transmission lines 4-12, 9-10 and 6-10 are the tie lines interconnecting areas A to B, 6-8 and 6-28 interconnecting areas A and C while only transmission line 24-25 is the tie line linking areas B to C. Outages of these tie lines were implemented and the ATCs obtained are as tabulated in Table 4.2. Outage of feeder line between bus 6 and 28 gives the minimum ATC of all the outages. This implies that the contingency of line 6-28 will impact on the capacity of the network to transfer power beyond this value. When compared with normal condition, outage of line 9-10, 6-8, and 24-25 will permit 0.665 MW, 0.607 MW and 0.178 MW power transfer respectively, above allowable limit of normal condition. Other ATC values for line outages are presented in the table.

Table 4. 2: ATC values for various line outage

| **Outage Tie Lines** | 4-12 | 9-10 | 6-10 | 6-8 | 6-28 | 24-25 |
|---|---|---|---|---|---|---|
| **ATC (MW)** | 4.128 | 4.840 | 4.108 | 4.782 | 3.894 | 4.353 |

#### 4.3.2.2 Generator outage contingency condition

Generator outage contingency should be restrained because it will change the power flow convention. This happens when other generator(s), especially the slack generator assumes the obligation of compensating debilitating effects of the outage [197]. However, the understanding of the system behavior in case of a generator outage especially in a deregulated environment is an indispensable tool in power planning and operations [15]. Table 4.3 below depicts various values of ATC obtained under this contingency condition. ATC value obtained on transmission line 22-24 with value -0.999 is the minimum. This is an indication of response to the loss of generator 5 via the stated line. A compelled generator outage has a grave consequence on the other generators as well as the transmission lines whose responsibility at that instant of time, are to compensate for the impacts of outage in order to keep the network alive. The loss of generator 4 led to concurrent thermal violation of two transmission lines 21-22 and 22-24. This of course can spell doom for the network as it can lead to blackout consequent of cascaded line outages. TLV as used in the table means thermal violation of transmission lines 21-22 and 22-24.

Table 4. 3: Values of ATC for various line outage

| Outage Generator | Bus Location | ATC (MW) | Transmission Line Involved |
|---|---|---|---|
| G1 | 2 | 4.25 | 15-23 |
| G2 | 13 | 0.95 | 15-23 |
| G3 | 22 | 0.617 | 16-17 |
| G4 | 23 | TLV | 21-22 & 22-24 |
| G5 | 27 | -0.999 | 22-24 |

### 4.4 ATC for power transaction conditions

Different power transactions including bilateral and multilateral trading are becoming the order of the day in power network operation because of open access. The nature and magnitude of trading also affect the network performance hence various trading are implemented for investigation in this section. ATC was obtained for bilateral and multilateral transactions.

#### 4.4.1 ATC for bilateral power transaction

Bilateral power transaction involves a seller and a buyer. During bilateral transaction, power transaction took place between source bus 8 and sink bus 3 where, 20 MW of power was transferred from bus 8 to bus 3. The active power at bus 8 reduced to 10 MW from 30 MW while that of bus 3 increased from 2.4 MW to 22.4 MW. Then ATC was computed, and values obtained are as shown in Fig. 4.5. This bilateral transaction has undoubtedly influenced the ATCs values obtained for the adjoining transmission lines. Transmission lines 6-8, 8-28, 3-4 and 1-3 experienced a significant drift in value while lines 1-2, 2-4, 2-6, 4-6, 4-12, 6-7, 6-9, 6-10, and 6-28 were also not spared from the influence of this transaction. The deviation of vales obtained in this case is a clear indication that with this type of transaction taking place on the network, ATC will be impacted. This implies that the capability of the transmission lines to accommodate market operators has changed due to transaction of 20 MW of power between bus 8 and 3.

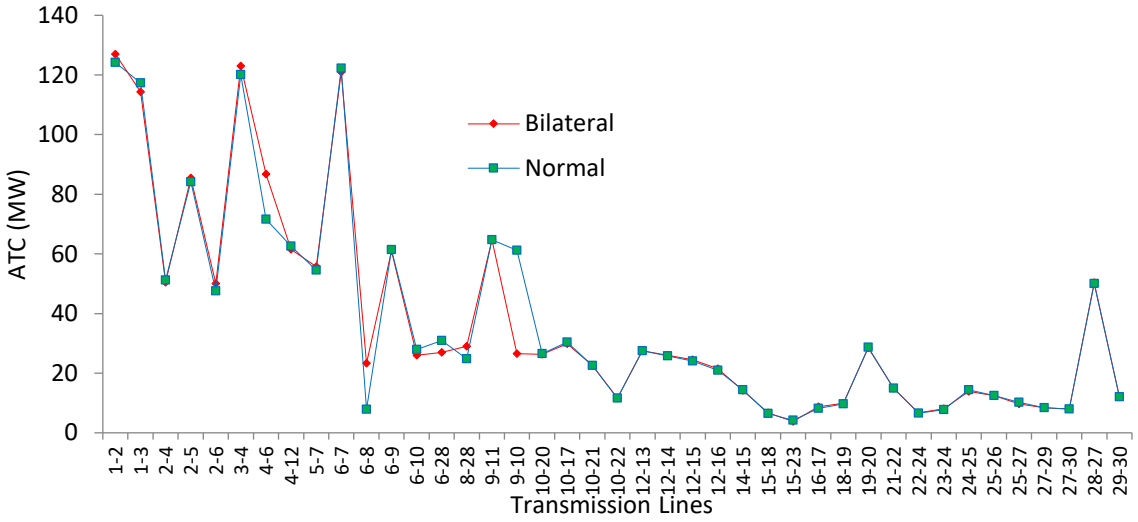


**Figure 4. 5: ATC values during normal case and bilateral transactions**

### 4.4.2 ATC for multilateral power transaction

Multilateral transaction involves more than one buyer and seller. In the case of multilateral transaction, there were exchange of power among source and sink buses. A total of 40 MW power was transferred from source buses 8 and 7 to the sink buses 10 & 12 and 16 & 20 respectively with buses 8 and 7 shedding 20 MW power each, while buses 10, 12, 16, and 20 benefitted 10 MW each. Before power transaction, bus 8, 7, 10, 12, 16 and 20 has 30 MW, 22.8 MW, 5.919 MW, 11.2 MW, 3.5 MW and 2.2 MW respectively. These values became 10 MW, 2.8 MW, 15.919 MW, 21.2 MW 13.5 MW and 12.2 MW after the transaction. With this transaction in place, ATC values obtained were compared with that of bilateral cases as shown in Fig. 4.6.

ATC values obtained during multilateral transactions were slightly high on transmission lines 1-3, 2-5, 5-7. 6-7, 6-28, 10-21, 16-17, 19-20, 22-24, 23-24, and 28-27. However, ATC value for other lines were higher during bilateral transaction.

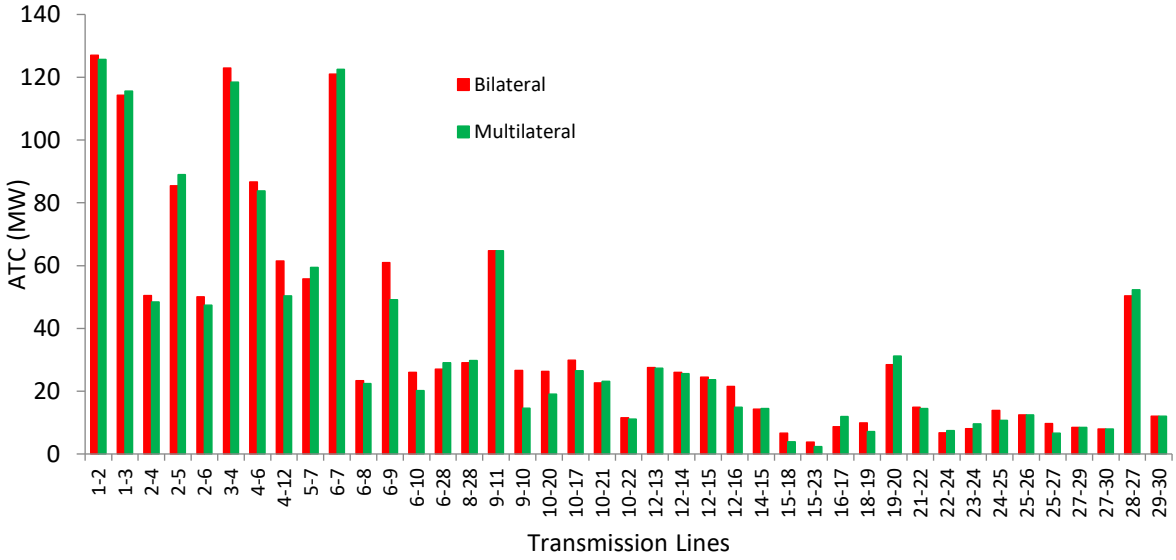


**Figure 4. 6: ATC values for bilateral and multilateral transactions**

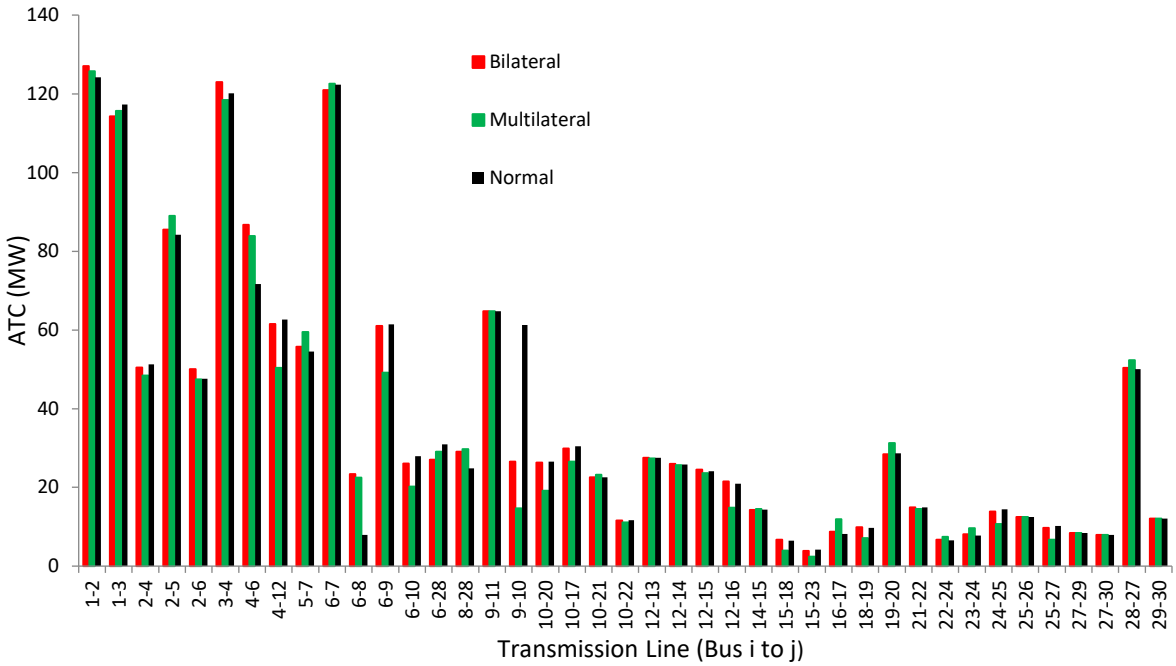


**Figure 4. 7: ATC for normal case, bilateral and multilateral transactions**

### 4.4.3 Comparison of ATC values for normal, bilateral and multilateral power transactions

ATC values for bilateral, multilateral and normal case study are shown in Fig. 4.7. There were significant changes in values of ATC obtained for both bilateral and multilateral cases compared with normal case. During bilateral transaction, there was an exchange of 20 MW power between bus 8 in Area C and bus 3 in Area A. This is reflected in the ATC for tie lines 4-12, 9-10 and 6-10. The transfer of 20 MW of power each from buses 7 and 8 in areas A and C respectively to buses 10, 12, 16 and 20 all in area B is also clearly depicted in the ATCs of tie lines 6-8, 6-28, (for area A to C), and 24-25 (for area B to C). The distinctions in ATC for line 6-9, is an indication of the fact that it is an extension of tie line 9-10. ATC value on line 9-10 during normal condition is significantly higher than values obtained during bilateral and multilateral transactions as presented.

### 4.4.4 Line outages for bilateral and multilateral power transactions

In Table 4.4, various values of ATC obtained for different line outages are presented. The minimum value of 1.997 MW was obtained during multilateral transaction when line 6-28 outage contingency was created. All the ATCs obtained for multilateral transactions were lower than the corresponding values for bilateral transaction. The corresponding values during bilateral also lower that that obtain during normal operation, except for line 4-12. The implication here is that network ATC is lowered with transaction and worsened with nature of transaction. The more the multiple transactions that is taken place, the less the accrued network ATC.

During bilateral condition, the contingency created consequent outage of line 4-12 can be managed without loss of supply to adjoining feeders through other tie lines. However, this was not so for multilateral situation, where thermal limit was violated because power flow increased in all transmission lines. This means that a well-

structured interconnected system rather than a radial system, due to its inertia, can withstand some level of contingencies. As presented in the table, TLV implies thermal limit of line 15-23 has been violated.

Table 4. 4: ATC values for various line outages during transactions

| Outage Tie Lines | Bilateral ATC (MW) | Multilateral ATC (MW) | Normal ATC(MW) |
|---|---|---|---|
| 4-12 | 4.395 | TLV | 4.128 |
| 9-10 | 4.488 | 3.507 | 4.840 |
| 6-10 | 3.767 | 2.544 | 4.108 |
| 6-8 | 4.084 | 2.653 | 4.782 |
| 6-28 | 3.319 | 1.997 | 3.894 |
| 24-25 | 4.174 | 3.679 | 4.353 |

### 4.5 Performance indices of various power system parameters

In this second section, performance index technique was applied to the test network system in Appendix A-2 but with thermal limits presented in Table A-1.1, through various system parameters for evaluation of contingency rankings as obtained in the analysis. The implementation of line outage and the subsequent ranking in order of severity obtained for real power, voltage and reactive power performance indices are presented in columns 3, 4, and 5 of Table 4.5. Voltage fused reactive power PI ranking is contained in column 6 while the values in column 7 were obtained from voltage fused real & reactive power PI.

Table 4. 5: Contingency ranking based on real power ($PI_{\_P}$), voltage ($PI_{\_V}$), reactive power ($PI_{\_Q}$), voltage & reactive power ($PI_{\_VQ}$), as well as real power & voltage & reactive power ($PI_{\_PVQ}$)

| L/N | Outage Line | Ranking | | | | | L/N | Outage Line | Ranking | | | | |
|---|---|---|---|---|---|---|---|---|---|---|---|---|---|
| | | PI_P | PI_V | PI_Q | PI_VQ | PI_PVQ | | | PI_P | PI_V | PI_Q | PI_VQ | PI_PVQ |
| 1 | 1-2 | 40 | 32 | 3 | 3 | 40 | 21 | 16-17 | 30 | 13 | 15 | 13 | 30 |
| 2 | 1-3 | 4 | 36 | 9 | 9 | 4 | 22 | 15-18 | 35 | 26 | 14 | 15 | 35 |
| 3 | 2-4 | 37 | 22 | 33 | 33 | 37 | 23 | 18-19 | 34 | 27 | 21 | 23 | 34 |
| 4 | 3-4 | 5 | 28 | 11 | 11 | 5 | 24 | 19-20 | 20 | 18 | 30 | 30 | 20 |
| 5 | 2-5 | 1 | 37 | 1 | 1 | 1 | 25 | 10-20 | 14 | 33 | 39 | 39 | 14 |
| 6 | 2-6 | 7 | 24 | 32 | 32 | 7 | 26 | 10-17 | 33 | 16 | 31 | 31 | 33 |
| 7 | 4-6 | 11 | 23 | 36 | 36 | 11 | 27 | 10-21 | 13 | 30 | 22 | 24 | 13 |
| 8 | 5-7 | 23 | 25 | 41 | 41 | 23 | 28 | 10-22 | 21 | 19 | 26 | 26 | 21 |
| 9 | 6-7 | 2 | 12 | 37 | 37 | 2 | 29 | 21-22 | 32 | 6 | 27 | 25 | 32 |
| 10 | 6-8 | 8 | 3 | 35 | 35 | 8 | 30 | 15-23 | 19 | 21 | 13 | 12 | 19 |
| 11 | 6-9 | 16 | 4 | 40 | 40 | 16 | 31 | 22-24 | 15 | 17 | 29 | 29 | 15 |
| 12 | 6-10 | 18 | 15 | 38 | 38 | 18 | 32 | 23-24 | 28 | 10 | 20 | 17 | 28 |
| 13 | 9-11 | 41 | 39 | 16 | 28 | 41 | 33 | 24-25 | 26 | 14 | 28 | 27 | 26 |
| 14 | 9-10 | 3 | 40 | 12 | 18 | 3 | 34 | 25-26 | 39 | 2 | 34 | 34 | 39 |
| 15 | 4-12 | 12 | 35 | 2 | 2 | 12 | 35 | 25-27 | 38 | 20 | 23 | 21 | 38 |
| 16 | 12-13 | 6 | 41 | 6 | 7 | 6 | 36 | 28-27 | 10 | 1 | 7 | 4 | 10 |
| 17 | 12-14 | 22 | 29 | 18 | 20 | 22 | 37 | 27-29 | 17 | 5 | 19 | 16 | 17 |
| 18 | 12-15 | 24 | 38 | 8 | 8 | 24 | 38 | 27-30 | 9 | 7 | 17 | 14 | 9 |
| 19 | 12-16 | 27 | 31 | 10 | 10 | 27 | 39 | 29-30 | 29 | 8 | 24 | 19 | 29 |
| 20 | 14-15 | 31 | 9 | 25 | 22 | 31 | 40 | 8-28 | 25 | 11 | 5 | 6 | 25 |
| | | | | | | | 41 | 6-28 | 36 | 34 | 4 | 5 | 36 |

This is replicated in columns 10, 11 and 12 as well as column 13 and 14 respectively. From the table, it can be deduced that there is lack of correlation among different rankings. Ranking based on reactive power and that of voltage fused reactive power correspond to each other for the first twelve transmission lines up to line 6-10. This is obvious because all the generators including the slack are located within these areas and reactive power limits regulation was enforced because, reactive power is responsible for the bus voltage regulation. However, the order of position in the subsequent transmission lines outside this vicinity does not align for these rankings.

Ranking of lines based on voltage fused real & reactive power takes after real power ranking because the magnitude of real power flow PI is far greater than the insignificant summation of values of voltage fused reactive power PI for the same line. This implies that for this summation, the ranking takes after the ranking order of real power PI. Howbeit, the magnitude of the real power PI, it cannot be substituted and does not replace the impacts of both the voltage and reactive power in ranking contingencies. This can also be explained for voltage fused reactive power ranking that has some correlations with reactive power ranking. Adequate attention must be paid to voltage and reactive power PI rankings because their values were also obtained with respect to limits violations. Therefore, further investigation was conducted on each of these rankings in order to establish the best system parameter to be engaged in determining the most severe outage line.

### 4.5.1 Contingency selection consequent of rankings

The summary of the first three outage rankings are as contained in Table 4.6. Contingency selection becomes difficult due to different ranking results obtained as presented in Table 4.5. Ranking based on real power, reactive power, voltage fused reactive power as well as voltage fused real & reactive power PI are the same for the first transmission lines. This ranking identified line 2-5 as the most severe contingency line, while voltage PI prioritized transmission line 28-27 as the most severe contingency line. Different orders of priority without correlation resulted from different methods of network rankings. However, if the selection was done based on voltage fused real & reactive power ($PI_{\_PVQ}$), a wrong severe contingency might have been chosen because a mis-ranking would have occurred. It should be observed that the major distinction occurs among real power, reactive power and voltage PI ranking for this first three severe lines. Therefore, these various rankings were further subjected to further scrutiny and analyses.

Table 4. 6: First three contingency rankings

| **Ranking** | **1** | **2** | **3** |
|---|---|---|---|
| **PI_P** | 2-5 | 6-7 | 9-10 |
| **PI_V** | 28-27 | 25-26 | 6-8 |
| **PI_Q** | 2-5 | 4-12 | 1-2 |
| **PI_VQ** | 2-5 | 4-12 | 1-2 |
| **PI_PVQ** | 2-5 | 6-7 | 9-10 |

### 4.5.2 Power flow analyses of selected contingency rankings

Here, the selections based on different PI ranking were subjected to further investigation. This was to eliminate ambiguity in the contingency selection when employing PI as a tool in ranking. Load flow analysis of each outage line was performed and pre and post outage conditions were then observed. This was repeated for all

transmission lines in the first three selected rankings. For emphasis, with the exemption of voltage PI ranking, transmission lines 2-5 ranked first based on reactive power, voltage fused reactive power, voltage fused real & reactive power rankings, while line 28-27 was first on voltage PI ranking.

#### 4.5.2.1 Selection based on real power ranking

The outage of transmission lines 2-5, 6-7 and 9-10 were further investigated using load flow analysis. Network responses to outage of these lines are summarized in Table 4.7. Outage of line 2-5 caused transmission line 5-7 to operate beyond its thermal limit, but other transmission lines in the ranking did not cause any thermal overload. Although, line 2-5 though ranked first in real power PI, its outage did not violate voltage limit bounds. The pre and post outage bus voltage profile for line 2-5 are as presented in Fig. 4.8. Pre and post outage voltages of line 6-7 and 9-10 are as shown in Figs. 4.9 and 4.10 respectively. It should be noted that outage of line 6-7 and 9-10 did not result into any MVA limit violation.

Table 4. 7: Network response to real power PI ranking order

| Overloaded Line | Line Flow (MW) | Line Flow (MVA) | Line Limit (MVA) |
|---|---|---|---|
| Pre-outage of line 2-5 | | | |
| 2-5 | 53.863 | 57.271 | 130 |
| 5-7 | 7.497 | 24.827 | 70 |
| Post-outage of line 2-5 | | | |
| 2-5 | nil | nil | 130 |
| 5-7 | 62.023 | 72.458 | 70 |
| Pre-outage of line 6-7 | | | |
| 6-7 | 30.607 | 33.56 | 130 |
| Post-outage of line 6-7 | | | |
| 6-7 | nil | nil | 130 |
| Pre-outage of line 9-10 | | | |
| 9-10 | 31.484 | 32.027 | 65 |
| Post-outage of line 9-10 | | | |
| 9-10 | nil | nil | 65 |

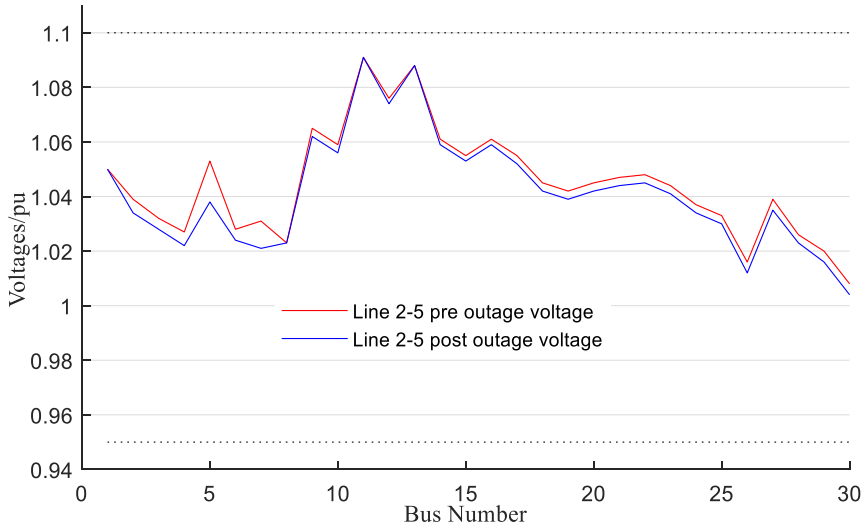


**Figure 4. 8: Pre and post outage voltage of line 2-5**

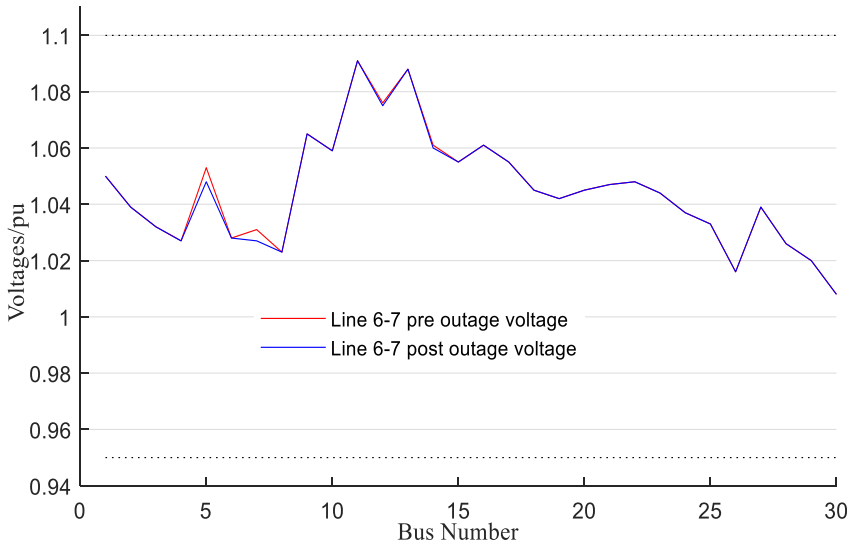


**Figure 4. 9: Pre and post outage voltage of line 6-7**

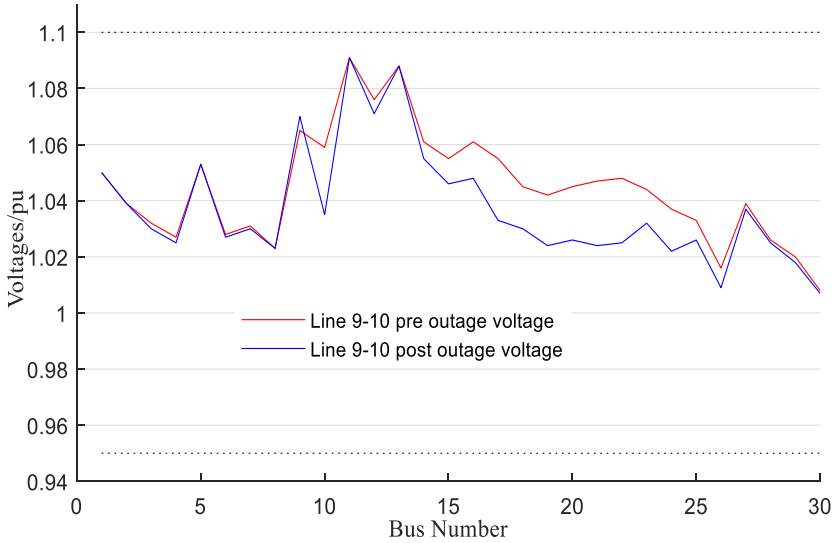


**Figure 4. 10: Pre and post outage voltage of line 9-10**

#### 4.5.2.2 Selection based on voltage ranking

Outage of lines 28-27, 25-26 and 6-8 were further investigated. The test system's responses to these outages are summarized in Table 4.8. The outage of line 28-27 caused thermal overload of transmission lines 22-24 and 24-25. As depicted in Fig. 4.11, this also resulted into voltage limits violations at the same time. Summarily, outage of line 28-27 resulted into thermal overloads of two transmission lines and a bus voltage violation. This was more severe compared to outage of line 2-5 which resulted into overloading of only one transmission line. Second in order of voltage ranking was line 25-26 whose outage also resulted into bus voltage limit violations. In Fig. 4.12, open circuit bus voltage resulted from tripping of protective devices isolating bus 26. Outage of line 6-8 did not result into any limit violations as shown in Fig. 4.13. In this analysis for the purposes of emphasis, outage of lines 25-26 and 6-8 did not result into any MVA limit violation.

Table 4. 8: Network response to voltage PI ranking order

| Overloaded Line | Line Flow (MW) | Line Flow (MVA) | Line Limit (MVA) |
|---|---|---|---|
| Pre-outage of line 28-27 | | | |
| 28-27 | 15.734 | 16.857 | 65 |
| 22-24 | 6.414 | 6.793 | 16 |
| 24-25 | 1.102 | 1.28 | 16 |
| Post-outage of line 28-27 | | | |
| 28-27 | nil | nil | 65 |
| 22-24 | 18.023 | 19.383 | 16 |
| 24-25 | 17.856 | 19.383 | 16 |
| Pre-outage of line 25-26 | | | |
| 25-26 | 3.528 | 4.246 | 16 |
| Post-outage of line 25-26 | | | |
| 25-26 | nil | nil | 16 |
| Pre-outage of line 6-8 | | | |
| 6-8 | 7.978 | 12.541 | 32 |
| Post-outage of line 6-8 | | | |
| 6-8 | nil | nil | 32 |

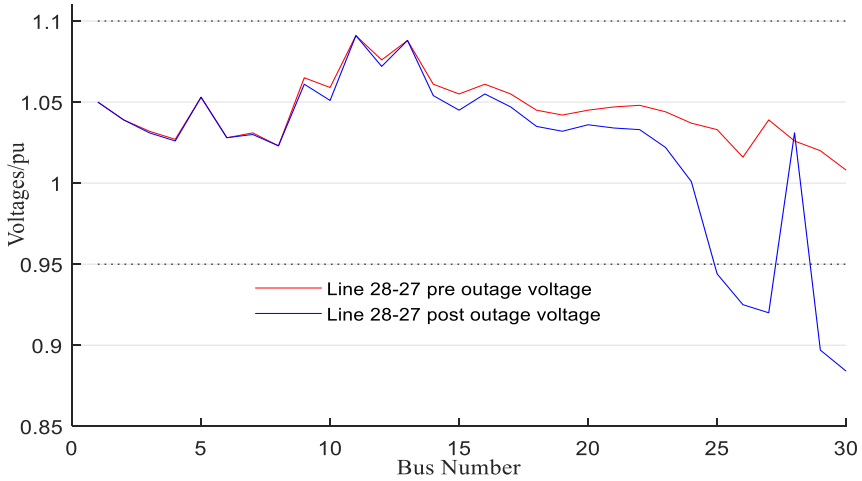


**Figure 4. 11: Pre and post outage voltage of line 28-27**

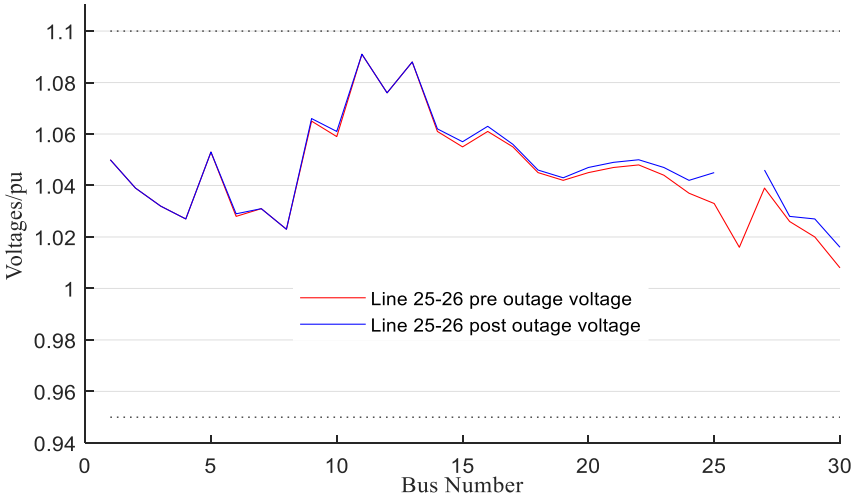


**Figure 4. 12: Pre and post outage voltage of line 25-26**

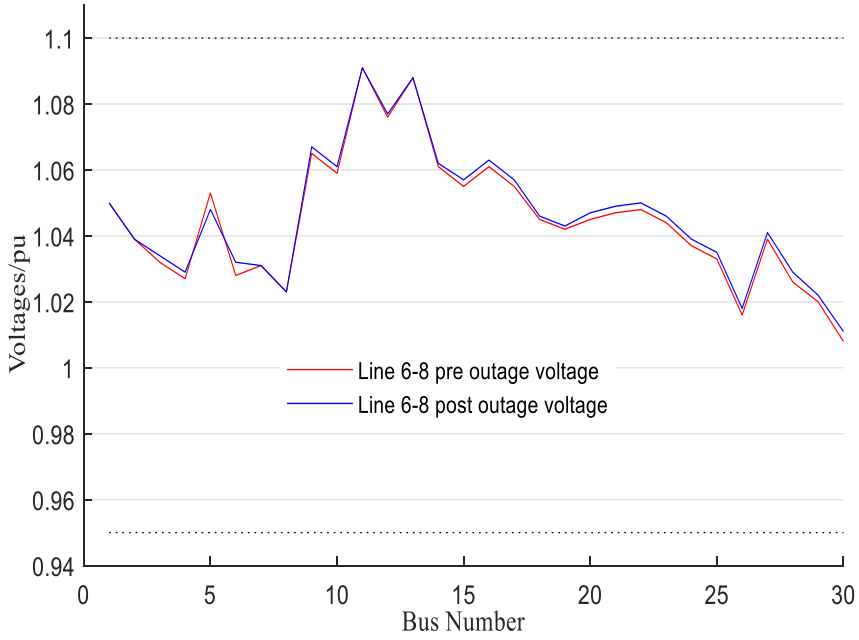


**Figure 4. 13: Pre and post outage voltage of line 6-8**

#### 4.5.2.3 Selection based on reactive power

The system's response to outages based on reactive power PI, where transmission lines 2-5, 4-12 and 1-2 were further investigated are summarized in Table 4.9. Load flow studies of transmission lines 4-12 and 1-2 outages revealed no line thermal overloads. Figs. 4.14 & 4.15 are pre and post outage bus voltages of line 4-12 and 1-2. All bus voltages were within the limits for these outages. In this analysis as well, outage of lines 4-12 and 1-2 did not result into any MVA limit violation.

Table 4. 9: Network response to reactive power PI ranking order

| Overloaded Line | Line Flow (MW) | Line Flow (MVA) | Line Limit (MVA) |
|---|---|---|---|
| Pre-outage of line 2-5 | | | |
| 2-5 | 53.863 | 57.271 | 130 |
| 5-7 | 7.497 | 24.827 | 70 |
| Post-outage of line 2-5 | | | |
| 2-5 | nil | nil | 130 |
| 5-7 | 62.023 | 72.458 | 70 |
| Pre-outage of line 4-12 | | | |
| 4-12 | 20.705 | 23.808 | 65 |
| Post-outage of line 4-12 | | | |
| 4-12 | nil | nil | 65 |
| Pre-outage of line 1-2 | | | |
| 1-2 | 76.824 | 77.098 | 130 |
| Post-outage of line 1-2 | | | |
| 1-2 | nil | nil | 130 |

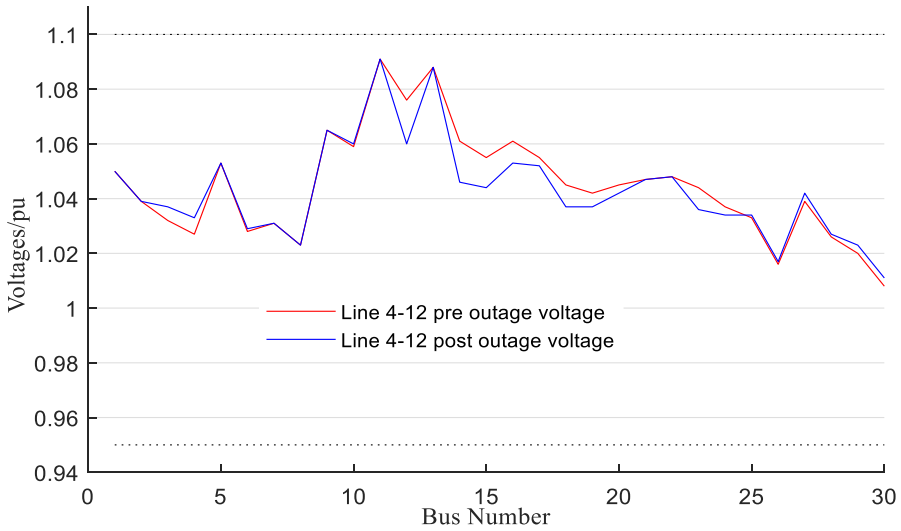


**Figure 4. 14: Pre and post outage voltage of line 4-12**

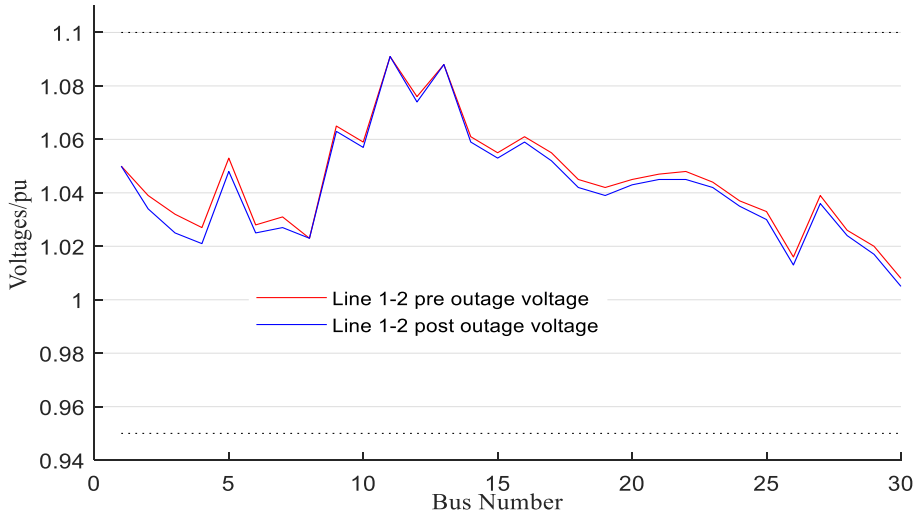


**Figure 4. 15: Pre and post outage voltage of line 1-2**

The comparison of post outage voltages for lines 2-5 and 28-27 is presented in Fig. 4.16. Table 4.10 summarizes the positions of the two transmission lines with ranking methods. Line 2-5 comes 1st in all rankings except for voltage ranking where it ranked 37th. No wonder its outage resulted into thermal overload of another line, but no bus voltage limits violation recorded. Line 28-27 ranked haphazardly in other methods but comes 1st in voltage ranking. Its outage violated bus voltage limits and caused line overloads on other transmission lines. Summarily, transmission line 28-27 outage which was the most severe contingency based on voltage PI ranking resulted into both line overloads and bus voltage limits violations, while outage of line 2-5 which was the most severe contingency consequent of real power PI ranking only resulted into line thermal limits violations. It can be inferred from the foregoing analysis that a system can be secured against real power overload but without being secured against voltage and reactive power limits violations because the disturbance that resulted in violation of one limit does not affect another. Therefore, a separate ranking based on different network parameter indices will produce better results.

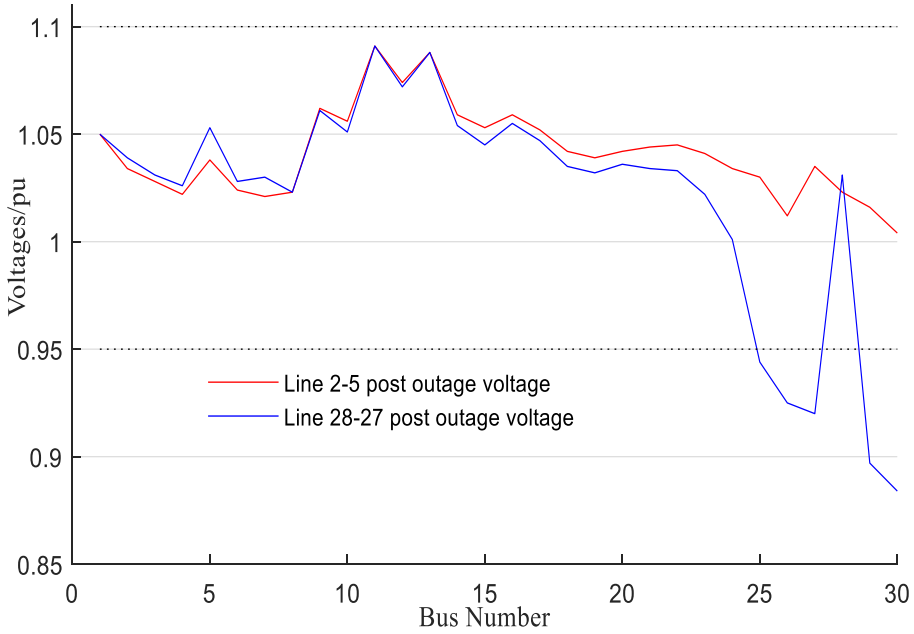


**Figure 4. 16: Post outage voltages of line 2-5 and 28-27**

Table 4. 10: Ranking comparison between line 2-5 and 28-27

| Ranking | PI_P | PI_V | PI_Q | PI_VQ | PI_PVQ |
|---|---|---|---|---|---|
| **2-5** | 1 | 37 | 1 | 1 | 1 |
| **28-27** | 10 | 1 | 7 | 4 | 10 |

### 4.6 Summary for chapter four

ATC computation is a vital tool in an interconnected system especially during deregulation for a better system planning and operation. RACPF method has been successfully implemented in determining the ATC of IEEE 30 bus RT system. The accuracy of this method has been established when compared with the results of previous work. Various operating conditions ranging from normal, contingency, bilateral and multilateral transactions were investigated as this is the case of modern power network operation. ATC has been established to decrease for all other transactions other than normal case. ATC values have also been obtained for contingency conditions. The least ATC value was observed when contingency was experienced during multilateral transaction. The importance of ATC to market participants in a deregulated power system has also been substantiated. This is inescapable in ensuring that succeeding transactions are practicable with considerations for system transmission constraints. The quantum of generation to be added, the sink(s) and source(s) buses for any specific bilateral/multilateral transactions can be distinctly described.

Likewise, performance index has been used as a tool for contingency ranking of IEEE 30 bus test system in this work. This was done with a view to presenting the most suitable method in deploying PI for contingency problems. The analyses of the ranked contingencies indicate the efficacy of PI in presenting the severity of line outage conditions for power network systems. The aftermath of post line outages for the most severe ranked lines based on real power and voltage PI also presented unique but important ranking order. The investigation conducted has demonstrated the behavioral attributes exhibited by different approaches of PI deployment. It

has therefore been established that the disturbance which resulted into lines overload did not necessarily cause bus voltage limits violations. Subsequently, voltage and real power indices should be treated differently in order to obtain a separate but meaningful contingencies rankings using PI, because the duo have been proven to be distinctly dissimilar.

With the efforts made in this chapter to determine ATC and contingency evaluation of deregulation and restructured network system, it is clear that an upsurge in power transaction subsists because of economic reasons. How then can the network performance as well as ATC be enhanced to cope with this upsurge in power demand/transaction amidst technical and economical restrictions of physical network expansion? These and other related questions are addressed in chronological order in the subsequent chapters.

# CHAPTER FIVE

# FACTS DEVICES ENHANCEMENT OF AVAILABLE TRANSFER CAPABILITY

## 5.1 Introduction

This chapter is divided into two sections. ATC enhancement with flexible alternating current transmission systems (FACTS) is presented in the first section. In this first part, static var compensator (SVC) and thyristor controlled series compensator (TCSC) models were incorporated into NR power flow equations for enhancement of available transfer capability (ATC) of a deregulated power network. Bus voltage profile improvement and real power loss minimization were also considered as part of objectives and were investigated during ATC enhancement. The performance of FACTS devices based on these objectives were analytically compared. These comparative analyses were conducted on IEEE 30 bus network system presented in Appendix A-1, and the implementation was done in MATLAB software environment.

Arising from the first section, an investigative study on the performance of FACTS device based on different methods of placements for available transfer capability enhancement (ATC), as inferred from the literature is presented in the second section. Here, total real power loss, real power performance index, real power loss sensitivity with respect to line reactance, power transfer distribution factor (PTDF), line thermal limitation, available transfer capability (ATC) value, and least bus voltage magnitude were the placement methods considered. Each of these methods was used independently for location of TCSC device for ATC enhancement. The comparative study was also conducted on same IEEE 30 bus test systems. The enhanced ATC values, bus voltage magnitudes and real power loss are then used in assessment of performance of TCSC with respect to locations.

## 5.2 FACTS and placement methods for ATC enhancement

The use of flexible alternating current transmission system for network performance enhancement is gaining attraction because of its several advantages in power system applications. FACTS devices can stabilise network systems, reduce power loses and enhance ATC [42]. The surge in power transactions, as a result of open access creation, through deregulation and restructuring warrants the need to enhance ATC. It has stated in [43], that adequate ATC is required for an economic power transaction while its sufficiency is needed for a competitive electricity trading. The orthodox ways of building new generation stations and transmission infrastructures in a bid to expand power transmission network capability are both technically and economically restricted. Issues such as right-of-way, environmental and high cost of power facilities are critical setback for power network expansions [67]. This triggers the exploration for optimization of the existing transmission network capability. Therefore, FACTS devices are becoming intrinsic parts of network systems, especially for enhancement of ATC among many other applications [67],[97]. Hence, researchers are intensifying efforts through diverse approaches in demonstrating capabilities of FACTS for ATC improvements. The alteration of natural electrical characteristics of transmission network system is inescapable in achieving target objective(s) especially when FACTS devices are employed. Therefore, the first section of this chapter compares the performance of SVC

with TCSC during ATC enhancement vis-à-vis bus voltage magnitude improvement and real power loss minimization.

Also, FACTS devices have proven to be effective in alleviating electrical power network problems such as transmission line thermal limits violations, bus voltage limits deviations, excessive power losses minimization, system instability among others [42]. Meanwhile, optimal placement of FACTS device can result into appropriate control of the desired network parameter(s) [67]. Although, the use of heuristic optimization algorithm is gaining attention in order to address the problems of FACTS devices settings nevertheless, placement of these devices still stands a challenge for ATC enhancement purposes. Most recent works in FACTS placement especially for ATC enhancement engaged one of earlier mentioned methods for device location and at times combine heuristic optimization techniques for device parameters settings. However, there is still need for further investigation on classified method of FACTS incorporation based on principles and hence this work. The second section of this chapter therefore investigates the performance of TCSC in ATC enhancement using each of the mentioned placement approaches independently. Here, only TCSC was considered for simplicity purposes and because of its proven capability to control line real power flow among other usefulness.

### 5.3 Results and discussions for ATC enhancement

The result presented here is an account of implementation of SVC and TCSC for ATC enhancement. Various values of network ATC during different transactions as improved by FACTS devices are dully reported in this section.

#### 5.3.1 Available transfer capability values

ATC of IEEE 30 bus system shown in Appendix A-2 was obtained using the described ACPTDF method. Three different transactions were implemented namely; Bilateral transaction T1 which comprises of 20 MW power transfer from generator bus 2 to load bus 20. Simultaneous transaction T2 involves 40 MW power transfer from generator 5 to load buses 16 & 18 while the third one is multilateral transaction of 40 MW power each from generator buses 5 & 8 to load buses 15 & 24. Table 5.1 presents ATC values obtained for the three transactions. In all the transactions, ATC of simultaneous trading was the minimum, while that of multilateral was the maximum as shown in the table.

Table 5. 1: ATC values for transactions T1, T2 and T3

| **Transactions** | **T1** | **T2** | **T3** |
|---|---|---|---|
| **ATC (MW)** | 162.11 | 106.18 | 171.68 |

##### 5.3.1.1 ATC values with incorporation of SVC and TCSC

In order to enhance ATC of the test network, SVC and TCSC were incorporated with test system at different time. At base case load flow, bus with least voltage magnitude was selected for SVC placement. This was because bus voltage profile improvement was one of the objectives in focus. SVC being a voltage regulating device was place at bus 30 with susceptance value in the range -0.25 to 0.25. Placement of TCSC was done

with the ranking of base case real power loss magnitude. This was also to fulfil the objective of real power loss control. Transmission line 12-15, having the highest real power loss magnitude was incorporated with TCSC. The reactance value of this TCSC was in the range of $-0.5 < X_{TCSC} < 0.5$. These locations applied to all the transactions. FACTS devices are not installed on lines that are already installed with transformer tap changing element as well as lines between buses installed with shunt compensators and generators even if sensitivity for placement favours such lines [6].

Table 5.2 presents the results obtained with incorporation of FACTS devices for the enhancement of the test system. SVC improved ATC with 14.11% while TCSC increased the value with 3.77% for bilateral transaction T1. An enhancement of 0.07% and 0.50% were recorded for SVC and TCSC for simultaneous transaction T2, while an improvement of 0.28% and 14.49% for SVC and TCSC respectively were obtained for multilateral transaction T3. Although, these devices responded differently to different transactions with varying magnification of enhancement, the duo improved ATC of the test system. Table 5.3 summarises the percentage enhancement of ATC. SVC performed well during bilateral enhancement more than TCSC while the reverse was the case for multilateral transaction. Both SVC and TCSC did not significantly enhanced ATC during simultaneous trading.

Table 5. 2: ATC values with and without FACTS

| **Transactions** | **T1** | **T2** | **T3** |
|---|---|---|---|
| **ATC (MW)** | 162.11 | 106.18 | 171.68 |
| **with SVC (MW)** | 184.99 | 106.25 | 172.16 |
| **with TCSC (MW)** | 168.22 | 106.71 | 196.56 |

Table 5. 3: Percentage enhancement of ATC

| | **Percentage (%)** | | |
|---|---|---|---|
| **Transactions** | **T1** | **T2** | **T3** |
| **with SVC (MW)** | 14.11 | 0.07 | 0.28 |
| **with TCSC (MW)** | 3.77 | 0.50 | 14.49 |

### 5.3.2 Bus voltage profile with incorporation of SVC and TCSC

Bus voltage magnitude during transaction T1 with incorporation of SVC and TCSC is presented in Fig. 5.1. TCSC maintained bus voltage magnitude throughout the transaction. However, network bus voltage between bus number 21 and 30 experienced a slight improvement with incorporation of SVC. A similar scenario was experienced during simultaneous transaction T2 as indicated in Fig. 5.2 in which voltage at buses numbers 21 to 30 were slightly improved with SVC. In the same way, TCSC when incorporated, maintained bus voltage magnitude for all buses. In multilateral transaction T3, a slight voltage dip occurred from bus number 14 to 26 with placement of TCSC for ATC enhancement. From the same bus 14 through to bus 30, an improved bus voltage profile was experienced with the integration of SVC to the test system. As shown in Fig. 5.3, voltage at bus 30 was held at 1.0 p.u. with placement of SVC and this aided the adjoining bus voltage magnitudes. This is because, shunt reactive compensation is capable of increasing voltage stability limit via the supplying of

reactive load and regulation of terminal voltage [13]. This was not the case for multilateral transaction with TCSC placement because, increase in line flow power affected contiguous bus voltage magnitudes. Within the location of generators in the network, bus voltage deviation was minimised because the reactive power control influence was enforced. This therefore kept bus voltage profile highly regulated from bus one to bus fifteen in all the transactions. The overlapping of all the curves from bus number 1 to 15 in the figures is an indication of this. Voltage magnitude deviation was more pronounced in the upper region of the test network for the obvious reasons of inadequacy of reactive power injection/absorption as required. The capability of SVC to provide appropriate reactive compensation resulted into optimal regulation of voltage profile within its influence. This was the situation in all the transactions as presented in Figs. 5.1 – 5.3.

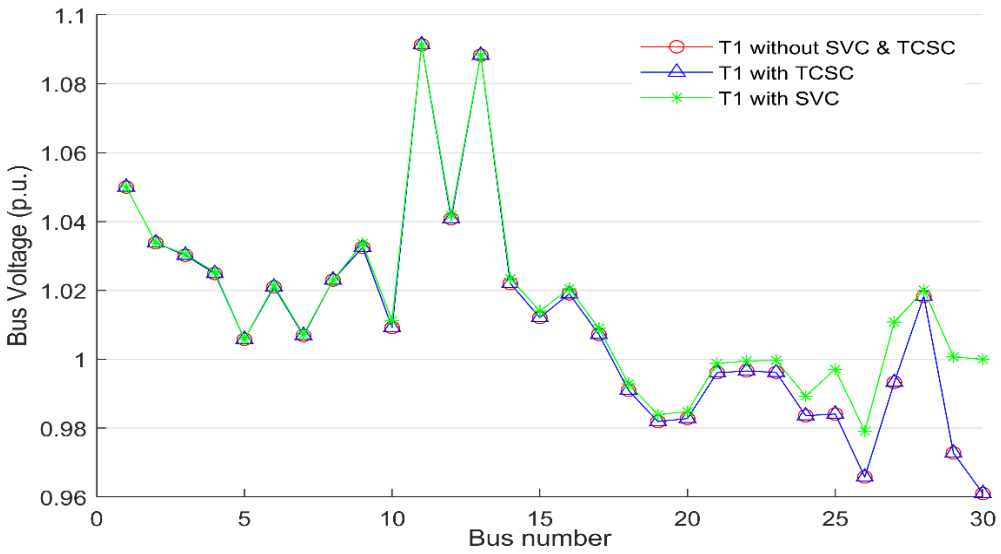


**Figure 5. 1: Bus voltage profile for T1 with SVC and TCSC**

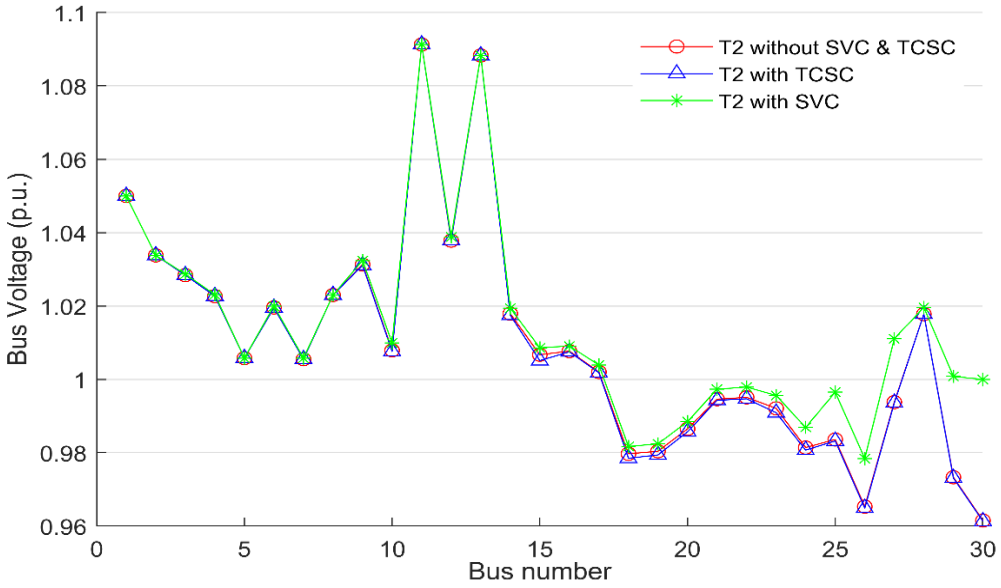


**Figure 5. 2: Bus voltage profile for T2 with SVC and TCSC**

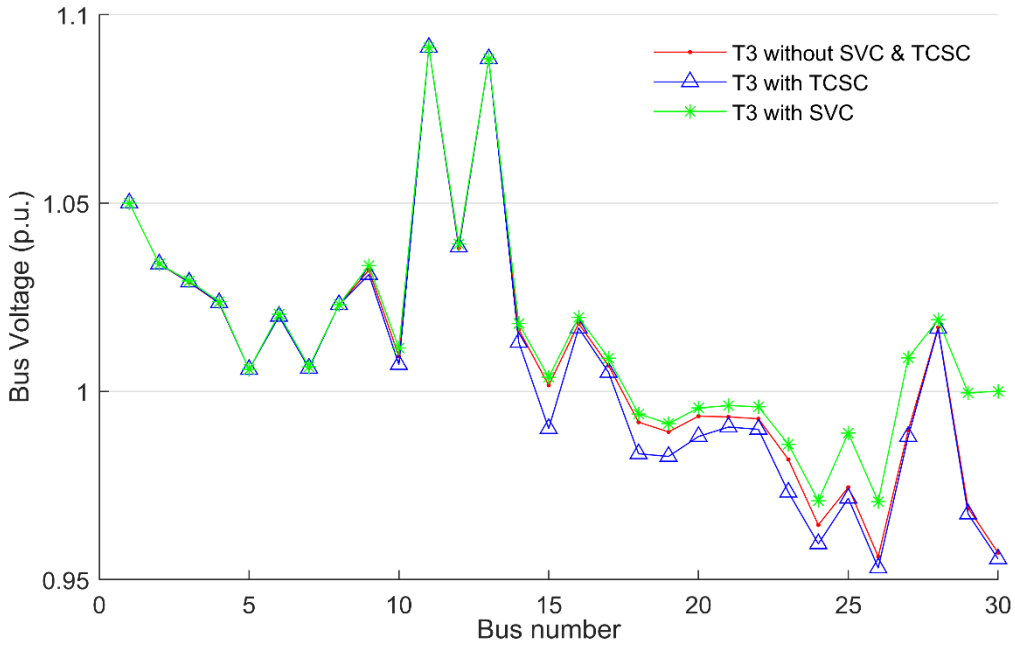


**Figure 5. 3: Bus voltage profile for T3 with SVC and TCSC**

### 5.3.3 Real power losses with incorporation of SVC and TCSC

The response of the test system real power loss to ATC enhancement consequent of FACT amalgamation is shown in Figs. 5.4 – 5.6. Placement of TCSC and SVC maintains system real power loss without further provocation during transaction T1. Both devices control real power loss approximately the same way, without significant different among them, as shown in Fig. 5.4. However, this was not the case during T2, where TCSC minimised real power loss on transmission line number 18 slightly more than SVC. A critical look at these figures 5.4 and 5.5 reveals the variation of system loss with FACTS for different transmission lines.

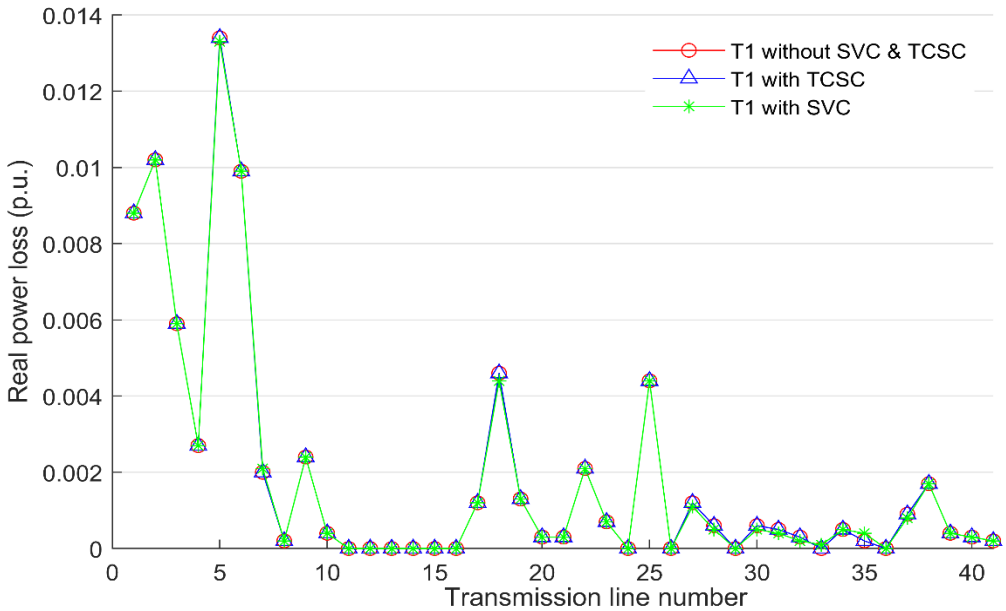


**Figure 5. 4: Real power loss during T1 with SVC and TCSC**

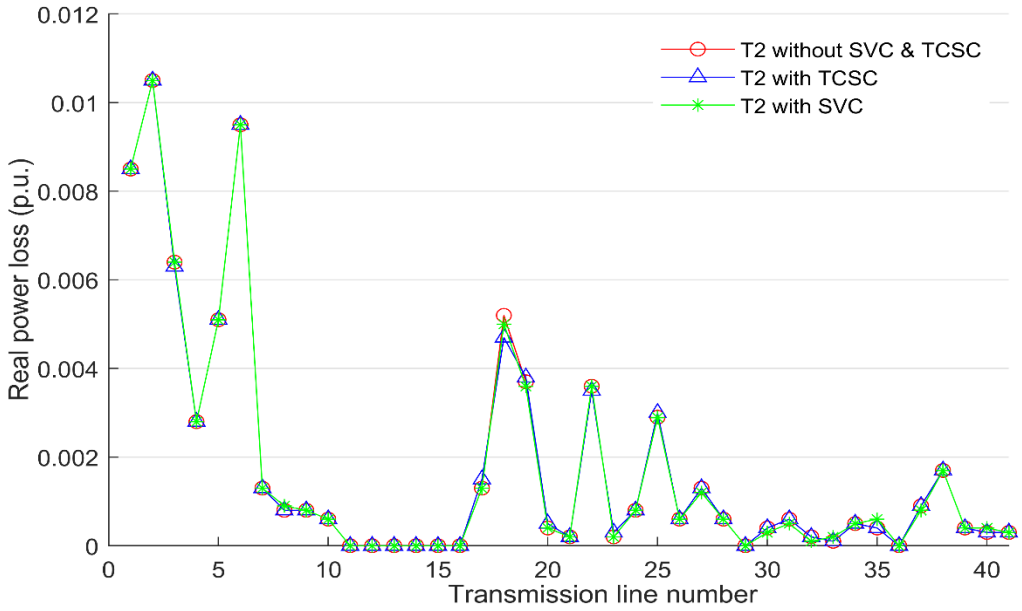


**Figure 5. 5: Real power loss during T2 with SVC and TCSC**

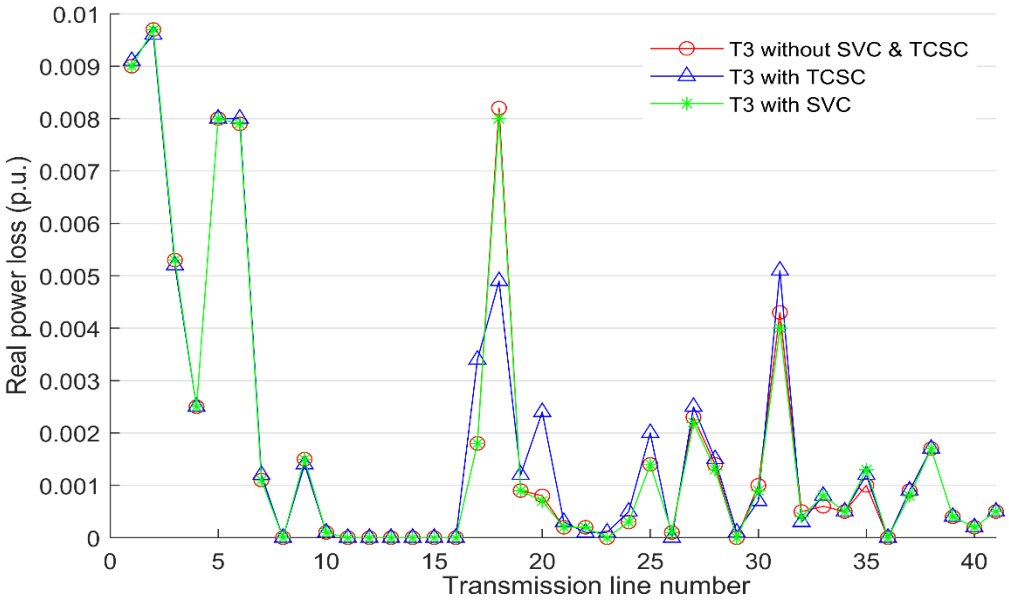


**Figure 5. 6: Real power loss during T3 with SVC and TCSC**

During transaction T3 however, as presented in Fig. 5.6, TCSC placement reduced system loss from 0.0081 p.u. to 0.005 p.u. on transmission line 12-15 where it was incorporated but increased losses slightly on line 14-15, 10-20 and 22-24 during multilateral transaction T3. In this situation, and for all these mentioned lines, SVC maintained and slightly reduced losses on line 12-15. The changes in the system loss is a function of nature of the transaction which predominantly occurred between sink buses 15 and 24. More power flow as experienced on the adjoining transmission lines led to more losses but with swift response of the FACTS devices. Unarguably, losses in the region of generator locations were controlled for all the three transactions as previously discussed.

Table 5.4 summarises the total real power loss for bilateral T1, simultaneous T2, and multilateral T3 transactions when TCSC and SVC were incorporated with test network. TCSC maintained the total loss at 0.0782 p.u. while SVC reduced the total loss with 0.0005 p.u. for T1. Total loss was minimised with 0.0003 p.u. by SVC while TCSC reduced it with 0.0001 p.u. during T2. During T3, SVC minimized losses to 0.0737 p.u. from 0.0743 p.u. while TCSC increased this total loss to 0.0764 p.u. Table 5.5 summarises real power loss minimization performance of these devices. It can be deduced from these values that minimization of system loss is more pronounced with SVC device because its incorporation in the test system resulted into loss minimization for all the scheduled transactions T1 to T3. However, TCSC minimised loss during T2, maintained loss level during T1 and slightly aggravated system loss during T3.

Table 5. 4: Total real power loss for the transactions

| **Transactions** | **T1** | **T2** | **T3** |
|---|---|---|---|
| **Losses without FACTS (p.u.)** | 0.0782 | 0.0729 | 0.0743 |
| **Losses with SVC (p.u.)** | 0.0777 | 0.0726 | 0.0737 |
| **Losses with TCSC (p.u.)** | 0.0782 | 0.0728 | 0.0764 |

Table 5. 5: Loss minimization values for SVC and TCSC

| **Transactions** | **T1** | **T2** | **T3** |
|---|---|---|---|
| **Losses with SVC (p.u.)** | -0.0005 | -0.0003 | -0.0006 |
| **Losses with TCSC (p.u.)** | 0.0000 | -0.0001 | +0.0021 |

### 5.4 Results and discussions for FACTS placement methods

In this second section, different methods of FACTS placement were adopted for through evaluation. This is because during the implementation of ATC enhancement conducted in first section of this chapter, it was discovered that location of FACTS devices in the network determines its utmost performance. Therefore, a research on performance of different placement approaches from the literature was harnessed in this section. The subsequent paragraphs present the results of findings as observed in the study conducted.

#### 5.4.1 Evaluation of TCSC placement techniques for ATC enhancement

In order to properly investigates the performance of TCSC based on different methods of placement, three different power transactions as considered in the first section were implemented. To recap, T1 comprises of bilateral transfer of 20 MW power from generator bus 2 to load bus 20. T2 involves simultaneous transaction of 40 MW of power between generator bus 5 and load buses 16 & 18, while transaction T3 is multilateral transfer of 40 MW power each from generator buses 5 & 8 to load buses 15 & 24. ATC of the test system was obtained using ACPTDF as discussed and the values obtained are as presented in Table 5.1. The need for same transactions was borne out of necessity for comparison purposes. However, these three transactions are used in verification of performance of TCSC in different locations as identified by various placement methods, for comparison basis.

### 5.4.2 Placement of TCSC for ATC values

Various placement methods presented in the literatures and as discussed in earlier chapters were implemented here. The methods were implemented one after the other and both the placement values and resultant ranking orders are presented. Table 5.6 presents the ranking values for first ten transmission lines obtained for different placement methods based on PTLB, PI, PTLS, XTL T1PTDF, T2PTDF and T3PTDF methods as discussed in chapter three. Table 5.7 shows transmission lines ranking based on these values. Ranking using TL and LBV are 15-23 and 29-30, while that of LTC are 15-18, 19-20 and 12-15 for T1, T2 and T3 (T1LTC, T2LTC and T3LTC) respectively. It should be recalled that, TCSC is not installed on lines containing transformer tap changing element as well as lines between buses containing shunt compensators and generators even if such lines have higher sensitivity as earlier stated.

Table 5. 6: Ranking values for different placement methods

| L/N | PTLB | PI | PTLS | -XLS | T1PTDF | T2PTDF | T3PTDF |
|---|---|---|---|---|---|---|---|
| 1 | 0.012 | 0.0048 | 0.02584 | 0.0001 | -0.7015 | -1.0000 | -0.8383 |
| 2 | 0.010 | 0.0024 | 0.01979 | 0.0001 | -0.3845 | -0.6882 | -0.7275 |
| 3 | 0.008 | 0.0018 | 0.00233 | 0.0003 | -0.3713 | -0.3453 | -0.6278 |
| 4 | 0.007 | 0.0017 | 0.00189 | 0.0007 | -0.3713 | -0.2925 | -0.5908 |
| 5 | 0.004 | 0.0014 | 0.0014 | 0.0007 | -0.3647 | -0.2858 | -0.5907 |
| 6 | 0.003 | 0.0013 | 0.00139 | 0.0008 | -0.3432 | -0.2827 | -0.3868 |
| 7 | 0.003 | 0.0010 | 0.00103 | 0.0011 | -0.3327 | -0.2240 | -0.372 |
| 8 | 0.002 | 0.0009 | 0.00094 | 0.0011 | -0.3287 | -0.1615 | -0.3485 |
| 9 | 0.002 | 0.0008 | 0.00086 | 0.0015 | -0.2525 | -0.0970 | -0.3412 |
| 10 | 0.002 | 0.0008 | 0.0006 | 0.0020 | -0.2473 | -0.0880 | -0.3302 |

Table 5. 7: Transmission line ranking for different placement methods

| L/N | PTLB | PI | PTLS | XLS | T1PTDF | T2PTDF | T3PTDF |
|---|---|---|---|---|---|---|---|
| 1 | 2-5 | 2-5 | 1-2 | **14-15** | 10-20 | 9-11 | 4-12 |
| 2 | 1-2 | 1-3 | 2-5 | 24-25 | 4-12 | 9-10 | **12-15** |
| 3 | 1-3 | 28-27 | **14-15** | 21-22 | 6-9 | 10-17 | 22-24 |
| 4 | 2-6 | 2-6 | 12-14 | 25-26 | 9-10 | 10-20 | 6-9 |
| 5 | 2-4 | 6-10 | 29-30 | 25-27 | 2-6 | 4-12 | 9-10 |
| 6 | **12-15** | 4-12 | 12-15 | 29-30 | **15-18** | **19-20** | 10-21 |
| 7 | 6-7 | **27-30** | 23-24 | 18-19 | 18-19 | 15-18 | 8-28 |
| 8 | 3-4 | 2-4 | 12-16 | 10-17 | 2-4 | 12-16 | 28-27 |
| 9 | 4-6 | 9-11 | 10-21 | 23-24 | 12-15 | 12-15 | 25-27 |
| 10 | 27-30 | 1-2 | 15-18 | 19-20 | 1-3 | 18-19 | 6-10 |

Therefore, the transmission lines highlighted in bold black on Table 5.7 represent the placement line as identified by each placement approaches. In the analysis however, some placement methods identified same locations in some occasions. Placement location of transmission line 12-15, identified by T3LTC and T3PTDF were the same as that of PTLB. Line 14-15 acknowledged by PTLS was also the same with that of XLS. T1PTDF and T1LTC pointed at same transmission line 15-18 while T2PTDF and T2LTC recognised position 19-20 as the optimal location for placement of TCSC. Ranking with LTC and PTDF were symmetrical for T1,

T2 and T3 and this is one on attributes of AC/DCPTDF method of ATC determination. TCSC range of reactance value for this investigation is as earlier stated.

### 5.4.3 ATC enhancement with TCSC at various locations

The various values obtained for ATC enhancement using TCSC are as presented in Table 5.8. Colum 1 presents different placement methods while the favoured transmission line locations are on column 2. Various enhanced ATC values for transactions T1, T2 and T3 are presented in columns 3, 4 and 5 respectively. Base case are ATC values obtained without the incorporation of TCSC as presented in Table 5.1. Enhanced ATC values during T1, T2, and T3 for various choices of locations are further explained subsequently.

Table 5. 8: ATC values obtained with TCSC at different line locations

| Method | Location | T1 | T2 | T3 |
|---|---|---|---|---|
| PTLB/T3PTDF/T3LTC | 12-15 | 168.22 | 106.71 | 196.56 |
| PI | 27-30 | 184.96 | 106.23 | 49.19 |
| PTLS/XLS | 14-15 | 183.05 | 106.31 | 172.68 |
| TIPTDF/T1LTC | 15-18 | 152.72 | 107.46 | 156.35 |
| T2PTDF/T2LTC | 19-20 | 118.62 | 106.20 | 159.40 |
| LBV | 29-30 | 184.96 | 106.18 | 171.68 |
| TL | 15-23 | 181.61 | 105.94 | 180.34 |
| **Base case** | **-** | **162.11** | **106.18** | **171.68** |

#### 5.4.3.1 Bilateral transaction T1 with incorporation of TCSC

TCSC has a wide range of performance in five out of seven locations for T1. The highest enhancement recorded with placement based on PI and LBV while the least improvement occurred when placement was achieved with PTLB/T3PTDF/T3LTC method. Location of TCSC based on T1PTDF/T1LTC and T2PTDF/T2LTC did not result into an enhancement but rather diminished the base case ATC as presented in Table 5.9. PTLS/XLS and TL enhanced ATC equally and significantly by 12%. Therefore, the highest enhancement performance of TCSC occurred with placement on lines 27-30 and 29-30 as optimized by PI and LBV placement methods respectively. In implementation of bilateral transaction of this kind with ATC enhancement in focus however, placement of TCSC using PI and LBV methods is optimal to achievement of the objective.

Table 5. 9: ATC enhancement ranking with TCSC during T1

| Method | Location | T1 | %ATC | Ranking |
|---|---|---|---|---|
| PI | 27-30 | 184.96 | 14. 095 | 1 |
| LBV | 29-30 | 184.96 | 14.095 | 2 |
| PTLS/XLS | 14-15 | 183.05 | 12.917 | 3 |
| TL | 15-23 | 181.61 | 12.029 | 4 |
| PTLB/T3PTDF/T3LTC | 12-15 | 168.22 | 3.769 | 5 |
| TIPTDF/T1LTC | 15-18 | 152.72 | -5.792 | 6 |
| T2PTDF/T2LTC | 19-20 | 118.62 | -26.827 | 7 |
| **Base case** | | **162.11** | | |

#### 5.4.3.2 Simultaneous transaction T2 with incorporation of TCSC

Table 5.10 gives the enhancement recorded during T2, having placed the device at various locations. No significant enhancement was recorded here other than 1.21% resulted from placement with T1PTDF/T1LTC which top the hierarchy as indicated in third column of the table. Likewise, no appreciable diminish in base case ATC besides 0.23% attributed to TL placement method. PTLB/T3PTDF/T3LTC, PTLS/XLS, PI, T2PTDF/T2LTC, and LBV placement approaches only regulate ATC value and did not have significant contribution to ATC improvement. It can be observed in this process that TCSC performance in ATC enhancement as optimized by TIPTDF/T1LTC placement method was not as significant as that recorded during T1.

Table 5. 10: ATC enhancement ranking with TCSC during T2

| Method | Location | T2 | %ATC | Ranking |
|---|---|---|---|---|
| TIPTDF/T1LTC | 15-18 | 107.46 | 1.21 | **1** |
| PTLB/T3PTDF/T3LTC | 12-15 | 106.71 | 0.50 | 2 |
| PTLS/XLS | 14-15 | 106.31 | 0.12 | 3 |
| PI | 27-30 | 106.23 | 0.05 | 4 |
| T2PTDF/T2LTC | 19-20 | 106.20 | 0.02 | 5 |
| LBV | 29-30 | 106.18 | 0.00 | 6 |
| TL | 15-23 | 105.94 | -0.23 | 7 |
| **Base case** | | **106.18** | | |

#### 5.4.3.3 Multilateral transaction T3 with incorporation of TCSC

The transaction T3 differs in response to these various placement methods as presented in Table 5.11. Placement done with TPLB/T3PTDF/T3LTC brought about a significant enhancement leaving a wide gap between the next placement method that resulted into a reasonable improvement. For this transaction, PTLB/T3PTDF/T3LTC, TL and PTLS/XLS methods improved ATC with 14.49%, 5.04% and 0.58% respectively. Value of ATC was impaired by 7.17%, 8.93% and 71.35% with T2PTDF/T2LTC, TIPTDF/T1LTC and PI methods respectively. However, LBV only maintained ATC value with no significant impact on ATC. Placement based on PI for this transaction diminished ATC greatly, having resulted into 49.19 MW with the presence of TCSC as against 171.68 MW without TCSC. With this type of multilateral transaction, TCSC significantly enhanced ATC when placed on transmission line 12-15 and moderately enhanced ATC value when placed on line 15-23, and 14-15.

Table 5. 11: ATC enhancement ranking with TCSC during T3

| Method | Location | T3 | %ATC | Ranking |
|---|---|---|---|---|
| PTLB/T3PTDF/T3LTC | 12-15 | 196.56 | **14.49** | **1** |
| TL | 15-23 | 180.34 | 5.04 | 2 |
| PTLS/XLS | 14-15 | 172.68 | 0.58 | 3 |
| LBV | 29-30 | 171.68 | 0.00 | 4 |
| T2PTDF/T2LTC | 19-20 | 159.40 | -7.15 | 5 |
| TIPTDF/T1LTC | 15-18 | 156.35 | -8.93 | 6 |
| PI | 27-30 | 49.19 | -71.35 | 7 |
| Base case | | **171.68** | | |

### 5.4.4 Voltage profile during ATC enhancement with TCSC

Bus voltage profile is also an important network parameter in establishing the performance of FACTS device when incorporated into the network. Therefore, the voltage profile of the test system with incorporation of TCSC under various power transactions are presented as follows;

#### 5.4.4.1 Bilateral transaction T1 with incorporation of TCSC

Buses 18, 19, 20, 21 and 22 experienced a slight improvement in bus voltage magnitude based on placement of TCSC on transmission line 19-20 identified by T2PTDF/T2LTC, although, ATC was declined with about 27% instead of enhancement during this placement. In contrast, a droop in bus terminal voltages was experienced on these same buses with location of TCSC based on identification by T1PTDF/T1LTC (line 15-18). With placement on this line 15-18, a decline in ATC of about 6% was experienced under this condition. As can be inferred from Fig. 5.7, there are no other significant changes in bus voltages for other placements during this transaction T1. Placement in other locations as indicated by other methods during transaction T1 only maintained bus voltage profile.

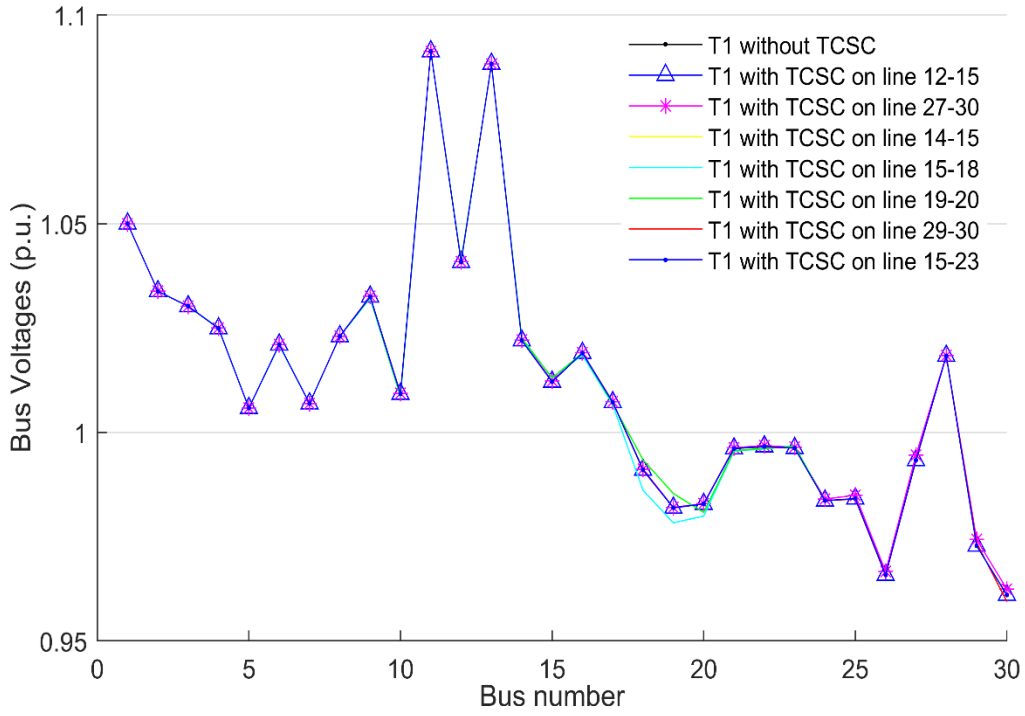


**Figure 5. 7: Comparison of bus voltage profile during T1**

#### 5.4.4.2 Simultaneous transaction T2 with incorporation of TCSC

During T2 and as depicts in Fig. 5.8, all the placement methods resulted into a slight decline in voltages magnitude from bus 14 to 24. However, voltage sag due to location of TCSC based on T1PTDF/T1LTC (15-18) and T2PTDF/T2LTC (19-20) were more intense. Moreover, these locations only resulted into 1.21% and 0.02% ATC enhancement. This implies that bus voltage profile deviation was aggravated during this transaction. Recall that hardly did TCSC improved ATC under this condition. Therefore, special attention

should be paid to any transaction involving power transfer of this nature, especially if inescapable. This is to ensure adequate consideration for network security whenever the system operator set for power dispatch especially in this era of liberalization.

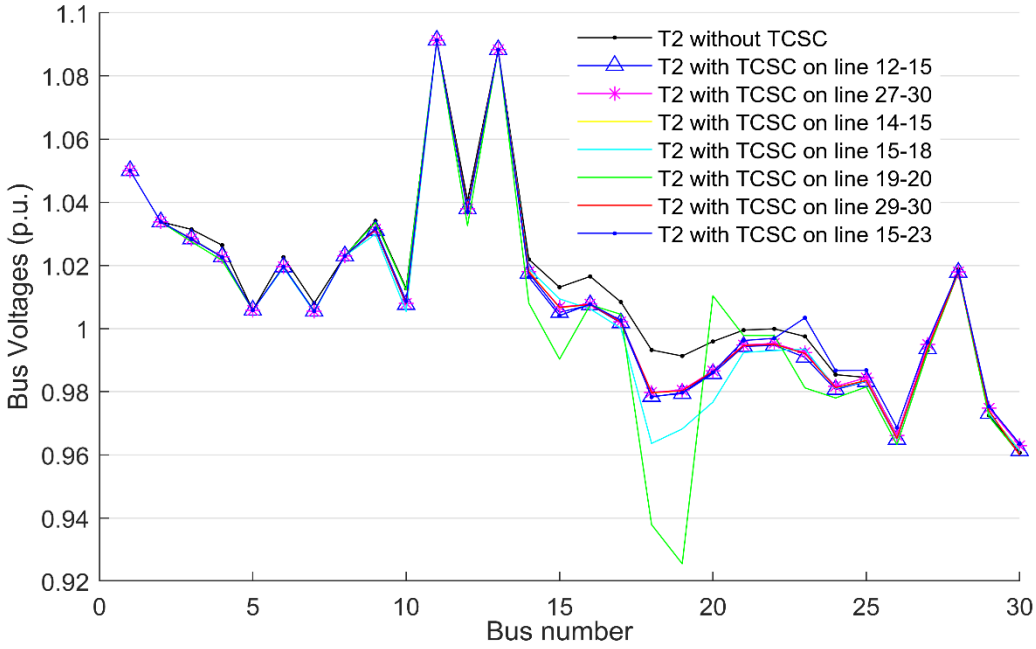


**Figure 5. 8: Comparison of bus voltage profile during T2**

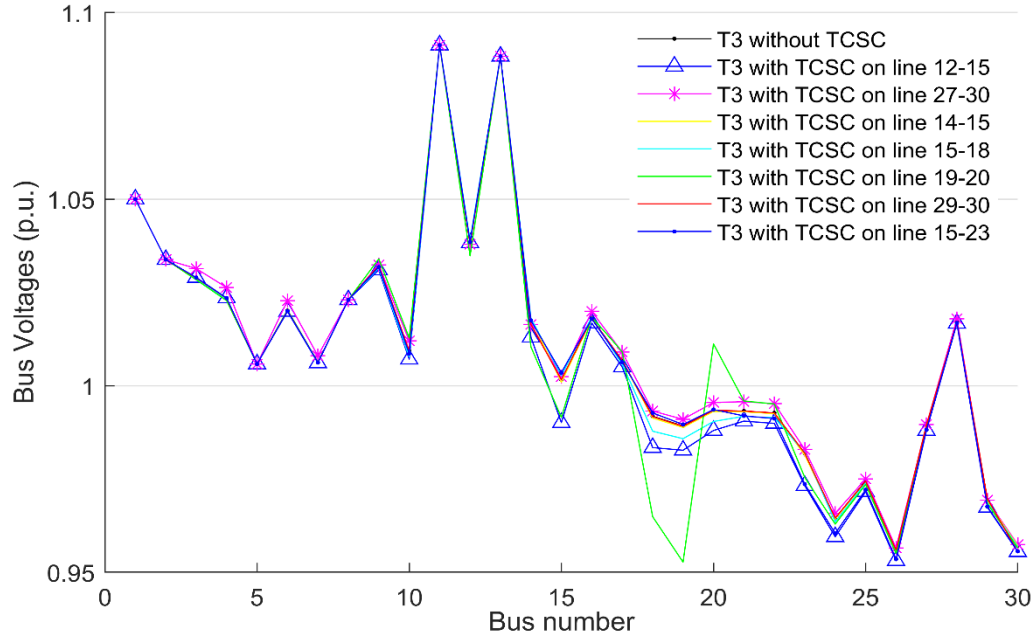


**Figure 5. 9: Comparison of bus voltage profile during T3**

#### 5.4.4.3 Multilateral transaction T3 with incorporation of TCSC

During T3 and as can be seen in Fig. 5.9, location based on PI (27-30) slightly improved bus voltages especially from bus 14 to 24, although, there was a colossal decline in ATC with this condition as earlier reported. Like previous transaction T2, T1PTDF/T1LTC placement method resulted into slight bus voltage deviation at bus 18, 19 and 20 as indicated by location line 15-18. In location line 19-20 as identified by T2PTDF/T2LTC, terminal voltage at bus 19 declined but improved at bus 20 as shown in the curve. The oscillation in terminal voltage because of placement in these locations are similar but with different peak of oscillation. These locations are radial in nature and hence they exhibit similar characteristics. Interestingly, these locations did not result into ATC improvement. There was a slight bus voltage deviation with PTLB/T3PTDF/T3LTC (12-15) placement however, an incomparable highest value of enhanced ATC of about 15% was recorded for this location.

### 5.4.5 Evaluation of real power loss with TCSC during ATC enhancement

The focus of this chapter concerns comparison of different placement approaches for ATC enhancement however, evaluation of system loss is also very important as part of the assessment. Although, it becomes a herculean task to expect more power flow without corresponding loss increase, notwithstanding, evaluation of real power loss associated with each placement method will be of noble assistance in justification of best approach.

#### 5.4.5.1 Real power loss during ATC enhancement with TCSC

The active power loss for the three transaction T1, T2, and T3 are presented in Figs. 5.10 - 5.12. In Fig. 5.10, placement on location line 27-30 resulted into loss minimization during transaction T1. Locating TCSC on line 15-18 regulate the real power loss but with a slight swell on the line number 25. In all other locations, incorporation of TCSC did not aggravate real power loss but rather maintain the loss magnitude as depicted in the figure.

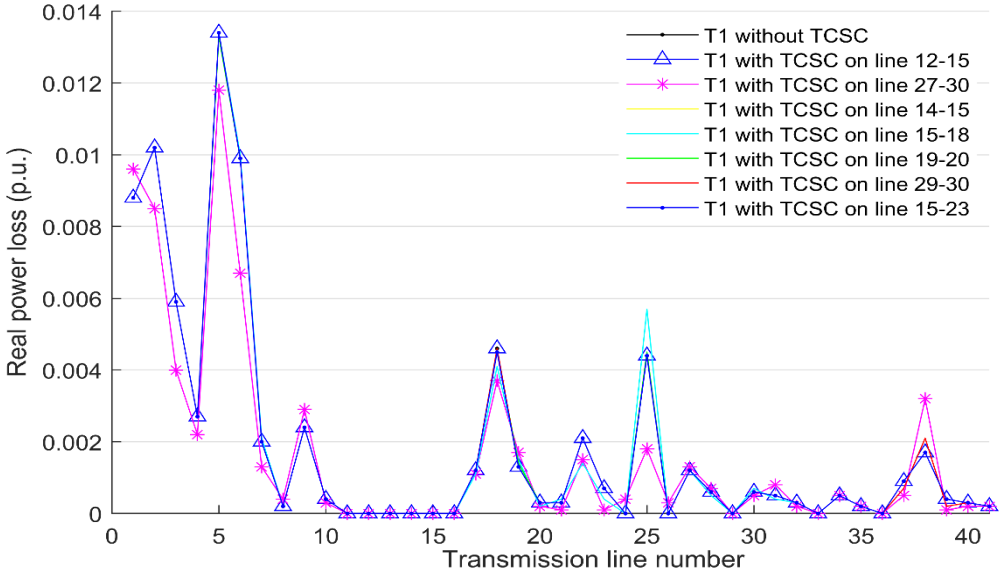


**Figure 5. 10: Real power loss during transaction T1**

#### 5.4.5.2 Real power loss during ATC enhancement with TCSC for transaction T2

The real power loss values for all the placement methods during T2 are plotted and presented in Fig. 5.11. In all these locations, TCSC ensured power loss control for line numbers 1 to 16. Placement on line 19-20 resulted into increase in loss magnitude for transmission line 12-15, 15-18 and 22-24. Also, placement on line 15-18 resulted into loss minimization on same line but with slight loss increase on line 10-20. When TCSC was located on line 27-30, it also led to slight increase in loss magnitude on same line. Details of loss minimization during T2 can be well understood through Fig. 5.11.

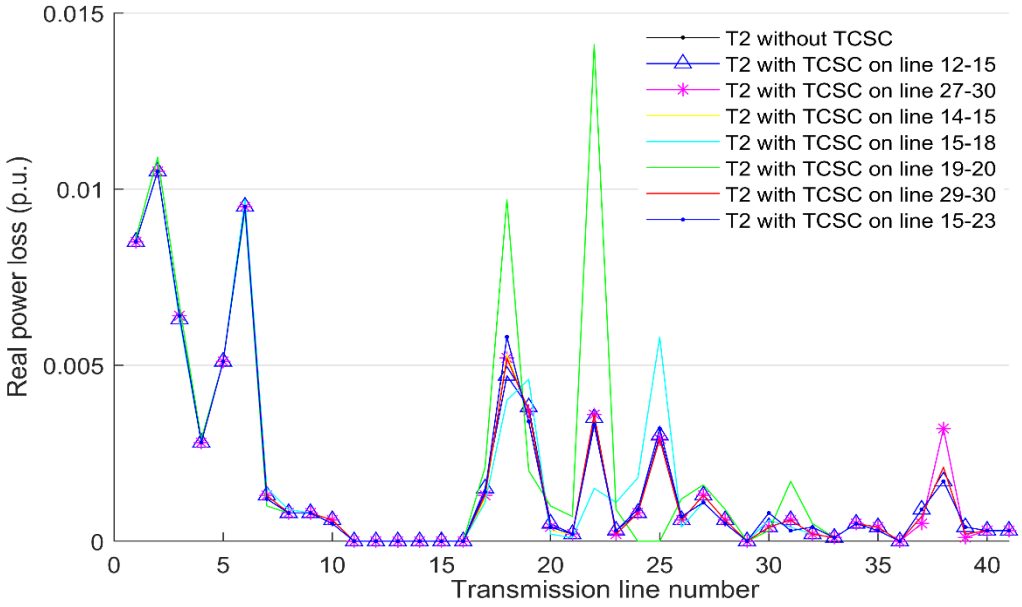


**Figure 5. 11: Real power loss during transaction T2**

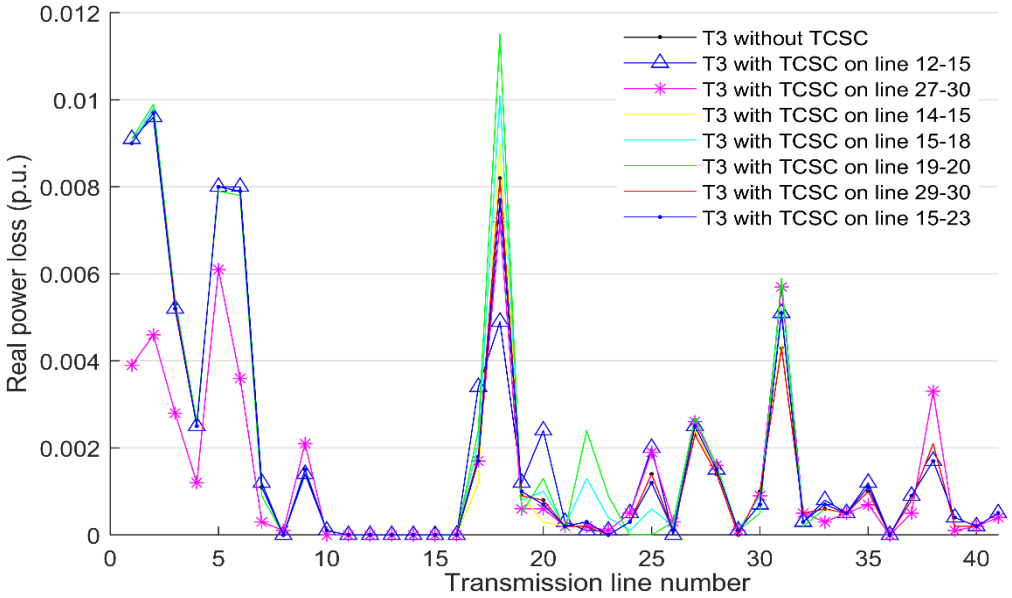


**Figure 5. 12: Real power loss during transaction T3**

#### 5.4.5.3 Real power loss during ATC enhancement with TCSC for transaction T2

Figure 5.12 presents active power loss for transaction T3. Placement of TCSC on transmission line 27-30 resulted into optimal loss minimization in all the transmission line except line 6-7, 10-20 and 27-30. When location of line 19-20 was used, loss magnitude increased on line numbers 15 and 22 with losses on other lines properly controlled. Similar result was obtained with placement on line 15-18 but with lower magnitude this time around. Details of network behavior with TCSC placement in other locations are well described in Fig. 5.12.

As indicated in Figs. 5.10 & 5.12, reduction in loss of 14% and 25% for T1 and T2 were observed with incorporation of TCSC based on PI (27-30). This is evident in Table 5.12. In transactions T2 and T3, an upsurge of real power losses was experienced in the range of 2.5% to 6% for T1PTDF/T1LTC placement. Also, an increase in active power loss of 20% for T2 and 10% for T3 were observed for placements resulted from T2PTDF/T2LTC. These are evident from Figs. 5.11 & 5.12. Loss deviations from base case values based on other placements for transaction T1, T2 and T3 remained insignificant. Table 5.12 presents summary of the total real power losses for all the implemented placement methods. Total real power loss for all these locations as compared base case scenario is contained and well spelt out in the table.

Table 5. 12: Total real power loss for ATC enhancement with TCSC

| Method | Location | T1 | T2 | T3 |
|---|---|---|---|---|
| **PTLB/T3PTDF/T3LTC** | 12-15 | 0.0782 | 0.0728 | 0.0764 |
| **PI** | 27-30 | 0.0670 | 0.0737 | 0.0554 |
| **PTLS/XLS** | 14-15 | 0.0782 | 0.0728 | 0.0742 |
| **TIPTDF/T1LTC** | 15-18 | 0.0782 | 0.0747 | 0.0783 |
| **T2PTDF/T2LTC** | 19-20 | 0.0782 | 0.0881 | 0.0814 |
| **LBV** | 29-30 | 0.0782 | 0.0729 | 0.0744 |
| **TL** | 15-23 | 0.0781 | 0.0733 | 0.0744 |
| **Base case** | | 0.0782 | 0.0729 | 0.0743 |

### 5.5 Summary of chapter five

In this chapter, ATC values were improved with incorporated of TCSC and SVC into IEEE 30 bus network system. These FACTS enhanced ATC for engaged bilateral, simultaneous and multilateral transactions. During enhancements, TCSC maintained bus voltage magnitude for bilateral and simultaneous transactions but with slight voltage droop during multilateral trading. In contrast, SVC slightly improved bus voltage profile for all the transactions. The introduction of SVC contributed to total system real power loss minimization for all the transactions while that of TCSC had no significant minimization for bilateral and simultaneous dealings but rather increased total real power loss for multilateral transaction. Real power loss minimization of up to 0.06 MW and voltage improvement of bus 21 to 30 were achieved with SVC, while ATC enhancement of up to 14% were recorded for both devices. ATC values, bus voltage magnitude profile and transmission line real power losses suggested an advantage of SVC over TCSC for ATC enhancement deployment**.** Therefore, for transfer capability enhancement with voltage improvement and real power loss minimization in focus, SVC is more relevant.

In the same vein, TCSC placement based on base case real power loss greatly enhanced ATC of multilateral transaction and maintained both bus voltage profile and real power losses. Placements using real power performance index and least bus voltage approaches enhanced ATC of bilateral transaction, maintained bus voltage and minimized losses. FACTS location considering PTDF increased losses and led to bus voltage deviations in all transactions. It greatly attenuated ATC for bilateral and multilateral trading without significant ATC enhancement for simultaneous transaction. Disparities in enhancement ranges between 2% and 85% were achieved while real power loss minimization of up to 25% was obtained based on different placement methods implemented in this second section. Arising from comparison of these placement methods, as applied to optimal placement of FACTS for ATC enhancement, therefore, bus voltage profile, real power loss and nature of transactions should be considered in adopting the right placement method.

The conclusion of implemented research in this chapter led to further inquisition as per the need to further optimize FACTS device placement for achievement of set objective(s) in network system. The subsequent chapters explore a better approach for optimal placement of FACTS device.

# CHAPTER SIX

# OPTIMIZATION OF THYRISTOR CONTROL SERIES COMPENSATOR WITH BRAIN STORM OPTIMIZATION ALGORITHM

## 6.1 Introduction

In this chapter, Brain storm optimization algorithms (BSOA) is engaged for the optimum setting of FACTS devices for enhancement of ATC of a deregulated electrical power system network. ATC enhancement, bus voltage deviation minimization and real power loss regulation were formulated into multi-objective problems for FACTS allocation purposes. TCSC was considered for simulation and analyses because of its fitness for active power control among other usefulness. ATC values were obtained for both normal and n-1-line outage contingency cases and these values were enhanced for different bilateral and multilateral power transactions. IEEE 30 bus system presented in Appendix A-2 was used for demonstration of the effectiveness of this approach in a MATLAB software environment. Obtained enhanced ATC values for different transactions during normal evaluation cases were then compared with enhanced ATC values obtained with particle swarm optimization (PSO) set TCSC technique under same trading. The performance of these two algorithms were presented and analysed.

## 6.2 Applications of BSOA

It was mentioned in the previous discussion that one of the consequences of electrical power deregulation and restructuring is the resultant competitive electrical power transactions. This results into an herculean task for power system operators in order to maintain a secured and economic power trading amidst system constraints and other bounded operating conditions. For emphasis, enhancement of ATC becomes imperative in a bid to handle the upsurge in power trading because sufficient and adequate ATC are necessary for both competitive and economic power transactions [43]. It has also been highlighted that applications of FACTS devices for enhancement of ATC is gaining attention due to economic and technical limits of the conventional methods involving physical network expansions. Apart from transmission capability enhancement, bus voltage deviation minimization, real and reactive power loss minimization, FACTS devices have been recognized to offer additional benefits including, voltage stability enhancement, power system stability enhancement, power system oscillation minimization, system loadability and operational band width enhancement among others [105],[118]. FACTS allocation which is sine-qua-non to its performance is a major problem and it is being addressed in recent time with heuristic algorithms. The comparative performance of different FACTS placement methods used in location of TCSC for ATC enhancement as obtained in the literature was implemented in chapter five. With fast response at lowest cost, TCSC is known to have a surpassing usefulness among FACTS devices because of its capability to advance system loadability, transient stability, power transmission capability and its ability to contain transmission loss as well as oscillation of network at low frequency [115]. Therefore, to effectively control these power network parameters, an optimal setting of TCSC is of paramount and inescapable. In this chapter, BSOA which is a new heuristic and predicting optimization algorithms, and which revolutionizes human brainstorming process was used for optimal setting of TCSC parameters having adopted

system real power loss placement method as investigated in the previous chapter. Metaheuristic algorithms are the contemporary direction for FACTS allocation optimization solutions because, these problems which are mostly multi-objective, multi-modal and restrained are as well complex in nature [63].

BSOA is a novel, swarm based intellectual algorithm which revolutionizes combined human brainstorming processes [184]. The application of this algorithm to most optimization problem is evolving but with a rare utilization in FACTS allocation problems [183]. In this chapter, BSO algorithm is utilized to solve FACTS multi-objective optimization problem and in summary, the followings are achieved in this chapter: An investigation into capability of BSOA heuristic procedure especially in the areas of power system optimization problem deployment was conducted with a view to further exploring its potency; This algorithm was applied to optimum setting of TCSC for solving multi-objective problems involving ATC enhancement, bus voltage deviation minimization and real power loss regulation; The test system response to optimally set TCSC placement for these objectives were also examined; Performance of BSOA set TCSC for various transactions during normal line intact condition were investigated; Network response to BSOA set TCSC for various n-1-line outage contingency conditions were also looked into; Comparison of BSO performance with that of PSO algorithm were also investigated and forthwith reported.

### 6.3 Network power and transactions description

The test system which has been modified as shown in Fig 6.1 comprises 6 generators including slack and 24 load nodes. The lower limits of voltage magnitude is 0.95 p.u. for all buses while the upper limit is 1.05 p.u. for all other buses except generator buses with specified upper limit of 1.1 p.u. Optimal settings of TCSC with BSOA was successfully validated on this test system. The modification was to allow for proper description of various power transactions as itemized in the subsequent paragraph.

#### 6.3.1 Description of undertaken transactions

Two major different bilateral and multilateral power transactions each for intact and for n-1-line outage contingencies were implemented. Bilateral transactions T1 and T2 are in red and green colors, while multilateral transactions T3 and T4 are in yellow and blue colors respectively in Fig. 6.1. These transactions are as characterized below.

- T1: 20 MW Bilateral transaction of power from seller bus 10 to buyer bus 23.
- T2: 20 MW Bilateral transaction of power from seller bus 12 to buyer bus 19.
- T3: 40 MW Multilateral transactions of power from seller buses 5 & 8 to buyer buses 15 & 24.
- T4: 40 MW Multilateral transactions of power from seller buses 10 & 12 to buyer buses 23 & 24.

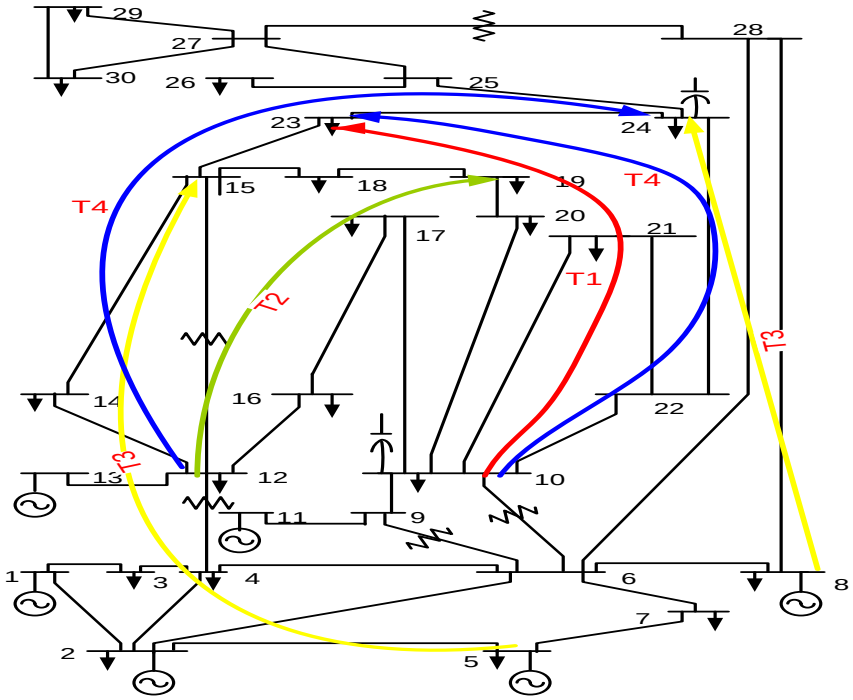


**Figure 6. 1: Modified basic line diagram of the IEEE 30 bus network test system**

### 6.3.2 Selection of line outage contingencies

Power flow analyses of test system were carried out for base case and n-1-line outage contingency conditions to obtain ATC. In implementation of n-1-line outage contingency in this chapter, due consideration was given to real power as well as voltage based PI contingency ranking of the transmission lines as presented in chapter two of this thesis. The entire transmission line divided into four and outage selection based on one line per quarter length. Lines 2-5, 6-9, 18-19 and 24-25 fall into 1$^{st}$ & 37$^{th}$, 16$^{th}$ & 4$^{th}$, 34$^{th}$ & 27$^{th}$ and 26$^{th}$ & 14$^{th}$ positions for real power and voltage contingency ranking respectively agreeable to 1$^{st}$, 2$^{nd}$, 3$^{rd}$ and 4$^{th}$ quarter of the total transmission line length, were selected for outage. One of the objectives here was to minimize real power loss in order to advance ATC, so highest ranked real power loss line was identified. The optimization process was implemented and optimal setting of TCSC was carried out. Branches 4-12, 6-9, 6-10 and 27-28 which contain transformer tap setting cannot be installed with TCSC and likewise, lines 1-2, 1-3, 2-4, 2-5, 2-6, 5-7, 6-8, 9-11, and 12-13 which are transmission lines between buses that contain generator can also not be installed with the device. In the same vein, lines 9-10, 10-17, 10-20, 10-21, 10-22, 22-24, 23-24 and 24-25 which are transmission lines between buses installed with shunt compensating elements are not candidates for TCSC device incorporation. PSO is also applied for same optimization problem for the purpose of comparison with BSOA performance. However, since the main objective was ATC enhancement, its associated scaling factor was the largest value of 0.8, while other objectives were allotted with 0.1 each. This implies that $\beta_1 = 0.8, \beta_2 = 0.1, and\ \beta_3 = 0.1$. Table 6.1 presents the parameters used for BSO and PSO algorithms. These algorithms were impartially compared with the parameters having the same value where possible as depicted in the table.

Table 6. 1: Parameters use for BSO and PSO algorithms

| **BSOA Parameters** | | **PSO Parameters** | |
|---|---|---|---|
| Parameters | Value | Parameters | Value |
| Population Size | 41 | Population Size | 41 |
| Dimension | 2 | Number of Decision Variable | 2 |
| Number of Cluster | 5 | Inertial weight | 0.88 - 0.38 |
| Prob. of cluster selection | 0.8 | Personal Learning Coefficient | 2 |
| Number of Runs | 50 | Global Learning Coefficient | 2 |
| Left of Dynamic range | -0.05 | Lower Bound of Variable | -0.05 |
| Right of Dynamic range | 0.05 | Upper Bound of Variable | 0.05 |
| Number of Iteration | 40 | Number of Iteration | 40 |

## 6.4 Results and Discussion

The above parameters were applied and implemented through respective algorithms and various specified transactions engaged. The following paragraphs describe in detail, the process and the outcomes of the investigation conducted.

### 6.4.1 ATC for bilateral and multilateral transactions with intact and n-1-line outage

Table 6.2 gives the values obtained for ATC of the network shown in Fig. 6.1 for both line intact and n-1-line outage contingency cases. Values for all the ATC during line intact were higher than that obtained during line outages except for the transaction T2 and T4 during outage of transmission line 2 – 5. This was because the network control system in reaction to this outage initiated additional power generation demand from the generator at bus 13 among others in order to maintain system stability. Therefore, transmission line 12 – 13 which happened to be the limiting line for these transactions but whose line thermal limit of 150 MW had not been exceeded experienced additional power flow. Limiting line 4 – 12 during line intact transactions had been shifted to line 12 – 13 for transactions T2 and T4 during line 2 – 5 outage. This was in addition to diversion of power to other adjoining transmission lines 1 – 2, 2 – 4 and 2 – 6, whose preset control system and thermal limits had not been exceeded.

Line outage contingency occurrence should be prevented because this limits ATC values whenever it occurs and thereby prevents the quantity of power that can be transacted especially in this era of power network deregulation. Table 6.3 depicts the percentage reduction in the allowable transfer power during line outages. A reduction of up to 55.5848% occurred during transaction T3 which grossly reduced the available transfer capability to 76.252 MW from 171.68 MW when lines were intact. The positive signs during outage of line 2 – 5 for T2 and T4 indicate an improvement in ATC values but the increment was infinitesimal compared reduction. The pictorial comparison of ATC values for all the transactions during line intact and different line outage conditions are shown in Fig. 6.2. Outage of line 6 – 9 severely affected transactions T1 and T4 unlike other line outages because this line conveys bulk power through bus 9 to bus 10 which interconnects other lines

via three different paths to deliver power to bus 23 and 24. In the same manner, outage of line 18 – 19 affected T2 mostly while that of line 2 – 5 greatly affected T3.

Table 6. 2: ATC values for intact and line outage contingency

| **Transactions** | **T1** | **T2** | **T3** | **T4** |
|---|---|---|---|---|
| ATC with line intact (MW) | 189.04 | 136.90 | 171.68 | 82.627 |
| ATC with n-1-line outage (MW) | | | | |
| 6-9 | 138.23 | 114.77 | 135.4 | 64.917 |
| 2-5 | 167.92 | 137.76 | 76.252 | 82.918 |
| 18-19 | 171.84 | 110.50 | 156.55 | 79.818 |
| 24-25 | 148.81 | 129.31 | 147.32 | 73.600 |

Table 6. 3: Percentage changes in ATC values during line outage contingency

| **Transactions** | **T1** | **T2** | **T3** | **T4** |
|---|---|---|---|---|
| ATC with n-1-line outage (%) | | | | |
| 6-9 | -26.8779 | -16.1651 | -21.1323 | -21.4337 |
| 2-5 | -11.1722 | +0.6282 | -55.5848 | +0.3522 |
| 18-19 | -9.0986 | -19.2841 | -8.81291 | -3.39962 |
| 24-25 | -21.2812 | -5.54419 | -14.1892 | -10.9250 |

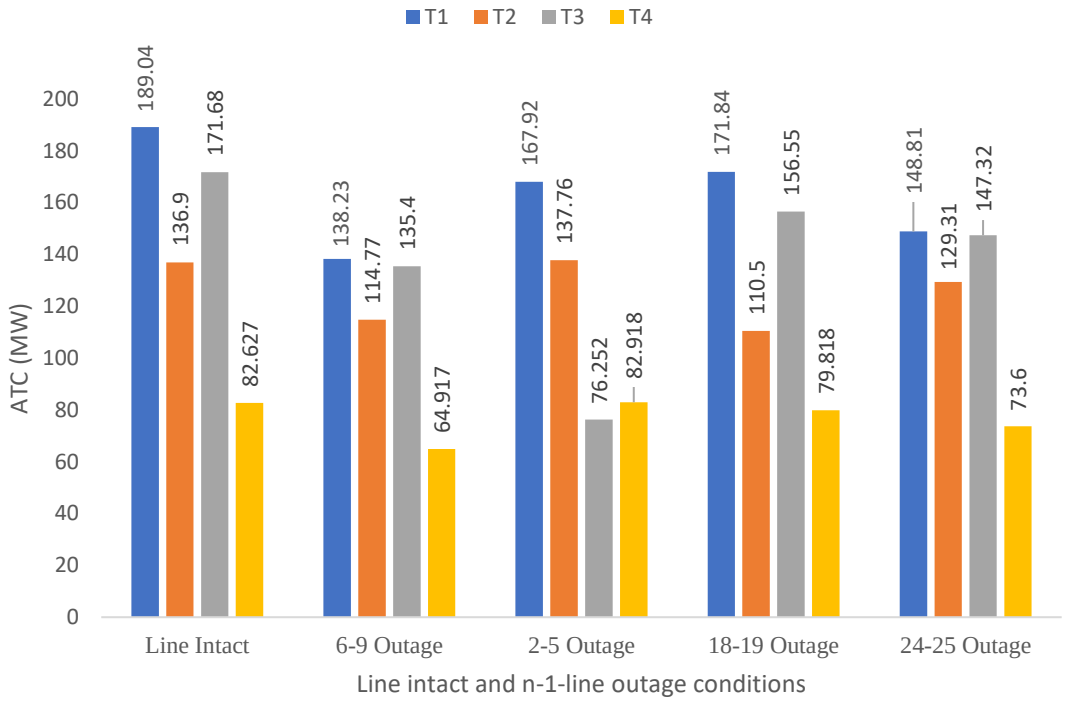


**Figure 6. 2: ATC for all transactions with intact and different n-1-line outages**

### 6.4.2 Enhanced ATC for bilateral and multilateral transactions with intact and n-1-line outage

The values in Table 6.4 are enhanced ATC values obtained when TCSC parameters were optimized with BSO and PSO algorithms. Values in row 2 and that of row 3 are the improved ATC for BSO and PSO algorithms respectively. These values are almost the same except for T3 where BSO set TCSC produced 209.95 MW and that of PSO resulted into 182.83 MW. This implies BSO apart from being efficient for optimization problems, still has some advantage over PSO. Rows 5 to 8 on the same table presents the enhanced ATC values during different line outages for BSO set TCSC. A critical look at these vales revealed a slight increase in values obtained for T1 during line 18 – 19 outage and T4 during line outage 2 - 5 above that of line intact.

Table 6. 4: Enhanced ATC values for intact and line outage contingency

| Transactions | T1 | T2 | T3 | T4 |
|---|---|---|---|---|
| ATC with line intact + TCSC (MW) | | | | |
| BSOA set TCSC | 198.13 | 148.31 | 209.95 | 95.144 |
| PSO set TCSC | 198.13 | 143.07 | 182.83 | 95.144 |
| ATC with n-1-line outage + BSOA set TCSC (MW) | | | | |
| 6-9 | 166.55 | 123.67 | 170.47 | 72.618 |
| 2-5 | 198.09 | 148.85 | 76.252 | 95.118 |
| 18-19 | 208.45 | 110.50 | 156.91 | 92.597 |
| 24-25 | 168.43 | 140.84 | 172.18 | 84.757 |

Table 6. 5: Percentage enhancement of ATC values during intact and line outage

| Transactions | T1 | T2 | T3 | T4 |
|---|---|---|---|---|
| ATC with line intact + TCSC (%) | | | | |
| BSOA set TCSC | 4.80851 | 8.33455 | 22.2915 | 15.1488 |
| PSO set TCSC | 4.80851 | 4.50693 | 6.49464 | 15.1488 |
| ATC with n-1-line outage + BSOA set TCSC (%) | | | | |
| 6-9 | 20.4876 | 7.75464 | 25.901 | 11.8628 |
| 2-5 | 17.9669 | 8.05023 | 0 | 14.7133 |
| 18-19 | 21.3047 | 0 | 0.22996 | 16.0102 |
| 24-25 | 13.1846 | 8.91656 | 16.8748 | 15.1590 |

Table 6.5 presents the percentage of enhancement obtained when TCSC parameters were optimized with these algorithms. An improvement ranging from of up to 22.3% were obtained with BSOA, while an increment of up to 15.1% was recorded using PSO to obtain optimal setting of TCSC for line intact conditions. Therefore, BSO perform better than PSO algorithm for ATC enhancement. Apart from T3 during line outage 2 – 5 and T2 during line outage 18 – 19 where ATC values hitherto obtained were maintained, an enhancement of up to 25.9% was

recorded during all the line outages and for all the power transactions. These various percentage improvement in ATC whose actual values were earlier presented in Table 6.4 are detailed in Table 6.5.

Just as in the case of ATC values for both line intact and outage, a critical look at Fig. 6.3 revealed how vital is line 6 – 9 to transactions T1 and T4. Outage of this line gravely affected T1 and T4 beyond other transactions. Line 18 – 19 outage affected T2 severely while that of line 2 – 5 had monumental impact on T3. Notwithstanding, a slight increase in ATC value was realized for T1 during line 18 – 19 outage above the obtained value during line intact.

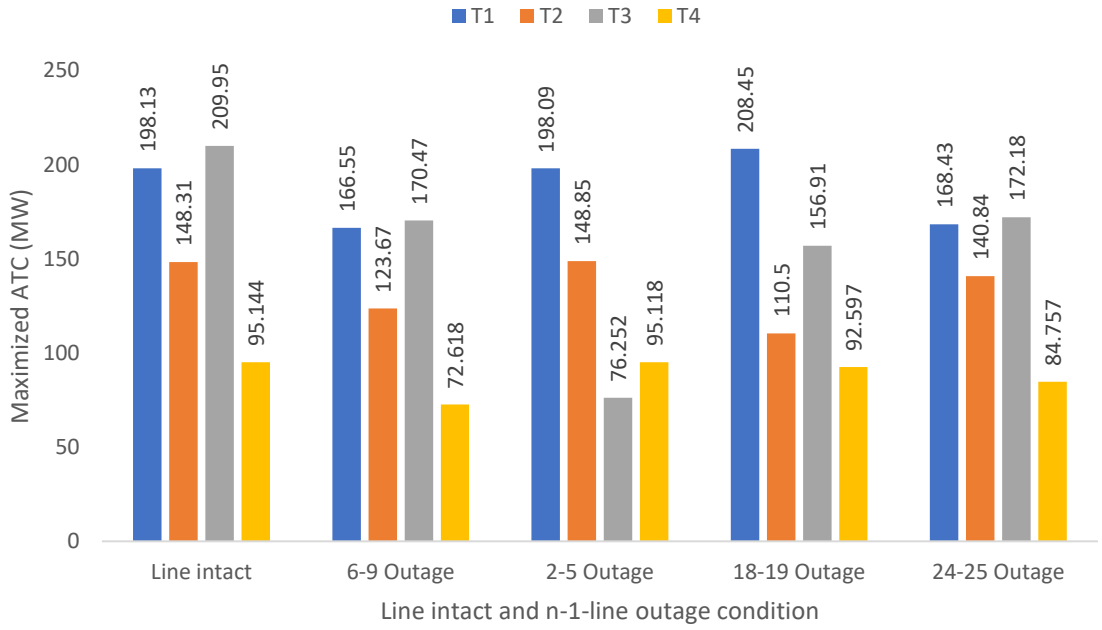


**Figure 6. 3: Enhanced ATC values for all transactions with intact and different n-1-line outages**

### 6.4.3 Bus voltage profile during line intact for bilateral and multilateral transactions

Bus voltage profiles during transactions T1 to T4 are presented in Figs. 6.4 – 6.7. The system bus response to the incorporation of TCSC based on the two optimization algorithms are very much alike. Both BSO and PSO set TCSC minimized bus voltage deviations as they restored bus voltage terminals. Although, small scaling factor was allocated to voltage deviation minimization, notwithstanding, the impacts of the optimization can be clearly seen in the figures.

#### 6.4.3.1 Bilateral transaction T1

As depicted in Fig. 6.4, bus voltage profile deviation during transaction T1 was minimized. The slight deviation between bus 14 and 25 towards lower voltage limit was controlled with incorporation of TCSC. The consequence of TCSC optimal setting with the two algorithm is the same here in that the two voltage profiles overlap each other.

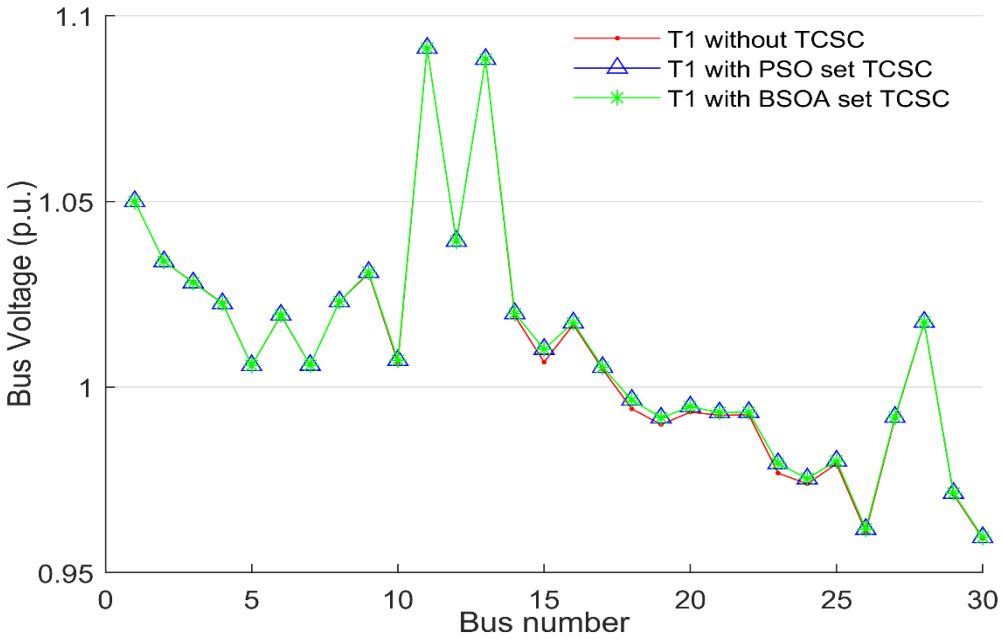


**Figure 6. 4: Bus voltage profile for transaction T1 during line intact with BSO and PSO set TCSC**

#### 6.4.3.2 Bilateral transaction T2

During transaction T2, the deviation of voltage profile without TCSC can be clearly visualized in Fig. 6.5, where between buses 14 and 25, voltage deviation towards lower limit of 0.95 is intense compare to that of T1. With the incorporation of the device, deviation minimization was achieved. During this transaction for instance, the voltage at bus 15 sag to 1.01 p.u. without TCSC but this was restored back to 1.02 p.u. which was pre-transaction terminal voltage when TCSC was incorporated.

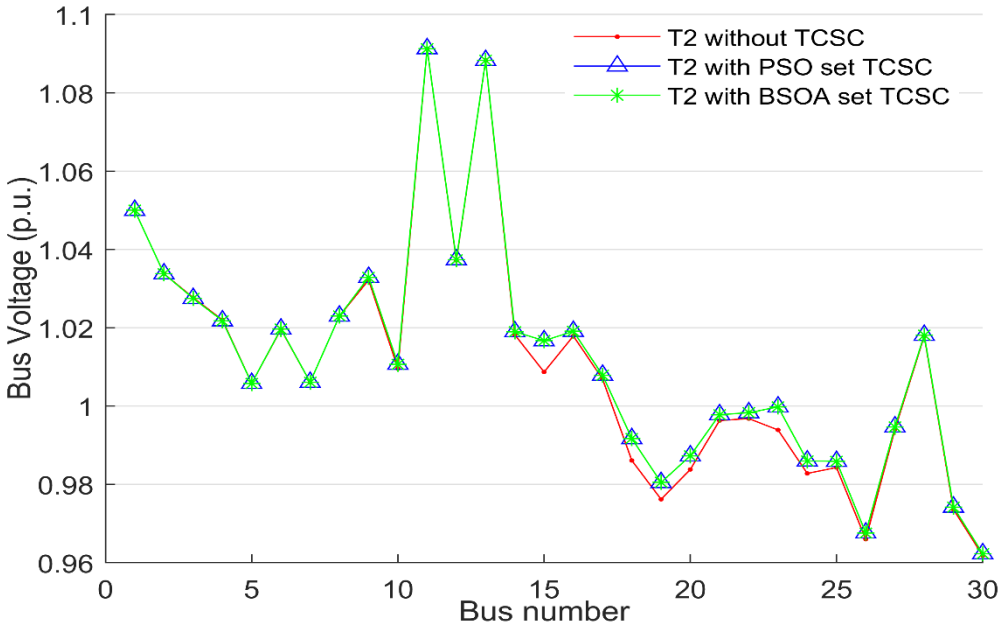


**Figure 6. 5: Bus voltage profile for transaction T2 during line intact with BSO and PSO set TCSC**

#### 6.4.3.3 Multilateral transaction T3

During transaction T3, no visible bus voltage profile deviation was experienced, with and without TCSC because all bus voltage profiles aligned as evident in Fig. 6.6. The nature of transaction definitely affects the bus voltage profile.

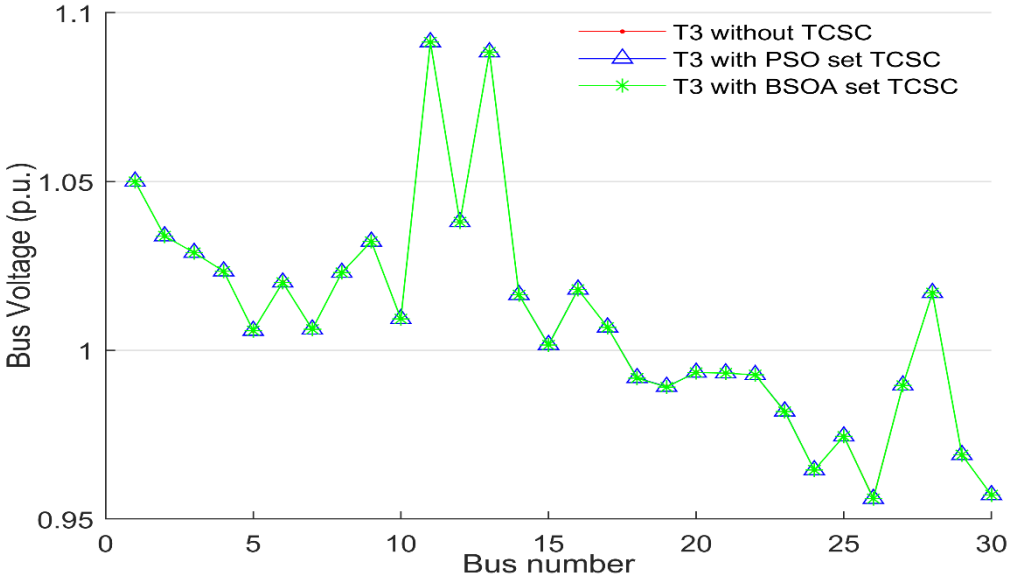


**Figure 6. 6: Bus voltage profile for transaction T3 during line intact with BSO and PSO set TCSC**

#### 6.4.3.4 Multilateral transaction T4

Fig. 6.7 presents bus voltage profile during transaction T4. A similar scenario to that of T2 occurred here but with mild intensity. Notwithstanding, the deviation was also minimized with incorporation of TCSC. Looking at bus 26, TCSC was able to minimize bus voltage deviation that was otherwise at the verge of violation of lower limit bound.

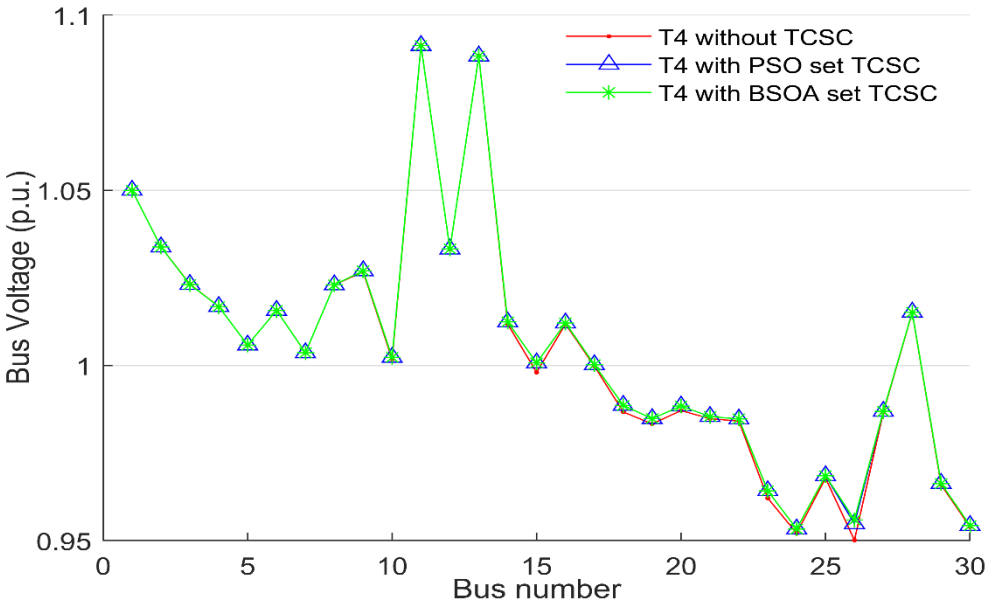


**Figure 6. 7: Bus voltage profile for transaction T4 during line intact with BSO and PSO set TCSC**

### 6.4.4 Bus voltage profile during n-1- line outage for bilateral and multilateral transactions

Bus voltage profiles for different transactions T1 to T4 during line outages are presented from Figs. 6.8 – 6.11. Here, TCSC device setting was achieved with BSOA only because PSO exhibits similar behavior to previous simulations.

#### 6.4.4.1 Bus voltage profile with line 6 – 9 outage

The response of terminal voltages during line 6 – 9 outage is depicted in Fig. 6.8. With optimal setting of TCSC, the device was able to minimize voltage deviations as presented in the figure. During T1, no significant voltage profile deviation as presented in Fig. 6.8 (a). FACTS device acted in line with the objective of minimizing voltage deviation as can be seen in Fig. 6.8 (b), (c) & (d). In these three cases, bus voltage experienced deviation towards lower limit of 0.95 p.u. but these were restored with incorporation of TCSC.

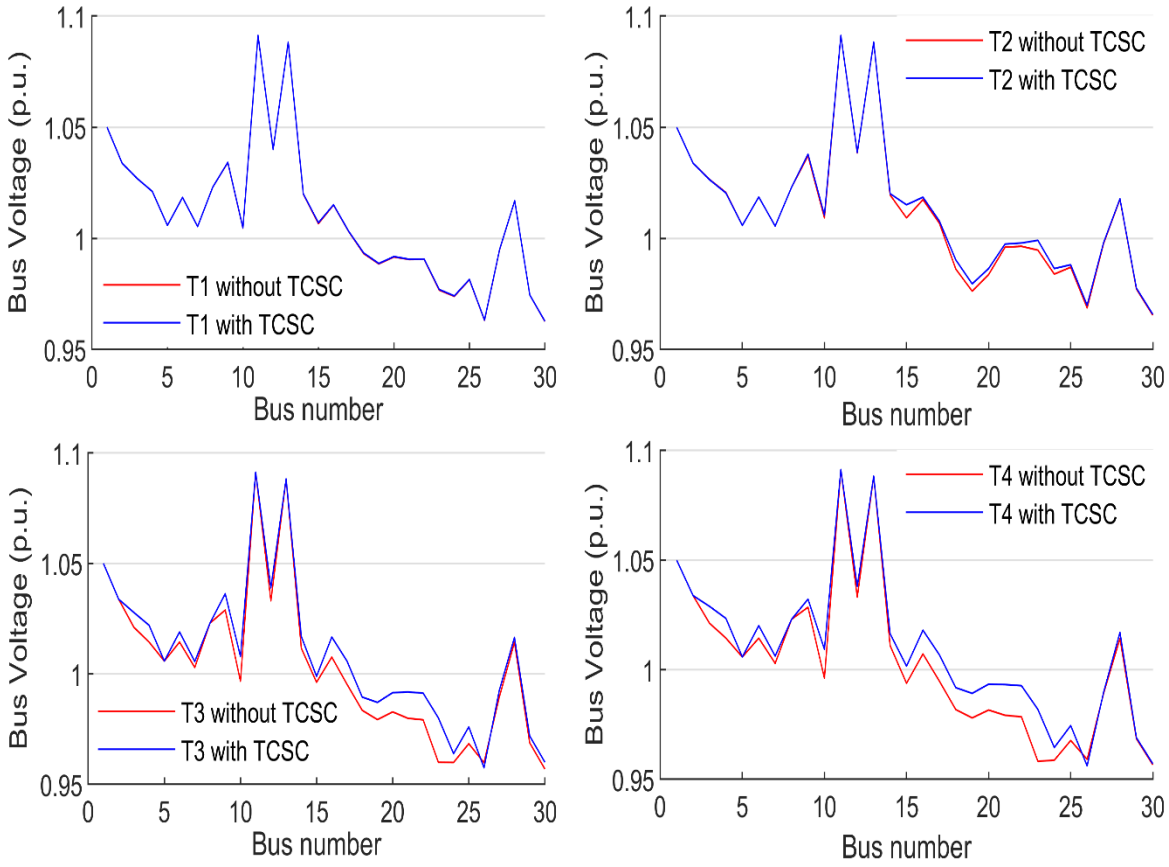


**Figure 6. 8: Bus voltage profile during line 6 – 9 outage with BSO set TCSC: (a) Bilateral transaction T1; (b) Bilateral transaction T2; (c) Multilateral transaction T3 and; (d) Multilateral transaction T4.**

#### 6.4.4.2 Bus voltage profile with line 2 – 5 outage

During line 2 – 5 outage, bus voltage profiles were maintained for transactions T3, for all the buses without any observable deviation. The superimposed bus voltage profiles curves with and without TCSC shown in Fig. 6.9 (c) is an indication. The slight deviations observed during T1 and T4 were restored in both cases as presented in Figs. 6.9 (a) & (d). Fig. 6.9 (b) describes voltage profile during transaction T2 with the deviation minimized.

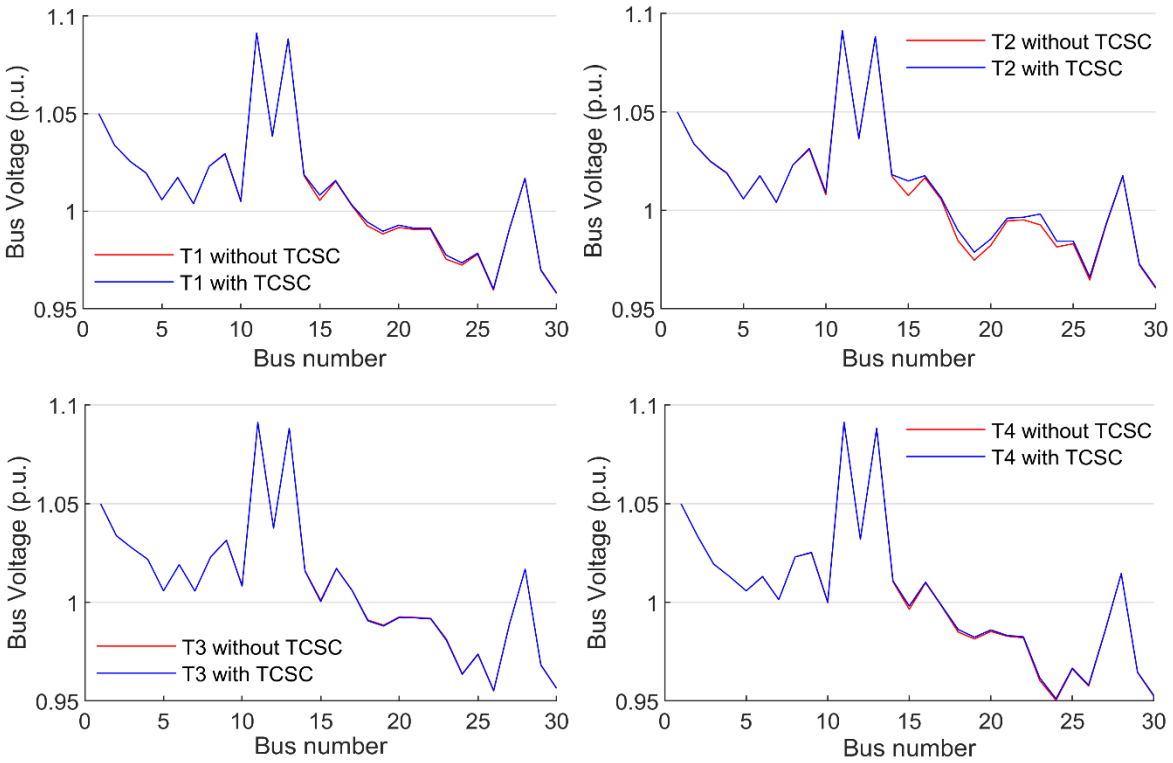


**Figure 6. 9: Bus voltage profile during line 2 – 5 outage with BSO set TCSC: (a) Bilateral transaction T1; (b) Bilateral transaction T2; (c) Multilateral transaction T3 and; (d) Multilateral transaction T4.**

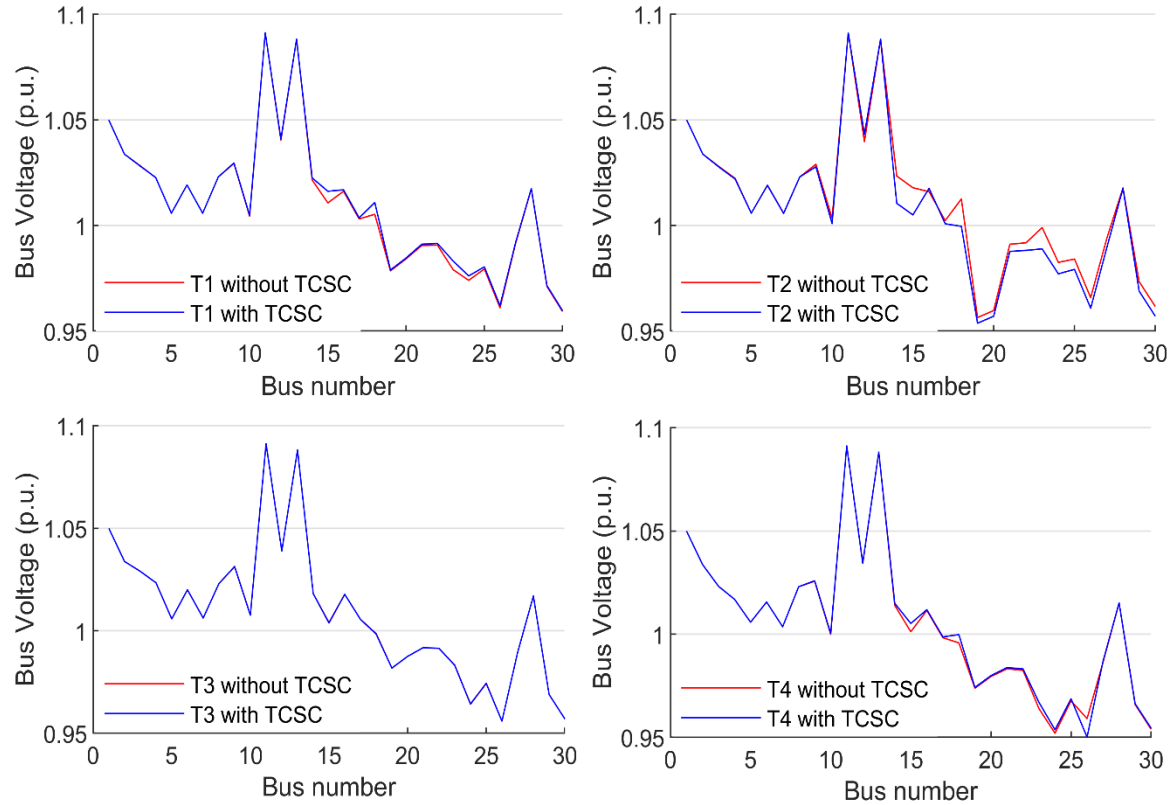


**Figure 6. 10:Bus voltage profile during line 18 – 19 outage with BSO set TCSC: (a) Bilateral transaction T1; (b) Bilateral transaction T2; (c) Multilateral transaction T3 and; (d) Multilateral transaction T4.**

#### 6.4.4.3 Bus voltage profile with line 18 – 19 outage

Figs. 6.10 (a) – (d) present test network bus voltage behavior to outage of line 18 – 19. For transaction T1, the achieved voltage deviation control is as shown in Fig. 6.10 (a) and this is clear for buses 15, 17 and 18. The voltage deviations at buses 15 18 and 23 towards upper limit of 1.05 during T2 were minimized as shown in Fig. 6.10 (b). No observable voltage deviation with and without TCSC as can be seen in Figure 13 (c) during T3. The slight deviation witnessed during T4 was also minimized in Fig. 6.10 (d)

#### 6.4.4.4 Bus voltage profile with line 24 – 25 outage

Effects of outage of line 24 – 25 on system bus voltage profiles can be seen in Fig. 6.11 (a) – (d). Voltage profiles before and after incorporation of TCSC are nearly the same for transactions T3 and T4. No observable bus voltage deviations occurred as evident in Fig. 6.11 (c) & (d). The slight deviations in the course of transaction T1 and T2 during this line outage were also minimized when TCSC was incorporated. Although, the scaling factor allocated to bus voltage minimization was small, yet optimal setting of TCSC device with BSOA played a tremendous role in ensuring this objective was met.

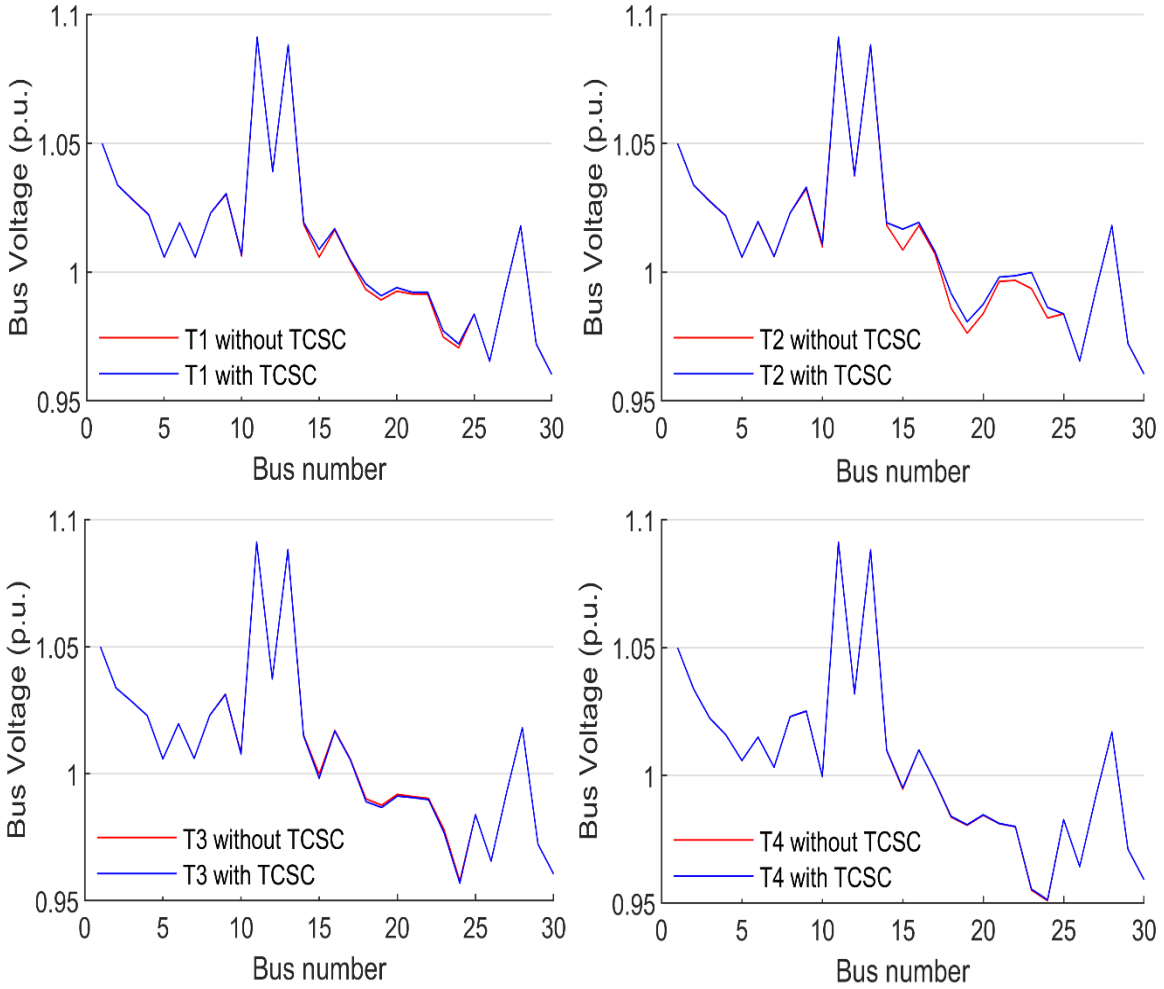


**Figure 6. 11: Bus voltage profile during line 24 – 25 outage with BSO set TCSC: (a) Bilateral transaction T1; (b) Bilateral transaction T2; (c) Multilateral transaction T3 and; (d) Multilateral transaction T4.**

### 6.4.5 Real power loss during line intact for bilateral and multilateral transactions

The patterns of real power loss curves for both BSO and PSO set TCSC are almost the same for the test network. BSO algorithm achieved optimum setting of TCSC parameters for the control of real power loss with no significant incremental loss due to increase in line power flow consequent of ATC enhancement. The real power loss for all the transactions T1 to T4 with and without TCSC are presented in Figs. 6.12 – 6.15. The capability of TCSC to control real power loss during ATC enhancement especially when its parameters were optimally set is succinctly depicted in the figures.

#### 6.4.5.1 Real power loss during bilateral transaction T1

During transactions T1, no observable increase in real power loss despite that the test system witnessed more power flow on the transmission lines. In Fig. 6.12, Real power losses were reduced to 0.0011, 0.0013, 0.0002, 0.0005, 0.0005, 0.0011 and 0.0002 p.u. from 0.0015, 0.0015, 0.0005, 0.0004, 0.0007, 0.0013 and 0.0003 p.u. on transmission lines 17, 19, 20, 21, 25, 31 and 32 respectively. This implies 26%, 13%, 60%, 25%, 28.5%, 15.3%, and 30% loss reduction. In that order. The instance of slight increase in losses are only recorded on lines 18, 22 and 30. Understandably, this was as a result of location of TCSC on line 18, which allowed more power flow on lines 22 and 30 that are directly connected to it.

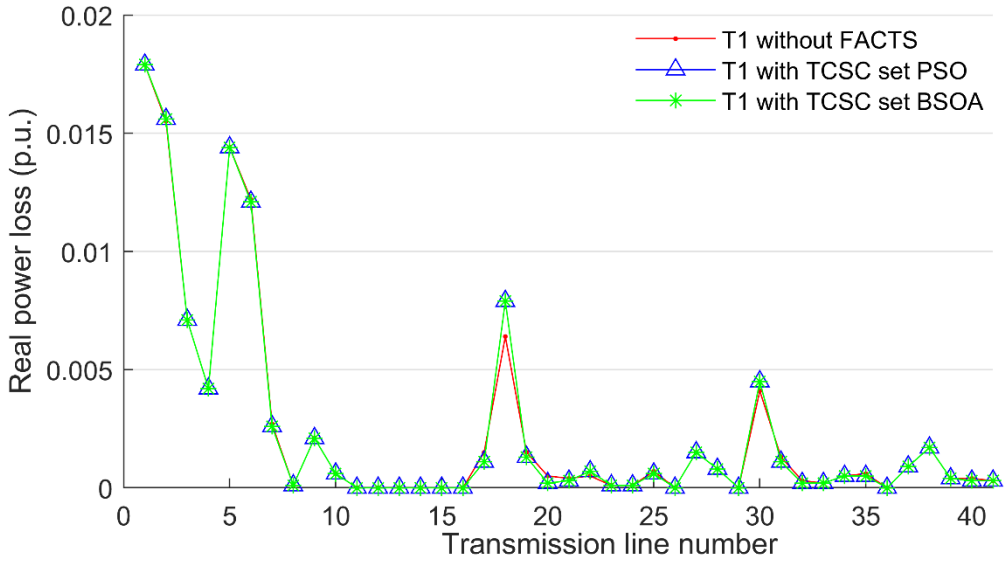


**Figure 6. 12: Real power loss for T1 during line intact with BSO and PSO set TCSC**

#### 6.4.5.2 Real power loss during bilateral transaction T2

Real power loss during T2 is presented in Fig. 6.13. There are reductions in losses to the tune of 63%, 12.5%, 23%, 24%, 7.6%, 16%, 42.9, and 100%, on transmission lines 17, 19, 24, 25, 27, 28, 31 and 33 respectively. The reduction in values of losses corresponding to these percentages are 0.005, 0.0007, 0.001, 0.0034, 0.0012, 0.0005, 0.0004 and 0.0000 p.u. from 0.0011, 0.0008, 0.0013, 0.0045, 0.0013, 0.0006, 0.0007 and 0.0001 p.u. respectively. The slight increase in real power loss on transmission lines 18, 22 and 30 from 0.004, 0.0021 and 0.0004 to 0.007, 0.003 and 0.0007 p.u. respectively was due to same reason earlier mentioned.

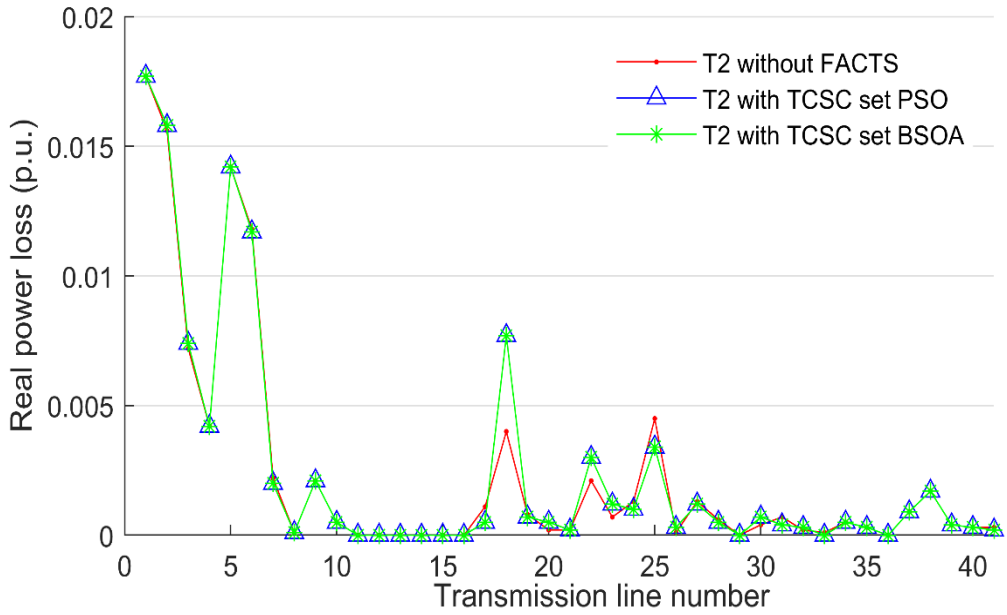


**Figure 6. 13: Real power loss for T2 during line intact with BSO and PSO set TCSC**

#### 6.4.5.3 Real power loss during multilateral transaction T3

Fig. 6.14 depicts the real power loss during T3. The losses here were controlled such that no noticeable changes occurred. The transmission lines 18, 22 and 30 interconnecting buyers 15 and 23 experienced more power flow also but these did not result into increase in real power loss but rather into ATC enhancement. Proper real power loss control was achieved here.

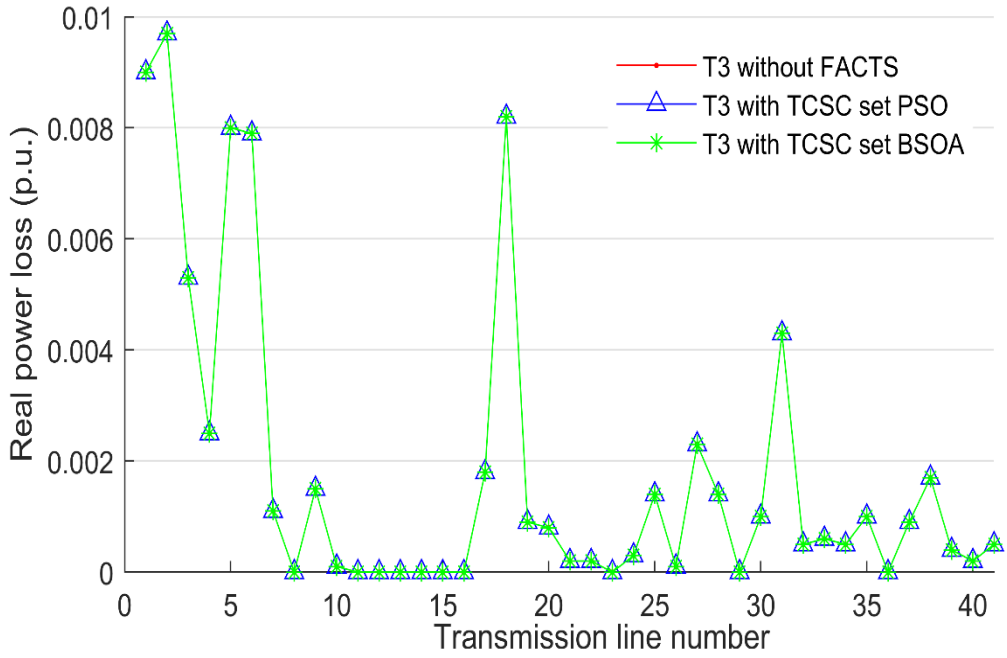


**Figure 6. 14: Real power loss for T3 during line intact with BSO and PSO set TCSC**

#### 6.4.5.4 Real power loss during multilateral transaction T4

As indicated in Fig. 6.15, losses here were also controlled with presence of TCSC. With same reasons and at the same transmission lines as for T1 and T2, a slight increase in real power losses were observed as indicated in Figure 18. However, the major losses reductions from 0.0017, 0.0011, 0.006, 0.003, 0.0011, 0.0016, 0.0055, and 0.0016 p.u. to 0.0013, 0.001, 0.0004, 0.0002, 0.0009, 0.0015, 0.0053 and 0.0015 p.u. among others were recorded on transmission lines 17, 19, 20, 21, 25, 28, 31 and 33 respectively. These reduction in loses are 23.5%, 9%, 93%, 93%, 18%, 6.2%, 3.6% and 6.3% for these transmission lines.

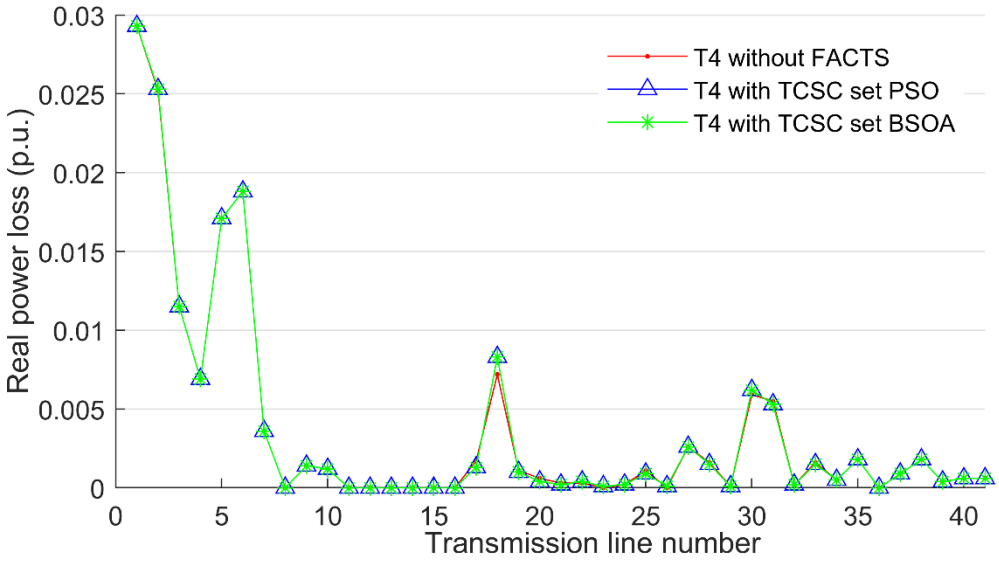


**Figure 6. 15: Real power loss for T4 during line intact with BSO and PSO set TCSC**

### 6.4.6 Real power loss during n-1- line outage for bilateral and multilateral transactions

Transmission line real power loss for all the implemented n-1-line outages are presented subsequently in Figs. 6.16 – 6.19. Optimal setting of TCSC with BSO resulted into proper regulation of real power loss for all the transactions.

#### 6.4.6.1 Real power loss during 6 – 9 line outage

Fig. 6.16 (a) – (d) present real power loss during line 6 - 9 outage. During transaction T1, adequate control of power loss occurred as can be seen in Fig. 6.16 (a). The system enjoyed losses reduction of 0.0001 each at lines 12-16, 14-15 and 24-25, without significant increase in loss during this transaction. In Fig. 6.16 (b), a decline in values recorded for losses from 0.0044 to 0.0003; 0.0013 to 0.0007; 0.0014 to 0.001; 0.0004 to 0.0002; 0.0036 to 0.0029; and 0.0011 to 0.0010 per units for transmission lines 8-28, 12-14, 12-16, 14-15, 16-17, 10-20, and 10-21 were obtained during T2. These stand for 93%, 38.5%, 28.5%, 50%, 19.4 and 9%, in terms of percentage loss reduction. A significant loss reduction on line 12-15 was obtained during T3, from 0.0095 to 0.0082 p.u. amounting to 13.7%, among other reductions as shown in Figure 19 (c). In Fig. 6.16 (d), similar loss reduction of 10.8%, from 0.0093 to 0.0083 p.u. on same line 12-15 was obtained among others for transaction T4.

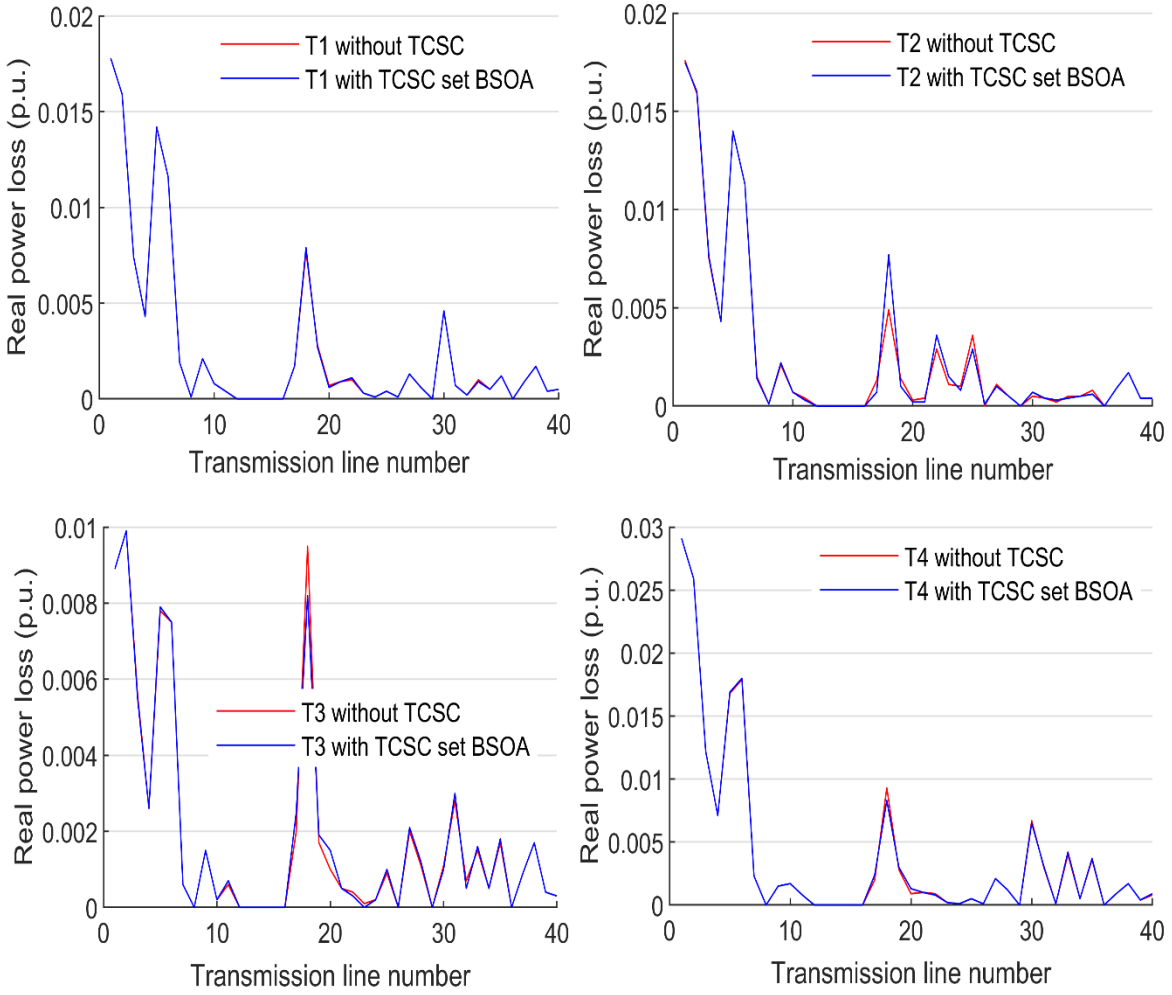


**Figure 6. 16: Real power loss for during line 6 – 9 outage with BSO set TCSC: (a)Bilateral transaction T1; (b) Bilateral transaction T2; (c) Multilateral transaction T3 and; (d) Multilateral transaction T4.**

#### 6.4.6.2 Real power loss during 2 – 5 line outage

Transaction T1 witnessed real power loss minimization on lines 12-14, 12-16, 14-15 and 16-17 to mention few. As depicted in Fig. 6.17 (a), values obtained on these lines reduced with 0.0004, 0.0001, 0.0003 and 0.0001 p.u. respectively. There were reductions in loss without as compared to that with TCSC as shown in Fig. 6.17 (b), during T2. Here, 0.0303, 0.0068, 0.0195, 0.0012, 0.0009 and 0.0013 p.u. became 0.0300, 0.0064, 0.0194, 0.0006, 0.0007, and 0.0009 p.u. in that order for transmission lines 2-6, 4-6, 6-7, 12-14, 12-16, and 19-20 among others. In percentile, these correspond to 1.0%, 5.9%, 0.51%, 22.2%, and 30.8%. The slight increase in loss on transmission lines 12-15, 15-18 and 15-23 was due to reasons already explained earlier. Line loss profile during transaction T3 is presented in Fig. 6.17 (c). Transmission lines here witnessed decay in loss from 0.0085 and 0.0011 to 0.0082 and 0.0010 p.u. respectively, achieving 3.5% and 9.1% loss reduction for lines 12-15 and 15-23. During transaction T4 with TCSC as shown in Fig. 6.17 (d), test network also experienced loss control. Values on transmission lines 12-14, 12-16 and 14-15 among other reduced by 0.0002 p.u. each for this trading.

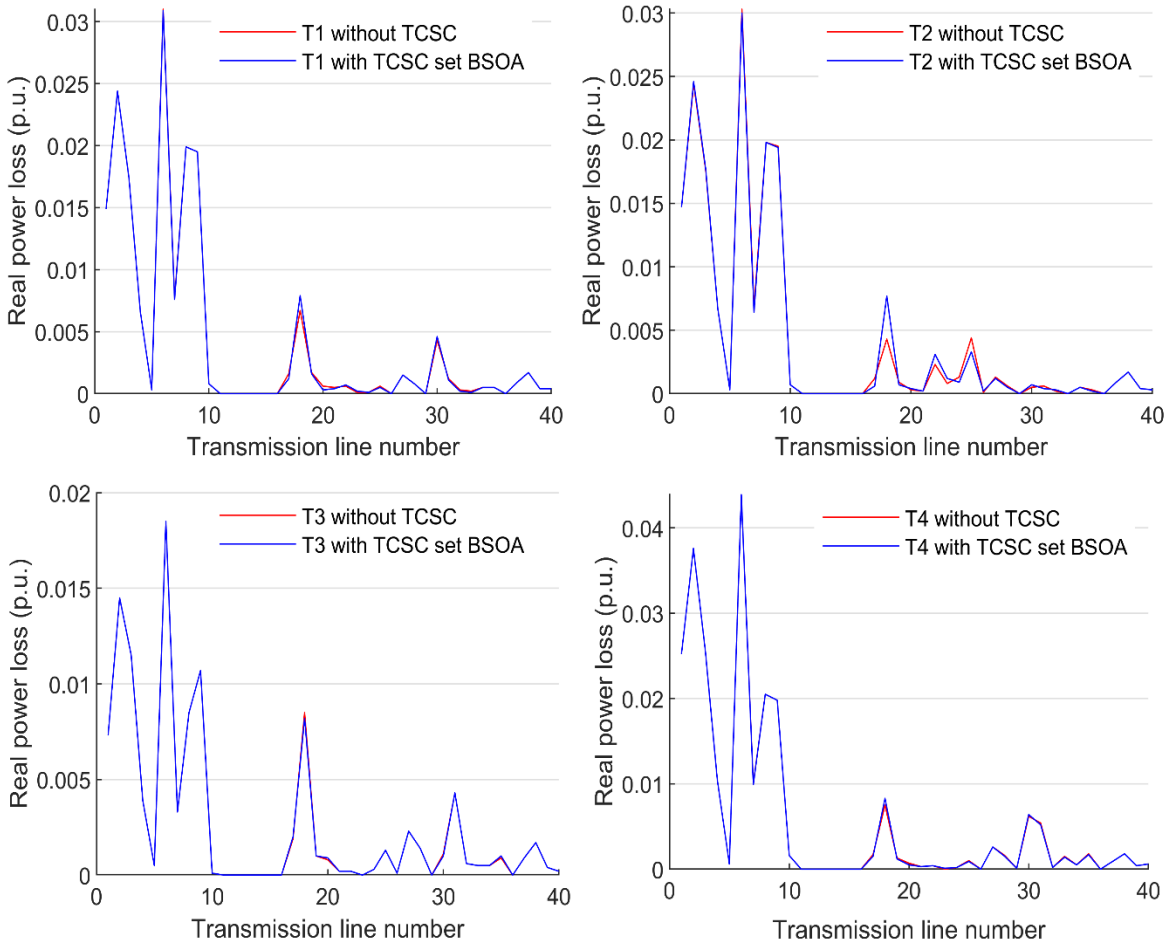


**Figure 6. 17: Real power loss for during line 2 – 5 outage with BSO set TCSC: (a)Bilateral transaction T1; (b) Bilateral transaction T2; (c) Multilateral transaction T3 and; (d) Multilateral transaction T4.**

#### 6.4.6.3 Real power loss during 18 – 19 line outage

In Fig. 6.18 (a) – (d), network real power losses during line outage 18 – 19 are presented. Transaction T1 according to Fig. 6.18 (a), witnessed real power control from 0.0014, 0.0018, 0.0004, 0.0014, 0.0003 and 0.0001 p.u. to 0.0008, 0.0016, 0.0001, 0.0013, 0.0001 and 0.0000 p.u. among others for transmission lines 12-14, 12-16, 14-15, 10-21, 23-24 and 24-25 respectively. During T2 and as depicted in Fig. 6.18 (b), lines 4-6, 6-8, 12-16, 8-28, 10-22, 24-25 and 25-27 experienced loss reduction from 0.0025, 0.0006, 0.0014, 0.0003, 0.0005, 0.0001, and 0.0003, to 0.0022, 0.0005, 0.0013, 0.0002, 0.0004, 0.0000, and 0.0002 p.u. respectively. Fig. 6.18 (c) gives the pictorial representation of real power loss regulation during T3 where losses in all the transmission lines were properly controlled despite additional power flow on them consequent ATC enhancement. In Fig. 6.18 (d), loss decline from 0.0016, 0.0013, 0.0006, 0.0026, 0.0015, 0.0052, 0.0016, and 0.0018, to 0.0011, 0.0012, 0.0002, 0.0025, 0.0014, 0.0047, 0.0015 and 0.0017 p.u. for transmission lines 12-14, 12-16, 14-15, 10-21, 10-22, 22-24, 24-25, and 25-27 respectively were achieved. These correspond to 31.3%, 7.7%, 60%, 3.8%, 6.6%, 9.6%, 6.3%, and 5.5% in that order. The slight increase in real power loss during all transactions with exception of T3 occurred on lines 12-15, 15-18 and 15-23 as previously explained.

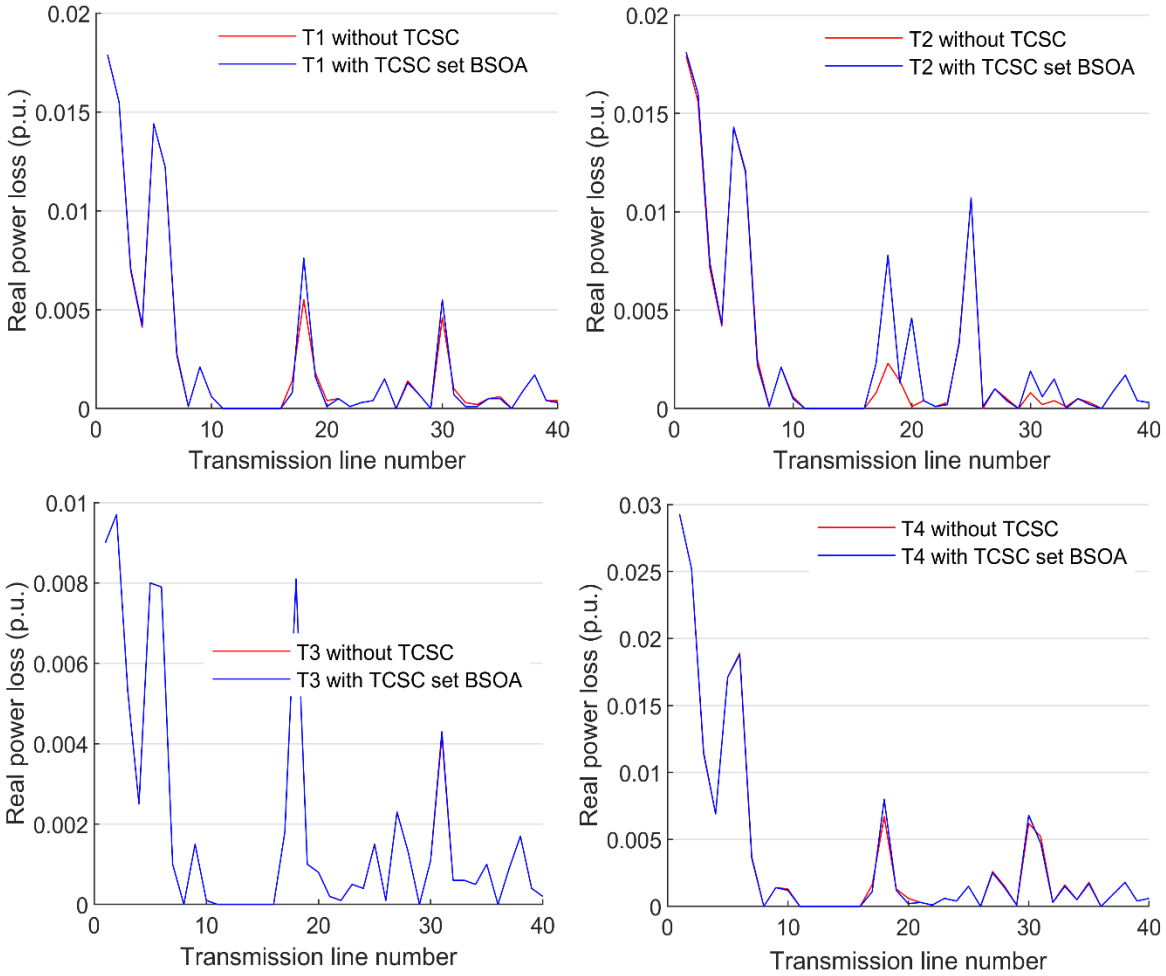


**Figure 6. 18: Real power loss for during line 18 – 19 outage with BSO set TCSC: (a)Bilateral transaction T1; (b) Bilateral transaction T2; (c) Multilateral transaction T3 and; (d) Multilateral transaction T4.**

#### 6.4.6.4 Real power loss during 24 – 25 line outage

Real power losses during 24-25 line outage are outlined in Figs. 6.19 (a) – (d). Transmission lines 12-14, 12-16, 14-15, 10-20, 10-21, and 22-24 witnessed loss diminution during transaction T1, from 0.0016, 0.0015, 0.0006, 0.0007, 0.0017 and 0.0018, to 0.0012, 0.0014, 0.0004, 0.0006, 0.0016 and 0.0016 p.u., corresponding to 25%, 6%, 30%, 14.3%, 5.9%, and 11.1% respectively, as depicted in Fig. 6.19 (a). Significant loss reduction during T2 occurred among others on lines 12-14, 12-16, 19-20, 10-20, and 22-24 with values reduced by 0.0006, 0.0001, 0.0003, 0.0011 and 0.0003 p.u. as shown in Fig. 6.19 (b). During T3, noticeable decline loss took place on lines 12-15, 15-23, and 23-24 as presented in Fig. 6.19 (c). Fig. 6.19 (d) gives the profile of real power loss during transaction T4. There were decrease in loss from 0.0002 to 0.0001 and 0.0091 to 0.0090 p.u. on lines 21-22 and 22-24 respectively. These amount to 50% and 1.1% loss reduction in that order on these line. Lines 12-15, 15-18 and 15-23 also experienced slight swell in real power loss as earlier explained. However, the slight swell did not result into increase in total real power loss for all transactions during intact and line outage transactions despite that more loss is associated with more power flow.

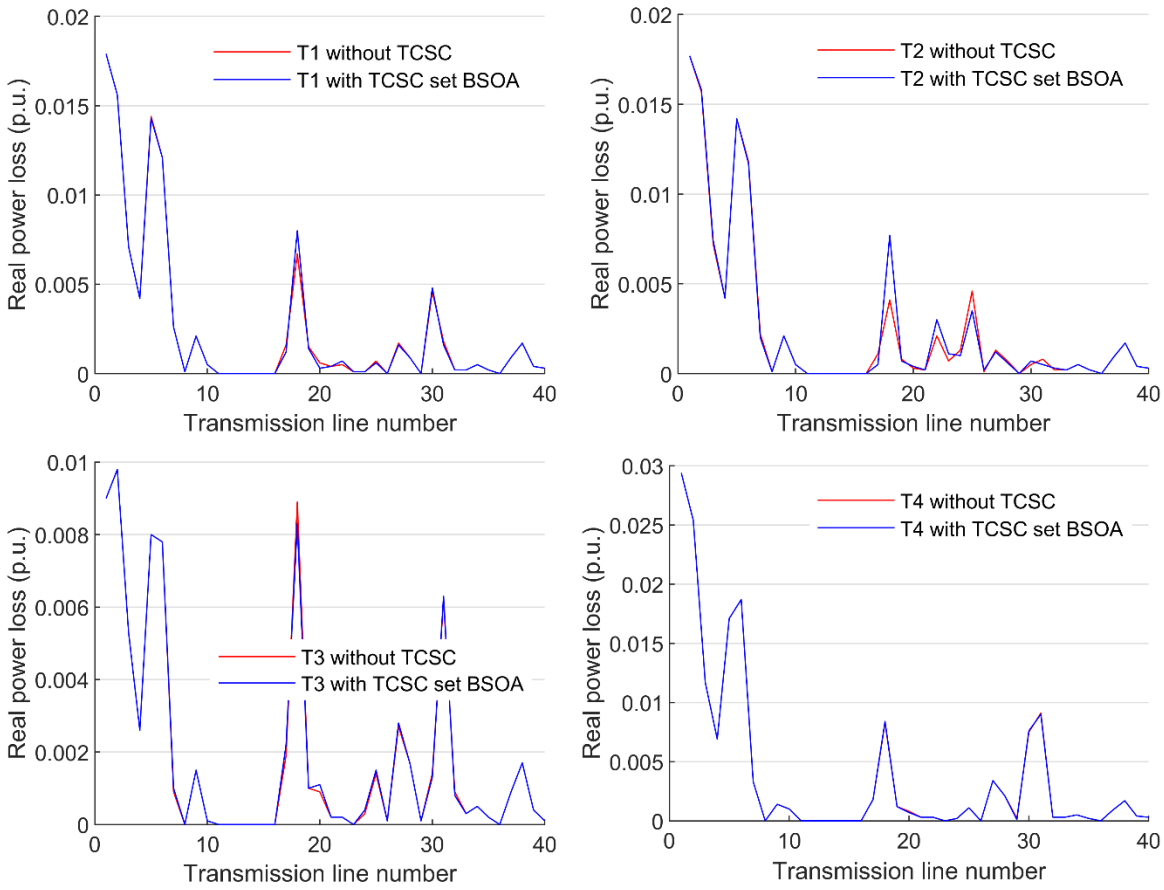


**Figure 6. 19: Real power loss for during line 24-25 outage with BSO set TCSC: (a)Bilateral transaction T1; (b) Bilateral transaction T2; (c) Multilateral transaction T3 and; (d) Multilateral transaction T4.**

### 6.5 Summary of chapter six

A novel optimization technique known as Brain Storm Optimization algorithm has been presented for the optimum setting of FACTS devices for multi-objective problem involving ATC enhancement, bus voltage profile deviation minimization and real power loss regulation. ATC values of IEEE 30 bus network system were obtained for different transactions with both line intact and n-1-line outage contingency cases. Enhanced ATCs for this network were achieved with TCSC device which was set with the presented BSO algorithm. The achieved bus voltage profile deviation minimization and real power loss control during ATC enhancement validate the innate fitness of BSO for solving multi-objective problems regarding FACTS. Likewise, BSO performance in comparison with PSO during the achievement of set objectives suggested an advantage of former over the latter. BSO behaved much like PSO throughout the achievements of other set objectives but performed better in ATC enhancement with 27.12 MW and 5.24 MW increase above enhanced ATC values achieved by the latter. The comparative of set objectives values relative to that obtained with PSO methods depict suitability and advantages of BSOA technique for optimal placement of FACTS devices. It has therefore been verified that BSO algorithm is effective in solving FACTS allocation multi-objective optimization problems.

# CHAPTER SEVEN

# SENSITIVITY BASED APPROACH FOR THYRISTOR CONTROL SERIES COMPENSATOR OPTIMIZATION

## 7.1 Introduction

In this chapter, a sensitivity based technique was developed for optimization of TCSC location in power network system. Here, FACTS device loss was incorporated with the general loss equation for the determination of optimum location for device placement in a deregulated power networks, with objectives of ATC enhancement, bus voltage profile improvement and loss reduction. A detailed mathematical model in terms of circuit system parameters was presented based on FACTS loss amalgamation approach. Like previous chapter, TCSC was considered for simulation and analysis because of its capability to control active power among other parameters. The TCSC location was established based on analysis of sensitivity factors obtained from partial derivatives of the resultant loss equations (including FACTS) with respect to control parameters. ATC values were obtained using alternating current power transfer distribution factor (ACPTDF) method and with TCSC in place, these values were enhanced for different bilateral and simltaneous power transactions. IEEE 5 bus system was used for the demonstration of the effectiveness of this approach.

## 7.2 Sensitivity based method

The increase in power transactions, consequent of open access brought about by deregulation and restructuring has resulted into challenges including but not limited to determination of ATC, transmission pricing, and congestion management. Among these issues, assessment of ATC is an indispensable tool for a secured and reliable power system planning and operations [144]. As earlier stated however, enhancement of ATC becomes imperative for economic power transaction and competitive electricity trading amidst increase in power trading [51]. The improvements as well as breakthroughs in power electronic devices coupled with restructuring of modern power network has created a renewed interest in FACTS applications [190]. The roles played by optimal location and settings of FACTS controllers in ATC enhancement and other benefits cannot be over emphasized. This is because, placement of these devices is a means to an end and it automatically affects the set objectives for which they were incorporated. Consequently, the choice of optimal location/method is critical for FACTS placement and utilization. Several models and approaches have been demonstrated for incorporation of FACTS for ATC enhancements as investigated in chapter five.

Summarily, approaches use in FACTS placement include but not limited to sensitivity based on DC/ACPTDF, loss sensitivities, line thermal limits, least bus voltage values as well as line with maximum ATC for the considered transactions. Adoption of any of these are being used in conjunction with meta-heuristics algorithms for parameter settings of FACTS devices. Although, meta-heuristic search algorithms like, BSOA, PSO, Generic, Firefly, Differential Evolution, Harmony Search and Artificial Bee Colony Algorithms are fast, robust and best suited for real power problems [97] however, their combination with a properly placed FACTS devices will bring about optimal location and setting for any desired objectives, since the problems of FACTS device location are combinatorial in principle and implementation.

The different approaches as highlighted above, have been demonstrated for placement of FACTS especially for ATC enhancement in previous chapter. However, none of the approaches accommodated and included FACTS loss in the process that culminated in its placement. Sensitivity based technique used in this work takes into cognizance, the effects and consequences of FACTS device loss on the system total loss in FACTS placement approach, having treated the total loss for network system containing FACTS as the algebraic sum of all the losses for both the system and FACTS. Sensitivity based techniques is a process of identifying system objective function as well as proposed optimizing FACTS devices control parameters and subsequently determine and obtain sensitivity factors through partial differentiation of identified objective function with respect to FACTS device control parameters. The objective function in this work is system total loss and the proposed FACTS device control parameters are magnitude and control voltage angle. This method leverages on the fact that optimal location of device is largely determined by partial derivatives of target function with respect to parameters affecting line power flow [190]. The voltage magnitude and injected voltage angle of TCSC series device are the parameters that influence line power flow for ATC enhancement in this case. In a bid to achieve this objective, TCSC has been modeled analytically for this purpose and has been presented in chapter three.

### 7.3 Results and Discussions

In order to determine the optimal location of TCSC, partial differentials of objective functions were obtained in chapter three with respective to voltage magnitude and control angle variables denoted by $V_s$ and $\theta_s$. Two sets of indices regarding total system loss sensitivity factors were obtained symbolized by $a_1^{TCSC}$ *and* $a_2^{TCSC}$. Optimal locations of FACTS devices are very important due to their high cost and for achievements of set objectives. However, ATC enhancement, bus voltage improvement and real power loss control are the main objectives of this chapter. This is because active power loss affects the quality of power and bus voltage regulation within the limit are critical to power network stability. The response of bus voltage profile and network system real power loss as a result of the introduction of TCSC during ATC enhancement are of great interest and focus of the research. Hence, the analyses of the results in this work were limited to these two objectives alongside ATC enhancement.

#### 7.3.1 IEEE 5-bus test system

IEEE 5-bus system obtained from [198] and modified as shown in Fig. 7.1, contains two generators located at buses 1 and 2 with generator 1 taken as slack. It also consists of four load buses and seven transmission lines. The details of the generators ratings, load ratings and transmission lines parameters as contained in [198] are presented in Appendix A-3.

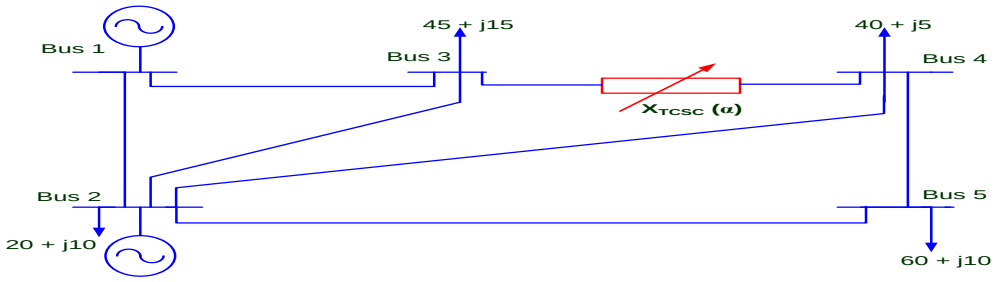


**Figure 7. 1: Modified IEEE 5-bus system**

### 7.3.2 Sensitivity factors for test system

Table 7.1 presents the total loss sensitivity value with respect to the magnitude of inserted voltage and that of angle of inserted voltage, represented as $a_1^{TCSC}$ *and* $a_2^{TCSC}$ respectively. Transmission line 3-4 has the least sensitivity value of 0.00096 as indicated on the column seven and row three of Table 7.1. However, line 3-4 has the highest absolute (most positive) loss sensitivity value with respect to phase angle of inserted voltage as appeared on column eight of row four of Table 7.1. These sensitivity values are presented graphically in Fig. 7.2 for easy understanding.

Table 7. 1: Loss sensitivity of test system to TCSC location

| **Line Number** | 1 | 2 | 3 | 4 | 5 | 6 | 7 |
|---|---|---|---|---|---|---|---|
| **Transmission Line** | 1-2 | 1-3 | 2-3 | 2-4 | 2-5 | 3-4 | 4-5 |
| $\boldsymbol{a_1^{TCSC} * 1e0}$ | 0.0105 | 0.0217 | 0.0144 | 0.0157 | 0.0185 | **0.00096** | 0.0039 |
| $\boldsymbol{a_2^{TCSC} * 1e-4}$ | -0.0251 | 1.1790 | -0.5396 | -0.6247 | -0.4408 | **-0.2080** | -0.0386 |

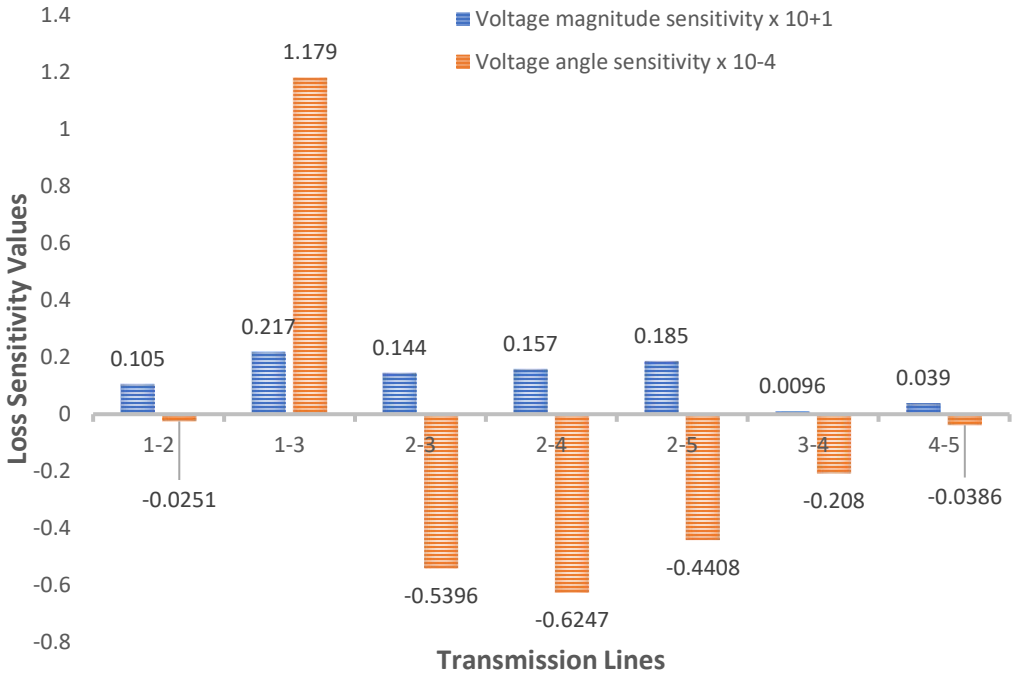


**Figure 7. 2: Voltage magnitude and angle sensitivities of the test system**

Table 7.2 presents other methods of FACTS location for the test system as inferred from literature. Base case active power loss [143], Base case reactive power loss [97], Performance index [138], PTDF for considered transaction [140],[144], highest ATC value [148], PTL Sensitivity [147], and QTL Sensitivity [145] (where loss sensitivity with respect to line reactance was implemented in FACTS location). Least bus voltage method [108], [141],[142] identified bus 5, while line thermal limits [139] pointed at line 3-4. The impacts of the losses and different FACTS approach solutions based on location in the network system are also clearly depicted in Fig. 7.3 for better comprehension.

Table 7. 2: Other approaches for FACTS location for the test system

| **Line number** | 1 | 2 | 3 | 4 | 5 | 6 | 7 |
|---|---|---|---|---|---|---|---|
| **Transmission line** | 1-2 | 1-3 | 2-3 | 2-4 | 2-5 | 3-4 | 4-5 |
| **Base case PLoss** | **0.0249** | 0.0152 | 0.0036 | 0.0046 | 0.0122 | 0.0004 | 0.0004 |
| **Base case QLoss** | 0.0109 | -0.0069 | -0.0287 | -0.0255 | 0.0073 | -0.0182 | **-0.0465** |
| **Performance Index** | 0.00127 | **0.00459** | 0.0010 | 0.00128 | 0.00228 | 0.00002 | 0.00014 |
| **PTL Sensitivity** | 0.0003 | **-0.1133** | -0.0088 | -0.0141 | -0.0125 | 0.0039 | 0.0410 |
| **QTL Sensitivity** | -1.5543 | -0.2372 | -0.0748 | -0.0959 | -0.3793 | -0.0501 | **-0.0067** |
| **PTDF/10MW/2-5** | 0.0200 | **-0.0720** | -0.0980 | -0.1250 | -0.7580 | -0.1610 | -0.2820 |
| **PTDF/10MW/2-4** | 0.1530 | -0.1930 | -0.2930 | -0.3710 | **-0.1880** | -0.4630 | -0.1810 |
| **ACT/10MW/2-5 x 10+3** | 1.5335 | **1.2054** | 0.55582 | 0.46168 | 0.19084 | 0.214 | 0.0766 |
| **ACT/10MW/2-4 x 10 $^{+3}$** | 0.2005 | 0.4497 | 0.1859 | 0.1556 | **0.7695** | 0.0743 | 0.0464 |

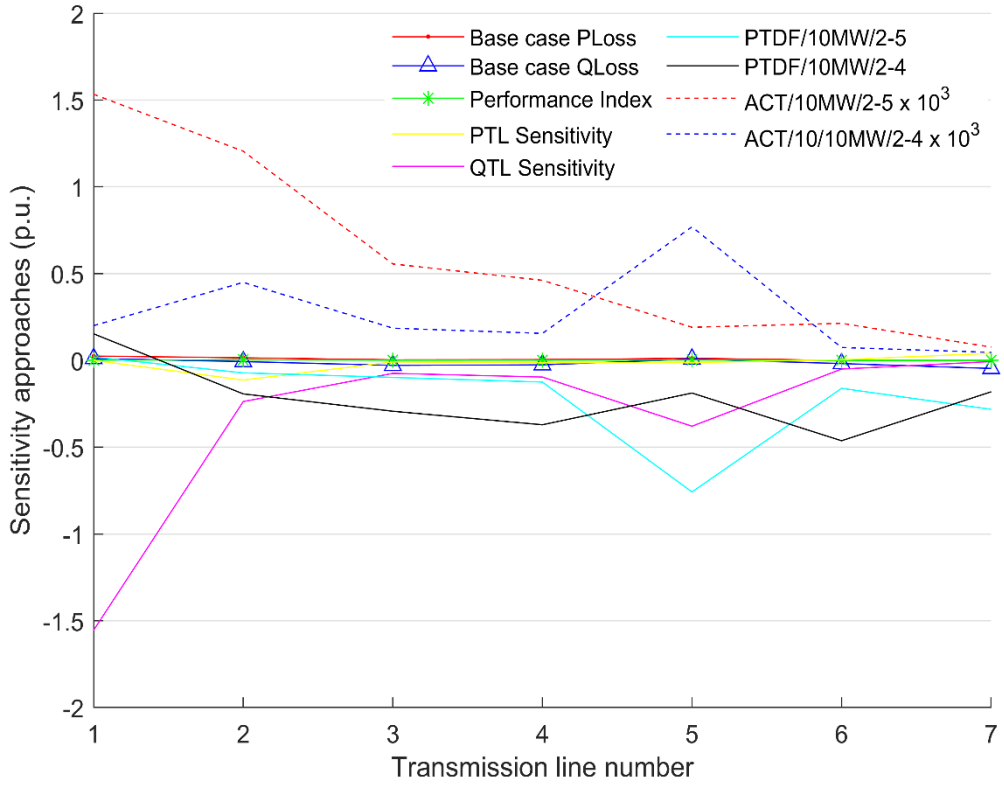


**Figure 7. 3: Test system response to various FACTS location approaches**

### 7.3.3 ATC evaluation during bilateral and simultaneous power transactions without TCSC

Two major trading termed bilateral and simultaneous transactions were implemented in this chapter. Transaction T1 (2-5) exists between generator 2 and load bus 5 while transaction T2 (2-4) occurs between generator 2 and load bus 4. Power transfer of 10 MW, 20 MW, 30 MW and 40 MW accompanied each transaction. Simultaneous transactions involving transfer of 20 MW and 40 MW power also occur between generator 2 and load bus 5 and 4.

#### 7.3.3.1 ATC evaluation during bilateral transaction without TCSC

ATCs were obtained for two major bilateral transactions as described above. Table 7.3 presents ATC values obtained for these various power transactions while Fig. 7.4 graphically compares transaction T1 with T2 for different quantities of power. Values of ATCs obtained during T1 are higher than that of T2 for all the magnitudes of power transfer as presented in the table. This is because bus 4 interconnects bus 2, 3 and 5 and bus 5 only interconnects bus 4 apart from bus 2, thereby making network demand on bus 4 higher than that of 5 at every instance.

Table 7. 3: ATC for bilateral transactions T1(2-5) and T2(2-4)

| **Power Transaction (MW)** | **10** | **20** | **30** | **40** |
|---|---|---|---|---|
| **T1(2-5) (MW)** | 76.596 | 76.460 | 76.146 | 75.923 |
| **T2(2-4) (MW)** | 46.409 | 46.409 | 46.409 | 54.892 |

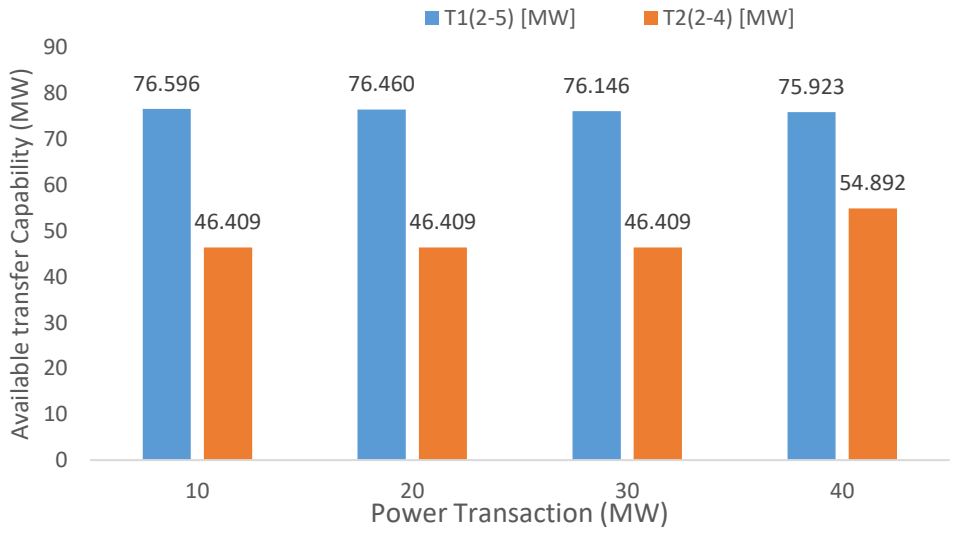


**Figure 7. 4: ATC values for different bilateral transactions**

#### 7.3.3.2 ATC evaluation during simultaneous transaction without TCSC

Values for the obtained ATC during simultaneous transaction are presented as follows in Table 7.4 and in Fig. 7.5 for clarity purposes. The value obtained for 20 MW and 40 MW are not too far from each other but that of 40 MW is smaller in magnitude because of the magnitude of power involved during this trading. This implies that magnitude of trading affects ATC values in deregulated network. Similar scenario occurs during bilateral transaction as presented in Table 7.3 above where ATC magnitude decreases with increase in magnitude of power transfer.

Table 7. 4: ATC for simultaneous transactions

| **Power Transaction (MW)** | **20** | **40** |
|---|---|---|
| **Bus 2 to Bus 5&4 (MW)** | 55.024 | 54.892 |

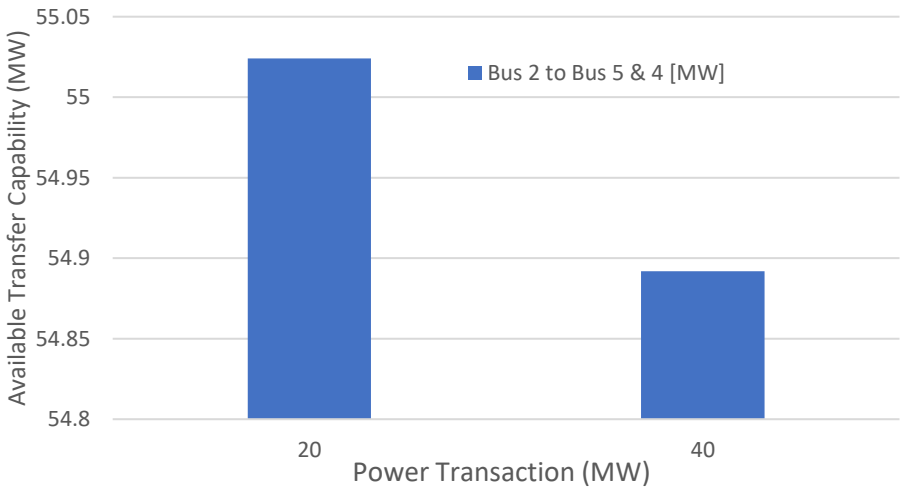


**Figure 7. 5: ATC values for multilateral transactions**

### 7.3.4 Bus voltage profile during bilateral and multilateral power transactions without TCSC

During these ATC improvement, bus voltage profile were investigated and reported for bilateral and multilatreral transactions in the subsequent paragraphs.

#### 7.3.4.1 Bus voltage profile during bilateral transactions

The bus voltage variation to various power transfer ranging from 10 MW to 40 MW for transactions T1 and T2 are as presented in Figs. 7.6 – 7.9. Voltage at bus 1 and 2 remained at their specified values while that of buses 3, 4 and 5 experienced droop. It is evident that the bus voltage deviation is a function of magnitude of power transactions. As the transaction increases from 10 MW to 40 MW, buses 3, 4 and 5 voltage magnitudes sag correspondingly. This can be well understood with critical comparison of bus voltage profile for both T1 and T2 as magnitude of trading increases. This is glaring when comparing terminal voltage at buses 3, 4 and 5 for T1, T2 and base case situations in all the figures. Benchmarking voltage profile of these buses for Fig. 7.6 and that of Fig. 7.9 reveals and picturises the voltage magnitude decline. Besides, the nature of transaction also affects bus terminal voltage. Transaction T1 and T2 influenced bus terminal voltage differently. The deviations in voltage magnitude from base case value for T1 and T2 demostrates that terminal voltage is well influenced

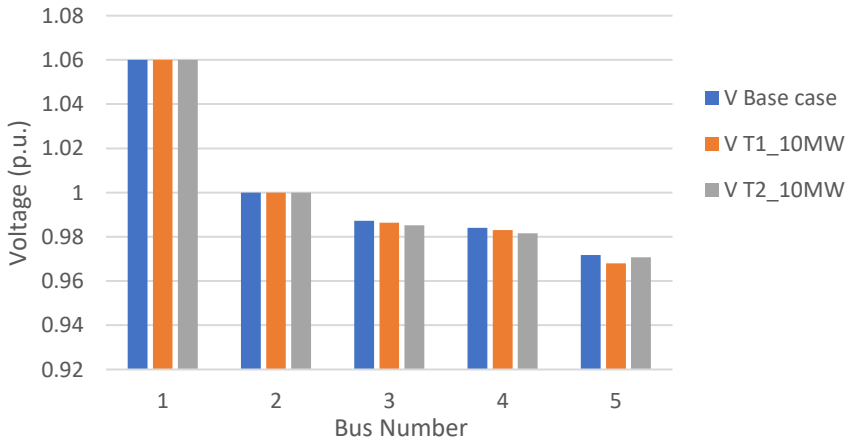


**Figure 7. 6: Bus voltage variation to 10 MW power transfer for T1(2-5) and T2(2-4)**

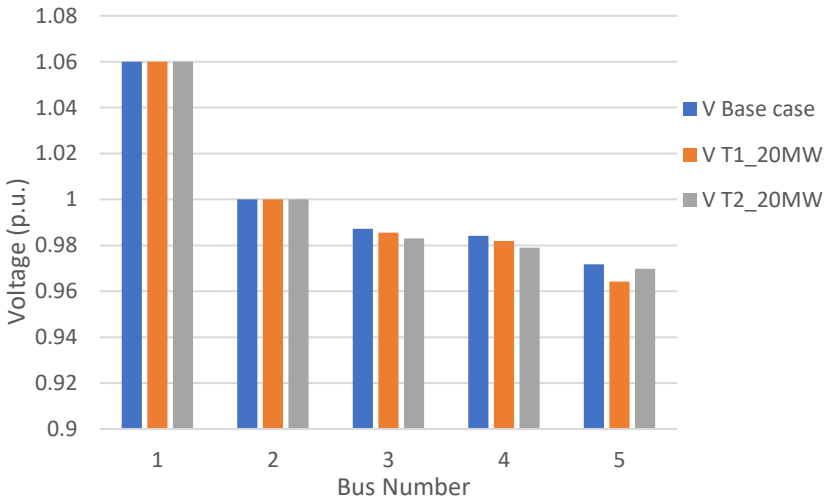


**Figure 7. 7: Bus voltage variation to 20 MW power transfer for T1(2-5) and T2(2-4)**

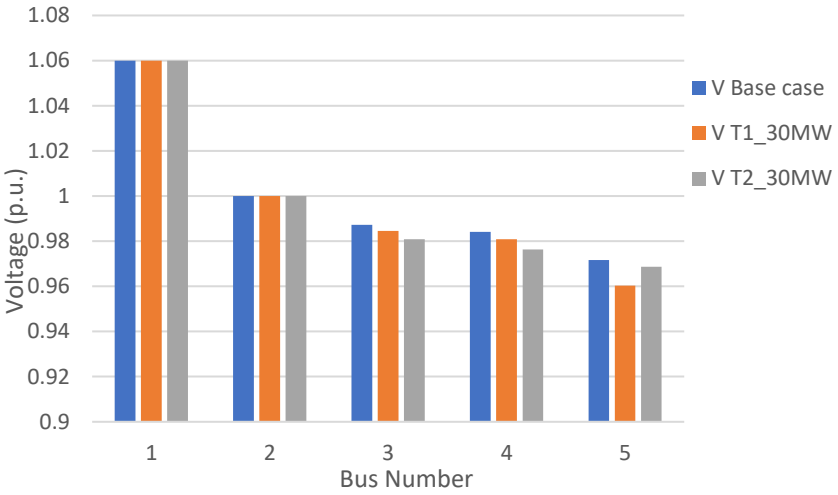


**Figure 7. 8: Bus voltage variation to 30 MW power transfer for T1(2-5) and T2(2-4)**

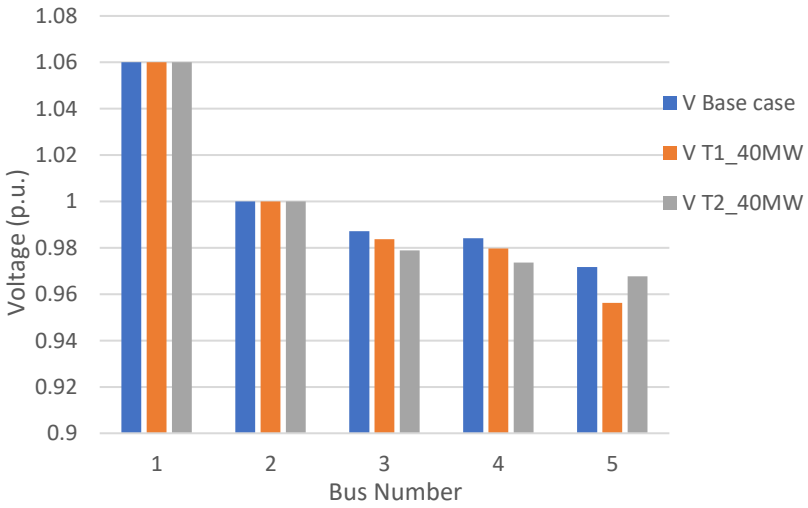


**Figure 7. 9: Bus voltage variation to 40 MW power transfer for T1(2-5) and T2(2-4)**

by the nature of transaction. This can be well understood in Figs. 7.6 – 7.9, having compared base case, T1 and T2 terminal voltage for buses 3, 4 and 5 during each magnitude of power trading in the figures.

#### 7.3.4.2 Bus voltage profile during simultaneous transactions

The bus voltage variation to 20 MW and 40 MW power transfer for simultaneous transaction is as presented in Fig. 7.10. Just like in the case of bilateral transaction, bus voltage deviation aggravates with magnitude of trading in this situation. It can be seen from deviation on bus 3, 4, and 5 that the more the magnitude of power involved in trading the more the deviation and this can lead to bus voltage limit violation if not properly controlled. It is of interest to note that voltage magnitude sag in this transaction is deeper in each situation when compared voltage deviations under bilateral transaction of the same transfer magnitude.

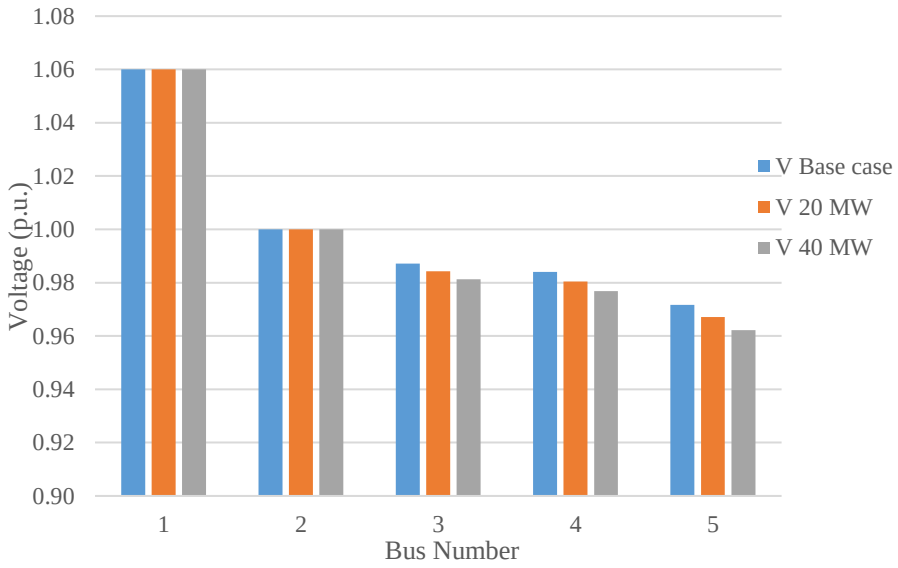


**Figure 7. 10: Bus voltage profile for simultaneous transaction for 20 MW and 40 MW power transfer**

### 7.3.5 Network loss during bilateral and simultaneous power transactions

The network loss as accompanied ATC determination in this investigation and as evaluated are as presented in the subsequent paragraphs. The losses during engaged trading for bilateral and simultaneous transactions are recorded and presented.

#### 7.3.5.1 Network power loss during bilateral power transactions

Figs. 7.11 and 7.12 depict active power losses for 10 MW to 40 MW power transfers for transactions T1 and T2. It can be observed from T1 that transmission line 2-5 recorded highest power loss of about 16.5 MW during 40 MW power transfer, while losses in other lines are insignificant compare to this. The power loss here is proportional to the magnitude of transferred power. This is an indication that more loss accompanies more power flows [134]. Increase in real power losses ranging from 0.09 MW to 0.61 MW were experienced during T2 on lines 1-3, 2-3, 2-4, and 2-5.

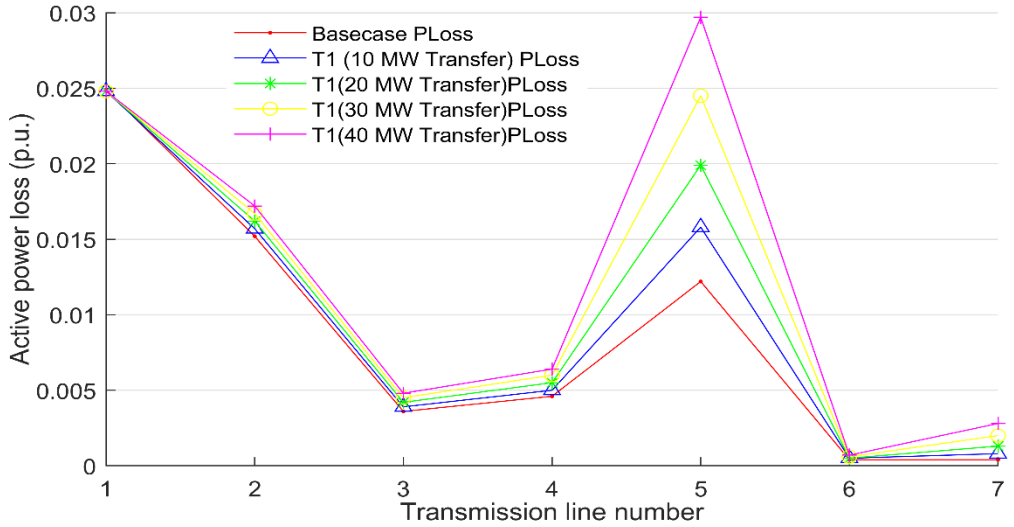


**Figure 7. 11: Transmission Line Real Power Losses for Power Transfer T1 (2-5)**

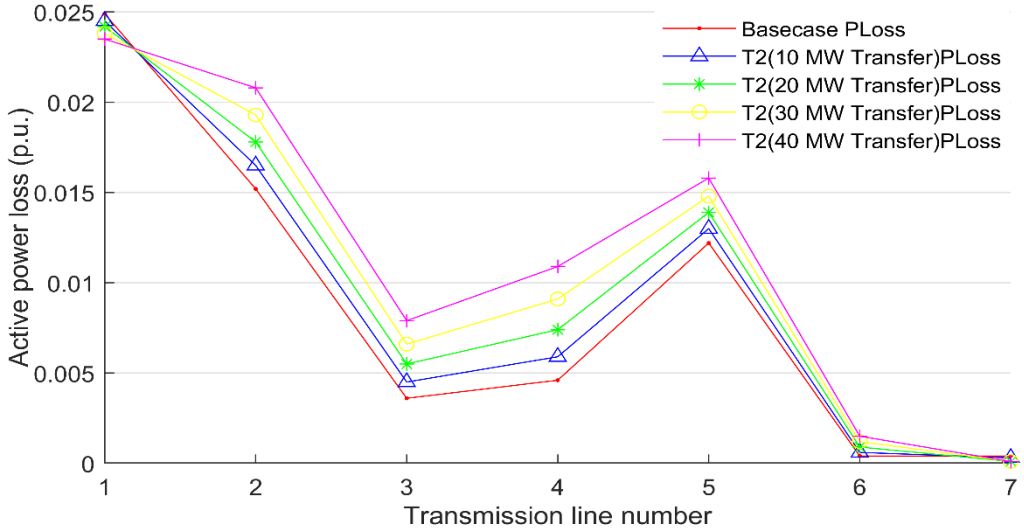


**Figure 7. 12: Transmission line real power losses for power transfer T2 (2-4)**

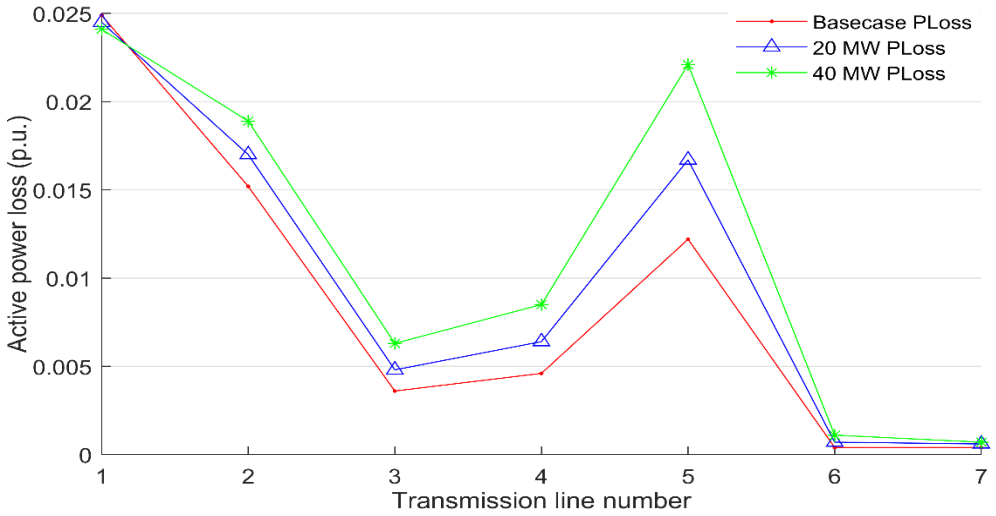


**Figure 7. 13: Transmission line real power losses for power transfer T2 (2-4)**

#### 7.3.5.2 Network power loss during simultaneous power transactions

In Fig. 7.13, active power losses for 20 MW and 40 MW power transfers during this transaction are depicted. Here also, it is demonstrated that the more the magnitude of power trading the more the loss. Apart from the magnitude, the nature of loss during simultaneous trading encompasses pattern of network loss as recorded for T1 and T2 during bilateral transactions.

### 7.3.6 ATC Enhancement with TCSC during bilateral and simultanous power transactions

TCSC was placed in between line 4-5 as indicated by sensitivity factors $a_1^{TCSC}$ and $a_2^{TCSC}$ presented in this work because, magnitude and angle of injected voltage of series converter is the parameter that influences power flow in a transmission line [190]. The objectives of TCSC placement are for ATC enhancement, voltage improvement and loss reduction. In order to explicitly demonstrate the potency of this method, TCSC was also place on line 3-4 for comparison. Line 3-4 is the location for placement identified by thermal limits location method use in [139].

In presentation of the results, four cases were investigated and reported. The values of the enhanced ATCs are as presented in Table 7.5. The observations recorded for T1(2-5) with TCSC at line 4-5, T1(2-5) with TCSC at line 3-4, T2(2-4) with TCSC at line 4-5, and T2(2-4) with TCSC at line 3-4 are presented under cases 1 to 4 below. Table 7.6 shows values of an enhanced ATCs for multilateral transactions with TCSC placed on line 4-5 and 3-4.

Table 7. 5: Enhanced ATC for bilateral transactions T1(2-5) and T2(2-4)

| **Power Transaction (MW)** | **10** | **20** | **30** | **40** |
|---|---|---|---|---|
| **T1(2-5) (MW), TCSC at line 4-5** | 141.42 | 140.75 | 140.09 | 139.37 |
| **T1(2-5) (MW), TCSC at line 3-4** | 94.18 | 93.96 | 93.76 | 93.45 |
| **T2(2-4) (MW), TCSC at line 4-5** | 53.36 | 56.34 | 56.29 | 55.24 |
| **T2(2-4) (MW), TCSC at line 3-4** | 23.50 | 23.50 | 56.21 | 81.07 |

Table 7. 6: Enhanced ATC for simultaneous transactions

| **Power Transaction (MW)** | **20** | **40** |
|---|---|---|
| **Bus 2 to Bus 5&4 (MW) without TCSC** | 55.024 | 54.892 |
| **Bus 2 to Bus 5&4 (MW), TCSC at line 4-5** | 56.090 | 55.940 |
| **Bus 2 to Bus 5&4 (MW), TCSC at line 3-4** | 62.480 | 62.110 |

#### 7.3.6.1 Case study 1: T1 (2-5), Transfer of 10 MW to 40 MW from bus 2 to 5 with TCSC on line 4-5

With TCSC in between bus 4 and 5, ATCs of bilateral power transfer were greatly enhanced to 84.6%, 84.1%, 84.0% and 83.6% for 10 MW, 20 MW, 30 MW and 40 MW transactions respectively. These enhanced values of ATC correspond to 141.42 MW, 140.75 MW, 140.09 MW and 139.37 MW respectively as presented in second row, columns two, three, four, and five of Table 7.5.

#### 7.3.6.2 Case study 2: T1 (2-5), Transfer of 10 MW to 40 MW from bus 2 to 5 with TCSC on line 3-4

When TCSC was placed on line 3-4, ATCs of bilateral power transfer were slightly enhanced to 22.9%, 22.9%, 23.1% and 23.08% for 10 MW, 20 MW, 30 MW and 40 MW transactions respectively. A reduction of 61.7%,

61.2%, 60.9% and 60.52% in the enhanced ATC earlier experienced in case study 1, were recorded. This implies that TCSC placed on line 4-5 performs far better than TCSC placed in line 3-4 for ATC enhancement. These values are 94.18 MW, 93.96 MW, 93.76 MW, and 93.45 MW respectively for 10 MW, 20 MW, 30 MW and 40 MW power transfer.

#### 7.3.6.3 Case study 3: T2 (2-4), Transfer of 10 MW to 40 MW from bus 2 to 4 with TCSC on line 4-5

For transaction T2 when TCSC was placed between bus 4 and 5, values of ATCs for bilateral power transfer of 10 MW, 20 MW, 30 MW and 40 MW were all enhanced with 15.0%, 21.4%, 21.29% and 0.63% respectively. These correspond to 53.36 MW, 56.34 MW, 56.29 MW and 55.24 MW ATC values. These values are far below the magnitude of enhanced ATC for the T1(2-5) with TCSC between buses 4-5 as earlier reported.

#### 7.3.6.4 Case study 4: T2 (2-4), Transfer of 10 MW to 40 MW from bus 2 to 4 with TCSC on line 3-4

Placement of TCSC on line 3-4 for this transaction reduced ATC values for 10 MW and 20 MW power transfer with 49.36% each. ATCs were found to be diminishing instead of enhancing. However, ATCs of power transfer of 30 MW and 40 MW from bus 2 to 4 under this placement experienced a boost of 21.1% and 47.69%. However, with nature of this transaction, the performance of TCSC in enhancing ATC when placed in between bus 4 and 5 outweigh the performance in location position 3-4 in this case.

#### 7.3.6.5 ATC values during simultaneous transaction

The values obtained during this transaction revealed that for both placement locations, ATC values are enhanced but with different magnitude. The nature of transaction here impacted on the enhanced ATC values and as previously reported, there was a reduction in the magnitude of values obtained during 40 MW power despatch as compared to 20 MW power transfer. This implies TCSC was able to influence network performance without impaired network parameters.

### 7.3.7 Voltage profile with TCSC during power transactions

The voltage values as obtained during different transactions as well as associated magnitude of despatched power are reported here. The influence of TCSC as affected bus voltage profile were well investigated and the performance of TCSC in relation to bus voltage profile in these two locations were then compared. These are presented in the following paragraphs.

#### 7.3.7.1 Case study 1: T1 (2-5) Transfer of 10 MW from bus 2 to 5, with TCSC on line 4-5 and 3-4

10 MW power transfer during T1 (2-5) was implemented with incorporation of TCSC on line 4-5 and 3-4 in each case. Fig. 7.14 presents bus terminal voltage of the situation for comparison. Like previous situation, reactive power control of generators located at buses 1 and 2 held terminal voltage constant at unity however, voltage at bus 3, 4, and 5 varies with power transaction. With TCSC on location 4-5, voltage at buses 3, 4, and 5 were made to improve whereas, with location 3-4, only voltage at bus 5 was improved while that of bus 3 and 4 experienced deviation to lower limit.

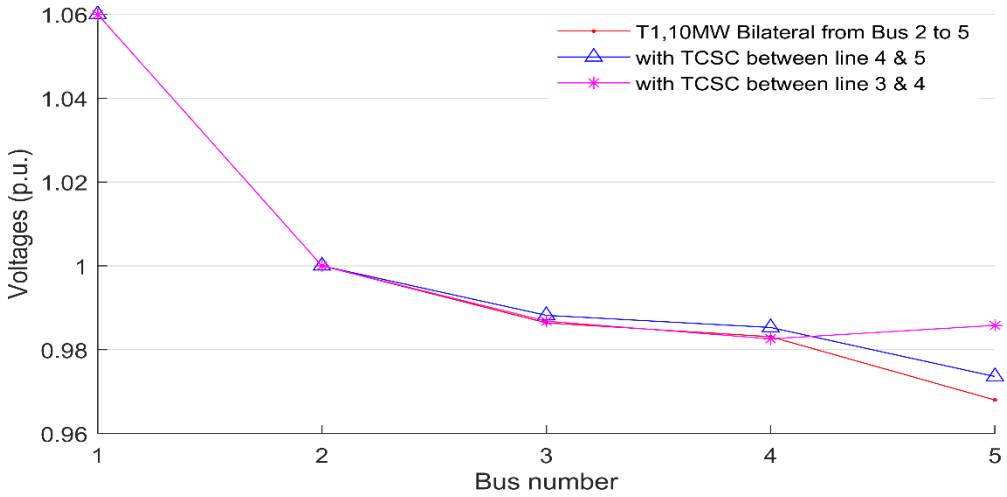


**Figure 7. 14: Bus voltage profile for T1 (2-5) 10 MW transfer with TCSC at 4-5 and 3-4**

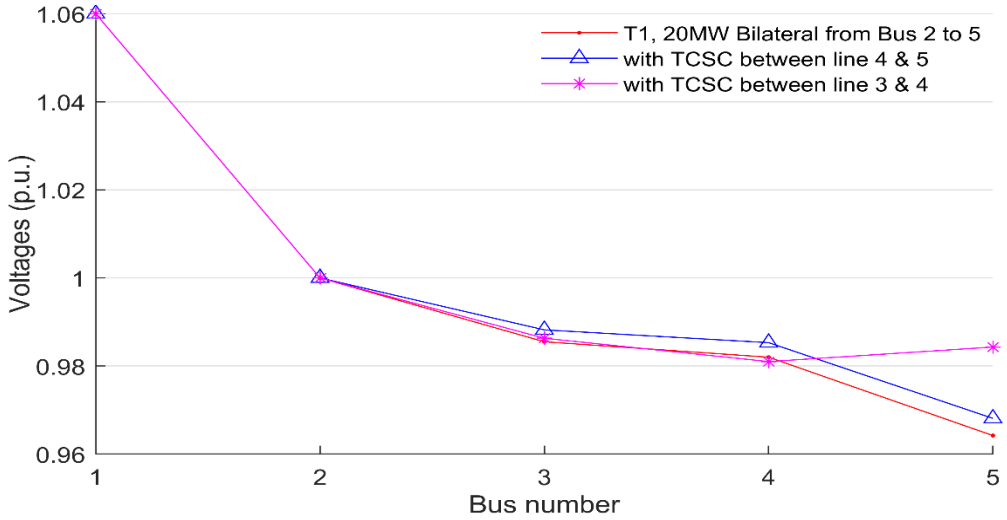


**Figure 7. 15: Bus voltage profile for T1 (2-5) 20 MW transfer with TCSC at 4-5 and 3-4**

#### 7.3.7.2 Case study 1: T1 (2-5) Transfer of 20 MW from bus 2 to 5, with TCSC on line 4-5 and 3-4

During 20 MW power transfer for T1 (2-5), the voltage profile is as presented in Fig 7.15. Similar bus voltage deviation minimization occurred when TCSC was in position line 4-5 as in the case of 10 MW power transfer. Voltages at buses 3, 4, and 5 were improved in this position but only bus 5 voltage was enhanced when the device was placed in location 3-4.

#### 7.3.7.3 Case study 1: T1 (2-5) Transfer of 30 MW from bus 2 to 5, with TCSC on line 4-5 and 3-4

When 30 MW power transfer for T1 (2-5), was implemented, the voltage profiles obtained are as presented in Fig. 7.16. The performance of TCSC in location 3-4 slightly improved with enhancement of voltage at bus 3 and 5 as against only bus 5 in the case of 10 MW and 20 MW transfer. However, placement of TCSC in location line 4-5 resulted into enhancement of voltage at buses 3, 4 and 5 as shown in the figure.

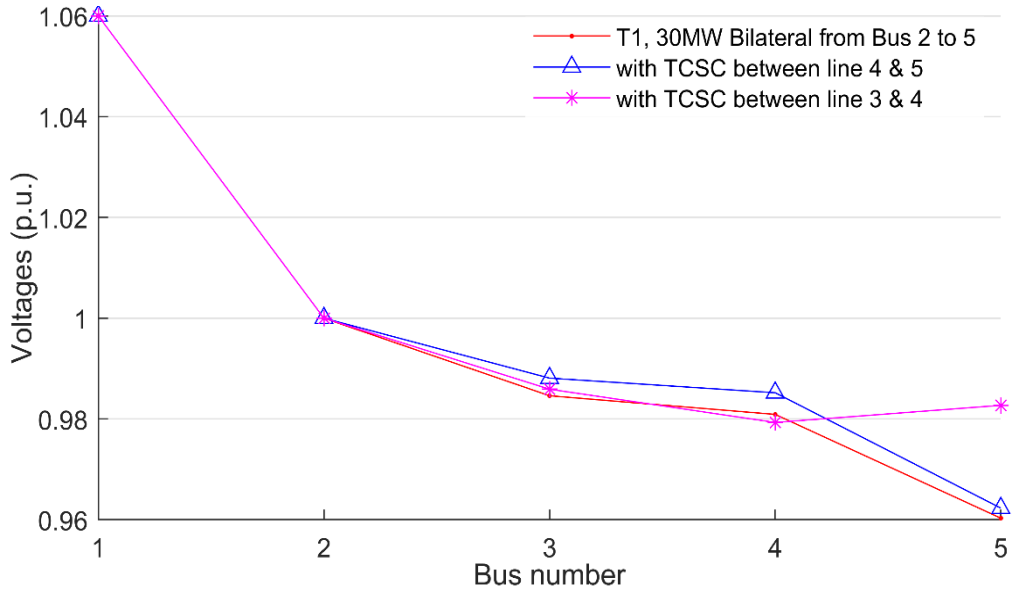


**Figure 7. 16: Bus voltage profile for T1 (2-5) 30 MW transfer with TCSC at 4-5 and 3-4**

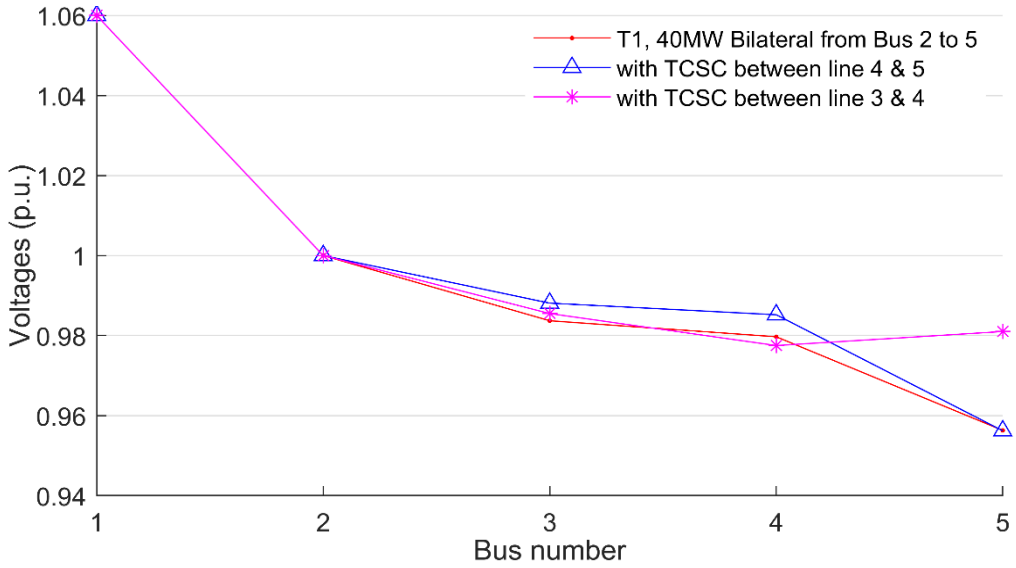


**Figure 7. 17: Bus voltage profile for T1 (2-5) 40 MW transfer with TCSC at 4-5 and 3-4**

#### 7.3.7.4 Case study 1: T1 (2-5) Transfer of 40 MW from bus 2 to 5, with TCSC on line 4-5 and 3-4

With TCSC in between bus 4 and 5, bus voltages for power transactions of 40 MW from generator bus 2 to load bus 5 are as presented in Fig 7.17. Blue colored graphs indicate the improvement in bus voltage, red graph is the pre-TCSC placement voltage. Likewise, with TCSC connected between transmission line 3-4, bus voltage is indicated in magenta colored graphs on the same figure. Only bus 5 witness voltage improvement with TCSC in this location. However, with TCSC between line 4 and 5, faster recovery of the voltage variable of the system was achieved. Regarding voltage improvement therefore, TCSC performance was optimized at location line 4-5 other than line 3-4 for all the implemented power transfer.

#### 7.3.7.5 Case study 2: T2 (2-4), Transfer of 10 MW from bus 2 to 4 with TCSC on line 4-5 and 3-4

The behavior of network voltage during transaction T2 for 10 MW power transfer is presented in Fig. 7.18. With this power magnitude, voltage deviation was minimal however just like case study 1, presence of TCSC on line 4-5 enhanced voltage profile at all the buses. This was not so for location 3-4 as shown in the figure because, there was a voltage dip at bus 4 despite TCSC incorporation as a result of location.

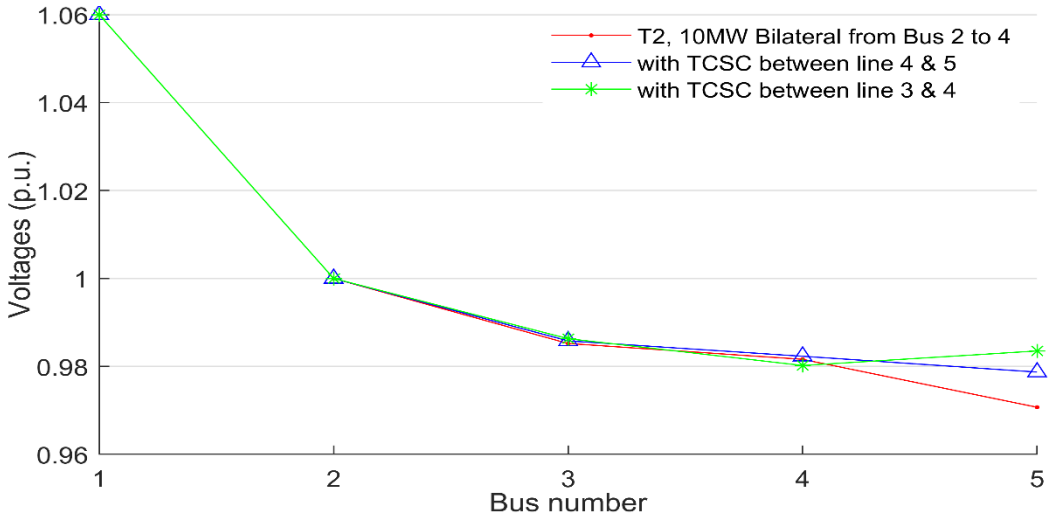


**Figure 7. 18: Bus voltage profile for T2 (2-4) 10 MW transfer with TCSC at 4-5 and 3-4**

#### 7.3.7.6 Case study 2: T2 (2-4), Transfer of 20 MW from bus 2 to 4 with TCSC on line 4-5 and 3-4

During 20 MW power transfer for this power transaction however, similar voltage profile as that of 10 MW power transfer was experience as presented in Fig. 7.19. TCSC placement in location line 3-4 improve voltage at bus 3 and 5 impaired voltage at bus 4 below pre-TCSC value. The scenario was different when TCSC was incorporated at location 4-5 as optimized by the sensitivity-based method as introduced in this chapter. The voltage profiles for this transfer is as presented in the figure for better understanding.

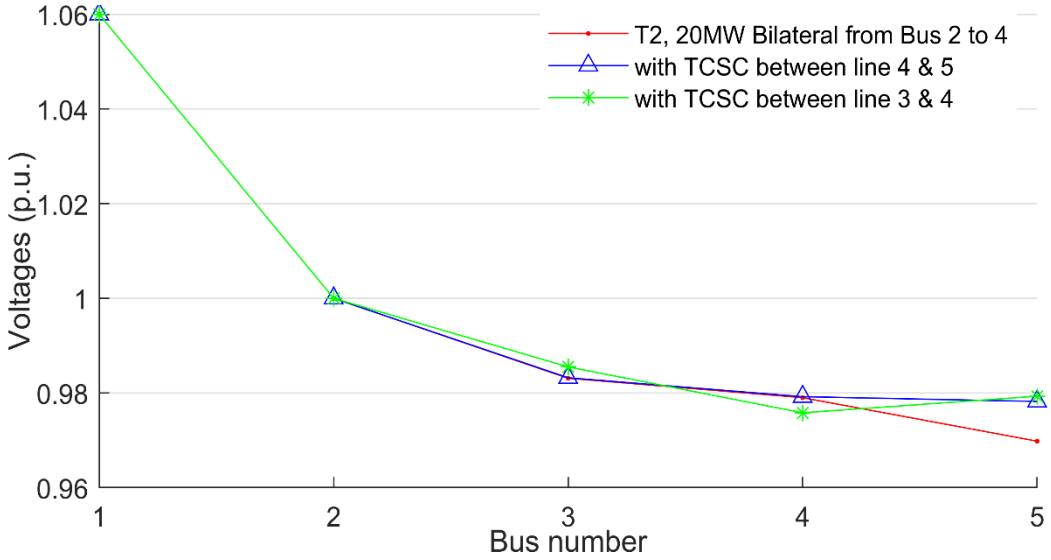


**Figure 7. 19: Bus voltage profile for T2 (2-4) 20 MW transfer with TCSC at 4-5 and 3-4**

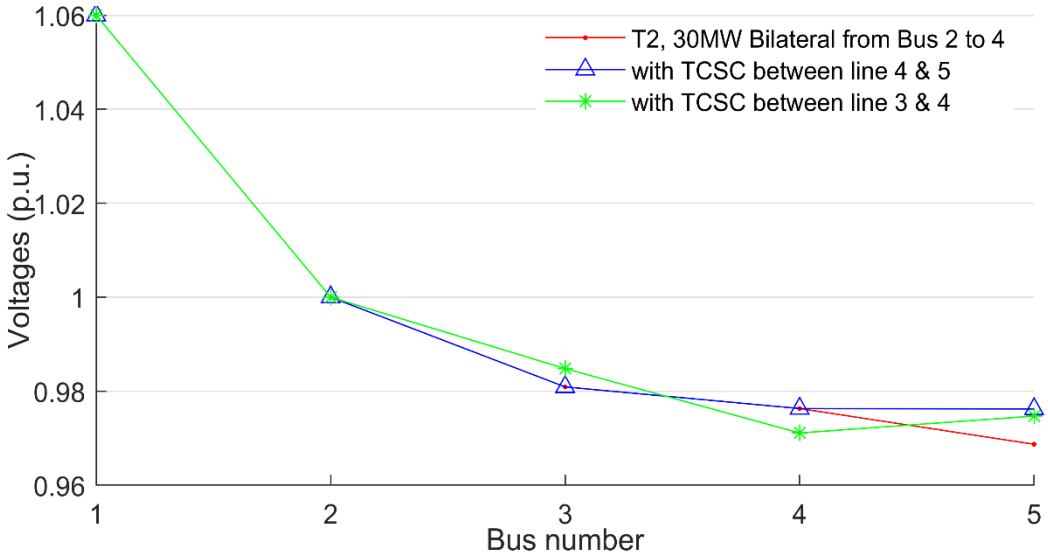


**Figure 7. 20: Bus voltage profile for T2 (2-4) 30 MW transfer with TCSC at 4-5 and 3-4**

#### 7.3.7.7 Case study 2: T2 (2-4), Transfer of 30 MW from bus 2 to 4 with TCSC on line 4-5 and 3-4

Response of network to 30 MW power transfer for this case study is presented in Fig. 7. 20. The situation is like that of 20 MW power transfer only with different magnitude of voltage deviation. Here, the voltage deviated towards lower limit at bus 4 when TCSC was on line 3-4 was this intense because of magnitude of power transfer as shown in Fig. 7.20. The performance of TCSC in location 4-5 surpasses that of 3-4 as presented.

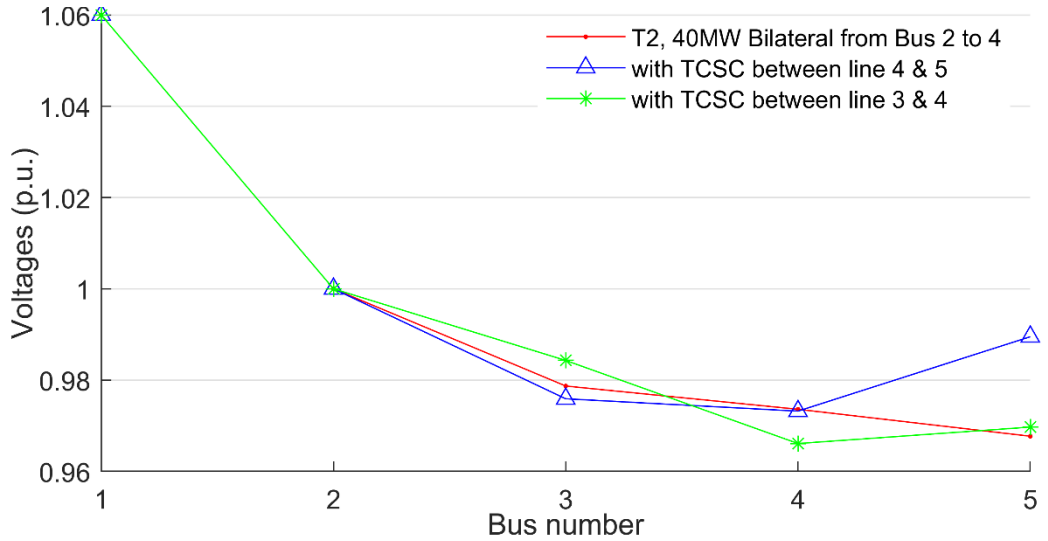


**Figure 7. 21: Bus voltage profile for T2 (2-4) 40 MW transfer with TCSC at 4-5 and 3-4**

#### 7.3.7.8 Case study 2: T2 (2-4), Transfer of 40 MW from bus 2 to 4 with TCSC on line 4-5 and 3-4

Figs. 7.21 depict bus voltage output with TCSC on line 4-5 and 3-4 during 40 MW power transfer between bus 2 and load bus 4. Under this arrangement, incorporation of TCSC on line 4-5 improved bus voltage for all the buses with slight reduction in voltage at bus 3. Notwithstanding, this is in connection with quantity of transacted power. However, the parameter setting of the device can further be optimized by such heuristic algorithms as

presented in chapter six, for better performance. In contrast, a critical look at these graphs revealed that bus 4 experienced a voltage drop for this 40 MW power despatch, when TCSC was placed on line 3-4 as against when FACTS was not incorporated. Summarily, with placement of TCSC in between line 3-4, bus voltage profile deviation towards lower limit was aggravated, whereas, placement of TCSC in between line 4-5 yielded minimization of bus voltage profile deviation as indicated on the graphs.

#### 7.3.7.8 Case study 3: Simultaneous transaction of 20 MW power from bus 2 to buses 4 & 5 with TCSC on line 3-4 and 4 – 5

Fig. 7.22 is the graph of bus voltage for simultaneous transaction of 20 MW power from bus 2 to buses 4 and 5. In comparison to when TCSC was not incorporated, placement of TCSC between bus 3 and 4 led to a deeper voltage dip at bus 2, 3 and 4, leaving only bus 5 voltage improved. In contrast, voltage at all the buses experienced a boost with inclusion of TCSC between bus 4 and 5.

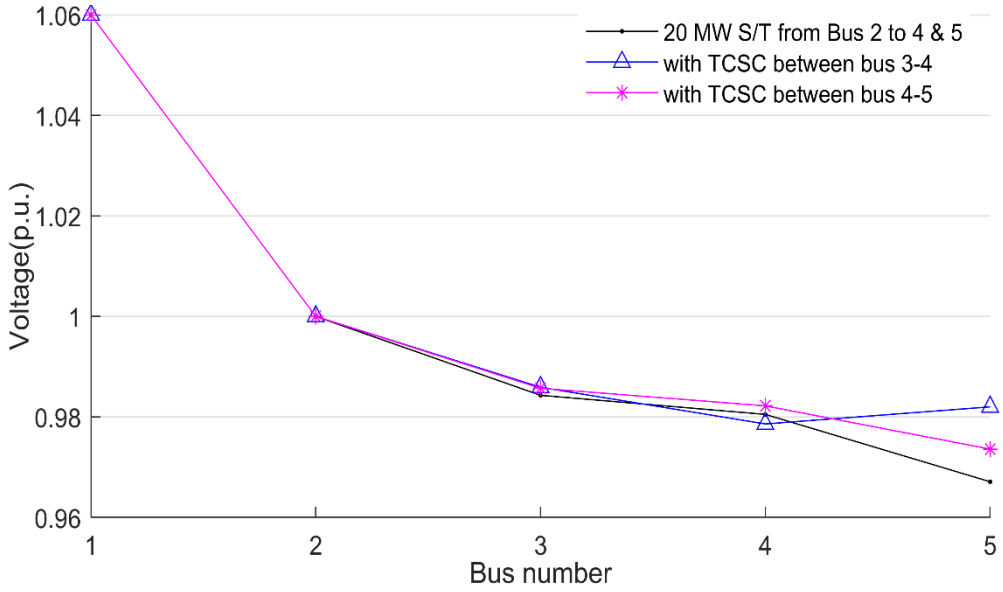


**Figure 7. 22: Bus voltage profile for simultaneous 20 MW power transfer from bus 2 to 4 & 5**

#### 7.3.7.8 Case study 4: Simultaneous transaction of 40 MW power from bus 2 to buses 4 & 5 with TCSC on line 3-4 and 4 – 5

The graph in Fig. 7.23 gives bus voltage profile for simultaneous transaction of 40 MW power from bus 2 to buses 4 and 5. When TCSC was incorporated between bus 4 and 5, this led to improvement of all bus voltages. This faster recovery of voltage variable of the test system is a pointer to the suitability of the location line 4-5. In contrast, voltage dip at bus 4 was exacerbated with inclusion of TCSC between bus 3 and 4.

During the investigation of bus voltage profile however, it has been observed that location line 4-5 led to fast voltage profile recovery in all the nature and type of implemented power transactions. Placement of TCSC in location line 4-5 optimized the performance of the device other than location line 3-4 for transactions and magnitude of trading.

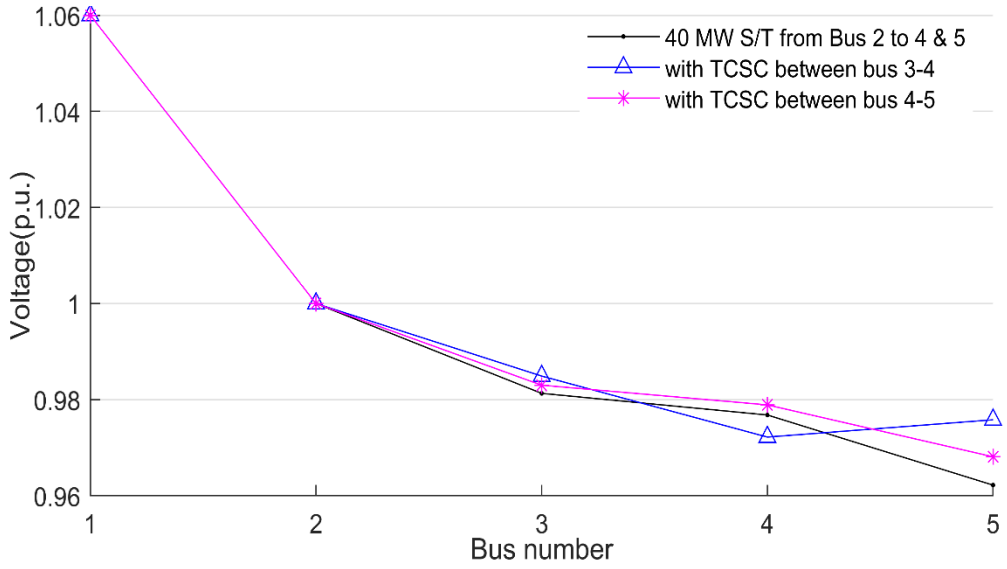


**Figure 7. 23: Bus voltage profile for simultaneous 40 MW power transfer from bus 2 to 4 & 5**

### 7.3.8 Active power loss profile with TCSC during power transactions

Test system power loss was also investigated as part of the objectives in this study. Placement of FACTS devices into network in this context was based on incorporation of TCSC device loss into network total loss, hence loss profile was also examined. The observations are reported as follows.

#### 7.3.8.1 Case study 1: T1 (2-5). Transfer of 10 MW – 40 MW from bus 2 to 5 with TCSC on line 4-5 and 3-4

The real power loss for the placement of TCSC device at the two locations 4-5 and 3-4 are presented in Figs. 7.24 – 7.27. It can be seen visually that with TCSC on line 4-5, active power loss was minimized in all the transmission lines during 10 MW power transfer. Major loss reduction was experienced on lines 1-3, 2-3, 2-4, 3-4 and 4-5. The slight increase in active power loss on transmission line 2-5 was as a result of increase in power flow subsequent of ATC enhancement because, more power loss accompanies more power flow on transmission lines as earlier stated. The situation is the same during other power transfers, for 20 MW, 30 MW, and 40 MW respectively but with different magnitude of loss reduction as presented in Figs. 7.25, 7.26 and 7.27 below. The situation is different for placement on line 3-4, where this location led to increase in system real power loss, as evident in all the figures. This location impairs loss reduction especially on transmission line number 1, 4, 5 and 6. Slight increase in loss which is proportional to power transfer magnitude was observed on line number 5, when TCSC was inserted on line 4-5. With this in mind, FACTS performance in this location outweighs the recorded loss reductions with placement of TCSC between line 3 and 4. The loss minimization and control capability of TCSC on location line 4-5 suggest suitability of this location for FACTS placement.

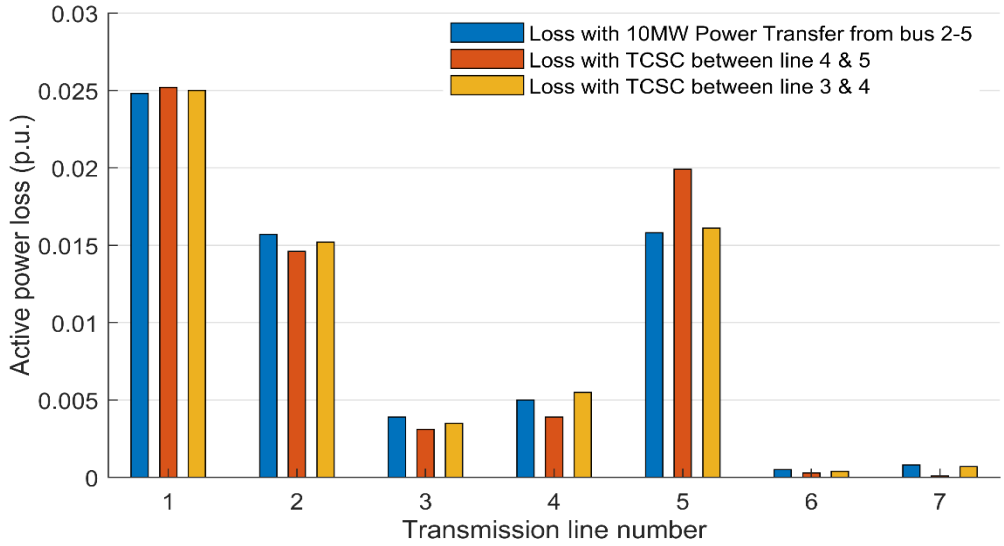


**Figure 7. 24: Line active power loss for T1 (2-5) 10 MW transfer with TCSC at 4-5 and 3-4**

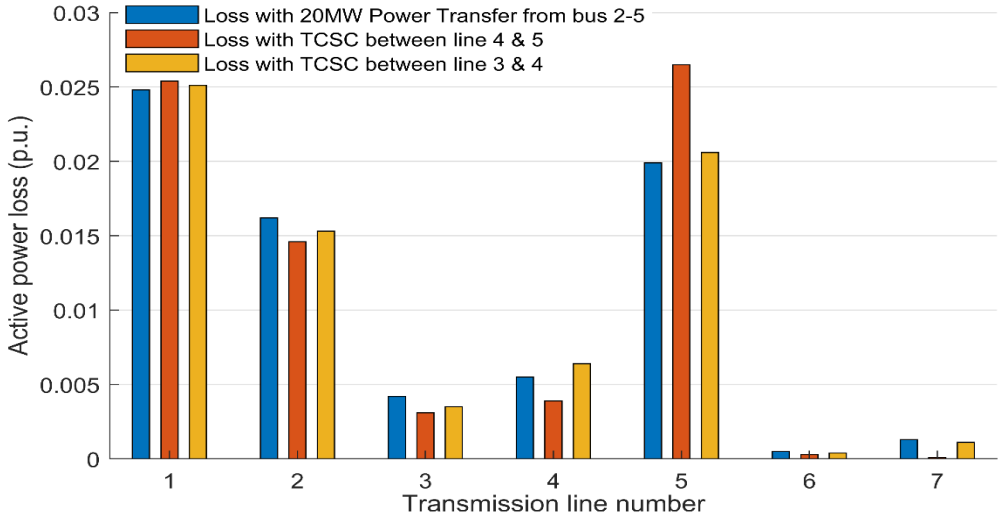


**Figure 7. 25: Line active power loss for T1 (2-5) 20 MW transfer with TCSC at 4-5 and 3-4**

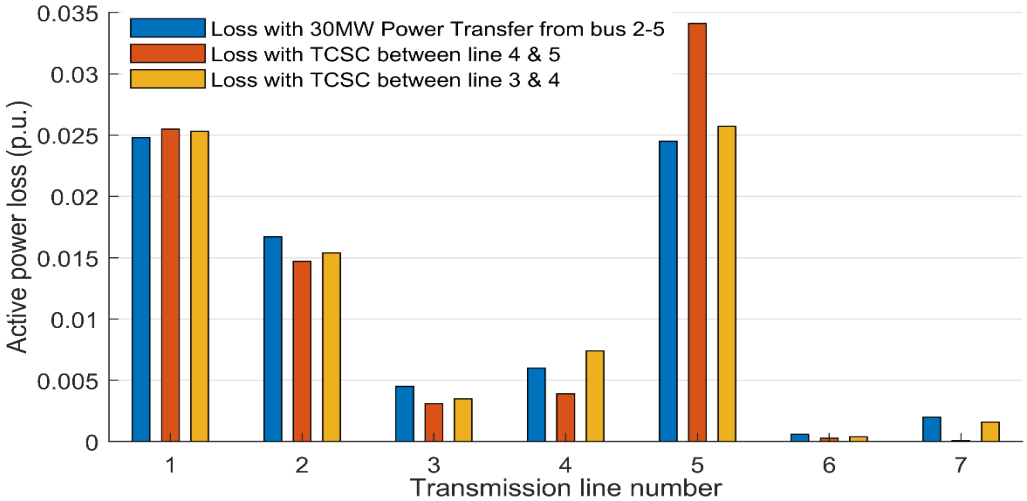


**Figure 7. 26: Line active power loss for T1 (2-5) 30 MW transfer with TCSC at 4-5 and 3-4**

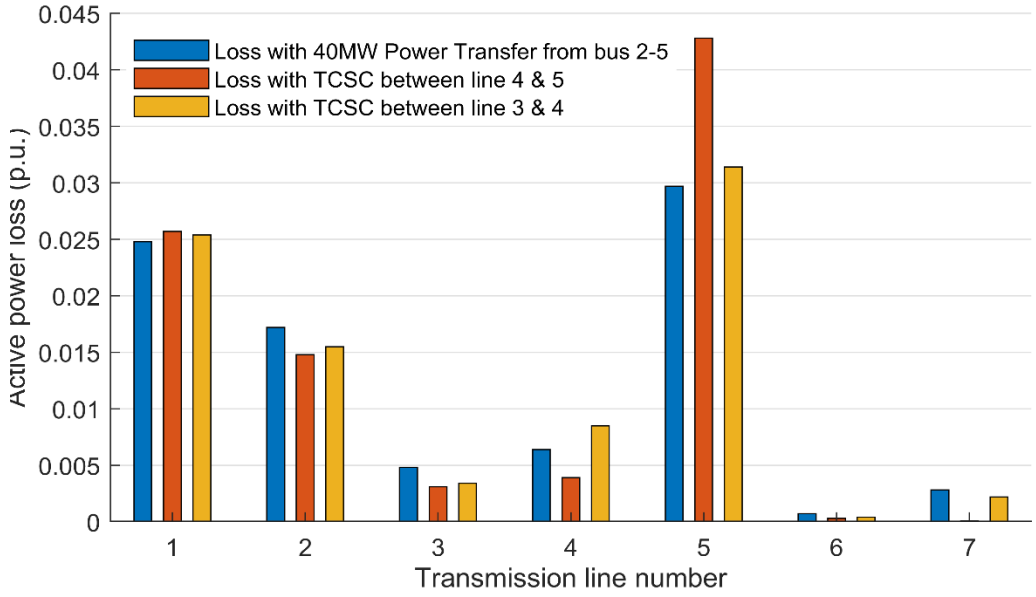


**Figure 7. 27: Line active power loss for T1 (2-5) 40 MW transfer with TCSC at 4-5 and 3-4**

#### 7.3.8.2 Case study 2: T2 (2-4). Transfer of 10 MW – 40 MW from bus 2 to 4 with TCSC on line 4-5 and 3-4

Active power loss for the case of power transfer between bus 2 and 4 are presented in Figs. 7.28 – 7.31. In Fig. 7.28, placement of TCSC on line 3-4 led to increase in real power loss in most cases on lines 2-4, 2-5, 3-4 and 4-5. Notwithstanding, lines 1-3 and 2-3 enjoyed loss reduction for same location. With placement of TCSC on line 4-5, transmission lines 1-3, 2-3, 2-4, 3-4 and 4-5 experienced decrease in active power loss. This situation of 10 MW power transfer is a replica of other power transfer for 20 MW, 30 MW and 40 MW but with slight changes in magnitude of power loss. Wherever location 4-5 leads to increase in power loss, the magnitude and instance is so small compared with that of 3-4 placement. Optimal real power loss control is achievable when TCSC is placed on line 4-5 because, this location favors loss reduction as part of set objectives.

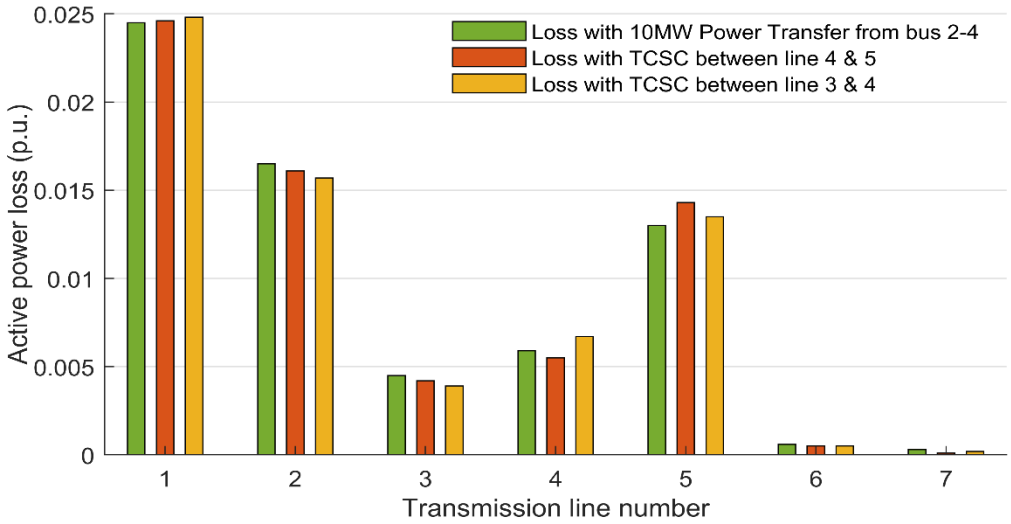


**Figure 7. 28: Line active power loss for T2 (2-4) 10 MW transfer with TCSC at 4-5 and 3-4**

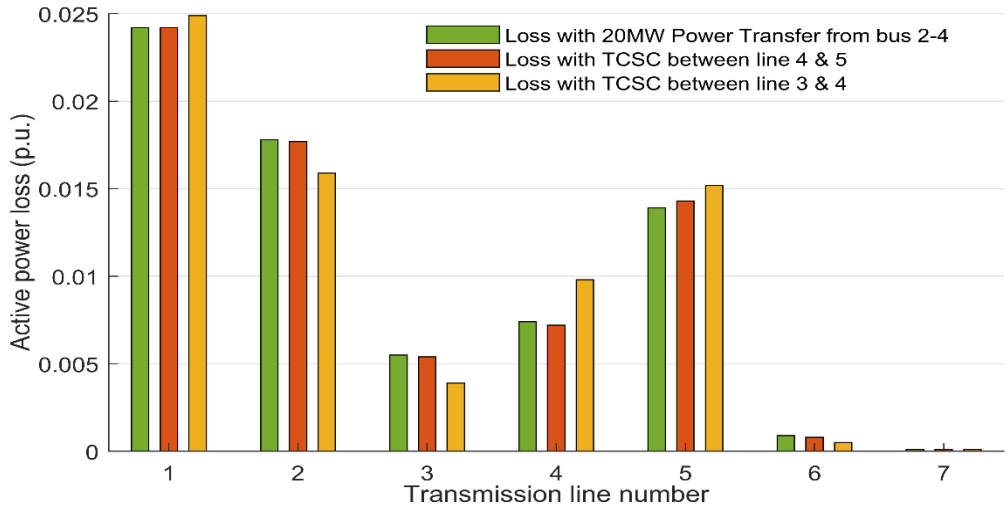


**Figure 7. 29: Line active power loss for T2 (2-4) 20 MW transfer with TCSC at 4-5 and 3-4**

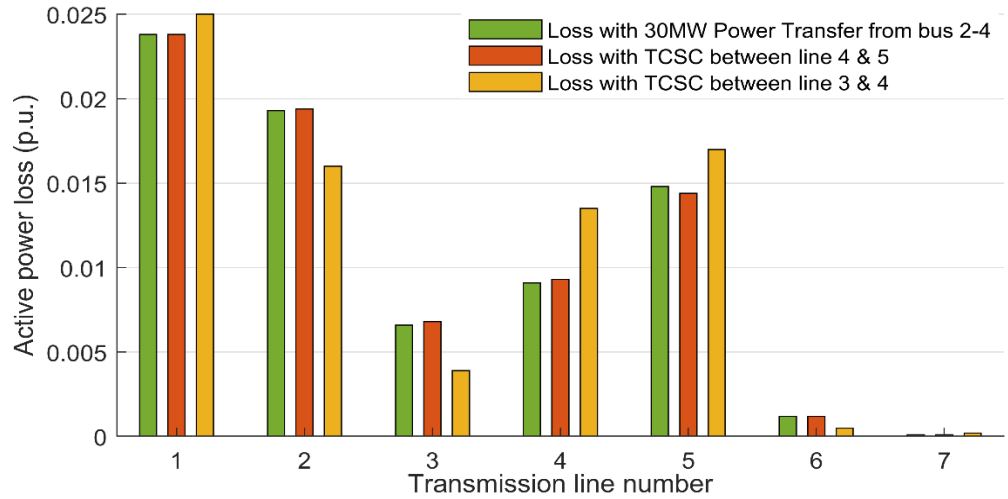


**Figure 7. 30: Line active power loss for T2 (2-4) 30 MW transfer with TCSC at 4-5 and 3-4**

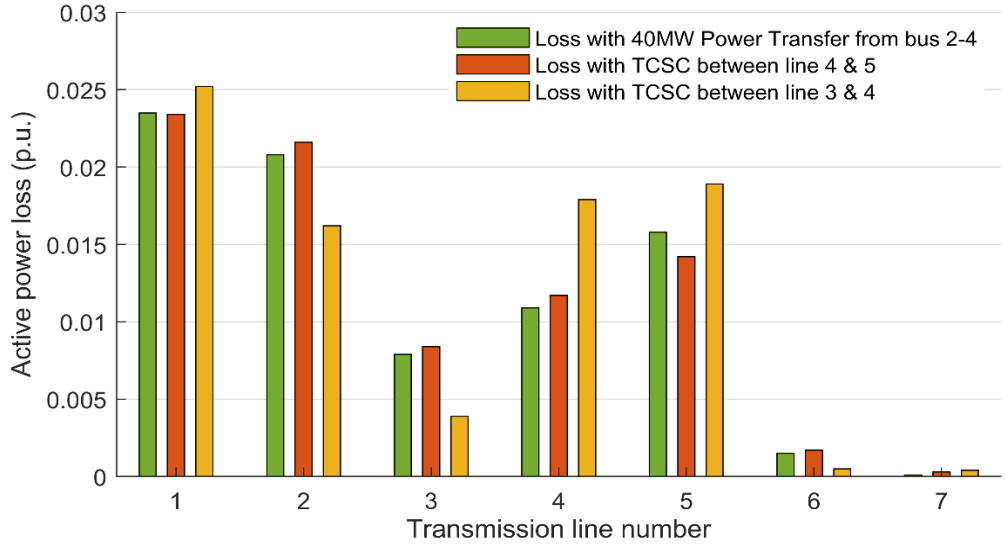


**Figure 7. 31: Line active power loss for T2 (2-4) 40 MW transfer with TCSC at 4-5 and 3-4**

#### 7.3.8.3 Case study 3: Simultaneous transaction of 20 MW power from bus 2 to buses 4 & 5 with TCSC on line 3 – 4 and 4 – 5

Fig. 7.32 is the graph of real power loss for simultaneous transaction of 20 MW power from bus 2 to buses 4 and 5. It can be observed that losses on all the transmission lines with exception of line 2-5 were minimized when TCSC was placed between bus 4 and 5. This is not the case for TCSC inclusion on line 3-4 because, real power losses were aggravated on transmission lines 1-2, 2-4 and 2-5. The location on line 4-5 also led to network performance improvement especially loss minimization in this type of trading, as recorded during bilateral transaction.

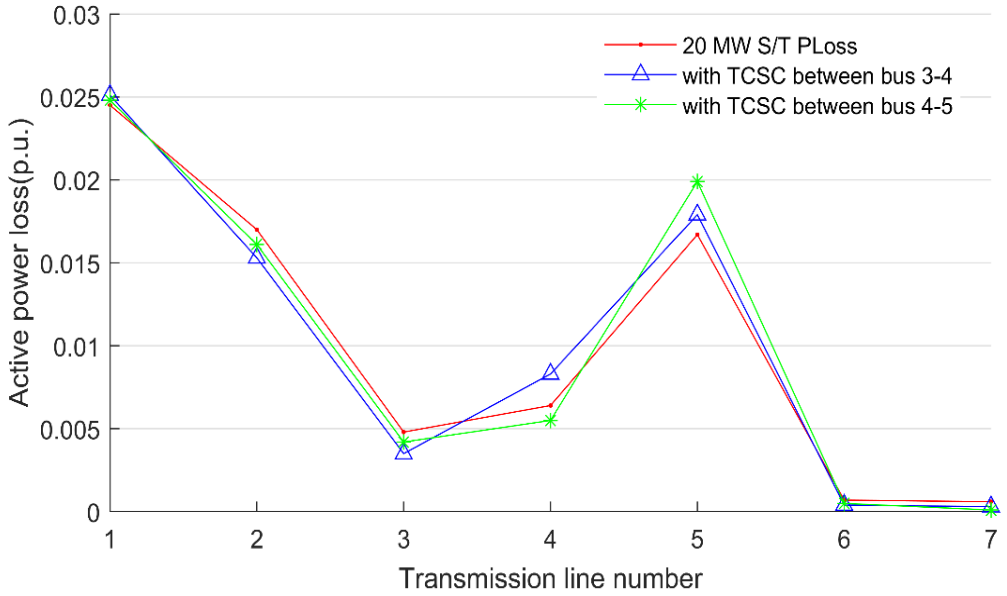


**Figure 7. 32: Line active power loss for simultaneous 20 MW transaction from bus 2 to 4 & 5**

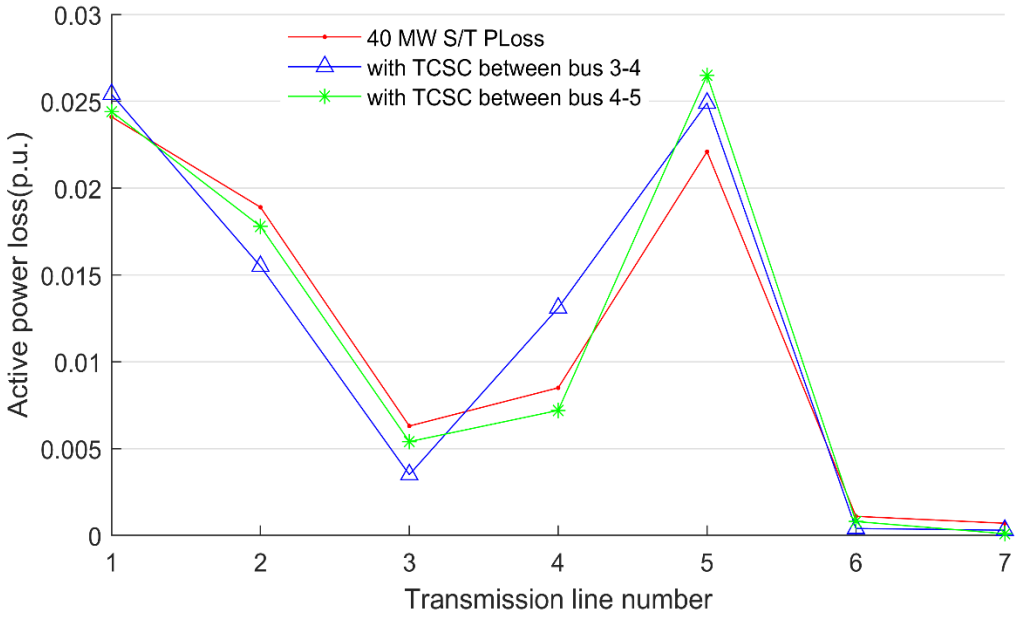


**Figure 7. 33: Line active power loss for simultaneous 40 MW transaction from bus 2 to 4 & 5**

#### 7.3.8.4 Case study 4: Simultaneous transaction of 40 MW power from bus 2 to buses 4 & 5 with TCSC on line 3-4 and 4 – 5

The active power loss pattern for this transaction as shown in Fig. 7.33 is like the one in Fig. 7.32, but with higher magnitude. There is loss minimization for all the transmission lines with an exception of line 2-5 for TCSC placement on line 4-5. Placement of TCSC between bus 3 and 4 led to increase in active power loss on transmission lines 1-2, 2-4 and 2-5. Loss reduction was limited to lines 1-3, 2-3 3-4 and 4-5. However, with active power loss control in focus especially during simultaneous transactions, the inclusion of TCSC between transmission line 4-5 is better that that of line 3-4. This is evident from the figures.

### 7.4 Summary of chapter seven

A universal method for FACTS optimal placement has been developed based on total real power loss minimization approach with the objectives of ATC enhancement, voltage profile improvement and active power loss minimization. TCSC has been implemented for this method with this device modeled analytically as SSSC for this purpose. Based on this model, the total real power loss was partially differentiated with respect to voltage magnitude and angle of injected voltage, the sensitivity of which were then used for identification of optimal location for TCSC device placement.

ATCs which were hitherto determined by ACPTDF approach were enhanced by optimal placement of TCSC in the position identified by this developed method. Comparative analyses of the optimal location based on this method and other existing approach revealed its advantage. It was also revealed that placement based on this method increases the effectiveness of FACTS devices on system performance. Placement with this method resulted into ATC enhancement of more than 60% well above the values obtained when TCSC was placed with thermal limit method. In addition, a substantial bus voltage improvement of up to 3% deviation minimization as well as up to 10% active power loss reduction was recorded with this placement.

The presented results and analyses of ATC values, bus voltage profiles and real power losses disclosed that ATCs were enhanced, bus voltage improved and that real power losses were also minimized with the presented sensitivity based optimal placement of TCSC device. With the performance of this sensitivity-based placement method, efforts were made to apply same for HVDC transmission system optimization for network performance enhancement in the subsequent chapters.

# CHAPTER EIGHT

# NETWORK PERFORMANCE ENHANCEMENT WITH HIGH VOLTAGE DIRECT CURRENT TRANSMISSION SYSTEMS

## 8.1 Introduction

This chapter presents the results of an investigation and analyses of the capability of voltage source converter (VSC) based high voltage direct current (HVDC) transmission system in enhancing power network performance. A sensitivity-based technique of optimal location as presented in chapter seven was applied for incorporation of VSC-HVDC transmission system in this chapter. This placement was achieved with recourse to magnitude of injected voltage and control angle variables of the device through its active participation in total system loss derivatives. Performances of VSC-HVDC based transmission system during different power transfers resulting from bilateral and simultaneous transactions were observed. Bus voltage deviation minimization and power loss control involved in these various transactions are presented and analysed.

## 8.2 VSC-HVDC transmission systems

There have been tremendous efforts by researchers to ensure sustainable and competitive electrical power transfer that will meet and even surpass the upsurge and ever increasing power demand created by the ongoing power system deregulation and restructuring [199]. Power transmission components are being stressed and operated near their limits because of this power demand. Hence, demonstration of applications of FACTS devices in power transfer capability enhancement and overload alleviations are being intensified through collaborative research [195]. HVDC transmission system has been found useful in various special applications apart from being highly efficient in transmitting bulk electrical energy over a long distance [200]. Vast electric power despatch over long distance with insignificant voltage drops and power losses are some of the major attributes of HVDC transmission systems. As earlier stated, applications of VSC based HVDC in transmission system is gaining attraction because of the recent recorded successes and improvements in VSC based power electronic systems. In point to point overhead power transmission beyond 800 km and for underground cable interconnection or distant offshore grid integration of wind energy in excess of 100 km, application of HVDC system is preferable [201]. It has been established that HVDC is an economic channel for long distance power transmission systems among other benefits, and its application is not only significant but will also determine future energy grid operations [151]. In comparison with HVAC, it has offered proficiency in interconnection of asynchronous grids, extended underground cable connections, fault current reductions, mitigation of network congestions and environmental impact extenuations among others [151],[202].

The realization of HVDC technology is achieved through converter based power electronic semiconductor devices which is classified into VSC and line commutated converter (LCC) [153]. However, VSC-HVDC has the capability for easy multiterminal connection, capability for black start operation, excellent ac fault response, independent active and reactive power control, optional bus terminal voltage control independent of reactive power, fast ac frequency response and damping support provision, short time requirement from

conceptualization to commissioning, and lower harmonic output content as against LCC-HVDC, which cannot operate reliably without absorbing reactive power from ac network for successful commutation of converters [180],[192],[203],[204]. Up till date, these characteristics argued in support of VSC-HVDC deployment successfulness as a solution to LCC-HVDC problems, thereby bringing the perceived high cost of implementation of former to no repute [205],[206]. Parts of the foreseeable improvement in future electrical grid operations and architecture will be achieved through increase in implementation of VSC-HVDC, which will lead to increase in transmission efficiency, growth in renewable generation integrations, additional grid connected distributed generations, capability expansion of bidirectional ac grids current flow, and overall enhancement of network reliability and security [156],[157]. An evidence of this future development is the formation of North Sea Region Offshore Grid Initiative (NSROGI) in 2010, by ten countries of North Sea Region for realization of VSC-HVDC infrastructure interconnection, to achieve the planned over 100 GW offshore wind power network by year 2030 [158].

VSC-HVDC is a new technology embedded with lots of inexhaustible potentials and while research interests have focused on its transient stability, dynamic stability, voltage supports, and oscillation damping, the focus of a renew thought of research is its deployment for the provision of ac network broad support benefits. Therefore, power flow enhancement capabilities of a VSC-HVDC embedded in ac power system network were investigated and analyzed in this chapter. Power network system that is in dire need of transmission capability expansion especially in the wake of upsurge in power demand due to power system deregulation and restructuring is the motivation for this study. The following were achieved in this chapter;

(a) Sensitivity based analysis of VSC-HVDC transmission system for its optimal placement in an ac network.

(b) Application and utilization of VSC-HVDC transmission system like other FACTS devices for power flow enhancement, bus voltage deviation minimization and power loss reduction purposes. These were made possible through the following;

   i. Static modelling of VSC-HVDC transmission line interconnecting two ac network buses based on lumped parameters π-equivalent representation for inclusion of HVDC line loss in total system loss as presented in chapter three.

   ii. Derivation of mathematical equations from system total loss based on the consideration and participation of power loss on the line containing VSC-HVDC resulting into sensitivity technique used in optimal placement as presented in chapter three.

   iii. Performance of psychoanalysis and ranking of the resultant voltage magnitude and control angle preferential sensitivities in order to optimize VSC-HVDC location in the network.

   iv. Implementation of load flow analyses with modified NR Jacobian elements as presented in chapter three due to VSC-HVDC inclusion in the transmission network.

### 8.2.1 Special consideration for using sensitivity based optimal location method

The followings were observed in implementing the developed sensitivity based method of optimal location of VSC-HVDC transmission system [127],[134],[207].

(a) VSC-HVDC transmission system was used to replace line with the minimum loss sensitivity resulting from voltage magnitude control.

(b) Considering voltage angle control, VSC-HVDC transmission system was used to replace line whose loss sensitivity was most positive.

(c) Lines installed with transformer tap changing elements were not considered for replacement with VSC-HVDC even with favoured loss sensitivity, next line on the ranking were considered.

(d) Likewise, lines that were located between buses containing shunt compensating elements or generators were also not considered for replacement with VSC-HVDC, preference was given to the next line on the ranking.

## 8.3 Results and discussions

The system loss objective function that was considered in locating VSC-HVDC on the ac network was differentiated with respect to magnitude of control voltage and angle of injected voltage of VSC. The sensitivity factors obtained from derivatives of these control variables were denoted by $\psi_1$ and $\psi_2$ for voltage magnitude and voltage angle control respectively. This resulted into two sets of variables for optimal location. The effectiveness of this approach was demonstrated on IEEE 5 bus network systems.

### 8.3.1 IEEE-5-bus test network system

The modified 5-bus system as presented in Fig. 8.1 consists of two generators connected at buses 1 and 2. This system is made up of seven transmission lines and four load buses. With generator 1 considered as the slack, the details of ratings of these generators, loads and parameters of transmission lines as contained in [198] are presented in Appendix A-3. The MW line limits in p.u. of 100 MVA base power are taken as 1.60, 0.60, 0.40, 0.40, 1.20, 0.50, and 0.30 for transmission lines 1-2, 1-3, 2-3, 2-4, 2-5, 3-4, and 4-5 respectively.

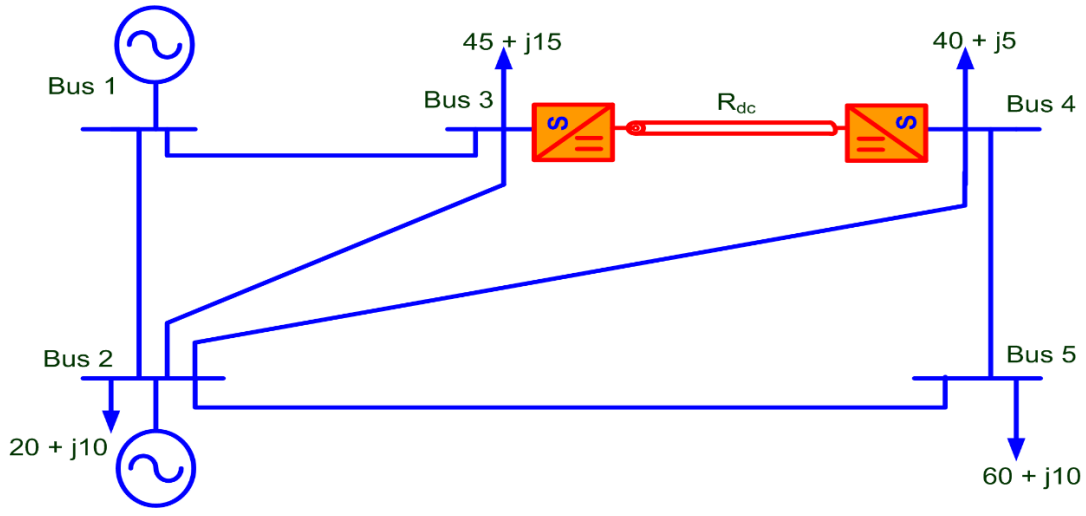


**Figure 8. 1: Modified 5-bus ac network with a VSC-HVDC transmission line interconnecting buses 3 and 4.**

### 8.3.2 Selection of optimal placement of VSC-HVDC transmission system

In determination of optimal location of VSC-HVDC transmission system in the network however, partial derivatives of system total loss with respect to voltage magnitude control parameter should be negatively large. Therefore, the value of maximum negative sensitivity factors $\psi_1$ determines the optimal location for placement with recourse to voltage magnitude control parameter. Likewise, partial derivatives that results into maximum absolute value with respect to angle of injected voltage control parameter is the suitable location for VSC-HVDC transmission system. Hence, maximum absolute value of sensitivity factors $\psi_2$ is the suitable location for HVDC based VSC transmission system.

The sensitivity factors $\psi_1$ and $\psi_2$ as obtained using the two control parameters of VSC are presented in Table 8.1. The least value of sensitivity to voltage magnitude control occurs on transmission line 3-4 with -19.8820 as appeared on sixth row of the third column in the table. This implies that maximum real power loss minimization will be obtained if the ac transmission line 3-4 is replaced outrightly with VSC-HVDC transmission system. However, maximum absolute sensitivity value to loss with respect to angle of inserted voltage, is most positive for line 3-4 as indicated on the fourth column of sixth row. The implication of this is that placement of VSC-HVDC transmission system in between buses 3-4 with negative angle of insertion will result into most real power loss reduction than any other location within the network.

Therefore, standard 5-bus network was modified with outright replacement of ac transmission line between bus 3-4 with VSC-HVDC transmission system as in Fig. 8.1. Bus 4 was taken as the rectifier station, for regulation of active and reactive power flow, while bus 3 was used as an inverter station for bus voltage regulation. Active and reactive power were to be regulated at 0.5 and 0.03 per unit, while voltage was to be regulated at unity. This was with a view to investigating power flow enhancement capability of VSC-HVDC transmission line on ac network system.

Table 8. 1: Sensitivity of test system loss to VSC-HVDC location

| Line No | Transmission Line | $\psi_1$ | $\psi_2$ |
|---|---|---|---|
| 1 | 1-2 | -9.6364 | -10.2340 |
| 2 | 1-3 | -1.2871 | -1.8261 |
| 3 | 2-3 | -3.3363 | -4.2927 |
| 4 | 2-4 | -3.2813 | -4.1726 |
| 5 | 2-5 | -5.0749 | -5.5643 |
| 6 | 3-4 | **-19.8820** | **-19.7390** |
| 7 | 4-5 | -4.0521 | -2.5438 |

## 8.4 AC network power flow with VSC-HVDC incorporation

The effects of VSC-HVDC transmission system in an ac network has been investigated in this section. With the technical and economic restrictions on physical network expansions, efforts are on the increase to optimize the networks with flexible ac transmission systems. VSC-HVDC is considered to offer great contribution to network power flow enhancement if incorporated. Power transactions that characterize power system deregulation and restructuring have been investigated with VSC-HVDC transmission system. Power transaction

that existed between generator 2 and bus 4 is termed T1 (2-4) while the transaction between same bus 2 and 5 is tagged T2 (2-5). Power transfer that accompanied these two main bilateral transactions were recorded and presented in the tabular form. The transfer of 20MW and 40 MW power were delivered in each case of the transactions. Besides, concurrent power wheeling of 20 and 40 MW power termed T3, existed between generator bus 2 and load buses 4 and 5 because of simultaneous transactions among them.

### 8.4.1 Basic power flow in the network with and without VSC-HVDC

Real power flow values of the test system are presented in Table 8.2. The basic ac network power flow values are presented in column 3 of table while the corresponding values of power flow are contained in column 4 when VSC-HVDC was incorporated into ac network. The flow on transmission line 3-4 was raised to 50 MW from 19.39 and power flow on line 4-5 which stood at 6.6 MW was increased to 29.60 MW, but flowing from line 5 to 4. Fig. 8.2 depicts the flow on all the transmission lines for base case ac network and ac network with VSC-HVDC for a better understanding.

Table 8. 2: Base case real power flow

| Line No | Transmission Line | Basic AC | with HVDC |
|---|---|---|---|
| 1 | 1-2 | 0.8933 | 0.8897 |
| 2 | 1-3 | 0.4179 | 0.4228 |
| 3 | 2-3 | 0.2447 | 0.2495 |
| 4 | 2-4 | 0.2771 | 0.1996 |
| 5 | 2-5 | 0.5466 | 0.6159 |
| 6 | 3-4 | 0.1939 | 0.5000 |
| 7 | 4-5 | 0.0660 | -0.2960 |

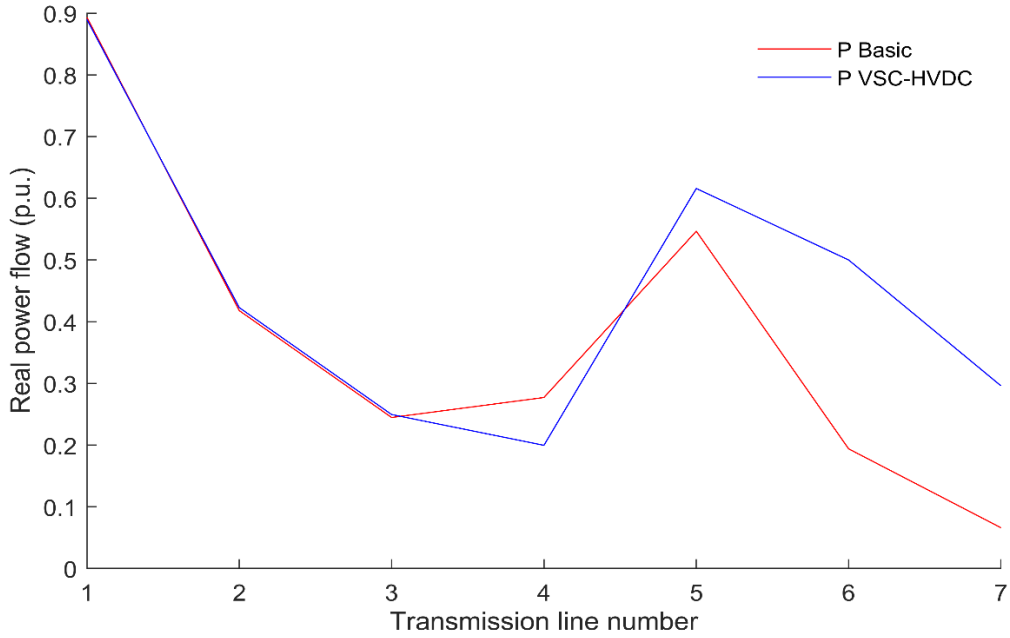


**Figure 8. 2: Test network basic ac power flow with and without VSC-HVDC transmission system**

The exchange of ac transmission line 3-4 with VSC-HVDC transmission system increased power flow on lines 2-5, 3-4 and 4-5 as shown in the figure. Hitherto flow on line 4-5 with limits 0.3 p.u. was 0.066 p.u. and that of line 2-4 with limits 0.4 p.u. was 0.2771 p.u. These power flows were enhanced thereby bringing flow on line 4-5 to 0.2960 p.u. and that of 2-4 to 0.1996 p.u, corresponding to 349% and 2.2% respectively.

### 8.4.2 Bilateral and simultaneous power transactions

Different power transactions were implemented and the obtained results for both the bilateral and simultaneous transactions are as presented in the subsequent paragraphs.

#### 8.4.2.1 20 MW transactions T1 (2-4) and T2 (2-5)

Table 8.3 presents the real power flow values for 20 MW power transfer for transactions T1 and T2. Except for transmission line numbers 1 and 4, there was an increase in flow on other transmission lines, due to incorporation of VSC-HVDC in the ac network during T1. However, during T2, an increase in real power flow amounting to 1.2%, 18.6%, 121% and 141.2% of basic flow occurred on lines 1, 5, 6 and 7 respectively. Lines 1 and 4 during T1 and 2, 3 and 4 during T2 were relieved of their loadings

Table 8. 3: Per unit real power flow for 20 MW bilateral transaction T1 and T2

| **20 MW Bilateral Power Transactions for T1 and T2** | | | | | |
|---|---|---|---|---|---|
| | | **T1(2-4)** | | **T2(2-5)** | |
| **Line No** | **Transmission Line** | **Basic AC** | **with HVDC** | **Basic AC** | **with HVDC** |
| 1 | 1-2 | 0.8631 | 0.8495 | 0.8899 | 0.9008 |
| 2 | 1-3 | 0.4567 | 0.4697 | 0.4325 | 0.4248 |
| 3 | 2-3 | 0.3033 | 0.3207 | 0.2643 | 0.2484 |
| 4 | 2-4 | 0.3514 | 0.2891 | 0.3022 | 0.1987 |
| 5 | 2-5 | 0.5842 | 0.6159 | 0.6987 | 0.8287 |
| 6 | 3-4 | 0.2866 | 0.5000 | 0.2264 | 0.5000 |
| 7 | 4-5 | 0.0298 | -0.1833 | 0.1225 | -0.2951 |

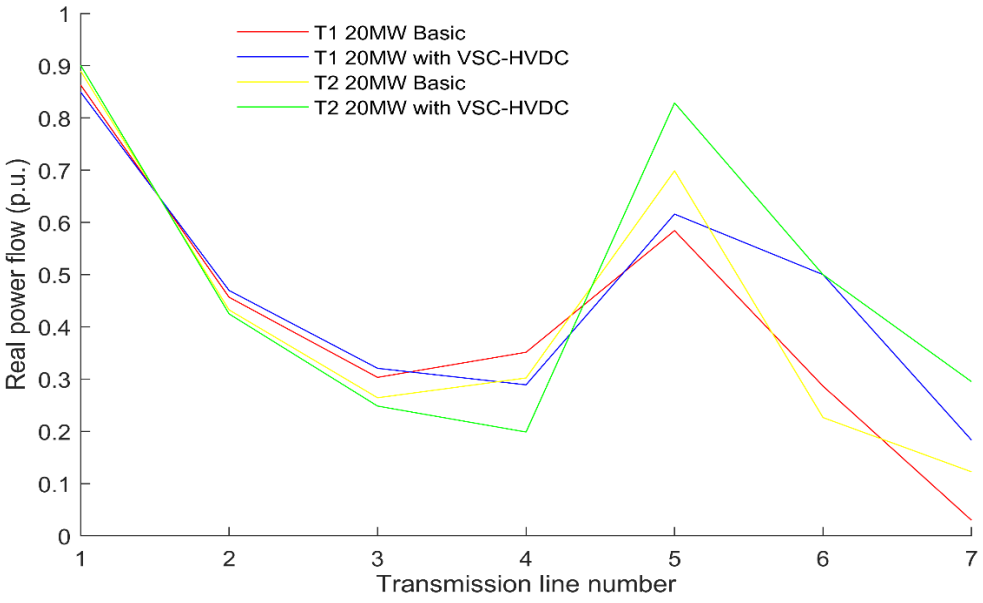


**Figure 8. 3: 20 MW transfer power flow with and without VSC-HVDC transmission system**

which could lead to thermal limit violation. The details of power flow enhancement are best understood from Fig. 8.3. There was a flow diversion through line 2-5 to bus 5 when the system was incorporated with VSC-HVDC leading to more power flow through line 4-5. The negative sign on the values obtained for flow on line 4-5 indicates change in flow direction. This led to optimization of line 4-5 whose flow ab-initio was less than 0.03 p.u. The indication is that the network can accommodate more power flow due to power flow enhancement capability of VSC-HVDC transmission system.

#### 8.4.2.2 40 MW transactions T1 (2-4) and T2 (2-5)

The power flow patterns under this power transfer are like the ones obtained during 20 MW power transfer for T1 and T2 as contained in Table 8.4, but, with different flow magnitudes. With the replacement of ac line 3-4 using VSC-HVDC, the network system real power flow was enhanced. Optimization of network in this regard

Table 8. 4: Per unit real power flow for 40 MW bilateral transactions T1 and T2

| 40 MW Bilateral Power Transactions for T1 and T2 | | | | | |
|---|---|---|---|---|---|
| | | T1(2-4) | | T2(2-5) | |
| Line No | Transmission Line | Basic AC | with HVDC | Basic AC | with HVDC |
| 1 | 1-2 | 0.8343 | 0.8109 | 0.8888 | 0.9156 |
| 2 | 1-3 | 0.4962 | 0.5175 | 0.4477 | 0.4274 |
| 3 | 2-3 | 0.3623 | 0.3926 | 0.2839 | 0.2470 |
| 4 | 2-4 | 0.4263 | 0.3794 | 0.3274 | 0.1975 |
| 5 | 2-5 | 0.6222 | 0.6159 | 0.8527 | 1.0458 |
| 6 | 3-4 | 0.3797 | 0.5000 | 0.2595 | 0.5000 |
| 7 | 4-5 | -0.0064 | -0.0700 | 0.1798 | -0.2940 |

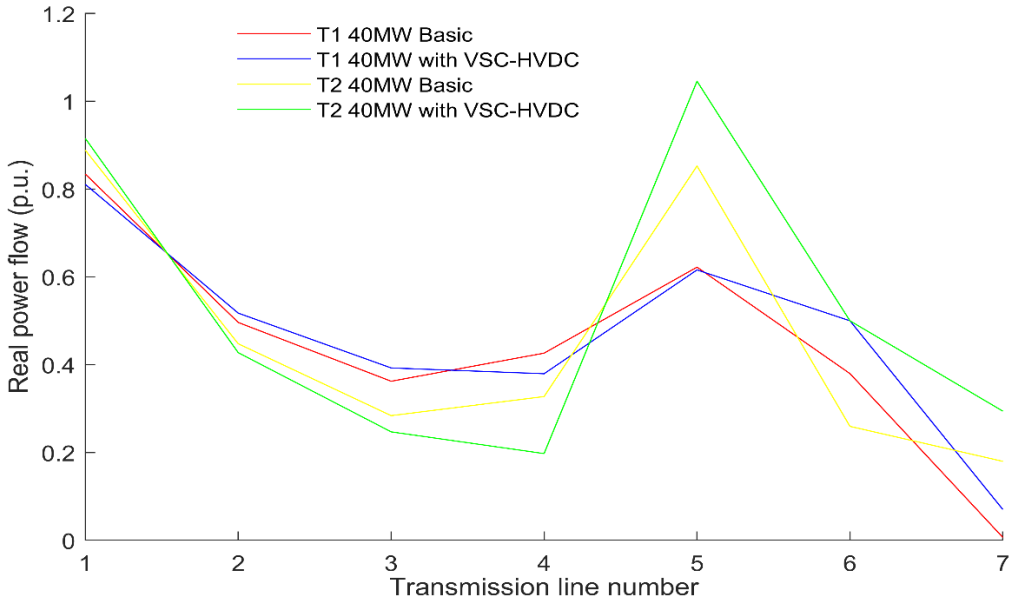


**Figure 8. 4: 40 MW transfer power flow with and without VSC-HVDC transmission system**

relieved lines 1 and 3 for T1 and lines 2, 3 and 4 for T2 of power flows that could lead to thermal limit violation. Power diversion into transmission corridors that were being underutilized was one of the achievements of the VSC-HVDC transmission system in this exercise. Fig. 8.4 gives a pictorial view of the flow with and without VSC-HVDC system as presented in Table 8.4. Wheeling of scheduled power to bus 5 was achieved via line 2-5, resulting into additional power flow through line 4-5 but in the direction 5-4 as indicated by negative real power flow. Effective deployment of network resources was therefore achieved with VSC-HVDC system. It worth note that none of the line thermal limits was violated and there was room for accommodation of more transactions.

#### 8.4.2.3 Simultaneous power transactions T3 from Bus 2 to buses 4 and 5

Table 8.5 presents the real power flow values for both 20 MW and 40 MW power transfer for transactions T3. Parts of power flows on lines 1 and 4 were diverted to other lines 2, 3, 5, 6 and 7, due to incorporation of VSC-HVDC in the ac network during 20 MW power transfer. However, power flow reduction occurred on lines 3 and 4 during 40 MW with a corresponding increase in real power flow lines 1, 2, 5, 6 and 7. Like previous bilateral transactions, the power diversion and reduction were to ensure relief of excessive loadings which could

Table 8. 5: Per unit real power flow for 20 MW and 40 MW simultaneous transaction T3

| Simultaneous Power Transactions T3 from Bus 2 to 4 & 5 | | | | | |
|---|---|---|---|---|---|
| | | 20 MW, T3 | | 40 MW, T3 | |
| **Line No** | **Transmission Line** | **Basic AC** | **with HVDC** | **Basic AC** | **with HVDC** |
| 1 | 1-2 | 0.8762 | 0.8745 | 0.8602 | 0.8606 |
| 2 | 1-3 | 0.4445 | 0.4470 | 0.4715 | 0.4717 |
| 3 | 2-3 | 0.2837 | 0.2845 | 0.3229 | 0.3196 |
| 4 | 2-4 | 0.3267 | 0.2438 | 0.3766 | 0.2882 |
| 5 | 2-5 | 0.6413 | 0.7218 | 0.7366 | 0.8287 |
| 6 | 3-4 | 0.2564 | 0.5000 | 0.3192 | 0.5000 |
| 7 | 4-5 | 0.0760 | -0.2393 | 0.0862 | -0.1824 |

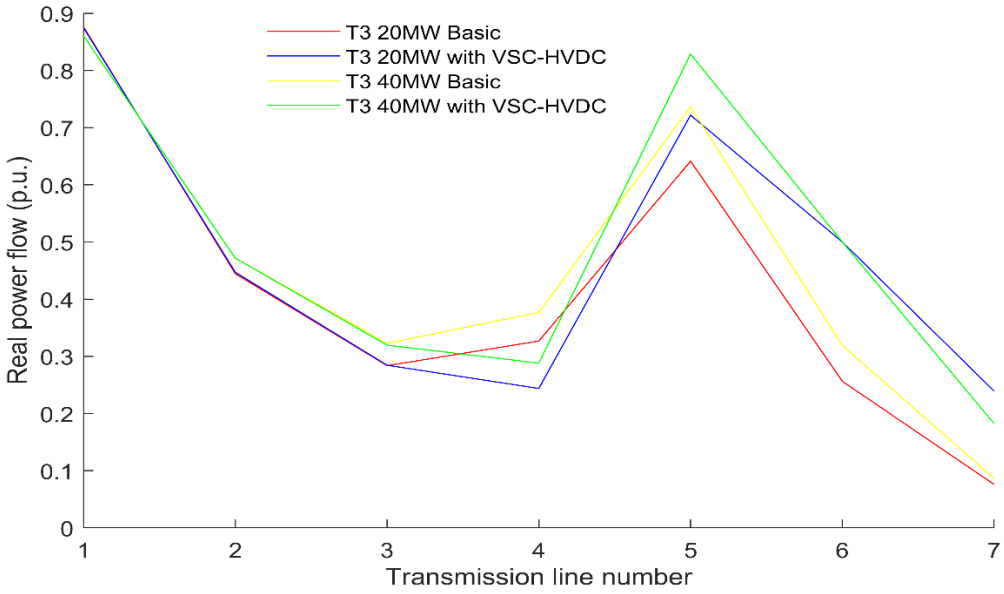


**Figure 8. 5: T3 simultaneous power transfer flow with and without VSC-HVDC transmission system**

lead to thermal limit violation. Fig. 8.5 gives details of power flow enhancement for better decipherment. Power flow diversion was made possible through line 2-5 to bus 5 with VSC-HVDC transmission system. In all the transfers, thermal limits of the transmission lines were not exceeded.

### 8.4.3 Network total real power flow

The total system power flow as enhanced with VSC-HVDC is presented in Table 8.6. The incorporation of VSC-HVDC transmission system into the network has enhanced power flow greatly. An additional power flow in the range of 35.31 MW to 46.00 MW were achieved during 20 MW transactions while 15.89 MW to 38.89 MW were recorded during 40 MW power transactions. These correspond to 12.28% to 15.66% and 5.08% to 11.96% for 20 MW and 40 MW transactions respectively. Therefore, ac network system containing VSC-HVDC transmission system can successfully cope with the upsurge in power transaction due to deregulation and restructuring. Similar scenarios played out for reactive power flow but could not be reported due to space constraints.

Table 8. 6: Per unit power flow enhancement of VSC-HVDC system for various transactions

| | 20 MW | | | | 40 MW | | | |
|---|---|---|---|---|---|---|---|---|
| **Power Transactions** | **Basic AC** | **with HVDC** | **Additional Power** | **% Increase** | **Basic AC** | **with HVDC** | **Additional Power** | **% Increase** |
| **T1 (2-4)** | 2.8751 | 3.2282 | 0.3531 | 12.28 | 3.1274 | 3.2863 | 0.1589 | 5.08 |
| **T2 (2-5)** | 2.9365 | 3.3965 | 0.4600 | 15.66 | 3.2398 | 3.6273 | 0.3875 | 11.96 |
| **T3 ( 2-(4&5))** | 2.9048 | 3.3109 | 0.4061 | 13.98 | 3.1732 | 3.4512 | 0.2780 | 8.76 |

### 8.4.4 Bus voltage profile

The effects of VSC-HVDC transmission system on bus voltage profile during network power flow and various power transfers for bilateral and multilateral transactions were investigated and recorded as follows.

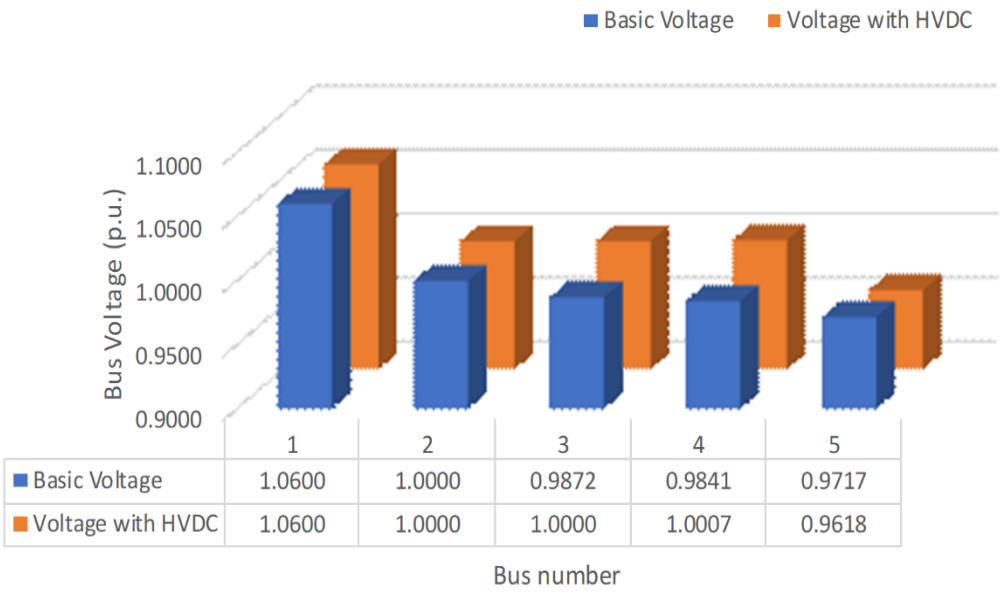


**Figure 8. 6: Bus voltage profile for basic and with VSC-HVDC transmission system**

#### 8.4.4.1 Bus voltage profile for power flow without power transactions

During normal power flow activities, the initial bus voltages which stood at 1.0000 p.u. dropped to 0.9871 p.u., 0.9841 p.u. and 0.9717 p.u. for buses 3, 4 and 5 respectively however, these values were raised to 1.0000, 1.0007 p.u. and 0.9618 p.u. when ac transmission line 3-4 was replaced with VSC-HVDC transmission system. The relationship between basic bus voltage profile and voltage profile with VSC-HVDC is depicted in Fig. 8.6, for better understanding. Bus voltage profile deviation was minimized leading to a better network performance.

#### 8.4.4.2 Bus voltage profile for 20 MW bilateral transactions T1 and T2

Fig. 8.7 shows the behaviors of system voltage profile for 20 MW transactions T1 and T2. During these trading, increase in power flow resulted into voltage sag at buses 3, 4 and 5. However, when VSC-HVDC transmission system was incorporated, voltage at bus 3 was raised back to 1.0000 p.u., while voltage deviations at buses 4 and 5 were well compensated for during T1. However, as can be inferred from the figure, during T2, bus 3 and 4 terminal voltage were restored to 1.0000 p.u., leaving voltage at bus 5 within its limits.

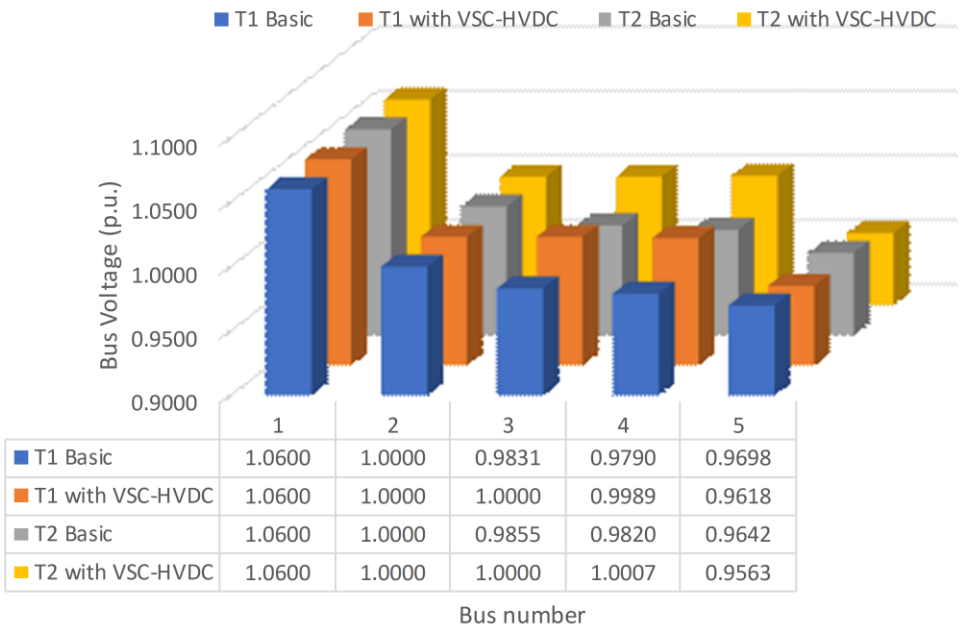


| | 1 | 2 | 3 | 4 | 5 |
|---|---|---|---|---|---|
| T1 Basic | 1.0600 | 1.0000 | 0.9831 | 0.9790 | 0.9698 |
| T1 with VSC-HVDC | 1.0600 | 1.0000 | 1.0000 | 0.9989 | 0.9618 |
| T2 Basic | 1.0600 | 1.0000 | 0.9855 | 0.9820 | 0.9642 |
| T2 with VSC-HVDC | 1.0600 | 1.0000 | 1.0000 | 1.0007 | 0.9563 |

**Figure 8. 7: Bus voltage profile for 20 MW T1 and T2, for basic and with VSC-HVDC transmission system**

#### 8.4.4.3 Bus voltage profile for 40 MW bilateral transactions T1 and T2

System network bus voltage profiles with 40 MW trading for T1 and T2 are depicted in Fig. 8.8. The magnitude and nature of these transactions impaired voltage profiles when the system was operated in an ac mode. The incorporation of VSC-HVDC transmission system improved the voltage at buses 3, 4 and 5. Values of the bus voltages for T1 and T2 differ with the nature of transactions. However, all the bus voltages operated within the limits.

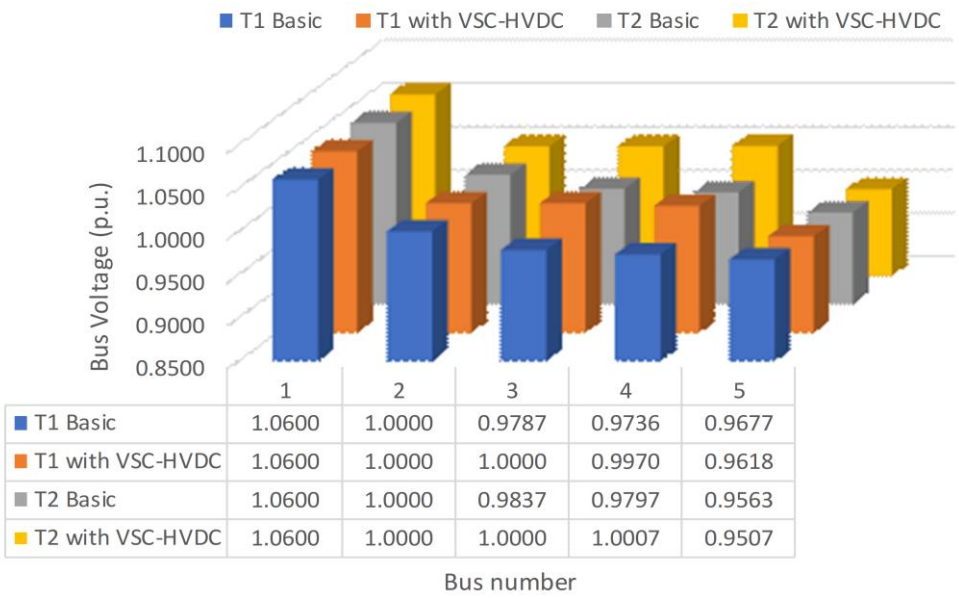


| | 1 | 2 | 3 | 4 | 5 |
|---|---|---|---|---|---|
| T1 Basic | 1.0600 | 1.0000 | 0.9787 | 0.9736 | 0.9677 |
| T1 with VSC-HVDC | 1.0600 | 1.0000 | 1.0000 | 0.9970 | 0.9618 |
| T2 Basic | 1.0600 | 1.0000 | 0.9837 | 0.9797 | 0.9563 |
| T2 with VSC-HVDC | 1.0600 | 1.0000 | 1.0000 | 1.0007 | 0.9507 |

**Figure 8. 8: Bus voltage profile for 40 MW T1 and T2, for basic and with VSC-HVDC transmission system**

#### 8.4.4.4 Bus voltage profile for 20 MW and 40 MW simultaneous transactions T3

Simultaneous transaction that existed concurrently among bus 2, 4 and 5 are also very common because of economy of power transactions especially in deregulated power network. The capability of power flow enhancement via VSC-HVDC transmission system with voltage profile improvement under concurrent transactions has been demonstrated in this work. Fig. 8.9 presents various bus voltage profiles during these transactions. The magnitude of transaction also affected voltage profile in such a way that the higher the system loading, the more the severity of bus voltage deviation. Notwithstanding, the voltage deviation was minimized

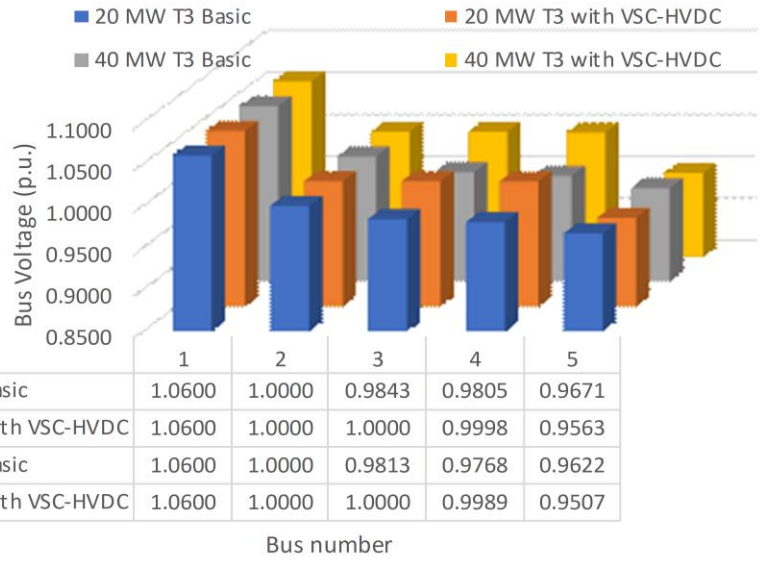


| | 1 | 2 | 3 | 4 | 5 |
|---|---|---|---|---|---|
| 20 MW T3 Basic | 1.0600 | 1.0000 | 0.9843 | 0.9805 | 0.9671 |
| 20 MW T3 with VSC-HVDC | 1.0600 | 1.0000 | 1.0000 | 0.9998 | 0.9563 |
| 40 MW T3 Basic | 1.0600 | 1.0000 | 0.9813 | 0.9768 | 0.9622 |
| 40 MW T3 with VSC-HVDC | 1.0600 | 1.0000 | 1.0000 | 0.9989 | 0.9507 |

**Figure 8. 9: Bus voltage profile during 20 MW and 40 MW T3, for basic and with VSC-HVDC transmission system**

with replacement of ac transmission line 3-4 using VSC-HVDC transmission system. Details of bus voltage deviation and the corresponding deviation minimization control as offered by VSC-HVDC system are contained in the figure.

### 8.4.5 Network real power loss

The real power loss control capability of VSC-HVDC transmission system on ac network was also investigated for basic ac network power flow and for various power transfers during different bilateral and simultaneous transactions.

#### 8.4.5.1 Real power loss for base case power flow without power transactions

VSC-HVDC transmission system demonstrated the capability to control real power loss on ac network system. Fig. 8.10 shows the loss pattern for basic ac network and a network containing VSC-HVDC system. Losses on transmission lines 1, 2, 4 and 5 were reduced by 0.01 MW, 0.11 MW, 0.19 MW and 0.04 MW respectively. Losses on lines 3 and 7 are almost of same magnitude, while the slight increase in loss on line 5 resulted from increase in power flow as a result of presence of VSC-HVDC transmission system in the network.

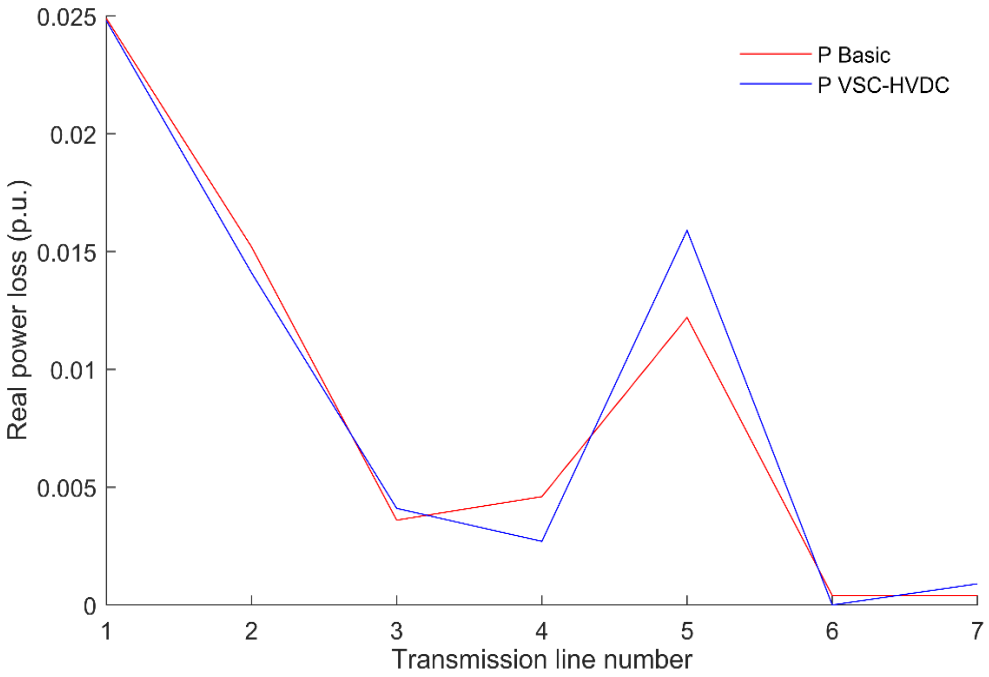


**Figure 8. 10: Real power loss for basic ac network and with VSC-HVDC transmission system**

#### 8.4.5.2 Real power loss for 20 MW bilateral transactions T1 and T2

The real power loss for T2 was minimized on all the transmission lines save line 5 when VSC-HVDC transmission system was incorporated into ac network as presented in Fig. 8.11. Reduction of 0.02 MW, 0.2 MW, 0.02 MW, 0.29 MW 0.05 MW and 0.04 MW were achieved for lines 1, 2, 3, 4, 6, and 7 respectively.

During T1, loss was equally minimized on lines 1, 2, 4, and 7, corresponding to 0.03 MW, 0.09 MW, 0.2 MW and 0.08 MW respectively. However, a slight increase in losses on line 5 during T1 and T2 corresponding to 0.12 MW and 0.66 MW was as a result of more power flow because more losses usually accompany more power flow [134]. Notwithstanding, other benefits recorded outweighed this slight increase in loss on line 5.

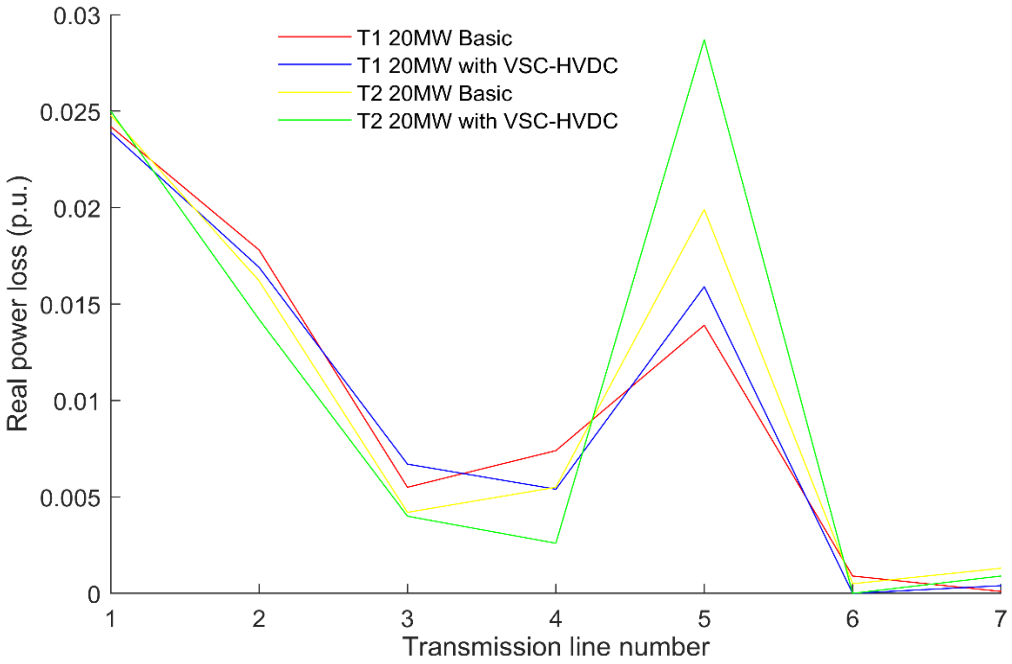


**Figure 8. 11: Real power loss during 20 MW T1 and T2, for basic ac network and with VSC-HVDC transmission system**

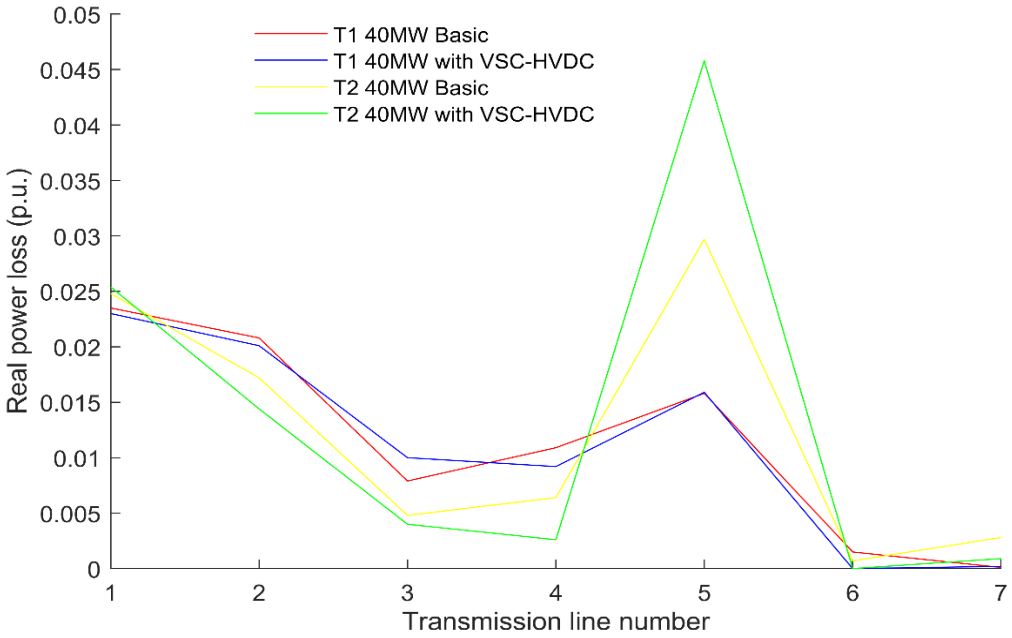


**Figure 8. 12: Real power loss during 40 MW T1 and T2, for basic ac network and with VSC-HVDC transmission system**

#### 8.4.5.3 Real power loss for 40 MW bilateral transactions T1 and T2

Real power loss during 40 MW transactions T1 and T2 as controlled by VSC-HVDC system is presented in Fig. 8.12. Reductions of 0.05 MW, 0.07 MW, 0.17 MW, 0.15 MW and 0.01 MW were recorded on lines corresponding to 1, 2, 4, 6 and 7 respectively for transaction T1. However, these were with diminutive loss increase of 0.021 MW, 0.01 MW on lines 3 and 5. Major power flow diversion through adjacent transmission line 2-5 resulted into major difference in power loss on this line number 5 during the transaction. Lines 2, 3, 4, 6 and 7 with loss reduction magnitude of 0.28 MW, 0.08 MW, 0.38 MW, 0.07 MW and 0.19 MW were major transmission lines where loss minimization were recorded during T2. Line 5 experienced slight increase in power loss due to reason earlier stated during this transaction.

#### 8.4.5.4 Real power loss for 20 MW and 40 MW simultaneous transactions T3

Under the Simultaneous transaction that co-existed among bus 2, 4 and 5, the real power loss for 20 MW and 40 MW power transfer are presented in Fig. 8.13. VSC-HVDC transmission system has been demonstrated to have capacity for loss control because of loss minimization achievement recorded during this type of transactions. During 20 MW power transfer, losses were minimized on lines 1, 2, 4, 6 and 7 but with a slight increase in loss magnitude on lines 3 and 5. The corresponding magnitude of the loss reductions are 0.0001, 0.0015, 0.0025, 0.0007 and 0.0001 p.u. respectively. During 40 MW power transfer, however, loses on all the lines were minimized except for transmission line 2-5 due to reason earlier explained. There are 0.0019, 0.0004, 0.0031, 0.0011 and 0.0003 p.u. loss reductions but with slight increase of 0.005 p.u. on line 5, during this 40 MW power transfer exercise. Details are as contained in Fig. 8.13 for better understanding.

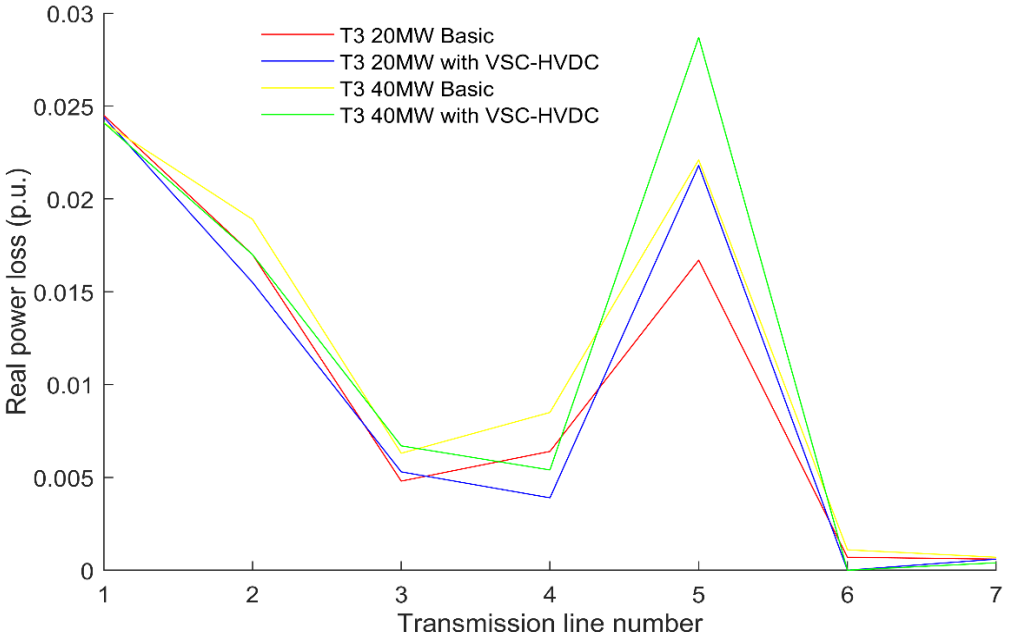


**Figure 8. 13: Real power loss during 20 MW and 40 MW T3, for basic ac network and with VSC-HVDC transmission system**

### 8.5 Summary of chapter eight

Power flow enhancement capability of VSC-HVDC transmission system incorporated into an ac transmission network has been presented in this study. VSC-HVDC described in steady state and static π-equivalent models to obtain appropriate power equations and for determination of power loss on HVDC line were also implemented in the research. Optimal location of VSC-HVDC transmission system has been achieved with derivatives of total network system loss alongside VSC-HVDC transmission system loss with respect to control parameters. The sensitivity resulted from magnitude of voltage and angle of injection of VSC-HVDC transmission system formed the basis for HVDC location. Various power transfers resulting from different types of bilateral and simultaneous transactions consequents of ongoing power system deregulation and restructuring were implemented and the corresponding power flow examined. The associated bus voltage profiles and real power loss were studied during these various power transfers. There were improvements in power flow up to 15.66% corresponding to 46 MW for various transactions, transmission line power loss minimization up to 0.38 MW and bus voltage profile deviation minimization with incorporation of a VSC-HVDC based transmission system in the ac network. Power flow were enhanced, bus voltage profile deviations were minimized, and real power loss magnitudes were also reduced. With the incorporation of VSC-HVDC transmission system in an ac network, an improvement in system performance has been recorded, therefore, HVDC based VSC transmission systems have the capacity to support and enhance system behavior especially during power transactions to achieve system reliability and security. Having demonstrated its competence in network performance enhancement, the next chapter is therefore dedicated to investigation of VSC-HVDV transmission system's ability to offer relief to network especially during n-1-line outage contingency.

# CHAPTER NINE

# CONTINGENCY MITIGATION WITH HIGH VOLTAGE DIRECT CURRENT TRANSMISSION SYSTEM

## 9.1 Introduction

This chapter presents the investigation of high voltage direct current (HVDC) based on voltage source converter (VSC) for power network contingency mitigation purposes. An optimized VSC-HVDC transmission system was applied for mitigation of bus voltage and line thermal limit violation as a result of n-1-line outage contingency occurrence during bilateral, simultaneous and multilateral transactions. Line contingency evaluation through real power performance index (RPPI) as earlier presented in chapter four was adopted for severe contingency identification purposes. Also as presented in chapter seven and as adopted in chapter eight, optimization of VSC-HVDC system was achieved through statically developed sensitivity-based analysis of VSC control parameters, while its performance for both steady state and contingency conditions were verified with IEEE 30 bus network presented in Appendix A-2 of this thesis.

## 9.2 Application of HVDC for contingency alleviation

There are accruing challenges for network operators whose determination hitherto, was to ensure economy of power operation with utmost consideration for maintenance of system security limits. This is because of renewed interest in power industry consequent of ongoing power network deregulation and restructuring. In order to obtain economic benefits in this regards, utility companies tend to operate network systems in the vicinity of their constraints which could result into congestion issue, affect network security, decrease system reliability and eventually lead to network contingency [208]. To alleviate these problems, system operators can manipulate network topology in favor of reliability and congestion reduction because the solutions to network complexity through generation and transmission expansions are both technically and economically bound [209].

In line with North American Electric Reliability Council (NERC) standard 51, system reliability and security are necessary for operation of power system [210]. This implies that power system planning, and operation should be such that an n-1 outage contingency of power components should not disrupt supply to the load. To salvage this situation, several methods which include optimal power flow (OPF), unit commitment (UC), security constrained OPF/UC, redispatch after continency, reconfiguration of network, contingency management and transmission switching have been in operation, however, some of them are not economically viable [211],[212],[213]. In the recent time, power electronics devices have made tremendous contributions to the urgency for network capacity enhancement, constrained with sustainability and reliability improvement, with due consideration for minimization of cost, through injection of supplementary controllability and flexibility of operation [149]. The advancement in voltage source converter based technology enables FACTS devices and HVDC systems to play these substantive roles in grid infrastructure sustainability and supports [150]. HVDC and other flexible alternating current transmission systems (FACTS) imbedded with VSC have established competence for noticeable diverse power network characteristics improvements. Among other benefits however, HVDC has

been established to be economical for power system transmission over long distance and its application apart from being significant, will determine network grid operation in the future [151]. As highlighted, HVDC surpasses HVAC in asynchronous interconnection of grids, broadened connection of underground cables, minimization of fault currents, mitigation of impacts on environment and network congestion control [152].

The technology of VSC-HVDC system is fast evolving, with entrenched countless potentials and its suitability in terms of transient stability, dynamic stability and oscillation damping have received increasingly great research attentions. However, wide range of ac network support benefits, and other ancillary services formed bulk of renewed research focus for deployment and application of VSC-HVDC systems. This chapter, therefore, investigates power network contingency control capability of an ac network embedded HVDC based VSC transmission system. The provision of ancillary support service which include system limits violation restoration at the instance of an n-1 line outage contingency was well investigated and analyzed. For emphasis, the need for increase in network transmission potentials to accommodate diverse nature of power transactions occasioned by power sector liberalization forms the motivation for the study. The following are the major achievement of this chapter among others;

(a) Investigation of power flow improvement and bus voltage profile deviation minimization of ac network embedded with VSC-HVDC transmission system.
(b) Investigation of VSC-HVDC transmission system ancillary support services during contingency. The following are the major steps taken to achieve the listed objectives;
    i. Application of mathematical equations of total system loss involving HVDC line loss for derivation of sensitivity-based solution for optimal placement.
    ii. Presentation and ranking of resultant sensitivity for voltage magnitude control and control angle of VSC-HVDC transmission system for optimization.
    iii. Performance of load flow of an ac network with alteration in Jacobian elements.
    iv. Ranking and selection of the most severe n-1 line outage contingency.
    v. Implementation of load flow with n-1 line outage contingency.

### 9.3 Results and discussions

VSC-HVDC transmission system incorporated into an ac network based on sensitivity optimization technique is presented as a solution to contingency management in the subsequent paragraphs. System performance under outage of the most severe ranked contingency line based on RPPI has been evaluated and properly reported. The effectiveness of VSC-HVDC transmission system for contingency alleviation has also been demonstrated on IEEE 30 bus network systems in MATLAB software environment. The special consideration for placement of VSC-HVDC transmission system has well been spelt out in chapter eight. This also holds in this chapter and is being considered for implementation.

### 9.3.1 Optimal placement of VSC-HVDC transmission system

Like previous chapter, total loss of the system containing VSC-HVDC transmission system was differentiated with respect to voltage magnitude and angle of control variables and the sensitivities factors obtained are denoted *x* and *y* respectively. However, for effective placement, the sensitivity regarding voltage magnitude must be predominantly negative, while the resulting absolute value of sensitivity for voltage angle control should be the largest. This implies that highest negative value of sensitivity factor *x* determines the optimal location of VSC-HVDC transmission system. Regarding voltage angle derivative, the transmission line where highest absolute value of sensitivity factor *y* occurs determines the optimal location. Fig. 9.1 presents the sensitivity factors *x* and *y* as obtained in this study. The highest negative value of *x* occurred on transmission line 21-22 meaning this is the optimal location for placement of VSC-HVDC transmission system. The maximum absolute value for sensitivity factor *y* also occurred on same line 21-22. Various values for *x* and *y* are well depicted in the figure, but to be precise, the optimal value of *x* and *y* which occurred on transmission line 21-22 are -33.6100 and 33.5940 respectively.

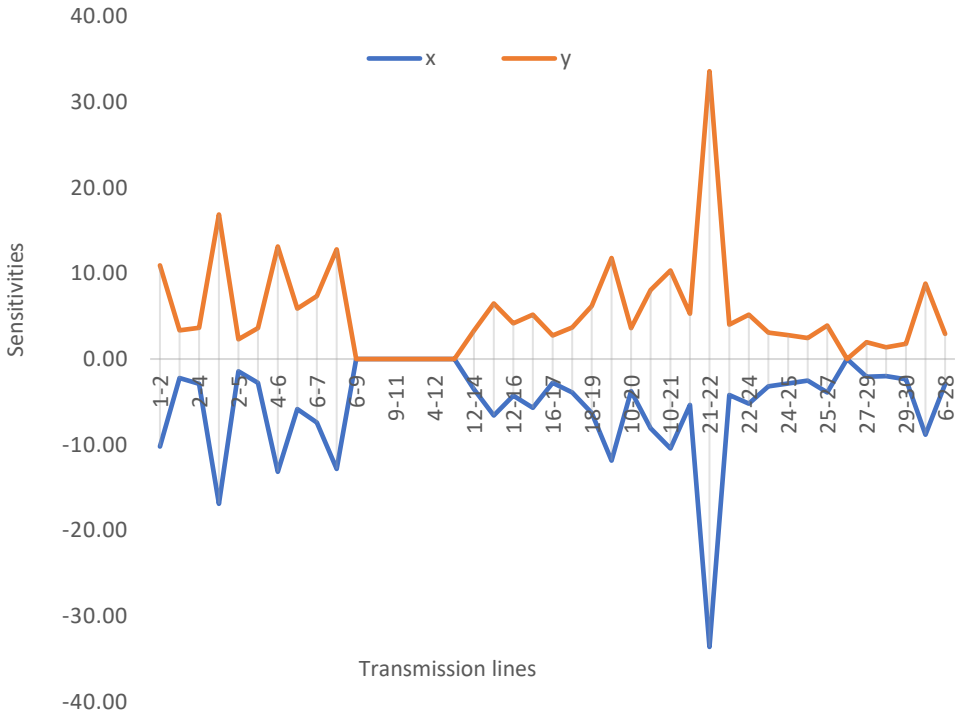


**Figure 9. 1: Sensitivity factors x and y for optimal placement**

### 9.3.2 Test network system

IEEE 30 bus network used for analysis in this study has been earlier described. The modified configuration is as shown in Fig. 9.2. However, network information, operating settings and line thermal limits as obtained from IEEE bus networks Appendix 2 data sheet, are detailed in Appendix A-2. In brief, bus voltage lower limits for all the buses including slack are taken as 0.95 p.u. and that of upper limit to be 1.05 p.u., with the exception of generator buses whose upper voltage limit is 1.1 p.u. VSC-HVDC transmission system has been used to

outrightly replace the existing ac line 21-22 in the network as depicted in the figure. This location is as optimized by the implemented sensitivity-based analysis method.

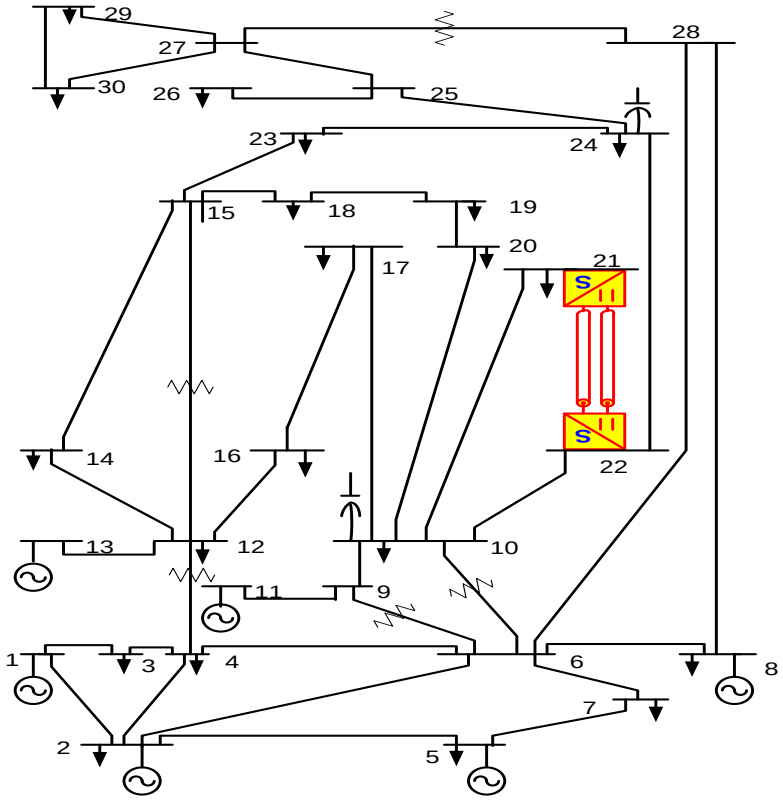


**Figure 9. 2: Modified IEEE 30 bus test network**

### 9.3.3 Severe contingency ranking and selection

In order to implement contingency ranking and eventual selection, as a quick recap, load flow was performed after outage of each transmission line on the test network prior to placement of VSC-HVDC transmission system. Ranking was done based on sensitivity of outage of each line to the disturbance. Order of ranking was determined by performance index sensitivity to the various line outages, in descending order from utmost severe to the least as earlier presented in chapter four. This presents line 2-5 as the most ranked severe contingency as appears on Table 9.1, containing the first five ranked severe outage lines. Chapter four contains the details of ranking processes.

Table 9. 1: Ranking of Contingency

| Ranking Order | Line No | Transmission Line | RPPI |
|---|---|---|---|
| 1 | 5 | 2-5 | 321.0613 |
| 2 | 9 | 6-7 | 262.0340 |
| 3 | 14 | 9-10 | 258.2439 |
| 4 | 2 | 1-3 | 247.1413 |
| 5 | 4 | 3-4 | 243.9255 |

### 9.3.4 Impacts of VSC-HVDC transmission system on network

The need to optimize network utilization amidst technical and economical restrictions confronted with physical network expansion calls for intensive research into applications of FACTS and HVDC transmission systems. Effects of VSC-HVDC transmission system on ac network especially during line outage contingency has been investigated in the subsequent paragraphs. The investigations were conducted within the attributes of a deregulated and restructured power network. Power transactions involving bilateral, simultaneous and multilateral trading were implemented and investigated amidst contingency in this study. Bilateral transaction of 40 MW power between generator bus 2 and load bus 20 is named T1, simultaneous transaction of 40 MW power trading between generator bus 5 and load buses 16 and 18 is termed T2, while multilateral transaction of 40 MW power among generator buses 5 & 8 and load buses 15 & 24 are tagged T3 for the purpose of distinction in this chapter.

### 9.3.5 Bus voltage profile with and without contingency

The impacts of VSC-HVDC transmission line on network bus voltage values during implemented bilateral, simultaneous and multilateral transactions are investigated and presented as follows.

#### 9.3.5.1 Bus voltage profile without transactions

Outage of transmission line 2-5 contingency was created here, and effects observed on the test network bus voltage profile. Fig. 9.3 presents bus voltage profile for normal power flow and flow during outage of line 2-5. During normal power flow, voltage profile deviation was pronounced in the upper region of the network where generators are not located. The deviation is glaring from bus 15 up to 30. However, replacement of ac transmission line 21-22 with VSC-HVDC transmission line minimizes this deviation as shown in the figure.

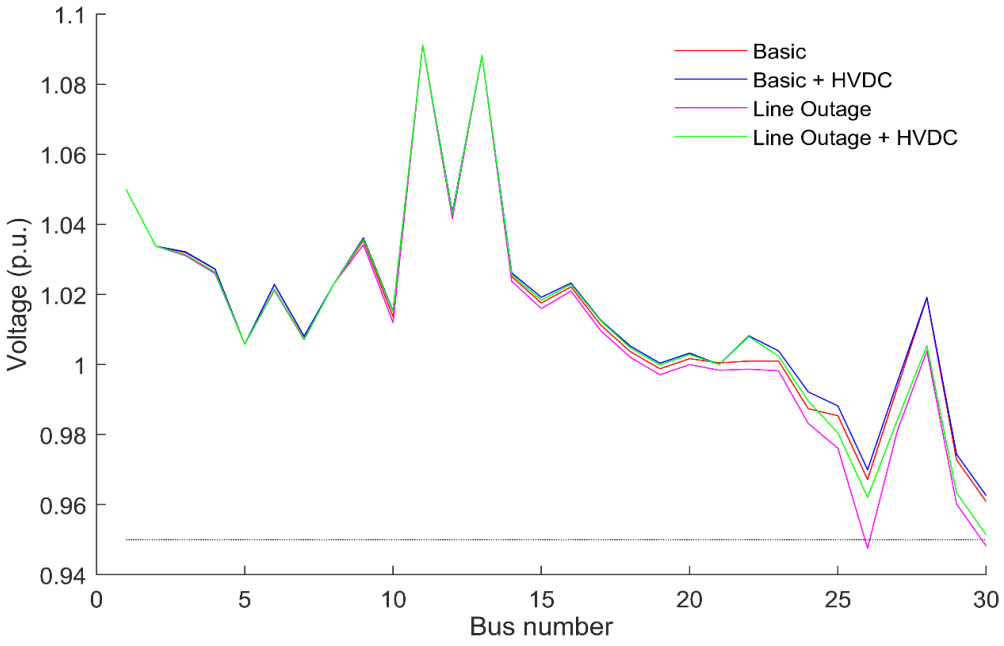


**Figure 9. 3: Bus voltage profile with and without contingency**

With the occurrence of contingency, bus limit violation occurred at buses 26 and 30 as indicated in magenta color in Fig. 9.3. Presence of HVDC in the network not only minimized bus voltage deviation but also restored violated bus limits. Bus 26 and 30 had their terminal voltage restored to 0.9621 p.u. and 0.9514 p.u. from 0.9476 p.u. and 0.9482 p.u. respectively as indicated by green color in the figure.

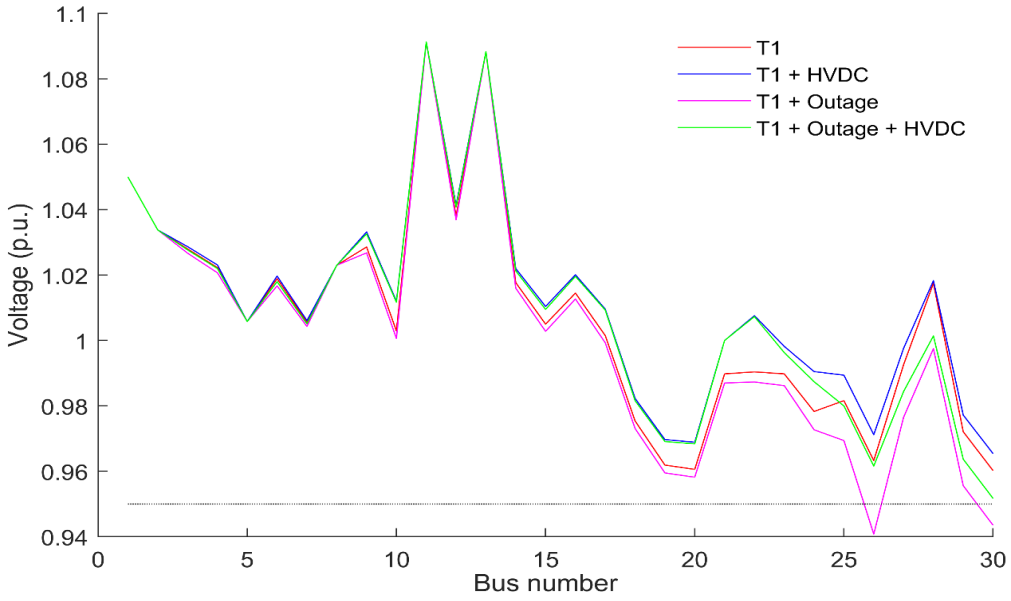


**Figure 9. 4: Bus voltage profile for bilateral transaction T1**

#### 9.3.5.2 Bus voltage profile for bilateral transaction T1

Bilateral transaction involves power trading between a seller and a buyer in a deregulated power sector. The bilateral trading in this situation involves transfer of 40 MW of power from generator bus 2 to load bus 20 and termed T1. Bus voltage profile associated with this transaction is depicted in Fig. 9.4. In this transaction, bus voltage profile deviation was more pronounced compared to voltage profile without power transaction for both normal network flow and contingency condition. In each case, voltage profile deviated towards the lower limits. When line 21-22 was replaced with HVDC, the deviation was minimized as evident from the figure. The blue color line indicates deviation minimization when compared with red colored curve that represents voltage profile without compensation. Bus voltage limit was violated at bus 26 and 30 when contingency occurred during this transaction. The depth of voltage dip at these buses transcends the depth when there were no transactions. Voltage at bus 26 was sagged to 0.9408, and that of bus 30 to 0.9435 p.u. but restored to 0.9616 and 0.9517 p.u. respectively with incorporation of HVDC into the network.

#### 9.3.5.3 Bus voltage profile for simultaneous transaction T2

Simultaneous transaction involves dispatching of power from the same generator to two or more load centers concurrently. This was also implemented with generator bus 2 transferring 40 MW of power to load buses 16 and 18 at the same time. The response of network bus voltage to this transaction is shown in Fig. 9.5 below. Voltage deviation profile was a bit relax unlike T1 because wheeling of power to these load buses flow through

different paths as can be inferred from Fig. 9.2. In the case of T1, the dispatch was from single seller to another single buyer but for T2 it was from single seller to two different buyers at the same time. This created room for flexibility in power flow.

Just like previous transactions, the inclusion of HVDC in ac network provided support for bus voltage as can be seen in the figure. Bus voltage at bus 21 was held around 1.0 p.u. while that of bus 22 was held constant at 1.0 p.u. This is depicted by blue and green line of the curves. As usual, voltage limit violation resulted from outage of line 2-5, but the violation at buses 26 and 30 was restored in this case as well. Voltages were reduced to 0.9434 p.u. at bus 26 and to 0.9456 p.u. at bus 30, however, with presence of HVDC in the tested ac network the violations were restored to 0.9615 p.u. and 0.9516 p.u. respectively.

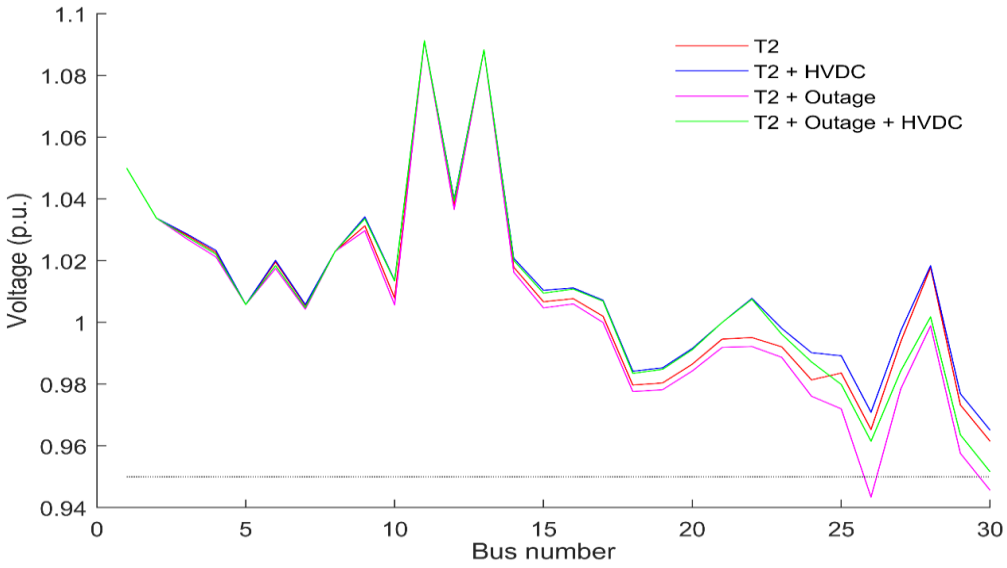


**Figure 9. 5: Bus voltage profile for simultaneous transaction T2**

#### 9.3.5.4 Bus voltage profile for multilateral transaction T3

Multilateral transaction involves multiple sellers and multiple buyers for concurrent power wheeling in a restructured power system. This type of transaction was also implemented, and the voltage profile obtained for 40 MW trading is as shown in Fig. 9.6. Multilateral transaction is more demanding on terminal voltage because of concurrent wheeling of power to and from multiple buses. The response of bus voltage profile to this transaction is as shown in the figure. Between bus one and thirteen where generators are located, the profile deviation was controlled, but reactive power control capability of these generators has been weakened in the upper region of the test network thereby giving room for significant deviation in voltage profile in the region, as experienced during T3 without contingency.

When contingency occurred, the reactive power control responsible for bus voltage regulation was loss totally thereby leaving bus 26 and 30 vulnerable. These buses operated below their lower limit bound at 0.9404 p.u. and 0.9438 p.u. respectively. However, with embedded HVDC system in the test network, these values were improved to 0.9571 p.u. and 0.9510 p.u. for buses 26 and 30 respectively.

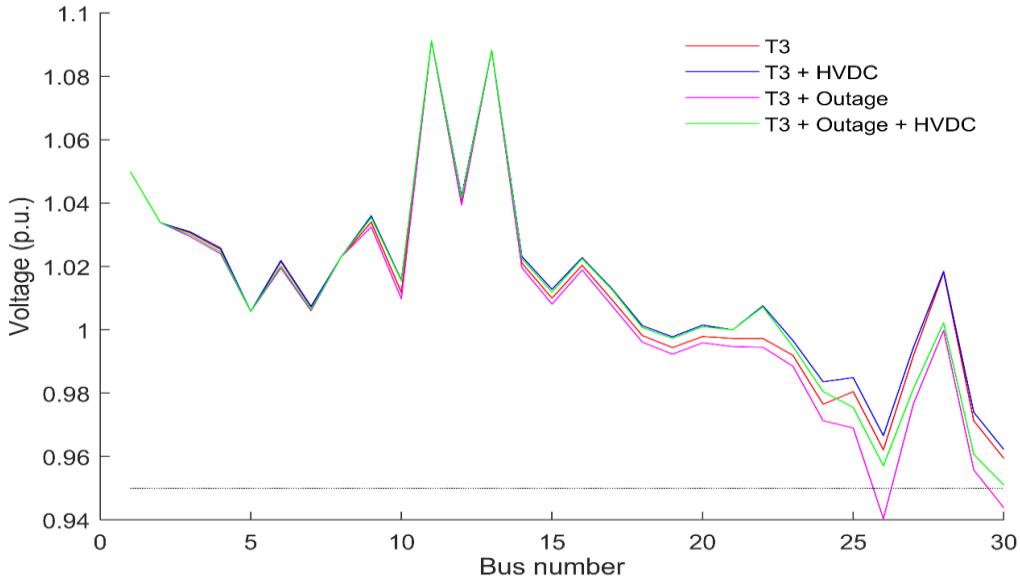


**Figure 9. 6: Bus Voltage profile for multilateral transaction T3**

### 9.3.6 Network power flow with and without contingency

The impacts of VSC-HVDC system on network power flow during various transactions as described are reported in this section. Power flow control capability of VSC-HVDC system especially during contingency is also reported in this section.

#### 9.3.6.1 Power flow without transaction and contingency

Fig. 9.7 presents transmission line flows without power transaction and contingency. HVDC transmission system alters the flow pattern when incorporated to replace transmission line 21-22 outrightly. The improvement in the flows on the transmission lines in the vicinity of lines 21-22 are of great interest.

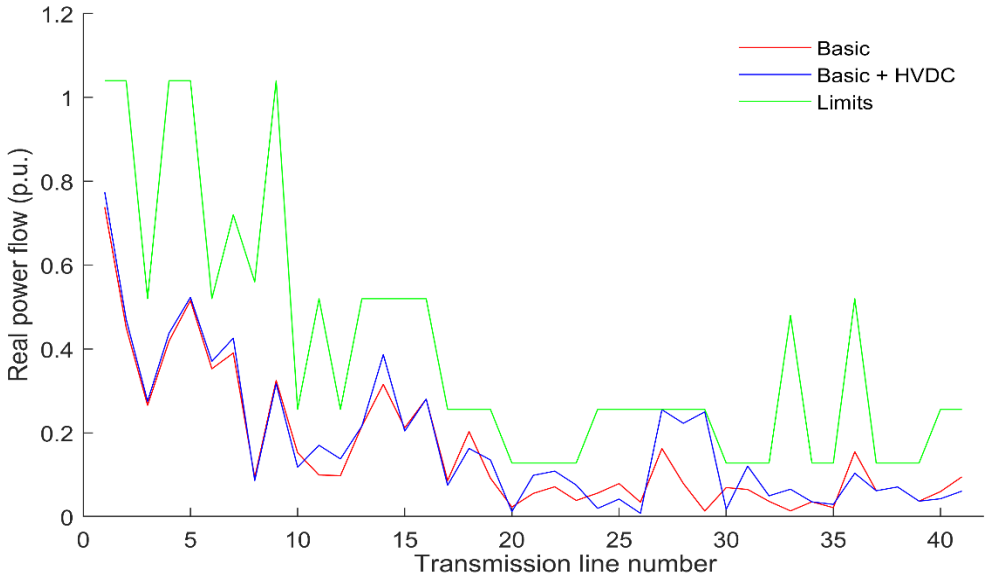


**Figure 9. 7: Network power flow without transaction and contingency**

More flows occurred on lines 10-21 and 10-22 but without thermal limit violation. Besides these lines, the influence of flow enhancement capability of HVDC system were also felt by other transmission lines.

#### 9.3.6.2 Power flow without transaction but with contingency

When contingency occurred as presented in Fig. 9.8, thermal limit violation occurred on transmission lines 4-6, 5-7 and 25-27 as indicated by line numbers, 6, 8, and 35 respectively. The overloading of these lines resulted into addition flow on them due to outage of line 2-5. With the presence of HVDC transmission system in the network, power flows were diverted to adjoining interconnected transmission lines, thereby forcing the lines operation within the limits. These initial flows which were 0.6781 p.u., 0.8639 p.u. and 0.1515 p.u. on lines 6, 8 and 35 reduced to 0.5137 p.u., 0.5174 p.u. and 0.0355 p.u. respectively. This is well depicted in the figure.

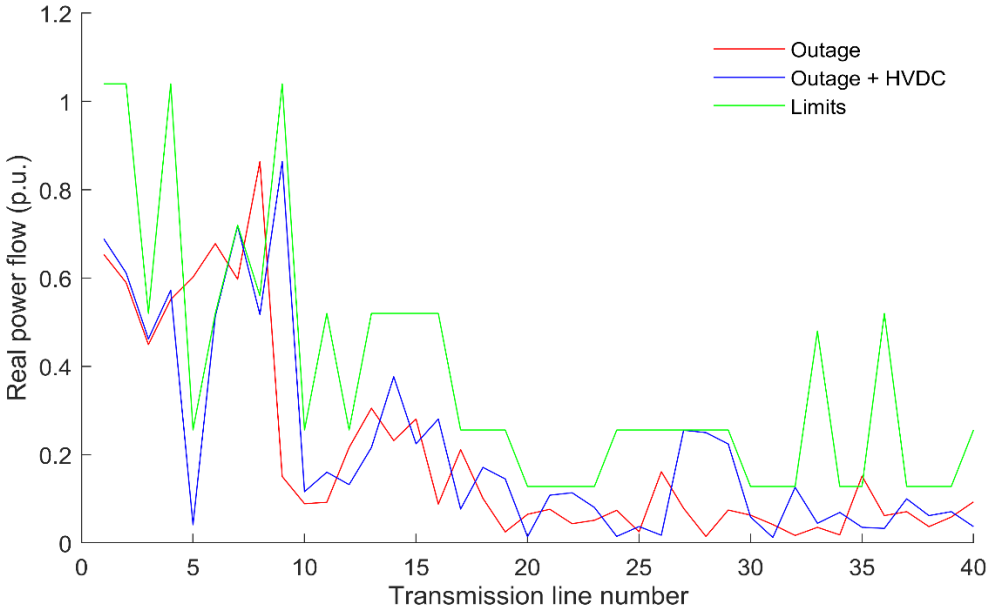


**Figure 9. 8: Network power flow without transaction but with contingency**

#### 9.3.6.3 Power flow during bilateral transaction T1 without contingency

Power trading due to liberalization constitutes additional burden to network operations which hitherto have been in the region of their limits. When there was no trading as presented in Fig. 9.7, none of transmission line limits were violated however, with 40 MW power transfer from generator 2 to load bus 20, thermal violation of lines 9-10, 18-19 and 10-20 occurred as presented in Fig. 9.9 in addition to increase in power flow on other transmission lines. These line overloads were properly controlled by HVDC transmission system as clearly presented in the figure. These loads were reduced from 0.3020 p.u., 0.1719 p.u. and 0.3596 p.u. to 0.2507 p.u., 0.1207 p.u. and 0.2324 p.u. agreeable to line limits 0.2560 p.u., 0.1280 p.u. and 0.2500 p.u. respectively for these lines.

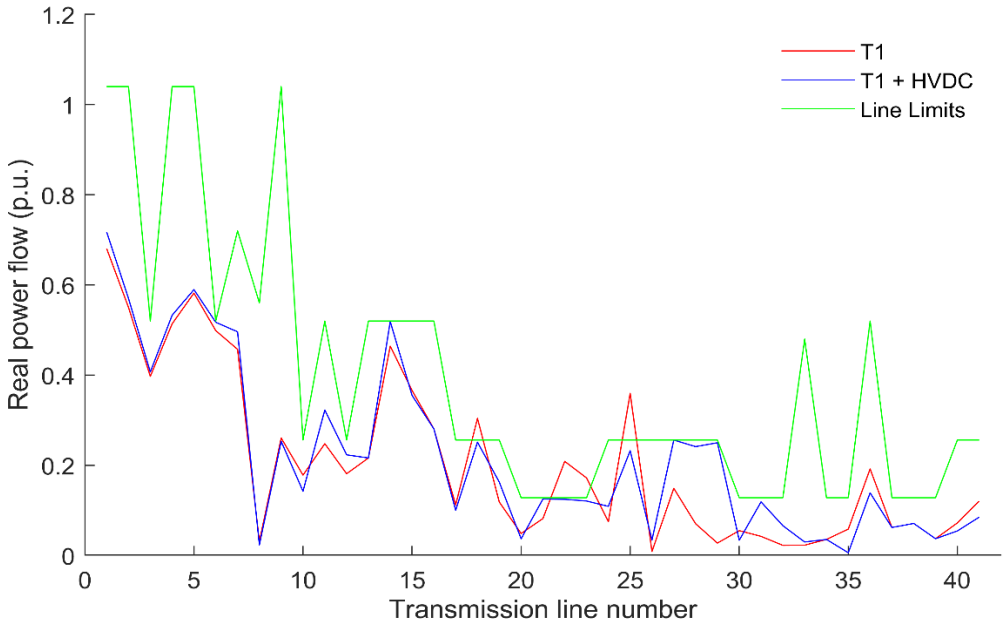


**Figure 9. 9: Network power flow for bilateral transaction T1 without contingency**

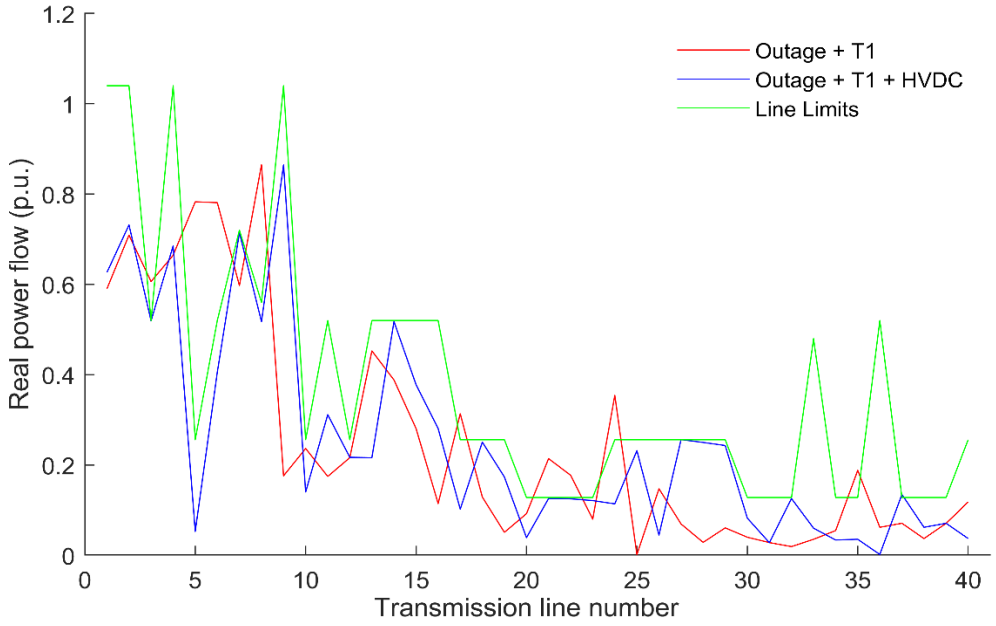


**Figure 9. 10: Network power flow for bilateral transaction T1 with contingency**

#### 9.3.6.4 Power flow during bilateral transaction T1 without contingency

In Fig, 9.10, the magnitude and number of occurrences of thermal overload increased due to outage of line 2-5. Line numbers 5, 6, 8, 17, 21, 22, 24, and 35 were affected as presented in the figure. Notwithstanding the overloads created by this contingency, HVDC system adequately controlled and restored the violations when it was incorporated into the ac network. In this condition, 0.7829 p.u., 0.7810 p.u., 0.8648 p.u., 0.3135 p.u., 0.2142

p.u., 0.1772 p.u., 0.3542 p.u. and 0.1882 p.u. controlled to 0.0527 p.u., 0.4055 p.u., 0.7143 p.u., 0.1023 p.u., 0.0391 p.u., 0.1258 p.u., 0.1212 p.u. and 0.0339 p.u. for lines 2-4, 6-28, 2-6, 5-7, 12-14, 15-18, 19-20, and 25-27 respectively.

#### 9.3.6.5 Power flow during simultaneous transaction T2 without contingency

Impacts of simultaneous transfer of power was as not as severe as that of bilateral trading on the network system. Thermal overloading of lines 18 and 22 resulted from this transaction without contingency as presented in Fig. 9.11. The flows which exceeded the rated values of 0.2560 p.u. and 0.1280 p.u. with 0.0109 p.u. and 0.0535 p.u. were controlled to 0.2255 p.u. and 0.1218 p.u. respectively, when HVDC transmission system was used to replace ac line 21-22 in the network.

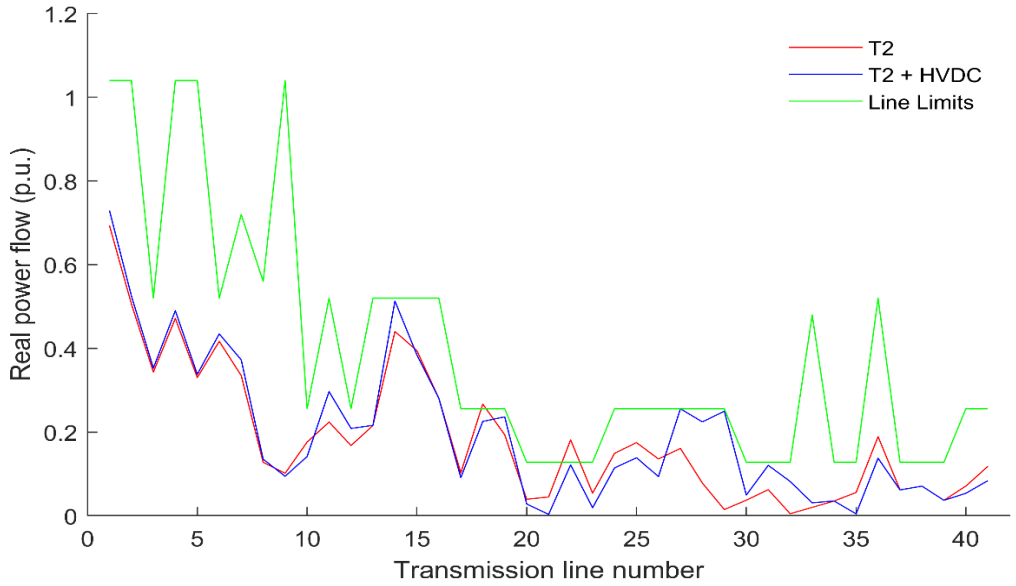


**Figure 9. 11: Network power flow for Simultaneous transaction T2 without contingency**

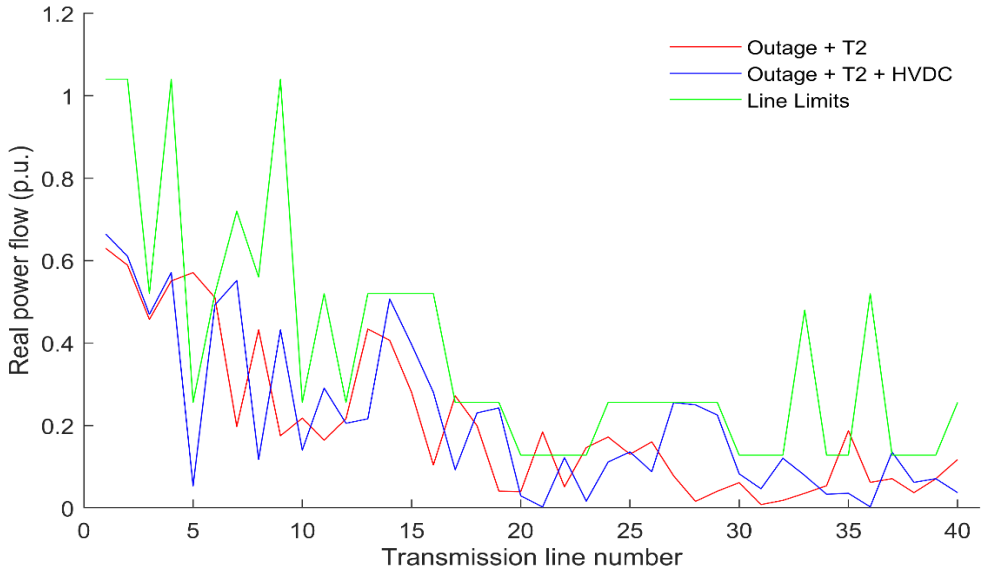


**Figure 9. 12: Network power flow for Simultaneous transaction T2 with contingency**

#### 9.3.6.6 Power flow during simultaneous transaction T2 with contingency

The occurrence of line outage contingency aggravated thermal limit violations. Transmission lines 6-28, 16-17, 18-19 and 25-27 had their thermal limit violated because shed off power that would have otherwise flown through line 2-5 flew through them. From Fig. 9.12, the flows which were 0.5709 p.u., 0.1845 p.u., 0.1465 p.u. and 0.1873 p.u. were properly controlled to 0.0531 p.u., 0.0023 p.u., 0.0164 p.u. and 0.0355 p.u. respectively when HVDC system was installed on the network.

#### 9.3.6.7 Power flow during multilateral transaction T3 without contingency

Apart from the previous trading, multilateral power transaction is another type of transaction which occurs in a deregulated network. The network responses to the implementation of 40 MW power transfer from seller generators buses 5 and 8 to buyer load buses 15 and 24 are as depicted in Fig 9.13. Transmission line number 18 which was overloaded during this trading was relieved with presence of HVDC system. No other line thermal violation was recorded meaning that the magnitude and the nature of this trading impacted less on the network as shown in Fig. 9.13.

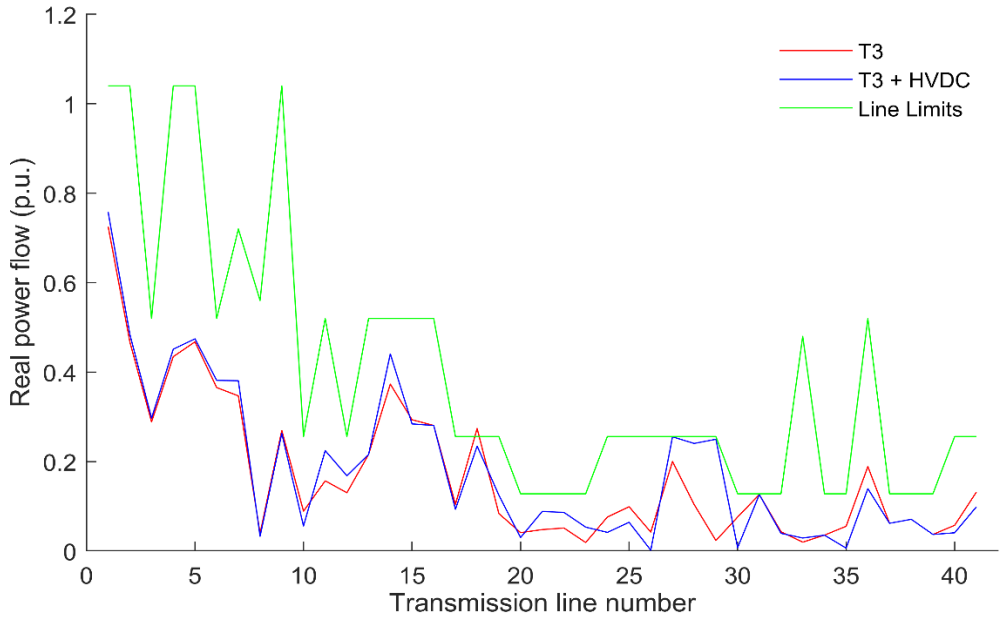


**Figure 9. 13: Network power flow for Multilateral transaction T3 without contingency**

#### 9.3.6.8 Power flow during multilateral transaction T3 with contingency

During contingency as presented in Fig. 9.14 however, transmission lines 5-7, 12-14, and 25-27 suffered thermal overload. With thermal ratings of 0.5600 p.u., 0.2500 p.u., and 0.1280 p.u., power flow on these lines were 0.7533 p.u., 0.2815 p.u. and 0.1860 p.u. respectively. These flows were controlled to fall within the limits, thereby suppressing these values to 0.4974 p.u., 0.0951 p.u., and 0.0355 p.u. when line 21-22 was replaced with HVDC transmission system. The incorporation of VSC-HVDC transmission system into ac network has enhanced network performance including contingency mitigation as can be inferred from the various results of implemented power flow analyses.

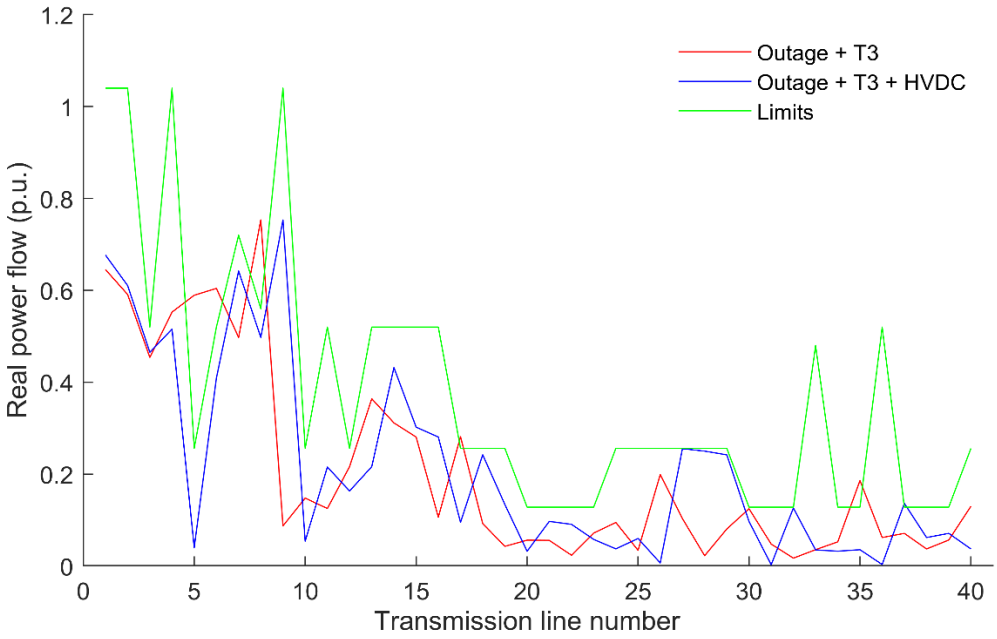


**Figure 9. 14: Network power flow for Multilateral transaction T3 with contingency**

### 9.4 Summary of chapter nine

Contingency control capability of VSC-HVDC system integrated into an ac network has been investigated in this chapter. Equivalent π model representation of transmission line lump parameters was deployed with a view to obtaining loss on the line containing VSC-HVDC system. This was mathematically embedded with steady state model equations of VSC-HVDC system for determination of its optimal location for placement in an ac network. The objective of using sensitivity analysis based on controlled parameters of VSC was discerned through consideration for the impacts of shunt devices on network loss characteristics. Thereafter, an n-1 transmission line outage contingency was created based on the most severe ranked outage line. Real power performance index ranking of the most severe outage line was adopted because of its effectiveness in identification of the critical line for contingency implementation as earlier presented in chapter four. Various power transactions which characterised deregulated and restructured power network were implemented on the standard IEEE 30 bus system used in the analyses. The incorporation of VSC-HVDC system in-between ac buses in a network minimized bus voltage profile deviation for steady state and restored violated bus voltage limits during contingencies. Power flow were enhanced during steady state and thermal limit violations occasioned by contingencies were adequately controlled. During bilateral, simultaneous and multilateral transactions however, the presence of HVDC in the ac network not only damped the impactful effects of power transfers on network dynamics but also control both voltage and thermal limit violations as a result of associated contingencies. Therefore, VSC-HVDC system incorporated into ac network has the capacity to influence system dynamics and it stands a solution to problems of contingency especially in a deregulated and restructured power network.

# CHAPTER TEN

# SUMMARY, CONCLUSION, RECOMMENDATIONS AND FUTURE RESEARCH

## 10.1 Summary and Conclusion

This thesis addresses the issues of power system performance enhancement of a deregulated and restructured network, using standard IEEE 5 and 30 bus reliability test systems. Initially, RACPF method was successfully implemented in determining the ATC of a deregulated and restructured system. Subsequently, ATC was obtained using ACPTDF method. The accuracy of RACPF method was established when compared with the results of previous work. Numerically to mention but few, 11.574 MW was obtained above the recorded ATC value for transmission line 1-2 while 29.014 MW was obtained below the recorded value for line 6-8. Various network operating conditions ranging from normal, contingency, bilateral, simultaneous and multilateral transactions were investigated with this method. ATC values have been established to decrease with increase in power transactions. It has also been established that least ATC occurs with contingency occurrence of multilateral transaction. With these investigations, the importance of ATC to market participants in a deregulated power system has been substantiated.

Performance index was also used as a tool for contingency ranking and evaluation of IEEE 30 bus test system. This was done with a view to presenting the most suitable method in deploying PI for contingency problems. The analyses of the ranked contingencies indicate the efficacy of PI in presenting the severity of line outage conditions for power network systems. The aftermath of post line outages for the most severe ranked lines based on real power and voltage PI also presented unique but important ranking order. The investigation conducted has demonstrated the behavioral attributes exhibited by these different approaches of PI. It has therefore been established that the disturbance which resulted into lines overload did not necessarily cause bus voltage limits violations. Subsequently, voltage and real power indices should be treated differently in order to obtain a separate but meaningful contingencies rankings using PI, because the duo have been proven to be distinctly dissimilar.

In order to enhance network performance, an up-to-date and comprehensive literature review of FACTS controllers starting from description, generations, classifications, categories and connection types, were carried out in this research work. It was discovered that FACTS devices optimal location and parameter settings are sine-qua-non to their performance therefore, placement techniques that are categorized into four major groups have also been exhaustively and properly discussed. Several cutting-edge applications of these controllers obtained from published articles were presented and discussed. Essentially, this review has shown that future of successful power network operations depends on applications of optimized FACTS controllers.

Based on this review, ATC values were improved with incorporation of TCSC and SVC into IEEE 30 bus network system. These FACTS enhanced ATC for engaged bilateral, simultaneous and multilateral transactions. During enhancements, TCSC maintained bus voltage magnitude for bilateral and simultaneous

transactions but with slight voltage droop during multilateral trading. In contrast, SVC slightly improved bus voltage profile for all the transactions. The introduction of SVC contributed to total system real power loss minimization for all the transactions while that of TCSC had no significant minimization for bilateral and simultaneous dealings but rather increased total real power loss for multilateral transaction. Therefore, for transfer capability enhancement with voltage improvement and real power loss minimization in focus, SVC is more relevant.

Consequently, application of different placement methods was implemented using TCSC for ATC enhancement of IEEE 30 bus system. TCSC placement based on base case real power loss greatly enhanced ATC of multilateral transaction and controlled both bus voltage profile and real power losses. Placements using real power performance index and least bus voltage approaches enhanced ATC of bilateral transaction, controlled bus voltage and minimized losses. FACTS location considering PTDF increased losses and led to bus voltage deviations in all transactions. It greatly attenuated ATC for bilateral and multilateral trading without significant ATC enhancement for simultaneous transaction. It has been concluded here that in optimal placement of FACTS for ATC enhancement, bus voltage profile, real power loss and nature of transactions should also be considered.

Based on the forgoing, an optimization technique known as BSO algorithm was proposed for optimum setting of FACTS devices for multi-objective problem involving ATC enhancement, bus voltage profile deviation minimization and real power loss regulation. ATC values of the tested network system were obtained for different transactions with both line intact and n-1-line outage contingency cases. Enhanced ATCs for this network were achieved with TCSC device which was set with the presented BSO algorithm. The achieved bus voltage profile deviation minimization and real power loss control during ATC enhancement validate the innate fitness of BSO for solving multi-objective problems regarding FACTS. Likewise, BSO performance in comparison with PSO during the achievement of set objectives suggested an advantage of former over the latter. It has therefore been verified that BSO algorithm is effective in solving multi-objective FACTS allocation and optimization problems.

Subsequently, a universal method for FACTS optimal placement was developed based on total real power loss minimization approach with the objectives of ATC enhancement, voltage profile improvement and active power loss minimization. TCSC which was modeled analytically as SSSC was implemented for this method. Based on this model, the total real power loss was partially differentiated with respect to voltage magnitude and angle of injected voltage, and the sensitivity of which were then used for identification of optimal location for TCSC device placement. ATCs which were hitherto determined by ACPTDF approach were enhanced by optimal placement of TCSC in the position identified by this developed method. Comparative analysis of optimal location based on this method and other existing approach revealed its advantage. It was also revealed that placement based on this method increases the effectiveness of FACTS devices on system performance. The

presented results and analyses indicate enhancement of ATCs, minimization of bus voltage profile deviation and reduction of real power loss.

Power flow enhancement capability of VSC-HVDC transmission system incorporated into an ac transmission network was also investigated and presented. VSC-HVDC described in steady state and static π-equivalent models to obtain appropriate power equations and for determination of power loss on HVDC line were also implemented in the research. Optimal location of VSC-HVDC transmission system had been achieved with derivatives of total network system loss alongside VSC-HVDC transmission system loss with respect to control parameters. The sensitivity resulted from magnitude of voltage and angle of injection of VSC-HVDC transmission system formed the basis for HVDC location. Various power transfers resulting from different types of bilateral and multilateral transactions consequents of ongoing power system deregulation and restructuring were implemented and the corresponding power flow examined. The associated bus voltage profiles and real power loss were studied during these various power transfers. Power flow were enhanced, bus voltage profile deviations were minimized, and real power loss magnitudes were also reduced. With the incorporation of VSC-HVDC transmission system in an ac network, an improvement in system performance was recorded, therefore, HVDC based VSC transmission systems have the capacity to support and enhance system behavior especially during power transactions to achieve system reliability and security.

In the same manner, contingency control capability of VSC-HVDC system integrated into an ac network was investigated in this study. In this study also, sensitivity-based approach was applied for placement purposes. The objective of using sensitivity analysis based on controlled parameters of VSC was discerned through consideration for the impacts of shunt devices on network loss characteristics. However, an n-1 transmission line outage contingency was created based on the most severe ranked outage line. Real power performance index ranking of the most severe outage line was adopted because of its effectiveness in identification of the critical line for contingency implementation. Various power transactions which characterised deregulated and restructured power network were also implemented on the tested system. The incorporation of VSC-HVDC system in-between ac buses in a network minimized bus voltage profile deviation for steady state and restored violated bus voltage limits during contingencies. Power flow were enhanced during steady state and thermal limits violation occasioned by contingencies were adequately controlled. During bilateral, simultaneous and multilateral transactions however, the presence of this HVDC in the ac network not only damped the impactful effects of power transfers on network dynamics but also control both voltage and thermal limit violations as a result of associated contingencies. Therefore, VSC-HVDC system incorporated into ac network has the capacity to influence system dynamics and it stands a solution to problems of contingency especially in a deregulated and restructured power network.

Deregulated and restructured network define the future of power systems, hence, different power trading including bilateral, simultaneous and multilateral transactions which characterize liberalised network were implemented alongside determination and enhancement of ATC, improvement of bus voltage profile,

enhancement of power flow and minimization of system loss using various FACTS devices in this thesis. The investigation, analyses and contributions in this work present approaches, techniques and future directions for operation of a restructured power network to researchers, system engineers, network operators and all the stakeholders in power business.

### 10.2 Recommendations and Future Research

The following recommendations and future research direction are proposed based on the outcome of this thesis;

- Literature review of FACTS deployment conducted in this work revealed high concentration of the research work focus on single objective, therefore future research should dwell more on multiple applications of FACTS because variation of one network objective could simultaneously lead to enhancement, diminution or delimitate others.
- FACTS optimization using metaheuristic optimization algorithms is making waves, however, efforts should be channeled and intensified into applying more hybrid techniques because of its attendant advantages ranging from accuracy of results, rapidity of convergence and computational efficiency.
- TCSC, SVC and VSC-HVDC formed the principal FACTS devices deployed in this thesis, for multi-objective applications. However, further research studies which will reveal innate capabilities of other controllers (series, shunt, series-series and series-shunt) should be engaged to encourage their applications.
- The use of multi-FACTS for same target objectives should be part of focus of future research to give room for comparison in terms of capabilities and performance of different controllers.
- Deregulation with several distributed generators describes future power networks, hence, research that will focus on FACTS utilization with incorporation of DG should be painstaking investigated.
- Efforts should be made in future, to conduct research into coordinated control of simultaneously installed DG and FACTS with a view to improving various power system network performance.
- Most importantly, research in the areas of economic benefits of FACTS deployment needs concerted efforts. Future research on these issues will assuredly lead to overall cost reduction and should be given due consideration.
- More research focus should go into HVDC based VSC transmission system to optimize its performance especially in the area of network performance enhancement.

# REFERENCES


[1] A. Meletiou, C. Cambini, and M. Masera, "Regulatory and ownership determinants of unbundling regime choice for European electricity transmission utilities," *Elsevier Util. Policy*, vol. 50, no. November 2016, pp. 13–25, 2018, doi: 10.1016/j.jup.2018.01.006.

[2] R. W. Bacon, "Privatization and Reform in the Global Electricity Supply Industry," *Annu. Rev. Energy Environ.*, vol. 20, pp. 119–143, 1995, doi: https://doi.org/10.1146/annurev.eg.20.110195.001003.

[3] D. Streimikiene and I. Siksnelyte, "Sustainability assessment of electricity market models in selected developed world countries," *Renew. Sustain. Energy Rev.*, vol. 57, pp. 72–82, 2016, doi: 10.1016/j.rser.2015.12.113.

[4] A. Alexandridis and H. E. Psillakis, "Challenges and Trends of Restructuring Power Systems due to Deregulation," in *Proceedings of the 5th International conference on Power Systems and Electromagnetic Compatibility*, 2014, no. August 2005, pp. 49–54.

[5] R. Wright, H. Shin, and F. Trentmann, "From World Power Conference to World Energy Council (90 Years of Energy Cooperation, 1923-2013)," *World Energy Counc.*, pp. 1–71, 2013.

[6] B. Marisekar and Somasundaram P L, "Computation of Available Transfer Capability(ATC) in the Open Access Transmission System(OATS) for various uncertainity conditions," in *IEEE 2015 International Conference on Circuit, Power and Computing Technologies (CCPCT)*, 2015, pp. 1–5, doi: 10.1109/ICCPCT.2015.7159357.

[7] A. . Abhyankar and S. A. Khaparde, "Introduction to Deregulation in Power Industry," *J. Power Energy Eng.*, vol. 2, no. 4, pp. 1–28, 2014, doi: 10.4236/ce.2012.37B011.

[8] S. Bose, C. Wu, Y. Xu, A. Wierman, and H. Mohsenian-Rad, "A Unifying Market Power Measure for Deregulated Transmission-Constrained Electricity Markets," *IEEE Trans. Power Syst.*, vol. 30, no. 5, pp. 2338–2348, 2015, doi: 10.1109/TPWRS.2014.2360216.

[9] K. Bhattacharya, M. H. J. Bollen, and D. E. Jaap, *Operation of Restructured Power Systems*. Kluwer Academic Publishers, 2001.

[10] V. Vittal, "Consequence and impact of electric utility industry restructuring on transient stability and small-signal stabilty analysis," *Proc. IEEE*, vol. 88, no. 2, pp. 196–207, 2000, doi: 10.1109/5.823998.

[11] R. W. Bacon, "Global Electric Power Reform, Privatization, and Liberalization of the Electric Power Industry in Developing Countries," *Annu. Rev. Energy Environ.*, vol. 26, pp. 331–360, 2001, doi: https://doi.org/10.1146/annurev.energy.26.1.331.

[12] D. Shukla, E. S. Lakshmi, and S. P. Singh, "Estimation of ATC using PS-NR," in *IEEE 2017 6th International Conference on Computer Applications in Electrical Engineering - Recent Advances, CERA 2017*, 2018, pp. 111–116, doi: 10.1109/CERA.2017.8343311.

[13] E. L. Da Silva, J. J. Hedgecock, J. C. Mello, and J. C. Luz, "Practical cost-based approach for the voltage ancillary service," *Proc. IEEE Power Eng. Soc. Transm. Distrib. Conf.*, vol. 1, no. 4, p. 46, 2002, doi: 10.1109/PESW.2002.984945.

[14] A. M. Bhaskar and A. A. Jimoh, "Available Transfer Capaility Using PTDF and Implementation of optimal Power Flow in Power Markets," in *IEEE 5th International Conference on Renewable Energy Reseach and Application*, 2016, pp. 219–223, doi: 10.1109/ICRERA.2016.7884541.

[15] S. S. Nayak, S. B. Panda, and S. Das Mohapatra, "State Estimation and Total Transfer Capability Calculation in Deregulated Power System," in *Proceedings of the IEEE 2017 International Conference on Computing Methodologies and Communication (ICCMC) State*, 2017, pp. 757–761, doi: 10.1109/ICCMC.2017.8282568.

[16] R. D. Christie and B. F. Wollenberg, "Transmission Management in the Deregulated Environment," *Proc. IEEE*, vol. 88, no. 2, pp. 170–195, 2000, doi: 10.1109/5.823997.

[17] G. C. Baker, "The Wave of Deregulation: Operational and Design Challenges," *IEEE Power Eng. Rev.*, vol. 19, no. 11, pp. 15–16, 1999, doi: 10.1109/MPER.1999.799637.

[18] S. Matthewman and H. Byrd, "Blackouts: A Sociology of Electrical Power Failure," 2014.

[19] D. Dochain, W. Marquardt, S. C. Won, O. Malik, and M. Kinnaert, "Monitoring and control of process and power systems: Towards new paradigms. Status report prepared by the IFAC Coordinating committee on Process and Power Systems," *Annu. Rev. Control*, vol. 30, no. 1, pp. 69–79, 2006, doi: 10.1016/j.arcontrol.2006.01.002.

[20] D. Streimikiene and I. Siksnelyte, "Sustainability assessment of electricity market models in selected developed world countries," *Renew. Sustain. Energy Rev.*, vol. 57, pp. 72–82, 2016, doi: 10.1016/j.rser.2015.12.113.

[21] N. K. Sharma, P. K. Tiwari, and Y. R. Sood, "Current status, policies and future perspectives of Indian power sector moving towards deregulation," in *2012 IEEE Students' Conference on Electrical, Electronics and Computer Science: Innovation for Humanity, SCEECS 2012*, 2012, pp. 1–6, doi: 10.1109/SCEECS.2012.6184730.

[22] H. Rudnick and J. Zolezzi, "Electric sector deregulation and restructuring in Latin America: Lessons to be learnt and possible ways forward," *IEE Proc. Gener. Transm. Distrib.*, vol. 148, no. 2, pp. 180–184, 2001, doi: 10.1049/ip-gtd:20010230.

[23] K. Varsha, P. Kamlesh, S. Sumeet, and S. Devashish, "Adaptive Neuro-Fuzzy Based AGC of Hydro-Thermal Reheat Deregulated Power System," in *IEEE 2017 Recent Developments in Control, Automation and Power Engineering (RDCAPE)*, 2017, pp. 1–6, doi: 10.1109/RDCAPE.2017.8358292.

[24] K. Mushfiq-Ur-Rahman, M. Saiduzzaman, M. N. Mahmood, and M. R. Khan, "Calculation of available transfer capability (ATC) of Bangladesh power system network," in *2013 IEEE Innovative Smart Grid Technologies - Asia, ISGT Asia 2013*, 2013, pp. 1–5, doi: 10.1109/ISGT-Asia.2013.6698716.

[25] S. Nagalakshmi, S. Kalyani, V. Alamelu Shobana, R. Naga Ranjeni, and P. Deepamangai, "Estimation of available transfer capability under normal and contingency conditions in deregulated electricity market," *IEEE-International Conf. Adv. Eng. Sci. Manag. ICAESM-2012*, pp. 453–459, 2012.

[26] G. S. Rao and K. R. Susmitha, "Determination of ATC using ACPTDF and RPF methods," in *IEEE International Conference on Power, Control, Signals and Instrumentation Engineering, ICPCSI 2017*, 2018, pp. 655–660, doi: 10.1109/ICPCSI.2017.8391794.

[27] A. B. Khairuddin, O. O. Khalifa, A. I. Alhammi, and R. M. Larik, "Deterministic Approach Available Transfer Capability ( ATC ) Calculation Methods," 2016, pp. 1–6.

[28] R. H. Bhesdadiya and P. M. Rajesh, "Available Transfer Capability Calculation Using Deterministic Methods: A Case Study of Indian Power System," in *IEEE International Conference on Electrical, Electronics, and Optimization Techniques (ICEEOT) - 2016 Available*, 2016, pp. 2261–2264.

[29] Shweta, V. K. Nair, V. A. Prakash, S. Kuruseelan, and C. Vaithilingam, "ATC Evaluation in A Deregulated Power System," *Elsevier Energy Procedia*, vol. 117, pp. 216–223, 2017, doi: 10.1016/j.egypro.2017.05.125.

[30] V. Agnes Idhaya Selvi, M. Karuppasamypandiyan, R. Narmathabanu, and D. Devaraj, "Artificial neural network approach for on-line ATC estimation in deregulated power system," in *IEEE 2014 International Conference on Power Signals Control and Computations, EPSCICON 2014*, 2014, pp. 1–5, doi: 10.1109/EPSCICON.2014.6887500.

[31] A. Gupta and A. Kumar, "ATC Determination with Heuristic techniques and Comparison with Sensitivity based Methods and GAMS," *Procedia Comput. Sci.*, vol. 125, no. 2017, pp. 389–397, 2018, doi: 10.1016/j.procs.2017.12.051.

[32] L. Wu, J. Gao, Y. Wang, and R. G. Harley, "A survey of contingency analysis regarding steady state security of a power system," in *2017 North American Power Symposium, NAPS 2017*, 2017, pp. 1–6, doi: 10.1109/NAPS.2017.8107215.

[33] T. Ding, C. Li, C. Yan, F. Li, and Z. Bie, "A Bilevel Optimization Model for Risk Assessment and Contingency Ranking in Transmission System Reliability Evaluation," *IEEE Trans. Power Syst.*, vol. 32, no. 5, pp. 3803–3813, 2017, doi: 10.1109/TPWRS.2016.2637060.

[34] G. C. Ejebe and B. F. Wollenberg, "Automatic Contingency Selection," *IEEE Trans. Power Appar. Syst.*, vol. 98, no. 1, pp. 97–109, 1979, doi: 10.1109/TPAS.1979.319518.

[35] D. Megha, D. Astik, and P. Vivek, "Optimization of Weighting Factors of Performance Index to improve Contingency Ranking," in *IEEE 2017 International Conference on Power Systems (ICPS)*, 2017, pp. 319–322, doi: 10.1109/ICPES.2017.8387313.

[36] E. F. Dela Cruz, A. N. Mabalot, R. C. Marzo, M. C. Pacis, and J. H. S. Tolentino, "Algorithm development for Power System Contingency screening and ranking using Voltage-Reactive Power Performance Index," *IEEE Reg. 10 Annu. Int. Conf. Proceedings/TENCON*, pp. 2232–2235, 2017, doi: 10.1109/TENCON.2016.7848425.

[37] S. B. Daram, P. S. Venkataramu, and M. S. Nagaraj, "Performance index based contingency ranking under line outage condition incorporating IPFC," *Int. Conf. Electr. Electron. Optim. Tech. ICEEOT 2016*, no. 3, pp. 2589–2593, 2016, doi: 10.1109/ICEEOT.2016.7755161.

[38] A. V. Hardas, V. Rajderkar, V. K. Chandrakar, and V. D. Hardas, "Optimum Location of Thyristor Controlled Phase Angle Regulator Based on Performance Index," *Proc. - 2018 Int. Conf. Smart Electr. Drives Power Syst. ICSEDPS 2018*, pp. 132–136, 2018, doi: 10.1109/ICSEDPS.2018.8536084.

[39] P. Sekhar and S. Mohanty, "Power system contingency ranking using Newton Raphson load flow method," *2013 Annu. IEEE India Conf. INDICON 2013*, pp. 1–4, 2013, doi: 10.1109/INDCON.2013.6725912.

[40] S. Burada, D. Joshi, and K. D. Mistry, "Contingency Analysis of Power System by using Voltage and Active Power Performance Index," in *IEEE 2016 1st International Conference on Power Electronics, Intelligent Control and Energy Systems (ICPEICES 2016)*, 2016, pp. 1–5, doi: 10.1109/ICPEICES.2016.7853352.

[41] M. A. Tikuneh and G. B. Worku, "Identification of system vulnerabilities in the Ethiopian electric power system," *Glob. Energy Interconnect.*, vol. 1, no. 3, pp. 358–365, 2018, doi: 10.14171/j.2096-5117.gei.2018.03.007.

[42] A. R. Jordehi, "Particle swarm optimisation (PSO) for allocation of FACTS devices in electric transmission systems: A review," *Renew. Sustain. Energy Rev.*, vol. 52, pp. 1260–1267, 2015, doi: 10.1016/j.rser.2015.08.007.

[43] Y. H. Song and Allan T. Johns, *Flexible AC Transmission Systems (FACTS)*, IET Power. London, UK: The Institution of Engineering and Technology, 2008.

[44] F. Blaabjerg, Y. Yang, D. Yang, and X. Wang, "Distributed Power-Generation Systems and Protection," *Proc. IEEE*, vol. 105, no. 7, pp. 1311–1331, 2017, doi: 10.1109/JPROC.2017.2696878.

[45] A. K. Singh and S. K. Parida, "A review on distributed generation allocation and planning in deregulated electricity market," *Renew. Sustain. Energy Rev.*, vol. 82, no. October 2017, pp. 4132–4141, 2018, doi: 10.1016/j.rser.2017.10.060.

[46] K. Joshi and N. Pindoriya, "Advances in Distribution System Analysis with Distributed Resources: Survey with a Case Study," *Sustain. Energy, Grids Networks*, vol. 15, pp. 86–100, 2018, doi: 10.1016/j.segan.2017.12.004.

[47] S. Dawn and P. K. Tiwari, "Improvement of economic profit by optimal allocation of TCSC & UPFC with wind power generators in double auction competitive power market," *Int. J. Electr. Power Energy*

*Syst.*, vol. 80, pp. 190–201, 2016, doi: 10.1016/j.ijepes.2016.01.041.

[48] R. Srinivasa Rao and V. Srinivasa Rao, "A generalized approach for determination of optimal location and performance analysis of FACTs devices," *Int. J. Electr. Power Energy Syst.*, vol. 73, pp. 711–724, 2015, doi: 10.1016/j.ijepes.2015.06.004.

[49] Y. Xu, A. Siddique, and F. M. Albatsh, "Implementation of series Facts devices SSSC and TCSC to improve power system stability," in *2018 13th IEEE Conference on Industrial Electronics and Applications (ICIEA)*, 2018, pp. 2291–2297, doi: 10.1109/ICIEA.2018.8398092.

[50] K. Lavanya and P. Shobha Rani, "A Review on Optimal Location and Parameter Settings of FACTS Devices in Power Systems Era: Models, Methods," *Int. J. Mod. Trends Sci. Technol.*, vol. 02, no. 11, pp. 2–112, 2016.

[51] N. G. Hingorani and L. Gyugyi, *Understanding FACTS Concepts and Technology of Flexible AC Transmission Systems*, 2000th ed. New York: IEEE Power Engineering Society, 2000.

[52] B. Bhattacharyya and S. Kumar, "Approach for the solution of transmission congestion with multi-type FACTS devices," *IET Gener. Transm. Distrib.*, vol. 10, no. 11, pp. 2802–2809, 2016, doi: 10.1049/iet-gtd.2015.1574.

[53] N. Singh and P. Agnihotri, "Power system stability enhancement using FACTS devices," *Int. J. Recent Technol. Eng.*, vol. 8, no. 4, pp. 3497–3500, 2019, doi: 10.35940/ijrte.D6495.118419.

[54] A. K. Mohanty and A. K. Barik, "Power system stability improvement using FACTS devices," *Int. J. Mod. Eng. Res.*, vol. 1, no. 2, pp. 666–672, 2011.

[55] B. Singh, R. P. Payasi, and V. Shukla, "A taxonomical review on impact assessment of optimally placed DGs and FACTS controllers in power systems," *Energy Reports*, vol. 3, pp. 94–108, 2017, doi: 10.1016/j.egyr.2017.07.001.

[56] S. Gasperic and R. Mihalic, "Estimation of the efficiency of FACTS devices for voltage-stability enhancement with PV area criteria," *Renew. Sustain. Energy Rev.*, vol. 105, no. February, pp. 144–156, 2019, doi: 10.1016/j.rser.2019.01.039.

[57] D. S. Nikam and V. N. Kalkhambkar, "STATCOM and Multilevel VSC Topology: A Review," *Proc. 2018 Int. Conf. Curr. Trends Towar. Converging Technol. ICCTCT 2018*, pp. 1–7, 2018, doi: 10.1109/ICCTCT.2018.8551170.

[58] L. Gyugyi, K. K. Sen, and C. D. Schauder, "The Interline power flow controller concept: A new approach to power flow management in transmission systems," *IEEE Trans. Power Deliv.*, vol. 14, no. 3, pp. 1115–1123, 1999, doi: 10.1109/61.772382.

[59] L. Gyugyi, "Dynamic compensation of AC transmission lines by solid-state synchronous voltage sources," *IEEE Trans. Power Deliv.*, vol. 9, no. 2, pp. 904–911, 1994, doi: 10.1109/61.296273.

[60] B. Blazic and I. Papic, "A new mathematical model and control of D STATCOM for operation under unbalanced conditions.pdf," *Electr. Power Syst. Res.*, vol. 72, pp. 279–287, 2004, doi: 10.1016/j.epsr.2004.04.012/Elsevier Enhanced Reader.

[61] A. Rathi, A. Sadda, L. Nebhnani, and V. M. Maheshwari, "Loss minimization with D-FACTS devices using sensitivity based technique," *India Int. Conf. Power Electron. IICPE*, 2012, doi: 10.1109/IICPE.2012.6450427.

[62] O. P. Mahela and A. G. Shaik, "A review of distribution static compensator," *Renewable and Sustainable Energy Reviews*, vol. 50. pp. 531–546, 2015, doi: 10.1016/j.rser.2015.05.018.

[63] A. Rezaee Jordehi, J. Jasni, N. Abd Wahab, M. Z. Kadir, and M. S. Javadi, "Enhanced leader PSO (ELPSO): A new algorithm for allocating distributed TCSC's in power systems," *Int. J. Electr. Power Energy Syst.*, vol. 64, pp. 771–784, 2015, doi: 10.1016/j.ijepes.2014.07.058.

[64] A. Saberian *et al.*, "Role of FACTS Devices in Improving Penetration of Renewable Energy," in *2013 IEEE, 7th International Power Engineering and Optimization Conference (PEOCO2013), Langkawi, Malaysia*, 2013, no. June, pp. 432–437, doi: 10.1109/PEOCO.2013.6564587.

[65] N. Rawat, A. Bhatt, and P. Aswal, "A review on optimal location of FACTS devices in AC transmission system," in *2013 IEEE International Conference on Power, Energy and Control (ICPEC)*, 2013, pp. 104–109, doi: 10.7498/aps/62.010302.

[66] B. Singh and G. Agrawal, "Enhancement of voltage profile by incorporation of SVC in power system networks by using optimal load flow method in MATLAB/Simulink environments," *Energy Reports*, vol. 4, pp. 418–434, 2018, doi: 10.1016/j.egyr.2018.07.004.

[67] D. Gaur and L. Mathew, "Optimal placement of FACTS devices using optimization techniques: A review," *IOP Conf. Ser. Mater. Sci. Eng.*, vol. 331, no. 1, pp. 0–15, 2018, doi: 10.1088/1757-899X/331/1/012023.

[68] T. Kang, J. Yao, T. Duong, S. Yang, and X. Zhu, "A hybrid approach for power system security enhancement via optimal installation of flexible ac transmission system (FACTS) devices," *Energies*, vol. 10, no. 9, 2017, doi: 10.3390/en10091305.

[69] A. AL Ahmad and R. Sirjani, "Optimal placement and sizing of multi-type FACTS devices in power systems using metaheuristic optimisation techniques: An updated review," *Ain Shams Eng. J.*, no. xxxx, 2019, doi: 10.1016/j.asej.2019.10.013.

[70] B. Singh, V. Mukherjee, and P. Tiwari, "A survey on impact assessment of DG and FACTS controllers in power systems," *Renew. Sustain. Energy Rev.*, vol. 42, pp. 846–882, 2015, doi: 10.1016/j.rser.2014.10.057.

[71] E. Barrios-Martínez and C. Ángeles-Camacho, "Technical comparison of FACTS controllers in parallel connection," *J. Appl. Res. Technol.*, vol. 15, no. 1, pp. 36–44, 2017, doi: 10.1016/j.jart.2017.01.001.

[72] A. Siddique, Y. Xu, W. Aslaml, and F. M. Albatsh, "Application of series FACT devices SSSC and TCSC with POD controller in electrical power system network," *Proc. 13th IEEE Conf. Ind. Electron. Appl. ICIEA 2018*, pp. 893–899, 2018, doi: 10.1109/ICIEA.2018.8397839.

[73] A. R. Gupta and A. Kumar, "Optimal placement of D-STATCOM using sensitivity approaches in mesh distribution system with time variant load models under load growth," *Ain Shams Eng. J.*, vol. 9, no. 4, pp. 783–799, 2018, doi: 10.1016/j.asej.2016.05.009.

[74] H. . A. Gabba and A. . A. Abdelsalam, "Microgrid energy management in grid-connected and islanding modes based on SVC," *Elsevier Energy Convers. Manag.*, vol. 86, pp. 964–972, 2014, doi: http:/dx.doi.org/10.1016/j.encomman.2014.06.070.

[75] A. M. Shaheen, S. R. Spea, S. M. Farrag, and M. A. Abido, "A review of meta-heuristic algorithms for reactive power planning problem," *Ain Shams Engineering Journal*, vol. 9, no. 2. pp. 215–231, 2018, doi: 10.1016/j.asej.2015.12.003.

[76] B. N. Nguyen, L. T. Le, Q. C. Le, T. H. Pham, C. T. Nguyen, and H. T. Nguyen, "Study of FACTS Device Applications for the 220kV Southwest Region of the Vietnam Power System," *Proc. 2018 4th Int. Conf. Green Technol. Sustain. Dev. GTSD 2018*, pp. 150–154, 2018, doi: 10.1109/GTSD.2018.8595603.

[77] J. Li, F. Liu, Z. Li, S. Mei, and G. He, "Impacts and benefits of UPFC to wind power integration in unit commitment," *Renewable Energy*, vol. 116. pp. 570–583, 2018, doi: 10.1016/j.renene.2017.09.085.

[78] X. Zhang, K. Tomsovic, and A. Dimitrovski, "Optimal allocation of series FACTS devices in large-scale systems," *IET Gener. Transm. Distrib.*, vol. 12, no. 8, pp. 1889–1896, 2018, doi: 10.1049/iet-gtd.2017.1223.

[79] A. Kumar and J. Kumar, "ATC with ZIP load model - A comprehensive evaluation with third generation FACTS in restructured electricity markets," *Int. J. Electr. Power Energy Syst.*, vol. 54, pp. 546–558,

2014, doi: 10.1016/j.ijepes.2013.08.003.

[80] A. Nikoobakht, J. Aghaei, M. Parvania, and M. Sahraei-Ardakani, "Contribution of FACTS devices in power systems security using MILP-based OPF," *IET Gener. Transm. Distrib.*, vol. 12, no. 15, pp. 3744–3755, 2018, doi: 10.1049/iet-gtd.2018.0376.

[81] A. Rezaee Jordehi and J. Jasni, "Parameter selection in particle swarm optimisation: A survey," *J. Exp. Theor. Artif. Intell.*, vol. 25, no. 4, pp. 527–542, 2013, doi: 10.1080/0952813X.2013.782348.

[82] J. Hao *et al.*, "Meta-heuristics and Artificial Intelligence," *A Guid. Tour Artif. Intell. Res. II, Springer*, pp. 1–28, 2019.

[83] M. Mohammadalizadeh-Shabestary, H. Hashemi-Dezaki, S. Mortazavian, H. Askarian-Abyaney, and G. Gharehpetian, "A general approach for optimal allocation of FACTS devices using equivalent impedance models of VSCs," *Int. Trans. Electr. energy Syst.*, pp. 1–17, 2014, doi: 10.1002/etep.1896.

[84] A. L. Ara, J. Aghaei, M. Alaleh, and H. Barati, "Contingency-based optimal placement of Optimal Unified Power Flow Controller (OUPFC) in electrical energy transmission systems," *Sci. Iran.*, vol. 20, no. 3, pp. 778–785, 2013, doi: 10.1016/j.scient.2013.04.007.

[85] K. Sabitha and S. J. Bhasha, "Enhancement of ATC with FACTS devices using Real-code Genetic Algorithm," *Int. J. Eng. Res. Technol.*, vol. 3, no. 8, pp. 1005–1012, 2014.

[86] S. R. Inkollu and V. R. Kota, "Optimal setting of FACTS devices for voltage stability improvement using PSO adaptive GSA hybrid algorithm," *Eng. Sci. Technol. an Int. J.*, vol. 19, no. 3, pp. 1166–1176, 2016, doi: 10.1016/j.jestch.2016.01.011.

[87] A. Rezaee Jordehi, "Brainstorm optimisation algorithm (BSOA): An efficient algorithm for finding optimal location and setting of FACTS devices in electric power systems," *International Journal of Electrical Power and Energy Systems*, vol. 69. pp. 48–57, 2015, doi: 10.1016/j.ijepes.2014.12.083.

[88] K. S. Kumar, B. Basavaraja, and B. V. Sanker Ram, "Optimal placement of facts devices with available transfer capability enhancement," *2014 Int. Conf. Smart Electr. Grid, ISEG 2014*, pp. 1–4, 2015, doi: 10.1109/ISEG.2014.7005597.

[89] B. Patil and S. B. Karajgi, "A review on optimal placement of FACTS devices in deregulated environment-a detailed perspective," *Int. Conf. Electr. Electron. Commun. Comput. Technol. Optim. Tech. ICEECCOT 2017*, vol. 2018-Janua, pp. 375–380, 2018, doi: 10.1109/ICEECCOT.2017.8284532.

[90] M. J. Afzal, A. Arshad, S. Ahmed, S. Bin Tariq, S. Ali, and A. Kazmi$^{o}$, "A review of DGs and FACTS in power distribution network: Methodologies and objectives," in *2018 International Conference on Computational , Mathematics and Engineering Technologies iCoMET 2018*, 2018.

[91] A. H. Sautua, M. A. R. Vidal, E. T. Iglesias, and P. E. Lopez, "Survey and crossed comparison of types, optimal location techniques, and power system applications of FACTS," *2013 IEEE Grenoble Conf. PowerTech, POWERTECH 2013*, 2013, doi: 10.1109/PTC.2013.6652451.

[92] K. J. Bhayani, "Review on Optimization Algorithm based Optimal Location and Size of FACTS Devices," in *Second International Conference on Smart Systems and Inventive Technology (ICSSIT 2019)*, 2019, pp. 531–535, doi: 10.1109/ICSSIT46314.2019.8987593.

[93] A. R. Jordehi, "Particle swarm optimisation (PSO) for allocation of FACTS devices in electric transmission systems: A review," *Renew. Sustain. Energy Rev.*, vol. 52, pp. 1260–1267, 2015, doi: 10.1016/j.rser.2015.08.007.

[94] K. Kavitha and R. Neela, "Optimal allocation of multi-type FACTS devices and its effect in enhancing system security using BBO, WIPSO & PSO," *J. Electr. Syst. Inf. Technol.*, vol. 5, no. 3, pp. 777–793, 2018, doi: 10.1016/j.jesit.2017.01.008.

[95] J. Xue, Y. Wu, Y. Shi, and S. Cheng, "Brain storm optimization algorithm for multi-objective optimization problems," *Lect. Notes Comput. Sci. (including Subser. Lect. Notes Artif. Intell. Lect.*

*Notes Bioinformatics)*, vol. 7331 LNCS, no. PART 1, pp. 513–519, 2012, doi: 10.1007/978-3-642-30976-2_62.

[96] Z. Beldi and M. Bessedik, "A New Brainstorming Based Algorithm for the Community Detection Problem," *2019 IEEE Congr. Evol. Comput. CEC 2019 - Proc.*, pp. 2958–2965, 2019, doi: 10.1109/CEC.2019.8789897.

[97] R. Agrawal, S. K. Bharadwaj, and D. P. Kothari, "Population based evolutionary optimization techniques for optimal allocation and sizing of Thyristor Controlled Series Capacitor," *J. Electr. Syst. Inf. Technol.*, vol. 5, no. 3, pp. 484–501, 2018, doi: 10.1016/j.jesit.2017.04.004.

[98] H. R. E. H. Bouchekara, M. A. Abido, and M. Boucherma, "Optimal power flow using Teaching-Learning-Based Optimization technique," *Electr. Power Syst. Res.*, vol. 114, pp. 49–59, 2014, doi: 10.1016/j.epsr.2014.03.032.

[99] T. Nireekshana, G. Kesava Rao, and S. Sivanaga Raju, "Available transfer capability enhancement with FACTS using Cat Swarm Optimization," *Ain Shams Eng. J.*, vol. 7, no. 1, pp. 159–167, 2016, doi: 10.1016/j.asej.2015.11.011.

[100] M. Venkateswara Rao, S. Sivanagaraju, and C. V. Suresh, "Available transfer capability evaluation and enhancement using various FACTS controllers: Special focus on system security," *Elsevier Ain Shams Eng. J.*, vol. 7, no. 1, pp. 191–207, 2016, doi: 10.1016/j.asej.2015.11.006.

[101] S. Sayah and A. Bekrar, "Whale optimization algorithm based optimal reactive power dispatch : A case study of the Algerian power system," *Elsevier Electr. Power Syst. Res.*, vol. 163, pp. 696–705, 2018, doi: https://doi.org/10.1016/j.epsr.2017.09.001.

[102] M. Sedighizadeh, H. Faramarzi, M. M. Mahmoodi, and M. Sarvi, "Hybrid approach to FACTS devices allocation using multi-objective function with NSPSO and NSGA-II algorithms in Fuzzy framework," *International Journal of Electrical Power and Energy Systems*, vol. 62. pp. 586–598, 2014, doi: 10.1016/j.ijepes.2014.04.058.

[103] R. Liang, J. Wang, Y. Chen, and W. Tseng, "An enhanced firefly algorithm to multi-objective optimal active / reactive power dispatch with uncertainties consideration," *Elsevier Electr. Power Energy Syst.*, vol. 64, pp. 1088–1097, 2015, doi: http://dx.doi.org/10.1016/j.ijepes.2014.09.008.

[104] F. H. Gandoman *et al.*, "Review of FACTS technologies and applications for power quality in smart grids with renewable energy systems," *Renewable and Sustainable Energy Reviews*, vol. 82. pp. 502–514, 2018, doi: 10.1016/j.rser.2017.09.062.

[105] V. Frolov, P. G. Thakurta, S. Backhaus, J. Bialek, and M. Chertkov, "Operations- and uncertainty-aware installation of FACTS devices in a large transmission system," *IEEE Trans. Control Netw. Syst.*, vol. 6, no. 3, pp. 961–970, 2019, doi: 10.1109/TCNS.2019.2899104.

[106] A. Ghorbani, S. Y. Ebrahimi, and M. Ghorbani, "Modeling generalized interline power-flow controller (GIPFC) using 48-pulse voltage source converters," *J. Electr. Syst. Inf. Technol.*, vol. 5, no. 1, pp. 68–82, 2018, doi: 10.1016/j.jesit.2017.01.002.

[107] S. Bagchi, R. Bhaduri, P. N. Das, and S. Banerjee, "Analysis of power transfer capability of a long transmission line using FACTS devices," *2015 Int. Conf. Adv. Comput. Commun. Informatics, ICACCI 2015*, pp. 601–606, 2015, doi: 10.1109/ICACCI.2015.7275675.

[108] J. G. Jamnani and M. Pandya, "Coordination of SVC and TCSC for management of power flow by particle swarm optimization," *Energy Procedia*, vol. 156, pp. 321–326, 2019, doi: 10.1016/j.egypro.2018.11.149.

[109] E. M. Malatji, T. Bhekisipho, and M. Nhlanhla, "Optimal Placement Model of Multi-Type FACTS Devices in Power System Networks on a Limited Budget," in *IEEE Africon 2017 Proceedings*, 2017, no. 1, pp. 1296–1300, doi: 10.1109/AFRCON.2017.8095669.

[110] S. Dash, K. R. Subhashini, and J. Satapathy, "Efficient utilization of power system network through

optimal location of FACTS devices using a proposed hybrid meta-heuristic Ant Lion-Moth Flame-Salp Swarm optimization algorithm," *Int. Trans. Electr. Energy Syst.*, pp. 1–30, 2020, doi: 10.1002/2050-7038.12402.

[111] J. G. Singh, H. W. Qazi, and M. Ghandhari, "Load curtailment minimization by optimal placement of Uni fi ed Power Flow Controller," *Int. Trans. Electr. Energy Syst.*, pp. 1–13, 2016, doi: 10.1002/etep.2209.

[112] A. S. Siddiqui, M. T. Khan, and F. Iqbal, "Determination of optimal location of TCSC and STATCOM for congestion management in deregulated power system," *Int. J. Syst. Assur. Eng. Manag.*, vol. 8, no. January, pp. 110–117, 2014, doi: 10.1007/s13198-014-0332-4.

[113] M. R. Shaik and A. S. Reddy, "Optimal placement and sizing of FACTS device to overcome contingencies in power systems," *Int. Conf. Signal Process. Commun. Power Embed. Syst. SCOPES 2016 - Proc.*, pp. 838–842, 2017, doi: 10.1109/SCOPES.2016.7955559.

[114] B. Q. Khanh, "A New Comparison of D-FACTS Performance on Global Voltage Sag Compensation in Distribution System," *2019 Asia Power Energy Eng. Conf. APEEC 2019*, pp. 126–131, 2019, doi: 10.1109/APEEC.2019.8720677.

[115] M. B. Shafik, H. Chen, G. I. Rashed, and R. A. El-Sehiemy, "Adaptive multi objective parallel seeker optimization algorithm for incorporating TCSC devices into optimal power flow framework," *IEEE Access*, vol. 7, pp. 36934–36947, 2019, doi: 10.1109/ACCESS.2019.2905266.

[116] V. Suresh and S. Sreejith, "Power flow analysis incorporating renewable energy sources and FACTS devices," *Int. J. Renew. Energy Res.*, vol. 7, no. 1, pp. 452–458, 2017, doi: 10.1234/ijrer.v7i1.5074.

[117] B. Bhattacharyya, V. K. Gupta, and S. Kumar, "UPFC with series and shunt FACTS controllers for the economic operation of a power system," *Ain Shams Eng. J.*, vol. 5, no. 3, pp. 775–787, 2014, doi: 10.1016/j.asej.2014.03.013.

[118] S. Chirantan, S. C. Swain, P. Panda, and R. Jena, "Enhancement of power profiles by various FACTS devices in power system," *Proc. 2nd Int. Conf. Commun. Electron. Syst. ICCES 2017*, vol. 2018-Janua, no. Icces, pp. 896–901, 2018, doi: 10.1109/CESYS.2017.8321212.

[119] M. Rani and A. Gupta, "Steady state voltage stability enhancement of power system using facts devices," *Proc. 6th IEEE Power India Int. Conf. PIICON 2014*, 2014, doi: 10.1109/34084POWERI.2014.7117724.

[120] S. D. Choudante and A. A. Bhole, "A Review: Voltage Stability and Power Flow Improvement by Using UPFC Controller," *7th IEEE Int. Conf. Comput. Power, Energy, Inf. Commun. ICCPEIC 2018*, pp. 462–465, 2018, doi: 10.1109/ICCPEIC.2018.8525161.

[121] S. Dutta, P. K. Roy, and D. Nandi, "Optimal location of STATCOM using chemical reaction optimization for reactive power dispatch problem," *Ain Shams Eng. J.*, vol. 7, no. 1, pp. 233–247, 2016, doi: 10.1016/j.asej.2015.04.013.

[122] R. Agrawal, S. K. Bharadwaj, M. Ieee, D. P. Kothari, and F. Ieee, "Transmission Loss and TCSC Cost Minimization in Power System using Particle Swarm Optimization," *Int. J. Innov. Res. Electr. Electron. Instrum. Control Eng.*, vol. 4, no. 3, pp. 226–231, 2016, doi: 10.17148/IJIREEICE.2016.4360.

[123] G. Selvaraj and K. Rajangam, "Multi - objective grey wolf optimizer algorithm for combination of network reconfiguration and D - STATCOM allocation in distribution system," pp. 1–21, 2019, doi: 10.1002/2050-7038.12100.

[124] A. Gupta and A. Kumar, "Impact of TCSC Installation on ATC in a System Incorporating Wind and Hydro Generations," *Procedia Technol.*, vol. 25, no. Raerest, pp. 743–750, 2016, doi: 10.1016/j.protcy.2016.08.168.

[125] M. Rashidinejad, H. Farahmand, M. Fotuhi-Firuzabad, and A. A. Gharaveisi, "ATC enhancement using TCSC via artificial intelligent techniques," *Electr. Power Syst. Res.*, vol. 78, no. 1, pp. 11–20, 2008,

doi: 10.1016/j.epsr.2006.12.005.

[126] N. Kalpana and G. Y. Sree Varshini, "Enhancement of available transfer capability using particle swarm optimization technique with interline power flow controller," *IET Conf. Publ.*, vol. 2012, no. 624 CP, pp. 331–334, 2012, doi: 10.1049/cp.2012.2234.

[127] M. V. Rao, S. Sivanagaraju, and Chintalapudi .V. Suresh, "Evaluation and enhancement of available transfer capability in the presence of static synchronous series compensator," in *IEEE International Conference on Power, Control, Signals and Instrumentation Engineering (ICPCSI-2017)*, 2017, pp. 1365–1371, doi: 10.1109/ICPCSI.2017.8391934.

[128] K. Ravinder and Kumar Ashwani, "Impact of STATCOM Control Parameters on Available Transfer Capability Enhancement in Energy Markets," *Elsevier 4th Int. Conf. Eco-friendly Comput. Commun. Syst.*, vol. 70, pp. 515–525, 2015, doi: https://doi.org/10.1016/j.procs.2015.10.094.

[129] R. K. Pandey and K. V. Kumar, "Multi agent system driven SSSC for ATC enhancement," *2016 Natl. Power Syst. Conf. NPSC 2016*, pp. 1–6, 2017, doi: 10.1109/NPSC.2016.7858953.

[130] A. Kumar and J. Kumar, "ATC with ZIP load model - A comprehensive evaluation with third generation FACTS in restructured electricity markets," *Int. J. Electr. Power Energy Syst.*, vol. 54, pp. 546–558, 2014, doi: 10.1016/j.ijepes.2013.08.003.

[131] S. Chansareewittaya and P. Jirapong, "Optimal allocation of multi-type FACTS controllers for total transfer capability enhancement using hybrid particle swarm optimization," *2014 11th Int. Conf. Electr. Eng. Comput. Telecommun. Inf. Technol. ECTI-CON 2014*, pp. 1–6, 2014, doi: 10.1109/ECTICon.2014.6839754.

[132] J. A. Momoh and S. S. Reddy, "Optimal location of FACTS for ATC enhancement," *IEEE Power Energy Soc. Gen. Meet.*, vol. 2014-Octob, no. October, pp. 1–5, 2014, doi: 10.1109/PESGM.2014.6939507.

[133] A. Kumar and J. Kumar, "ATC enhancement in electricity markets with GUPFC and IPFC - A comparison," *Int. J. Electr. Power Energy Syst.*, vol. 81, pp. 469–482, 2016, doi: 10.1016/j.ijepes.2016.02.047.

[134] M. Venkateswara Rao, S. Sivanagaraju, and C. V. Suresh, "Available transfer capability evaluation and enhancement using various FACTS controllers: Special focus on system security," *Ain Shams Eng. J.*, vol. 7, no. 1, pp. 191–207, 2016, doi: 10.1016/j.asej.2015.11.006.

[135] N. Sinha, S. Karan, and S. K. Singh, "Modified de based ATC enhancement using FACTS devices," *Proc. - 1st Int. Conf. Comput. Intell. Networks, CINE 2015*, pp. 3–8, 2015, doi: 10.1109/CINE.2015.11.

[136] J. A. Momoh and S. S. Reddy, "Optimal location of FACTS for ATC enhancement," *IEEE Power Energy Soc. Gen. Meet.*, vol. 2014-Octob, no. October, pp. 1–5, 2014, doi: 10.1109/PESGM.2014.6939507.

[137] S. Chansareewittaya and P. Jirapong, "Optimal allocation of multi-type FACTS Controllers by using hybrid PSO for Total Transfer Capability Enhancement," *ECTI Trans. Comput. Inf. Technol.*, vol. 9, no. 1, pp. 55–63, 2015, doi: 10.37936/ecti-cit.201591.54404.

[138] S. M. Prajapati and P. R. Gandhi, "Impact of Facts Device for ATC Enhancement in Deregulated Market," *2018 Int. Conf. Power Energy, Environ. Intell. Control. PEEIC 2018*, pp. 482–487, 2019, doi: 10.1109/PEEIC.2018.8665458.

[139] N. B. Dev Choudhury and R. Jena, "Available Transfer Capability enhancement in constrained network conditions using TCSC," *2014 Int. Conf. Adv. Eng. Technol. Res. ICAETR 2014*, pp. 1–7, 2014, doi: 10.1109/ICAETR.2014.7012804.

[140] M. M. Karthiga, S. C. Raja, and P. Venkatesh, "Enhancement of available transfer capability using TCSC devices in deregulated power market," *2017 Innov. Power Adv. Comput. Technol. i-PACT 2017*, vol. 2017-Janua, pp. 1–7, 2017, doi: 10.1109/IPACT.2017.8244904.

[141] R. Kumar and A. Kumar, “Impact of SSSC Control Parameters on Available Transfer Capability Enhancement,” *Proc. - 2015 Int. Conf. Comput. Intell. Commun. Networks, CICN 2015*, pp. 1520–1526, 2016, doi: 10.1109/CICN.2015.291.

[142] R. Kumar and A. Kumar, “Impact of STATCOM Control Parameters on Available Transfer Capability Enhancement in Energy Markets,” *Procedia Comput. Sci.*, vol. 70, pp. 515–525, 2015, doi: 10.1016/j.procs.2015.10.094.

[143] V. Rao M, S. S, and C. V. Suresh, “Evaluation and Enhancement of Available Transfer Capability in the Presence of Static Synchronous Series compensator,” in *IEEE International Conference on Power, Control, Signals and Instrumentation Engineering (ICPCSI-2017)*, 2017, pp. 1365–1371.

[144] K. Bavithra, S. C. Raja, and P. Venkatesh, “Optimal setting of FACTS devices using particle swarm optimization for ATC enhancement in deregulated power system,” *IFAC-PapersOnLine*, vol. 49, no. 1, pp. 450–455, 2016, doi: 10.1016/j.ifacol.2016.03.095.

[145] B. Alekhya and J. S. Rao, “Enhancement of ATC in a deregulated power system by optimal location of multi-facts devices,” *2014 Int. Conf. Smart Electr. Grid, ISEG 2014*, pp. 1–9, 2015, doi: 10.1109/ISEG.2014.7005599.

[146] N. S. Rao, J. Amarnath, and V. P. Rao, “Comparison for performance of multitype FACTS devises on available transfer capability in a deregulated power system,” *2014 Int. Conf. Smart Electr. Grid, ISEG 2014*, pp. 1–6, 2015, doi: 10.1109/ISEG.2014.7005611.

[147] N. S. Rao, A. J., and P. Rao, “Comparison for Performance of Multitype FACTS Devises on Available Transfer Capability in a Deregulated Power System,” in *IEEE Computational Intelligence Magazine2014 International Conference on Smart Electric Grid (ISEG)*, 2014, pp. 1–6, doi: 10.1109/ISEG.2014.7005611.

[148] S. V. Padmavathi, S. Sahu, and A. Jayalakshmi, “Available transfer capability enhancement by using Particle Swarm Optimization algorithm based FACTS allocation,” *Asia Pacific Conf. Postgrad. Res. Microelectron. Electron.*, no. December, pp. 184–187, 2012, doi: 10.1109/PrimeAsia.2012.6458650.

[149] T. Joseph, C. E. Ugalde-Loo, J. Liang, and P. F. Coventry, “Asset management strategies for power electronic converters in transmission networks: Application to Hvdc and FACTS devices,” *IEEE Access*, vol. 6, pp. 21084–21102, 2018, doi: 10.1109/ACCESS.2018.2826360.

[150] S. M. Amrr and S. Member, “A Comprehensive Review of Power Flow Controllers in Interconnected Power System Networks,” *IEEE Access*, vol. 8, pp. 18036–18063, 2020, doi: 10.1109/ACCESS.2020.2968461.

[151] E. Pierri, O. Binder, N. G. A. Hemdan, and M. Kurrat, “Challenges and opportunities for a European HVDC grid,” *Elsevier Renew. Sustain. Energy Rev.*, vol. 70, pp. 427–456, 2017, doi: http://dx.doi.org/10.1016/j.rser.2016.11.233.

[152] B. Van Eeckhout, D. Van Hertem, M. Reza, K. Srivastava, and R. Belmans, “Economic comparison of VSC HVDC and HVAC as transmission system for a 300 MW offshore wind farm,” *Wiley Eur. Trans. Electr. Power*, no. 20, pp. 661–671, 2010, doi: 10.1002/etep.359.

[153] Y. S. Borovikov *et al.*, “A hybrid simulation model for vsc hvdc,” *IEEE Trans. Smart Grid*, vol. 7, no. 5, pp. 2242–2249, 2016, doi: 10.1109/TSG.2015.2510747.

[154] G. Li, J. Liang, S. Member, F. Ma, and C. E. Ugalde-loo, “Analysis of Single-Phase-to-Ground Faults at the Valve-Side of HB-MMCs in HVDC Systems,” *IEEE Trans. Ind. Electron.*, vol. 66, no. 3, pp. 2444–2453, 2019, doi: 10.1109/TIE.2018.2829666.

[155] G. E. N. Li *et al.*, “Feasibility and Reliability Analysis of LCC DC Grids and LCC / VSC Hybrid DC Grids,” *IEEE Access*, pp. 22445–22456, 2019, doi: 10.1109/ACCESS.2019.2898387.

[156] L. Liu and C. Liu, “VSCs-HVDC may improve the Electrical Grid Architecture in future world,” *Elsevier Renew. Sustain. Energy Rev.*, vol. 62, pp. 1162–1170, 2016, doi:

http://dx.doi.org/10.1016/j.rser.2016.05.037.

[157] T. An, G. Tang, and W. Wang, “Research and application on multi-terminal and DC grids based on VSC-HVDC technology in China,” *IET J. Insitution Eng. Technol.*, vol. 2, pp. 1–10, 2017, doi: 10.1049/hve.2017.0010.

[158] V. Akhmatov *et al.*, “Technical Guidelines and Prestandardization Work for First HVDC Grids,” *IEEE Trans. Power Deliv.*, vol. 29, no. 1, pp. 327–335, 2014, doi: 10.1109/TPWRD.2013.2273978.

[159] F. Schettler, H. Huang, and N. Christl, “HVDC Transmission Systems using Voltage Sourced Converters - Design and Applications,” in *2000 Power Engineering Society Summer Meeting (Cat. No.00CH37134)*, 2000, vol. 2, pp. 715–720, doi: 10.1109/PESS.2000.867439.

[160] Y. Wang, Y. Zhou, D. Li, D. Shao, K. Cao, and K. Zhou, “The Influence of VSC – HVDC Reactive Power Control Mode on AC Power System Stability,” *MDPI Energies J.*, vol. 13, no. 7, pp. 1–11, 2020, doi: doi:10.3390/en13071677.

[161] X. Guo, J. Yan, G. Xu, J. Hu, and T. Bi, “Control of VSC-HVDC connected wind farms for system frequency support,” *Int. Trans. Electr. Energy Syst.*, vol. 30, no. 5, pp. 1–13, 2020, doi: 10.1002/2050-7038.12352.

[162] S. Sayed and A. Massoud, “Minimum transmission power loss in multi-terminal HVDC systems: A general methodology for radial and mesh networks,” *Alexandria Eng. J.*, vol. 58, no. 1, pp. 115–125, 2019, doi: 10.1016/j.aej.2018.12.007.

[163] T. Mariano, L. Assis, S. Member, S. Kuenzel, and B. C. Pal, “Impact of Multi-Terminal HVDC Grids on Enhancing Dynamic Power Transfer Capability,” *IEEE Trans. Power Syst.*, vol. 32, no. 4, pp. 1–11, 2017, doi: 10.1109/TPWRS.2016.2617399.

[164] S. Kim, A. Yokoyama, Y. Takaguchi, T. Takano, K. Mori, and Y. Izui, “Small-signal stability-constrained optimal power flow analysis of multiterminal VSC-HVDC systems with large-scale wind farms,” *IEEJ Trans. Electr. Electron. Eng.*, vol. 14, no. 7, pp. 1033–1046, 2019, doi: 10.1002/tee.22898.

[165] A. Fuchs, S. Member, M. Imhof, S. Member, T. Demiray, and M. Morari, “Stabilization of Large Power Systems Using VSC – HVDC and Model Predictive Control,” *IEEE Trans. Power Deliv.*, vol. 29, no. 1, pp. 480–488, 2014, doi: 10.1109/TPWRD.2013.2280467.

[166] Y. Shu, G. Tang, and H. Pang, “Study on Yu’e back-to-back VSC-HVDC system,” *IEEE-CSEE J. Power Energy Syst.*, vol. 6, no. 1, pp. 67–71, 2020, doi: 10.17775/cseejpes.2018.01280.

[167] M. E. Montilla-djesus and D. Santos-martin, “Optimal Power Transmission of Offshore Wind Power Using a VSC-HVdc Interconnection,” *MDPI Energies J.*, vol. 10, no. 7, pp. 1–16, 2017, doi: 10.3390/en10071046.

[168] A. Wu, Z. Yuan, H. Rao, B. Zhou, and H. Li, “Analysis of power transmission limit for the VSC-HVDC feeding weak grid,” in *14th IET International Conference on AC and DC Power Transmission (ACDC 2018)*, 2019, pp. 2916–2920, doi: 10.1049/joe.2018.8475.

[169] K. Jia, R. Chen, Z. Xuan, Z. Yang, Y. Fang, and T. Bi, “Fault characteristics and protection adaptability analysis in VSC-HVDC-connected offshore wind farm integration system,” *IET Renew. Power Gener.*, no. Special issue, pp. 1547–1554, 2018, doi: 10.1049/iet-rpg.2017.0793.

[170] I. Mart *et al.*, “Dynamic Overload Capability of VSC HVDC Interconnections for Frequency Support,” *IEEE Trans. Energy Convers.*, vol. 32, no. 4, pp. 1544–1553, 2017, doi: 10.1109/TEC.2017.2712909.

[171] S. Sayed and A. Massoud, “Minimum transmission power loss in multi-terminal HVDC systems : A general methodology for radial and mesh networks,” *Elsevier Alexandria Eng. J.*, vol. 58, pp. 115–125, 2019, doi: https://doi.org/10.1016/j.aej.2018.12.007.

[172] S. D. Tavakoli, E. Prieto-Araujo, E. Sánchez-Sánchez, and O. Gomis-Bellmunt, “Interaction assessment and stability analysis of the MMC-based VSC-HVDC link,” *MDPI Energies J.*, vol. 13, no. 8, pp. 1–

19, 2020, doi: 10.3390/en13082075.

[173] H. S. Ramadan, A. Fathy, and M. Becherif, "Optimal gain scheduling of VSC-HVDC system sliding mode control via artificial bee colony and mine blast algorithms," *IET Gener. Transm. Distrib.*, pp. 661–669, 2017, doi: 10.1049/iet-gtd.2017.0935.

[174] A. L. I. Raza *et al.*, "Multi-Objective Optimization of VSC Stations in Multi-Terminal VSC-HVdc Grids , Based on PSO," *IEEE Access*, pp. 62995–63004, 2018, doi: 10.1109/ACCESS.2018.2875972.

[175] R. F. Mochamad, S. Member, R. Preece, and S. Member, "Assessing the Impact of VSC-HVDC on the Interdependence of Power System Dynamic Performance in Uncertain Mixed AC / DC Systems," *IEEE Trans. Power Syst.*, vol. 35, no. 1, pp. 63–74, 2020, doi: 10.1109/TPWRS.2019.2914318.

[176] P. F. Barber, F. W. T. Boston, T. Bowe, R. W. Cummings, and J. E. Dagle, "North American Electric Reliability Council," *North Am. Electr. Reliab. Counc.*, pp. 8540–5731, 2004.

[177] J. Preetha Roselyn, D. Devaraj, and S. S. Dash, "Multi-Objective Genetic Algorithm for voltage stability enhancement using rescheduling and FACTS devices," *Ain Shams Eng. J.*, vol. 5, no. 3, pp. 789–801, 2014, doi: 10.1016/j.asej.2014.04.004.

[178] H. Saadat, *Power-System-Analysis-by-Hadi-Saadat-Ele.pdf*. Mexico City: WCB/McGraw-Hill, 1999.

[179] E. Acha, C. R. Fuerte-Esquivel, H. Ambriz-Perez, and C. Angeles-Camacho, *FACTS Modelling and Simulation in Power Networks*. 2004.

[180] X. Zhang, C. Rehtanz, and B. Pal, *Flexible AC Transmission Systems: Modelling and Control*. Germany: Springer-Verlag Berlin Heidelberg, New York, 2006.

[181] G. Koundal and S. L. Shimi, "Recent Trends on Real Time Simulation of FACTS: A Review," *2018 Int. Conf. Comput. Charact. Tech. Eng. Sci. CCTES 2018*, pp. 230–235, 2019, doi: 10.1109/CCTES.2018.8674160.

[182] N. G. Hingorani, "FACTS technology - State of the art, current challenges and the future prospects," *2007 IEEE Power Eng. Soc. Gen. Meet. PES*, pp. 11–14, 2007, doi: 10.1109/PES.2007.386032.

[183] S. Cheng *et al.*, "A comprehensive survey of brain storm optimization algorithms," *2017 IEEE Congr. Evol. Comput. CEC 2017 - Proc.*, pp. 1637–1644, 2017, doi: 10.1109/CEC.2017.7969498.

[184] K. Ravi and Rajaram, "Optimal location of FACTS devices using Enhanced Particle Swarm Optimization," in *IEEE International Conference on Advanced Communication Control and Computing Technologies (ICACCCT)*, 2012, vol. 1, no. 978, pp. 414–419.

[185] S. Cheng, J. Chen, X. Lei, and Y. Shi, "Locating Multiple Optima via Brain Storm Optimization Algorithms," *IEEE Access*, vol. 6, pp. 17039–17049, 2018, doi: 10.1109/ACCESS.2018.2811542.

[186] L. Ke, "A brain storm optimization approach for the cumulative capacitated vehicle routing problem," *Memetic Comput.*, vol. 10, no. 4, pp. 411–421, 2018, doi: 10.1007/s12293-018-0250-0.

[187] D. P. Rini, S. M. Shamsuddin, and S. Y. Siti, "Particle Swarm Optimization: Technique, System and Challenges," *Int. J. Appl. Inf. Syst.*, vol. 1, no. 1, pp. 33–45, 2011, doi: 10.5120/ijais-3651.

[188] X. Wu, M. Zhao, and Y. Qu, "Particle Swarm Optimization Programming," in *IEEE Proceedings - International Conference on Computational Aspects of Social Networks, CASoN'10*, 2010, pp. 397–400, doi: 10.1109/CASoN.2010.96.

[189] A. Mishra and V. N. K. G., "Congestion management of deregulated power systems by optimal setting of Interline Power Flow Controller using Gravitational Search algorithm," *J. Electr. Syst. Inf. Technol.*, vol. 4, no. 1, pp. 198–212, 2017, doi: 10.1016/j.jesit.2016.09.001.

[190] R. Srinivasa Rao and V. Srinivasa Rao, "A generalized approach for determination of optimal location and performance analysis of FACTs devices," *Int. J. Electr. Power Energy Syst.*, vol. 73, pp. 711–724, 2015, doi: 10.1016/j.ijepes.2015.06.004.

[191] H. F. Latorre and M. Ghandhari, “Electrical Power and Energy Systems Improvement of power system stability by using a VSC-HVdc,” *Elsevier Electr. Power Energy Syst.*, vol. 33, pp. 332–339, 2011, doi: 10.1016/j.ijepes.2010.08.030.

[192] N. Flourentzou, S. Member, V. G. Agelidis, S. Member, and G. D. Demetriades, “VSC-Based HVDC Power Transmission Systems : An Overview,” *IEEE Trans. Power Electron.*, vol. 24, no. 3, pp. 592–602, 2009, doi: 10.1109/TPEL.2008.2008441.

[193] G. Asplund, “Application of HVDC Light to Power System Enhancement,” in *IEEEWinter Meeting, Session on Development and Application of Self-commutated Converters in Power Systems, Singapore*, 2000, pp. 2498–2503, doi: 10.1109/PESW.2000.847202.

[194] E. Acha, P. Roncero-Sanchez, A. de la V. Jaen, L. M. Castro, and B. Kazemtabrizi, “Power Flows,” in *VSC FACTS HVDC: Analysis, Modelling and Simulation in Power Grids*, John Wiley and Sons Limited, 2019, pp. 99–157.

[195] B. O. Adewolu and A. K. Saha, “Available transfer capability enhancement with FACTS: Perspective of performance comparison,” in *2020 IEEE International SAUPEC/RobMech/PRASA Conference, Cape Town*, 2020, pp. 1–6, doi: 10.1109/SAUPEC/RobMech/PRASA48453.2020.9040995.

[196] A. Masood, A. Xin, S. Salman, M. U. Jan, S. Iqbal, and H. U. Rehman, “Performance Analysis of FACTs Controller for Congestion Mitigation in Power System,” in *IEEE 2020 3rd International Conference on Computing, Mathematics and Engineering Technologies (iCoMET)*, 2020, pp. 1–6, doi: 10.1109/iCoMET48670.2020.9073800.

[197] S. Deka, “Available transfer capability calculations considering outages,” in *IEEE International Conference on Power and Embedded Drive Control, ICPEDC 2017*, 2017, pp. 161–166, doi: 10.1109/ICPEDC.2017.8081080.

[198] P. K. Gouda, A. Sahoo, and P. Hota, “Optimal Power Flow Including Unified Power Flow Controller in a Deregulated Environment,” *Int. J. Appl. Eng. Res.*, vol. 10, no. 1, pp. 505–522, 2015.

[199] O. O. Mohammed, M. W. Mustafa, D. S. S. Mohammed, and A. O. Otuoze, “Available transfer capability calculation methods: A comprehensive review,” *Int. Trans. Electr. Energy Syst.*, vol. 29, no. 6, pp. 1–24, 2019, doi: 10.1002/2050-7038.2846.

[200] K. H. S. and Y. A., “Enhancement of Power System Stability with VSC-HVDC Transmission,” in *2016 North American Power Symposium (NAPS)*, 2016, pp. 1–5, doi: 10.1109/NAPS.2016.7747907.

[201] A. Alassi, S. Bañales, O. Ellabban, G. Adam, and C. MacIver, “HVDC Transmission: Technology Review, Market Trends and Future Outlook,” *Renew. Sustain. Energy Rev.*, vol. 112, no. October 2018, pp. 530–554, 2019, doi: 10.1016/j.rser.2019.04.062.

[202] M. P. Bahrman and B. k. Johnson, “The ABCs of HVDC Transmission Technology,” *IEEE Power & Energy Magazine March/April 2007*, vol. 5, no. 2, pp. 31–44, 2007.

[203] Y. Li, L. Luo, C. Rehtanz, S. Member, and R. Sven, “Realization of Reactive Power Compensation Near the LCC-HVDC Converter Bridges by Means of an Inductive Filtering Method,” *IEEE Trans. Power Electron.*, vol. 27, no. 9, pp. 3908–3923, 2012, doi: 10.1109/TPEL.2012.2189587.

[204] D. Jovcic, “HVDC with Voltage Source Converters: VSC HVDC Applications and Topologies , Performance and Cost Comparison with LCC HVDC,” in *High Voltage Direct Current Transmission: Converters, Systems and DC Grids*, John Wiley & Sons, Ltd, The Atrium, Southern Gate, Chichester, West Sussex PO19 8SQ, England, 2019, pp. 137–143.

[205] M. F. M. Arani and Y. A. R. I. Mohamed, “Analysis and impacts of implementing droop control in dfig-based wind turbines on microgrid/Weak-grid stability,” *IEEE Trans. Power Syst.*, vol. 30, no. 1, pp. 385–396, 2015, doi: 10.1109/TPWRS.2014.2321287.

[206] J. Renedo, A. García-cerrada, L. Rouco, and L. Sigrist, “Coordinated Control in VSC-HVDC Multi-Terminal Systems to Improve Transient Stability : The Impact of Communication Latency,” *MDPI*

*Energies J.*, vol. 12, pp. 1–32, 2019, doi: 10.3390/en12193638.

[207] B. O. Adewolu and A. K. Saha, "FACTS Devices Loss Consideration in Placement Approach for Available Transfer Capability Enhancement," *Int. J. Eng. Res. Africa*, vol. 49, pp. 104–129, 2020, doi: https://doi.org/10.4028/www.scientific.net/JERA.49.104.

[208] Y. U. Huang, Q. Xu, S. Abedi, T. Zhang, X. Jiang, and G. Lin, "Stochastic Security Assessment for Power Systems With High Renewable Energy Penetration Considering Frequency Regulation," *IEEE Access*, vol. 7, pp. 6450–6460, 2019, doi: 10.1109/ACCESS.2018.2880010.

[209] S. B. Jain *et al.*, "Transmission Network Expansion Planning Considering Transmission Switching and Pumped- Storage," in *2017 IEEE International WIE Conference on Electrical and Computer Engineering (WIECON-ENE)*, 2017, pp. 161–164.

[210] NERC, "North America Electric Reliability Council: Standard 51, Transmission System Adequacy and Security," *Available online @ www.nerc.com*, pp. 1–111, 2005.

[211] M. Majidi-qadikolai, S. Member, and R. Baldick, "Integration of N - 1 Contingency Analysis With Systematic Transmission Capacity Expansion Planning: ERCOT Case Study," *IEEE Trans. Power Syst.*, vol. 31, no. 3, pp. 2234–2245, 2016, doi: 10.1109/TPWRS.2015.2443101.

[212] M. Majidi-Qadikolai and R. Baldick, "Reducing the Candidate Line List for Practical Integration of Switching into Power System Operation," in *22nd International Symposium on Mathematical Programming, Pittsburgh*, 2015, pp. 1–15.

[213] H. Peng, M. I. N. Su, S. Li, C. Li, and S. Member, "Static Security Risk Assessment for Islanded Hybrid AC / DC Microgrid," *IEEE Access*, vol. 7, pp. 37545–37554, 2019, doi: 10.1109/ACCESS.2019.2899347.

## APPENDIX A-1

The structure of IEEE 30 bus network and system data as presented here are as obtained from Appendix B of IEEE 30 bus data. The network structure is presented in Fig. A-1, while the transmission line data is presented in Table A-1.1. Table A-1.2 contains bus data, Table A-1.3 presents transformer tap setting and Table A-1.4 contains shunt capacitor data. The data as appeared on the tables are on 100MVA base. The maximum and minimum voltage magnitude limits are taken to be 1.05 p.u. and 0.95 p.u. respectively.

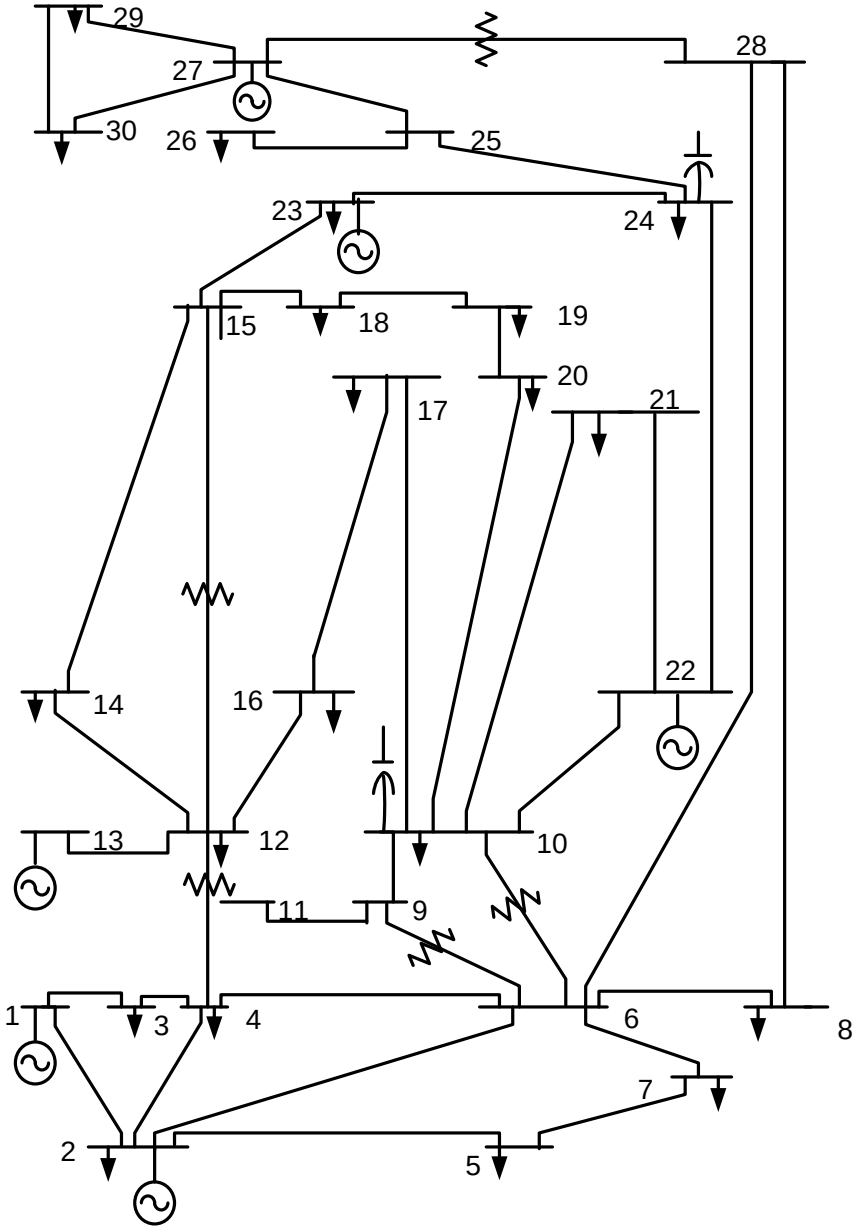


**Fig. A-1. Structure of IEEE 30 bus network**

**Table A-1.1: Transmission Line Data**

| Line Number | From Bus | To bus | Resistance (p.u.) | Reactance (p.u.) | Half Line Charging Susceptance (p.u.) | MVA Rating |
|---|---|---|---|---|---|---|
| 1 | 1 | 2 | 0.02 | 0.06 | 0.03 | 130 |
| 2 | 1 | 3 | 0.05 | 0.2 | 0.02 | 130 |
| 3 | 2 | 4 | 0.06 | 0.18 | 0.02 | 65 |
| 4 | 2 | 5 | 0.05 | 0.02 | 0 | 130 |
| 5 | 2 | 6 | 0.06 | 0.18 | 0.02 | 65 |
| 6 | 3 | 4 | 0.01 | 0.04 | 0 | 130 |
| 7 | 4 | 6 | 0.01 | 0.04 | 0 | 90 |
| 8 | 4 | 12 | 0 | 0.23 | 0 | 65 |
| 9 | 5 | 7 | 0.05 | 0.12 | 0.01 | 70 |
| 10 | 6 | 7 | 0.03 | 0.08 | 0 | 130 |
| 11 | 6 | 8 | 0.01 | 0.09 | 0 | 32 |
| 12 | 6 | 9 | 0 | 0.21 | 0 | 65 |
| 13 | 6 | 10 | 0 | 0.56 | 0 | 32 |
| 14 | 6 | 28 | 0.07 | 0.06 | 0.01 | 32 |
| 15 | 8 | 28 | 0.06 | 0.2 | 0.02 | 32 |
| 16 | 9 | 11 | 0 | 0.21 | 0 | 65 |
| 17 | 9 | 10 | 0 | 0.11 | 0 | 65 |
| 18 | 10 | 20 | 0.09 | 0.21 | 0 | 32 |
| 19 | 10 | 17 | 0.03 | 0.09 | 0 | 32 |
| 20 | 10 | 21 | 0.03 | 0.08 | 0 | 32 |
| 21 | 10 | 22 | 0.07 | 0.15 | 0 | 32 |
| 22 | 12 | 13 | 0 | 0.14 | 0 | 65 |
| 23 | 12 | 14 | 0.12 | 0.26 | 0 | 32 |
| 24 | 12 | 15 | 0.07 | 0.13 | 0 | 32 |
| 25 | 12 | 16 | 0.01 | 0.12 | 0 | 32 |
| 26 | 14 | 15 | 0.22 | 0.12 | 0 | 16 |
| 27 | 15 | 18 | 0.11 | 0.22 | 0 | 16 |
| 28 | 15 | 23 | 0.1 | 0.21 | 0 | 16 |
| 29 | 16 | 17 | 0.08 | 0.19 | 0 | 16 |
| 30 | 18 | 19 | 0.06 | 0.13 | 0 | 16 |
| 31 | 19 | 20 | 0.03 | 0.07 | 0 | 32 |
| 32 | 21 | 22 | 0.01 | 0.22 | 0 | 32 |
| 33 | 22 | 24 | 0.11 | 0.18 | 0 | 16 |
| 34 | 23 | 24 | 0.13 | 0.27 | 0 | 16 |
| 35 | 24 | 25 | 0.19 | 0.33 | 0 | 16 |
| 36 | 25 | 26 | 0.25 | 0.38 | 0 | 16 |
| 37 | 25 | 27 | 0.11 | 0.21 | 0 | 16 |
| 38 | 27 | 29 | 0.22 | 0.4 | 0 | 16 |
| 39 | 27 | 30 | 0.32 | 0.6 | 0 | 16 |
| 40 | 28 | 27 | 0 | 0.4 | 0 | 65 |
| 41 | 29 | 30 | 0.24 | 0.45 | 0 | 16 |

**Table A-1.2: Bus Data**

| | Voltage | | Load | | Generation | | Limits | |
|---|---|---|---|---|---|---|---|---|
| **Bus Number** | **Magnitude (p.u.)** | **Phase angle (Degree)** | **Real Power (MW)** | **Reactive Power (MVAR)** | **Real Power (MW)** | **Reactive Power (MVAR)** | **Qmin (MVAR)** | **Qmax (MVAR)** |
| 1 | 1 | 0 | 0 | 0 | 24.963 | -4.638 | -20 | 150 |
| 2 | 1 | 0 | 21.7 | 12.7 | 60.97 | 27.677 | -20 | 60 |
| 3 | 1 | 0 | 2.4 | 1.2 | 0 | 0 | 0 | 0 |
| 4 | 1 | 0 | 7.6 | 1.6 | 0 | 0 | 0 | 0 |
| 5 | 1 | 0 | 0 | 0 | 0 | 0 | 0 | 0 |
| 6 | 1 | 0 | 0 | 0 | 0 | 0 | 0 | 0 |
| 7 | 1 | 0 | 22.8 | 10.9 | 0 | 0 | 0 | 0 |
| 8 | 1 | 0 | 30 | 30 | 0 | 0 | 0 | 0 |
| 9 | 1 | 0 | 0 | 0 | 0 | 0 | 0 | 0 |
| 10 | 1 | 0 | 5.919 | 2 | 0 | 0 | 0 | 0 |
| 11 | 1 | 0 | 0 | 0 | 0 | 0 | 0 | 0 |
| 12 | 1 | 0 | 11.2 | 7.5 | 0 | 0 | 0 | 0 |
| 13 | 1 | 0 | 0 | 0 | 37 | 13.949 | -15 | 44.7 |
| 14 | 1 | 0 | 6.2 | 1.6 | 0 | 0 | 0 | 0 |
| 15 | 1 | 0 | 8.2 | 2.5 | 0 | 0 | 0 | 0 |
| 16 | 1 | 0 | 3.5 | 1.8 | 0 | 0 | 0 | 0 |
| 17 | 1 | 0 | 9 | 5.8 | 0 | 0 | 0 | 0 |
| 18 | 1 | 0 | 3.2 | 0.9 | 0 | 0 | 0 | 0 |
| 19 | 1 | 0 | 9.5 | 3.4 | 0 | 0 | 0 | 0 |
| 20 | 1 | 0 | 2.2 | 0.7 | 0 | 0 | 0 | 0 |
| 21 | 1 | 0 | 19.669 | 11.2 | 0 | 0 | 0 | 0 |
| 22 | 1 | 0 | 0 | 0 | 31.59 | 40.34 | -15 | 62.5 |
| 23 | 1 | 0 | 3.2 | 1.6 | 22.2 | 8.13 | -10 | 40 |
| 24 | 1 | 0 | 15 | 6.7 | 0 | 0 | 0 | 0 |
| 25 | 1 | 0 | 1 | 0 | 0 | 0 | 0 | 0 |
| 26 | 1 | 0 | 3.5 | 2.3 | 0 | 0 | 0 | 0 |
| 27 | 1 | 0 | 0 | 0 | 28.91 | 10.97 | -15 | 48.7 |
| 28 | 1 | 0 | 0 | 0 | 0 | 0 | 0 | 0 |
| 29 | 1 | 0 | 3.659 | 0.9 | 0 | 0 | 0 | 0 |
| 30 | 1 | 0 | 12 | 1.9 | 0 | 0 | 0 | 0 |

**Table A-1.3: Transformer Tap Setting Data**

| From Bus | To Bus | Tap Setting value (p.u.) |
|---|---|---|
| 6 | 9 | 1.0155 |
| 6 | 10 | 0.9629 |
| 4 | 12 | 1.0129 |
| 28 | 27 | 0.9581 |

**Table A-1.4: Shunt Capacitance Data**

| Bus number | Susceptance (p.u.) |
|---|---|
| 10 | 19 |
| 24 | 4 |

## APPENDIX A-2

The structure of IEEE 30 bus network and system data as presented here are as obtained from Appendix 2 of IEEE 30 bus data. The network structure is presented in Fig. A-2, bus data is contained in Table A-2.1, while transmission line data is presented in Table A-2.2. The data as appeared on the tables are on 100MVA base. The maximum and minimum voltage magnitude limits are taken to be 1.05 p.u. and 0.95 p.u. respectively.

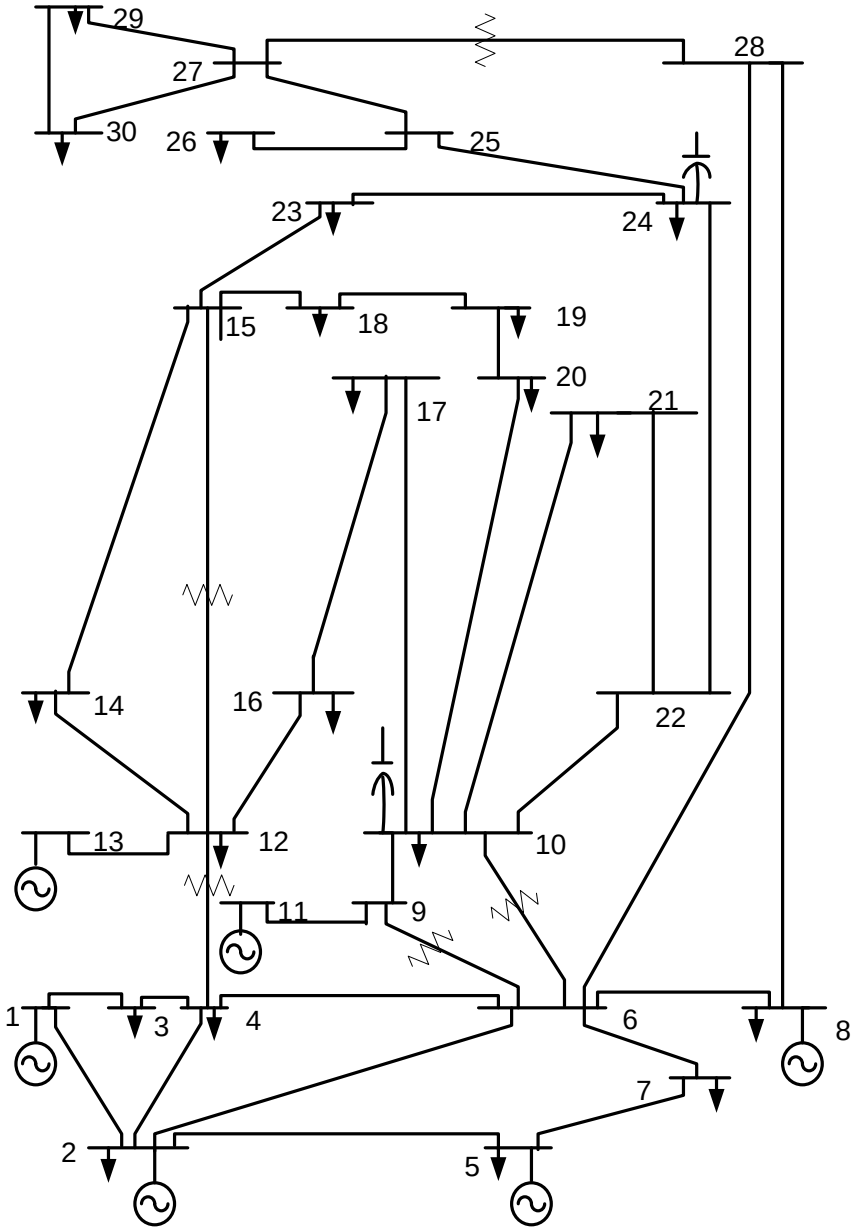


**Fig. A-2. Structure of IEEE 30 bus network**

**Table A-2.1. Bus Data**

| | Bus Voltage | | Generation | | Load | | Limits | |
|---|---|---|---|---|---|---|---|---|
| **Bus Number** | **Magnitude (p.u.)** | **Phase angle (Degree)** | **Real Power (MW)** | **Reactive Power (MVAR)** | **Real Power (MW)** | **Reactive Power (MVAR)** | **Qmin (MVAR)** | **Qmax (MVAR)** |
| 1 | 1.05 | 0 | 138.48 | -2.79 | 0 | 0 | -15 | 100 |
| 2 | 1.0338 | 0 | 57.56 | 2.47 | 21.7 | 12.7 | -20 | 60 |
| 3 | 1.0313 | 0 | 0 | 0 | 2.4 | 1.2 | 0 | 0 |
| 4 | 1.0263 | 0 | 0 | 0 | 7.6 | 1.6 | 0 | 0 |
| 5 | 1.0058 | 0 | 24.56 | 22.57 | 94.2 | 19 | -15 | 62.5 |
| 6 | 1.0208 | 0 | 0 | 0 | 0 | 0 | 0 | 0 |
| 7 | 1.0069 | 0 | 0 | 0 | 22.8 | 10.9 | 0 | 0 |
| 8 | 1.023 | 0 | 35 | 34.84 | 30 | 30 | -15 | 50 |
| 9 | 1.0332 | 0 | 0 | 0 | 0 | 0 | 0 | 0 |
| 10 | 1.0183 | 0 | 0 | 0 | 5.8 | 2 | 0 | 0 |
| 11 | 1.0913 | 0 | 17.93 | 30.78 | 0 | 0 | -10 | 40 |
| 12 | 1.0399 | 0 | 0 | 0 | 11.2 | 7.5 | 0 | 0 |
| 13 | 1.0883 | 0 | 16.91 | 37.83 | 0 | 0 | -15 | 45 |
| 14 | 1.0236 | 0 | 0 | 0 | 6.2 | 1.6 | 0 | 0 |
| 15 | 1.0179 | 0 | 0 | 0 | 8.2 | 2.5 | 0 | 0 |
| 16 | 1.0235 | 0 | 0 | 0 | 3.5 | 1.8 | 0 | 0 |
| 17 | 1.0144 | 0 | 0 | 0 | 9 | 5.8 | 0 | 0 |
| 18 | 1.0057 | 0 | 0 | 0 | 3.2 | 0.9 | 0 | 0 |
| 19 | 1.0017 | 0 | 0 | 0 | 9.5 | 3.4 | 0 | 0 |
| 20 | 1.0051 | 0 | 0 | 0 | 2.2 | 0.7 | 0 | 0 |
| 21 | 1.0061 | 0 | 0 | 0 | 17.5 | 11.2 | 0 | 0 |
| 22 | 1.0069 | 0 | 0 | 0 | 0 | 0 | 0 | 0 |
| 23 | 1.0053 | 0 | 0 | 0 | 3.2 | 1.6 | 0 | 0 |
| 24 | 0.9971 | 0 | 0 | 0 | 8.7 | 6.7 | 0 | 0 |
| 25 | 1.0086 | 0 | 0 | 0 | 0 | 0 | 0 | 0 |
| 26 | 0.9908 | 0 | 0 | 0 | 3.5 | 2.3 | 0 | 0 |
| 27 | 1.0245 | 0 | 0 | 0 | 0 | 0 | 0 | 0 |
| 28 | 1.0156 | 0 | 0 | 0 | 0 | 0 | 0 | 0 |
| 29 | 1.0047 | 0 | 0 | 0 | 2.4 | 0.9 | 0 | 0 |
| 30 | 0.9932 | 0 | 0 | 0 | 10.6 | 1.9 | 0 | 0 |

**Table A-2.2. Transmission Line Data**

| Line Number | Transmission Line | Resistance (p.u.) | Reactance (p.u.) | Half Line Charging Susceptance (p.u.) | MW Limit (pu) |
|---|---|---|---|---|---|
| 1 | 1-2 | 0.0192 | 0.0575 | 0.0528 | 1.0400 |
| 2 | 1-3 | 0.0452 | 0.1652 | 0.0408 | 1.0400 |
| 3 | 2-4 | 0.0570 | 0.1737 | 0.0368 | 0.5200 |
| 4 | 3-4 | 0.0132 | 0.0379 | 0.0084 | 1.0400 |
| 5 | 2-5 | 0.0472 | 0.1983 | 0.0418 | 1.0400 |
| 6 | 2-6 | 0.0581 | 0.1763 | 0.0374 | 0.5200 |
| 7 | 4-6 | 0.0119 | 0.0414 | 0.0090 | 0.7200 |
| 8 | 5-7 | 0.0460 | 0.1160 | 0.0204 | 0.5600 |
| 9 | 6-7 | 0.0267 | 0.0820 | 0.0170 | 1.0400 |
| 10 | 6-8 | 0.0120 | 0.0420 | 0.0090 | 0.2560 |
| 11 | 6-9 | 0 | 0.2080 | 0 | 0.5200 |
| 12 | 6-10 | 0 | 0.5560 | 0 | 0.2560 |
| 13 | 9-11 | 0 | 0.2080 | 0 | 0.5200 |
| 14 | 9-10 | 0 | 0.1100 | 0 | 0.5200 |
| 15 | 4-12 | 0 | 0.2560 | 0 | 0.5200 |
| 16 | 12–13 | 0 | 0.1400 | 0 | 0.5200 |
| 17 | 12–14 | 0.1231 | 0.2559 | 0 | 0.2560 |
| 18 | 12–15 | 0.0662 | 0.1304 | 0 | 0.2560 |
| 19 | 12–16 | 0.0945 | 0.1987 | 0 | 0.2560 |
| 20 | 14–15 | 0.2210 | 0.1997 | 0 | 0.1280 |
| 21 | 16–17 | 0.0524 | 0.1923 | 0 | 0.1280 |
| 22 | 15–18 | 0.1073 | 0.2185 | 0 | 0.1280 |
| 23 | 18–19 | 0.0639 | 0.1292 | 0 | 0.1280 |
| 24 | 19–20 | 0.0340 | 0.0680 | 0 | 0.2560 |
| 25 | 10–20 | 0.0936 | 0.2090 | 0 | 0.2560 |
| 26 | 10–17 | 0.0324 | 0.0845 | 0 | 0.2560 |
| 27 | 10–21 | 0.0348 | 0.0749 | 0 | 0.2560 |
| 28 | 10–22 | 0.0727 | 0.1499 | 0 | 0.2560 |
| 29 | 21–22 | 0.0116 | 0.0236 | 0 | 0.2560 |
| 30 | 15–23 | 0.1000 | 0.2020 | 0 | 0.1280 |
| 31 | 22–24 | 0.1150 | 0.1790 | 0 | 0.1280 |
| 32 | 23–24 | 0.1320 | 0.2700 | 0 | 0.1280 |
| 33 | 24–25 | 0.1885 | 0.3292 | 0 | 0.4800 |
| 34 | 25–26 | 0.2544 | 0.3800 | 0 | 0.1280 |
| 35 | 25–27 | 0.1093 | 0.2087 | 0 | 0.1280 |
| 36 | 28–27 | 0 | 0.3960 | 0 | 0.5200 |
| 37 | 27–29 | 0.2198 | 0.4153 | 0 | 0.1280 |
| 38 | 27–30 | 0.3202 | 0.6027 | 0 | 0.1280 |
| 39 | 29–30 | 0.2399 | 0.4533 | 0 | 0.1280 |
| 40 | 8-28 | 0.0636 | 0.2000 | 0.4028 | 0.2560 |
| 41 | 6-28 | 0.0169 | 0.0599 | 0.0130 | 0.2560 |

## APPENDIX A-3

The structure of IEEE 5 bus network and system data as presented here are as obtained from Appendix 1 of IEEE 5 bus data. The network structure is presented in Fig. A-3, bus data is contained in Table A-3.1, while transmission line data is presented in Table A-3.2. The data as appeared on the tables are on 100MVA base. The maximum and minimum voltage magnitude limits are taken to be 1.05 p.u. and 0.95 p.u. respectively.

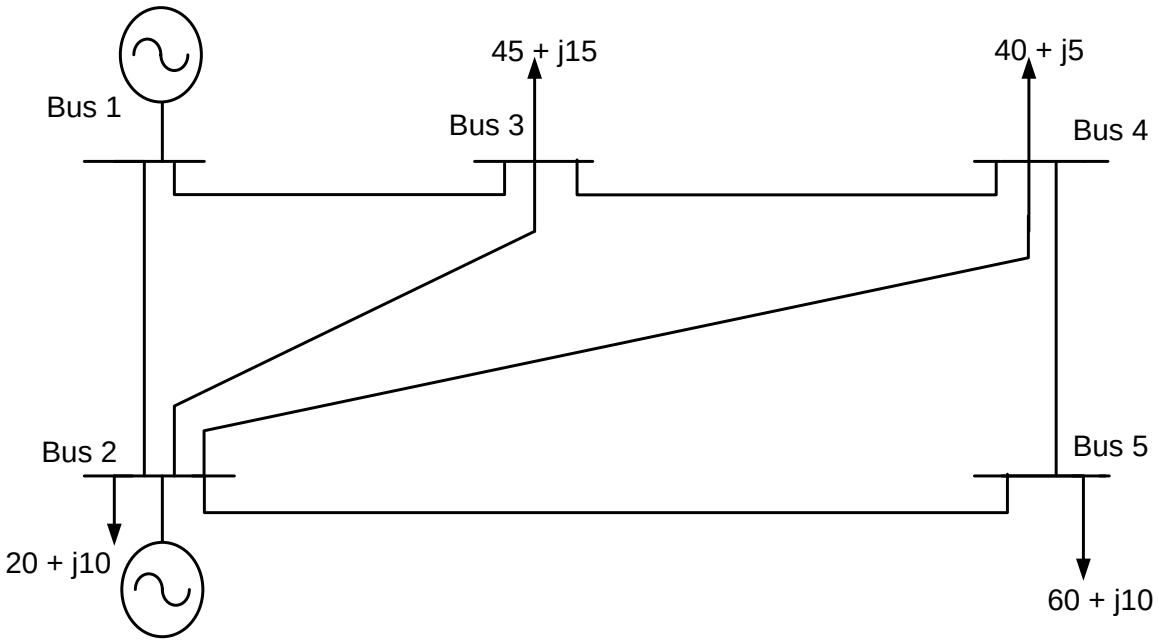


**Fig. A-3. Structure of IEEE 5 bus network**

**Table A-3.1: Bus Data**

| Bus Code | Bus Voltage | Real Power (MW) | Reactive Power (MVAR) | Real Power (MW) | Reactive Power (MVAR) |
|---|---|---|---|---|---|
| 1 | 1.06 + j0.0 | 0 | 0 | 0 | 0 |
| 2 | 1.0 + j0.0 | 40 | 30 | 20 | 10 |
| 3 | 1.0 + j0.0 | 0 | 0 | 45 | 15 |
| 4 | 1.0 + j0.0 | 0 | 0 | 40 | 5 |
| 5 | 1.0 + j0.0 | 0 | 0 | 60 | 10 |

**Table A-3.2. Transmission Line Data**

| Line Number | Transmission Line | Resistance (p.u.) | Reactance (p.u.) | Half Line Charging Susceptance (p.u.) |
|---|---|---|---|---|
| 1 | 1-2 | 0.02 | 0.06 | X per unit |
| 2 | 1-3 | 0.08 | 0.24 | 0.0 + j0.025 |
| 3 | 2-3 | 0.06 | 0.25 | 0.0 + 0.020 |
| 4 | 2-4 | 0.06 | 0.18 | 0.0 + j0.020 |
| 5 | 2-5 | 0.04 | 0.12 | 0.0 + j0.015 |
| 6 | 3-4 | 0.01 | 0.03 | 0.0 + j0.010 |
| 7 | 4-5 | 0.08 | 0.24 | 0.0 + j0.025 |